

IntechOpen

Industrial Applications of Ionic Liquids

Edited by Fabrice Mutelet



Industrial Applications of Ionic Liquids

Edited by Fabrice Mutelet

Published in London, United Kingdom

Industrial Applications of Ionic Liquids
<http://dx.doi.org/10.5772/intechopen.100788>
Edited by Fabrice Mutelet

Contributors

Ganesan Killivelu, Kisor Kumar Sahu, Kajari Chatterjee, M. K. Sridhar, Akhilesh Kumar Singh, Rajendra Kumar Singh, Dipika Meghnani, Toshio Kamiyo, Hiroyuki Arafune, Takashi Morinaga, Takaya Sato, Darko Lovrec, Vito Tič, Pradip K. Bhowmik, Si L. Chen, Haesook Han, Khairul Anwar Ishak, Thamil Selvi Velayutham, Umama Bendaoud, Alfonso Martinez-Felipe, Arvind Kumar, Praveen Singh AGehlot

© The Editor(s) and the Author(s) 2023

The rights of the editor(s) and the author(s) have been asserted in accordance with the Copyright, Designs and Patents Act 1988. All rights to the book as a whole are reserved by INTECHOPEN LIMITED. The book as a whole (compilation) cannot be reproduced, distributed or used for commercial or non-commercial purposes without INTECHOPEN LIMITED's written permission. Enquiries concerning the use of the book should be directed to INTECHOPEN LIMITED rights and permissions department (permissions@intechopen.com).

Violations are liable to prosecution under the governing Copyright Law.



Individual chapters of this publication are distributed under the terms of the Creative Commons Attribution 3.0 Unported License which permits commercial use, distribution and reproduction of the individual chapters, provided the original author(s) and source publication are appropriately acknowledged. If so indicated, certain images may not be included under the Creative Commons license. In such cases users will need to obtain permission from the license holder to reproduce the material. More details and guidelines concerning content reuse and adaptation can be found at <http://www.intechopen.com/copyright-policy.html>.

Notice

Statements and opinions expressed in the chapters are these of the individual contributors and not necessarily those of the editors or publisher. No responsibility is accepted for the accuracy of information contained in the published chapters. The publisher assumes no responsibility for any damage or injury to persons or property arising out of the use of any materials, instructions, methods or ideas contained in the book.

First published in London, United Kingdom, 2023 by IntechOpen
IntechOpen is the global imprint of INTECHOPEN LIMITED, registered in England and Wales,
registration number: 11086078, 5 Princes Gate Court, London, SW7 2QJ, United Kingdom

British Library Cataloguing-in-Publication Data

A catalogue record for this book is available from the British Library

Additional hard and PDF copies can be obtained from orders@intechopen.com

Industrial Applications of Ionic Liquids

Edited by Fabrice Mutelet

p. cm.

Print ISBN 978-1-80356-221-6

Online ISBN 978-1-80356-222-3

eBook (PDF) ISBN 978-1-80356-223-0

We are IntechOpen, the world's leading publisher of Open Access books Built by scientists, for scientists

6,200+

Open access books available

168,000+

International authors and editors

185M+

Downloads

156

Countries delivered to

Our authors are among the
Top 1%

most cited scientists

12.2%

Contributors from top 500 universities



WEB OF SCIENCE™

Selection of our books indexed in the Book Citation Index
in Web of Science™ Core Collection (BKCI)

Interested in publishing with us?
Contact book.department@intechopen.com

Numbers displayed above are based on latest data collected.
For more information visit www.intechopen.com



Meet the editor



Fabrice Mutelet is an Associate Professor of Chemical Engineering Thermodynamics at Ecole Nationale Supérieure des Industries Chimiques – University of Lorraine (ENSIC-LRGP), France, where he obtained his doctorate in 2001. He is a reviewer for more than twenty leading international journals and he has published more than 120 research papers. His research interests include suitable sustainable solvents for chemical processes, the reduction of CO₂ emissions, and the measurement and correlation of phase diagrams for complex systems.

Contents

Preface	XI
Section 1	
Applications of Ionic Liquids in Batteries	1
Chapter 1	3
Ionic Liquids: Applications in Rechargeable Lithium Batteries <i>by Dipika Meghnani and Rajendra Kumar Singh</i>	
Chapter 2	27
High Ionic Conductivities of Ionic Materials as Potential Electrolytes <i>by Pradip K. Bhowmik, Si L. Chen, Haesook Han, Khairul Anwar Ishak, Tamil Selvi Velayutham, Umama Bendaoud and Alfonso Martinez-Felipe</i>	
Chapter 3	43
Application of Ionic Liquids in Rechargeable Li-Ion Batteries: A Comprehensive Guide to Design, Synthesis and Computational Aspects <i>by Kajari Chatterjee, M.K. Sridhar, Akhilesh Kumar Singh and Kisor Kumar Sahu</i>	
Section 2	
Specific Ionic Liquids for Industrial Applications	73
Chapter 4	75
Perspective Chapter: Applications of Novel Ionic Liquids as Catalyst <i>by Ganesan Kilivelu</i>	
Chapter 5	95
Iron-Based Ionic Liquids for Magnetic Resonance Imaging Application <i>by Praveen Singh Gehlot and Arvind Kumar</i>	
Chapter 6	117
Compatibility of Filter Materials Used with Ionic Liquids' Uses in Hydraulic Drive Control Systems and a Filterability Test <i>by Darko Lovrec and Vito Tič</i>	
Chapter 7	135
Development of Low-Friction Ion Gels for Industrial Applications <i>by Toshio Kamijo, Hiroyuki Arafune, Takashi Morinaga and Takaya Sato</i>	

Preface

Ionic liquids (ILs) have received considerable attention in recent years as potential alternative solvents. The non-volatile nature and the high thermal and chemical stability of these solvents facilitate their use as solvent media for high-temperature chemical reactions. Using judicious combinations of cations and anions, their physico-chemical properties and their solubilizing character can be fine-tuned, in turn modifying the miscibility of the IL with water and organic solvents. ILs have been used as adsorbents in gas separation membranes, as stationary phases in gas-liquid chromatography, as entrainers in extractive azeotropic distillations, and as solvents in micro-extraction devices. In the field of heat absorption transformers, $\{H_2O + ILs\}$ working fluids have been shown to be successful as replacements for the conventional system $\{H_2O + LiBr\}$. Numerous ILs have been proposed as absorbents for absorption cycles. They have also been found efficient for biomass pretreatment, the production of bioethanol, and the extraction of high value-added compounds from biomass.

This book includes contributions from experts in different domains. The first section, “Applications of Ionic Liquids in Batteries,” begins with a chapter on the various properties of IL-based electrolytes and their application in rechargeable lithium batteries. The next chapter discusses the synthesis and characterization of new dicationic ILs, which are efficient in energy devices such as fuel cells, batteries, supercapacitors, and solar cells. The final chapter in this section presents a comprehensive guide for the design, synthesis, and computational aspects of ILs in rechargeable Li-ion batteries.

The second section, “Specific Ionic Liquids for Industrial Applications” is devoted to the use of specific ILs in industrial applications. The first chapter in this section discusses the catalytic importance and the plausible organic reaction mechanisms of novel mono, di, and trimeric imidazolium and pyridinium salts as a catalyst in aldol condensation, Biginelli reaction, Erlenmeyer reaction, Mannich reaction, and Pechmann reaction. The second chapter proposes the use of paramagnetic ILs in magnetic resonance imaging techniques. These paramagnetic ILs have shown superior features over other existing and reported contrast agents such as better dual-mode contrast properties, a biofriendly nature, the involvement of a non-toxic magnetic center (Fe), stable aqueous solutions, a better image intensity at low concentration level, and easier syntheses. The third chapter evaluates the compatibility of filter materials used with ILs. The last chapter presents the development of low-friction ion gels for industrial applications.

Fabrice Mutelet
University of Lorraine,
Nancy, France

Section 1

Applications of Ionic Liquids in Batteries

Chapter 1

Ionic Liquids: Applications in Rechargeable Lithium Batteries

Dipika Meghnani and Rajendra Kumar Singh

Abstract

World is passing through the energy crises due to the rapid depletion of fossil fuels. To address this crisis and to fulfill the energy demands worldwide, development of energy storage devices have increased rapidly. Also, renewable energy resources are intermittent, and therefore nevertheless, this energy resources are not always available. In that context, rechargeable lithium batteries are most promising energy storage devices owing to high energy and power density. Although, the development of the component of rechargeable battery such as anode, cathode and electrolyte are in progress as they play major role in enhancing the electrochemical performance of lithium-ion battery. Among them, electrolyte plays crucial role as it provides the path for diffusion of Li^+ ions between the electrodes. In that context, ionic liquid-based electrolytes are widely used as it acts as plasticizer and thus increases the conductivity of electrolyte considerably. In this chapter, we have discussed basics of ionic liquids and its application in electrolyte system. Also, in this chapter, we have discussed various properties of ionic liquid-based electrolytes and their application in rechargeable lithium battery.

Keywords: ionic liquid, rechargeable battery, IL-based polymer electrolyte, ionic conductivity, lithium-ion conductivity

1. Introduction

During the past decades, lithium-ion batteries (LIBs) have drawn more attention of researchers in the area of energy storage due to high energy density (~ 250 Wh/kg) and high-power density, good cycle life etc. Also, LIBs are considered as the most efficient energy storage devices that can store the vast amount of energy from the renewable energy sources (such as wind, solar etc.) and thus help us in making the “Fossil free world”. Furthermore, in order to maximize the energy and power density, several industries and R&D groups have continuously worked hard on the improvement of electrochemical performance of electrode materials as well as electrolytes for LIBs [1–5]. Due to high power and energy density, good cycle life and bring light weight, lithium-ion batteries are widely used and industrialized in transportation devices as well as hybrid and electric vehicles [6] as shown in **Figure 1**. Commercial rechargeable LIBs have three components mainly anode, cathode and electrolyte. Each component of battery has significant role in enhancing the performance of LIBs. Among them,



Figure 1.
Schematic presentation of various application of Lithium-ion battery.

electrolyte provides the path for the diffusion of ions between the electrodes and also act as separator. Initially, organic based conventional electrolytes are commonly used in LIBs due to their high ionic conductivity (10^{-3} to 10^{-2} s/cm) [7]. Organic liquid electrolytes are usually lithium salts that are dissolved in organic solvents such as ethyl methyl carbonate (EMC), ethylene carbonate (EC), propylene carbonate (PC) etc. However, they are highly flammable in nature, highly reactive towards the lithium electrode which causes the unwanted lithium metal electrode growth commonly known as lithium dendrite growth [8–10] as shown in the **Figure 2**. This inevitable lithium dendrite growth is the major problem of short circuiting of battery. Therefore, from the safety concern point, development of organic liquid-based electrolyte is restricted on large-scale applications. To address the above problem, solid polymer electrolytes are promising candidate as they have good mechanical strength, better thermal and chemical stability, good electrochemical stability window. Also, growth of lithium dendrite can be suppressed by such type of quasi-solid electrolytes.

However, they suffer from low room temperature ionic conductivity ($<10^{-6}$ s/cm) [11, 12]. In order to enhance the ionic conductivity of solid polymer electrolyte, several strategies [13, 14] are adopted such as:

1. Use of ethyl methyl carbonate (EMC), ethylene carbonate (EC), propylene carbonate (PC) as conventional plasticizer.

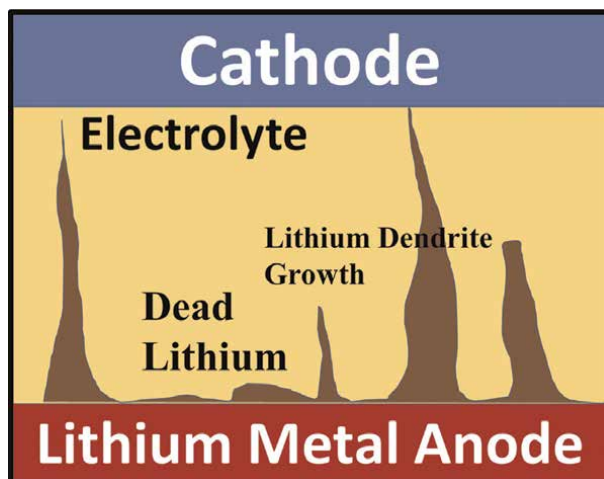


Figure 2.
Showing the lithium dendrite growth in rechargeable lithium batteries.

2. Use of additive/nano size filler such as Al_2O_3 , SiO_2 , TiO_2 etc.
3. Blending of polymer
4. Copolymerization.

By adopting this approach, considerable increase in the ionic conductivity of solid polymer electrolyte has been achieved but it needs to be increased further for Li-ion battery applications. For that, a new class of material known as the ionic liquid has been introduced in the solid polymer electrolyte that has flexible nature, good ionic conductivity, better mechanical stability and wide electrochemical window and ease of processibility as well as portability and is free from the corrosion and leakage problem [15–18]. Ionic liquids have enormous effect on the research field due to its wide range of properties that have a good impact on the development of energy technologies. Ionic liquids are generally molten salts having large organic cation and organic/inorganic anion and therefore the ionic forces between them are weaker and thus low melting temperature. ILs have generally melting temperature less than 100°C and some ionic liquids are liquid at or below the room temperature usually known as room temperature ionic liquids (RTILs) [19, 20]. Also, RTILs have gained increasing attention in the electrochemical device due to their excellent properties such as nonvolatility & nonflammability and thermal stability. In addition, ILs have low vapor pressure, display wide electrochemical stability window (ESW), have high ionic conductivity and display high thermal and chemical stabilities. Few common anions and cations used in the formation of ILs [21, 22] are shown in the **Figure 3**. The choice of anions and cations plays a crucial role on the physical properties of ILs because these cations and anions can combine in millions of possible ways to give the IL having the specific properties for a particular interest. Due to these properties, ionic liquids are also known as “*Designer Solvents*” [23]. Therefore, due to their uniqueness in properties ionic liquids are widely used as plasticizer in solid polymer electrolytes. Ionic liquid based solid electrolytes are usually composed of polymer host matrix, lithium salts and ionic liquid. Ionic liquid-based polymer electrolytes not only have

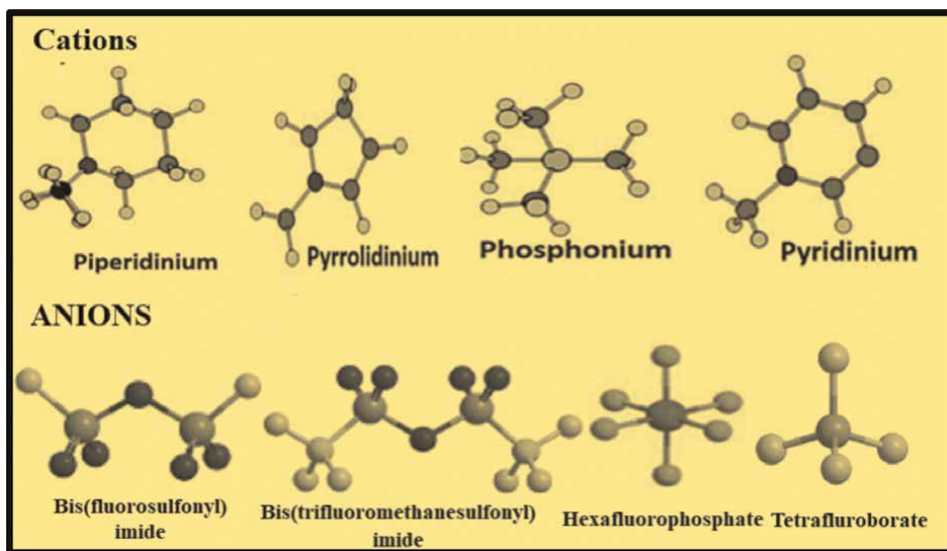


Figure 3.
Some of cations and anions used in the formation of ionic liquids.

high ionic conductivity but have good electrode-electrolyte contact like liquid electrolyte, good mechanical strength, flexibility, wide electrochemical window and good thermal stability and chemical stability also. Therefore, in electrochemical devices especially, in lithium-ion batteries, ionic liquid-based electrolytes are widely used.

In this chapter, we discussed the physical, thermal, structural and electrochemical properties of IL-based polymer electrolytes and its application as electrolyte in lithium polymer batteries.

2. Different role of ionic liquids in lithium batteries

2.1 Pure Ionic liquids as electrolytes

Nowadays, room temperature ionic liquids are replaced by conventional organic carbonate-based electrolytes due to their unique features, such as (a) wide ECW, (b) non-flammability, (c) low vapor pressure (d) higher conductivity (e) wide operation range of temperature (f) non-toxicity (g) non-flammability. Surprisingly, some electrode materials show good performance with pure IL-based electrolytes, compromising of lithium salt and IL which are not working with the conventional organic carbonate-based electrolyte [24]. However, practical applications of ionic liquid electrolyte are limited due to their high viscosity. As the conductivity is affected by viscosity, higher the viscosity, it will be more difficult for Li^+ ions to migrate. Among different types of ILs, 1-ethyl-3-methylimidazolium bis(trifluoromethylsulfonyl) imide ([EMIM][TFSI]) IL has highest conductivity ($\sim 10^{-2}$ S/cm at room temperature) due to smallest viscosity [25]. Ishikawa et al. [26] reported pure ionic liquid electrolytes such as the 0.8 M LiTFSI/EMI-TFSI, 0.8 M LiTFSI/EMI-FSI, or 0.8 M LiTFSI/P13-FSI and studied their electrochemical behavior using natural graphite as a negative electrode and Li as a counter electrode. They found that LiTFSI/EMI-TFSI shows outstanding performance than that of LiTFSI/EMI-FSI or LiTFSI/P13-FSI

electrolyte and reversible capacity of a graphite negative electrode with LiTFSI/EMI-FSI as the electrolyte is ~ 360 mAh g^{-1} at C/5 rate remains stable during 30 cycles which favorably is comparable with that of the EC + DEC solvent.

Also, the Li-salt concentration greatly affects the conductivity of ionic liquid system. Shiro Seki et al. [27] have reported effect of lithium salt concentration in 1,2-dimethyl-3-propyl imidazole bis(trifluoromethylsulfonyl) imide ([DMP][ImTFSI])-based binary electrolyte on the electrolyte/electrode interfacial resistance, charge-discharge performance, and ionic conductivity. They found that ionic conductivity of DMPIMTFSI-LiTFSI mixed electrolyte is decreased with on decreasing LiTFSI concentration and also with optimized mixed binary electrolyte with LiCoO₂ cathode, Li-cell shows high reversibility during charge-discharge performance for more than 100 cycles.

2.2 Conventional carbonate-based electrolyte with added ILs

Due to strong ion-ion interaction, ionic liquids have high viscosity and low ionic conductivity which limits their application in batteries. In order to solve these mentioned problems, organic solvents such as ethylene carbonate (EC), diethylene carbonate (DEC), dimethyl carbonate (DMC) are added to ILs which significantly reduce the viscosity and enhance the ionic conductivity of system than that of pure ionic liquid electrolyte system [28]. Marco Agostini et al. [29] added ethylene carbonate (EC): dimethyl carbonate (DMC) in N-butyl-N-methyl-pyrrolidinium bis(trifluoromethanesulfonyl) imide, lithium bis(trifluoromethanesulfonyl)imide (Py_{1,4} TFSI-LiTFSI) ionic liquid-based system and found that ionic conductivity as well as lithium-ion transference number increases from 10^{-3} to 10^{-2} S/cm and 0.25 to 0.38 respectively. This increase in lithium-ion transference number and ionic conductivity is due to the solvation of Li⁺-ions and dissociation of Li-salts due to more conductive system.

2.3 Quasi solid-state electrolytes containing ionic liquid

Quasi solid-state electrolyte containing ionic liquids are also known as ionic liquid-based electrolyte which have gained significantly more attention due to their high mechanical and chemical stability, good thermal and wide electrochemical stability, highly flexible in nature, non-flammability in nature and high ionic conductivity. In such system, ionic liquid is added into the polymer-based electrolyte as plasticizer which helps to improve the ionic conductivity, electrochemical window as well as Li-transference number. Singh et al. [30] added the 1-butyl-3-methylimidazolium bis(trifluoromethylsulfonyl)imide ([BMIM][TFSI]) ionic liquid into PEO + 20 wt.% of LiTFSI polymer electrolyte system and found the ionic conductivity of optimized ionic liquid-based polymer electrolyte (PEO + 20 wt.% LiTFSI) + 20 wt.% BMIMTFSI around $\sim 1.5 \times 10^{-4}$ S/cm at 30°C. Furthermore, addition of ILs in to polymer-based electrolyte, increases the amorphicity as well as ionic conductivity of polymer electrolyte system due to the plasticizing effect of ILs. Simonetti et al. [31] have reported the PEO-based polymer electrolyte containing N-methyl-N-propylpyrrolidinium bis (fluorosulfonyl)imide ionic liquid and ionic conductivity values $\sim 3.46 \times 10^{-4}$ and 2.43×10^{-3} S/cm at -20 and 20°C , respectively, with electrochemical stability window ~ 4.5 V vs. Li/Li⁺. Furthermore, Kumar et al. [32] have also reported the effect of 1-ethyl 3-methyl imidazolium trifluoromethanesulfonate (EMITf) IL on the PEO and lithium trifluoromethanesulfonate (LiCF₃SO₃ or LiTf) (in the ratio ~ 25) polymer electrolyte system. They found that PEO₂₅.LiTf +40 wt.% (EMITf) electrolyte system

IL based PEO-polymer system	Electrical conductivity (S.cm ⁻¹)	Transference number (Ion/cation)	Electrochemical stability window	References
PEO + 20 wt.% LiFSI +20 wt.% BMPyTFSI	4.05×10^{-5}	0.99/0.37	4.2	[8]
PEO-LiTFSI- PYR13FSI	2.43×10^{-3} at 20°C	—	4.5	[31]
(PEO) ₂₀ LiTFSI + PYR ₁₃ FSI	$\sim 10^{-4}$	—	—	[22]
PEO25.LiTf+40 wt.% EMITf	3.0×10^{-4}		4.9 V	[32]
PEO + 20 wt.% LiTFSI + [P _{6,6,6,14}] [Ntf ₂]	4.2×10^{-5}	0.99/0.37	3.34	[33]
PEO + 20 wt.% LiTFSI +12.5 wt.% EMIMTFSI	2.08×10^{-4}	0.99/0.39	4.6	[34]
P(EO) ₂₀ LiTFSI - BMPyTFSI	6.9×10^{-4} at 40°C	—	4.8–5.3	[35]
P(EO) ₂₀ LiTFSI + 1.27PP1.3TFSI	2.06×10^{-4}	0.339	4.5–4.7	[36]
PEO + 20wt%LiFSI+ 7.5wt% EMIMFSI	2.89×10^{-4}	0.99/0.28	3.8	[37]
PEO-NaMS- BMIM-MS	1.05×10^{-4}	0.99/0.46	4–5	[38]
PEO ₂₀ LiDFOB + 40 wt.% IL EMImTFSI	$\sim 1.85 \times 10^{-4}$	—	2.5–4.0 V	[39]

Table 1. Properties of ionic liquid-based polymer electrolyte system.

shows ionic conductivity of $\sim 3 \times 10^{-4}$ S/cm at RT with wide electrochemical stability window (~ 4.9 V vs. Li/Li⁺) and excellent thermal stability which proves the suitability of electrolyte in various energy storage/conversion devices. Also, such IL-based polymer electrolytes have freestanding and flexible nature along with excellent thermal and mechanical stabilities which proves the suitability of such electrolytes in Li-ion battery. Some of the IL-based polymer electrolyte systems are listed in **Table 1** along with some properties such as ionic conductivity, Li-ion transference number and electrochemical stability window (ESW). From the **Table 1**, it can be seen that IL incorporation in the polymer and salt electrolyte system has increased the ionic conductivity as well ESW which proves the suitability of IL-based polymer electrolytes for Li-battery. In this chapter, we mainly discuss the physical, thermal, structural and electrochemical properties of IL-based polymer electrolyte system and its application in lithium metal battery (LMB).

3. Structural, thermal and ionic transport properties of ionic liquid-based polymer electrolytes

3.1 Structural properties of ionic liquid-based polymer electrolytes

It is reported in the literature that on addition of IL in the PEO-based polymer electrolyte system, its amorphicity is increased and hence mobility of free ions which in turn increases the ionic conductivity of IL-based polymer electrolyte system. Such

increase in the amorphicity is observed by the X-ray Diffraction study (XRD) of IL-based polymer electrolyte system. Meghnani et al. [8] have reported that when in the PEO + 20 wt.% LiFSI system, 1-butyl-3-methylpyridinium bis(trifluoromethyl-sulfonyl) imide (BMPyTFSI) IL is added, the amorphous nature of polymer electrolyte system increases which in turn increases the mobility of charge carrier due to free volume. **Figure 4** shows the XRD pattern of pristine PEO and polymer electrolytes PEO + 20 wt.% LiFSI + X wt.% IL (b) X = 0, (c) X = 10, (d) X = 15, and (e) X = 20 at room temperature and it can be seen that on addition of ionic liquid in polymer electrolyte system, the halo region as well as FWHM increases which in turn decreases the crystallinity of the system. Gupta and Singh et al. [30, 33] observed the similar behavior, they reported the effect of addition of phosphonium based IL and BMIMTFSI IL in the PEO + 20 wt.% LiTFSI, and observed that the halo region of peak increases which makes the polymer system amorphous. This amorphous nature of polymer electrolyte system favors the Li ion diffusion and hence enhances the Li-ion conductivity.

Besides that, addition of ionic liquid does not only affect the XRD pattern of polymer electrolyte system, but also affects the surface morphology of it. It is reported in the literature that on addition of IL, surface of polymer electrolyte becomes smooth than that of without ionic liquid. We [40] have reported that addition of BMPyTFSI IL into PEO-based electrolyte system makes the surface of polymer electrolyte system smoother as shown in the **Figure 5**. Same behavior is also observed by Gupta et al. [33] They have reported the smoother surface morphology of IL based polymer electrolyte

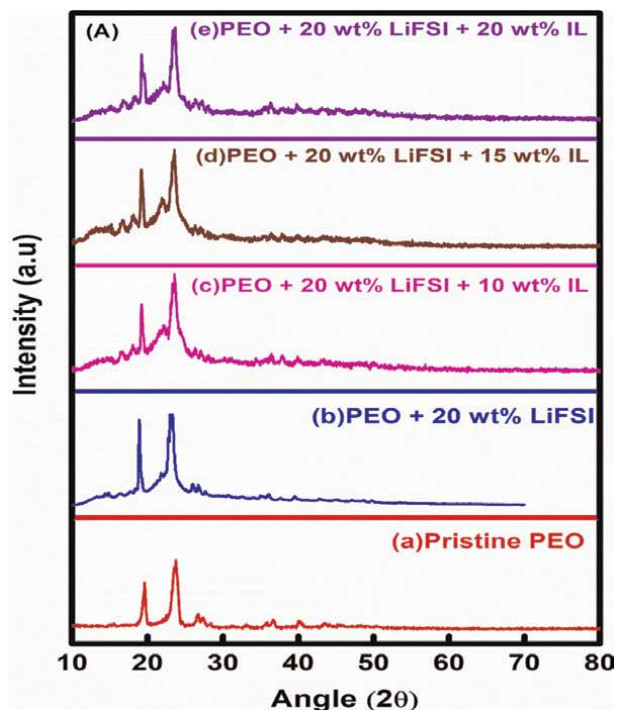


Figure 4. X-ray diffraction patterns of (a) PEO and PEO + 20 wt.% LiFSI + X wt.% IL (b) X = 0, (c) X = 10, (d) X = 15, and (e) X = 20 polymer electrolytes at RT.

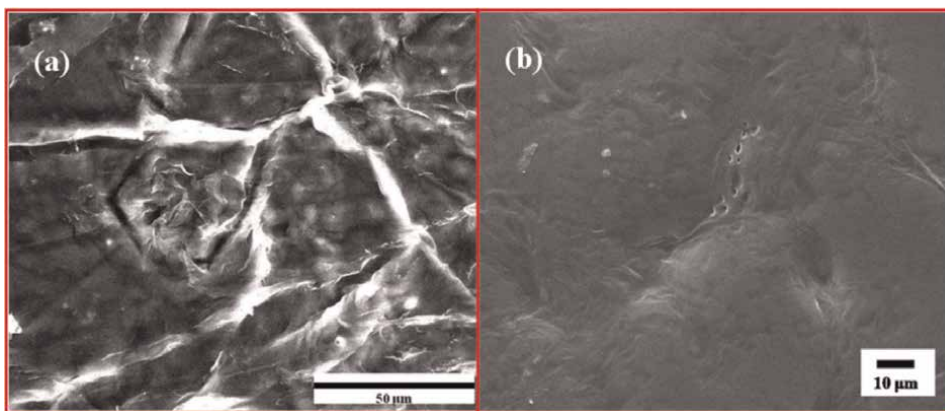


Figure 5. SEM images of (a) Pristine PEO (b) PEO + 20 wt.% LiFSI + 20 wt.% IL.

and found that addition of IL into polymer electrolyte system increases the amorphicity of the system and thus makes it surface smoother.

3.2 Effect of IL on the thermal behavior of polymer electrolyte system

The effect of IL on the thermal stability of polymer electrolyte system is examined by Thermogravimetric and Differential scanning calorimetry analysis using Mettler Toledo DSC/TGA system (TGA and DSC study). For practical application of IL-based polymer electrolyte system in lithium batteries at high temperature, it is necessary to know the thermal stability as well as melting temperature of IL based polymer electrolyte system. Meghnani et al. [41] synthesized the IL-based polymer electrolytes PEO + 20 wt.% LiFSI + X wt.% N-methyl-N-propyl piperidinium bis(fluorosulfonyl) imide (PP₁₃FSI) (X = 10, 20, 30 and 40) by solution cast technique [8] and found the thermal stability $\sim 210^\circ\text{C}$ as shown in the **Figure 6(a)**. The authors have also reported the melting temperature as well as degree of crystallinity of IL-based polymer electrolytes by DSC technique. They found that on increasing the IL concentration in PEO + 20 wt.% LiFSI system, melting temperature (T_m) is shifted towards the lower temperature ($\sim 47.6^\circ\text{C}$) and also area under the endothermic curve decreases due to decrease in the crystallinity of the system. This decrease in the crystallinity of the system is calculated by the formula [42]:

$$\text{Degree of Crystallinity} = \frac{\Delta H_m}{\Delta H_m^0} \times 100\% \quad (1)$$

Where ΔH_m and ΔH_m^0 are the enthalpy value of electrolyte and pristine PEO respectively. The value of ΔH_m is the area under the endothermic peak related to melting curve whereas the value of ΔH_m^0 is 213.7 Jg^{-1} for 100% crystalline polymer PEO. It is found that on addition of IL, the melting temperature as well as degree of crystallinity decrease and the lowest value is found to be for 40 wt.% IL containing polymer electrolyte (see **Figure 6(b)**). This is due to the enhancement of the amorphicity of the polymer electrolyte system which result in the increase of the segmental motion of polymeric chain.

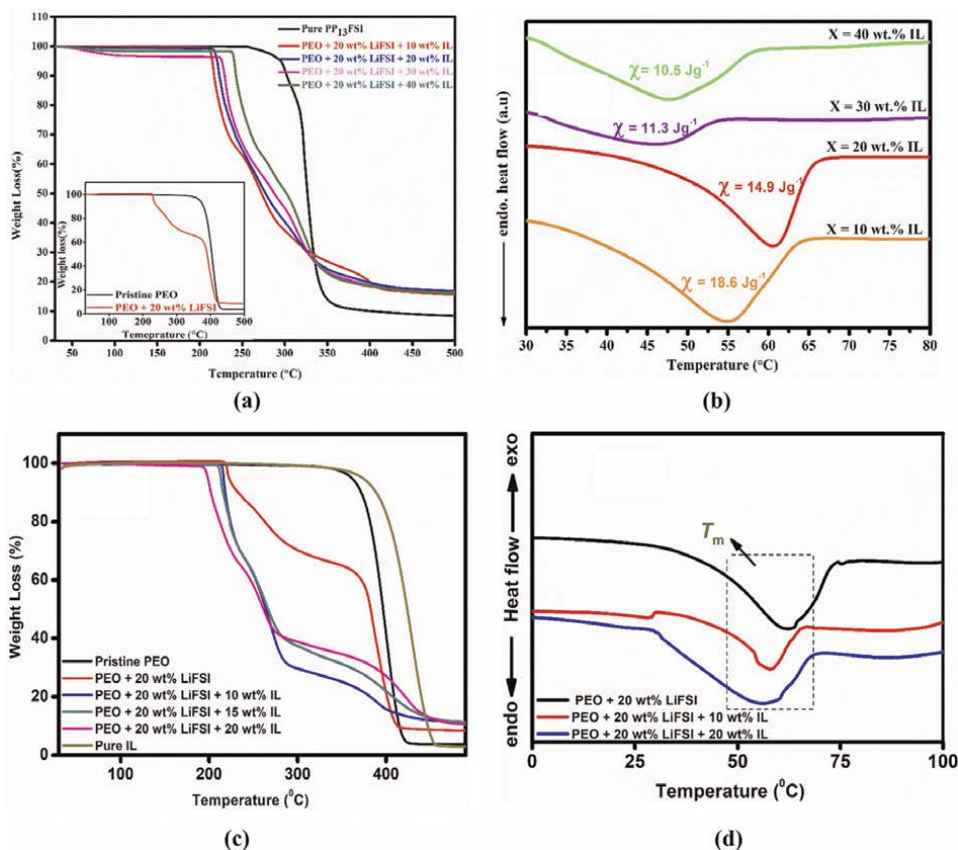


Figure 6. (a) Thermal stability, (b) DSC thermograms of polymer electrolyte PEO + 20 wt.% LiFSI + X wt.% PP₁₃FSI (X = 0, 10, 20, 30, 40) and (c) TGA thermogram and (d) DSC thermograms of pristine PEO, polymer electrolytes films PEO + 20 wt.% LiFSI + X wt.% IL (X = 0, 10, 15, and 20).

Meghnani et al. [8] also reported the effect of BMPyTFSI IL on the thermal stability of PEO-based electrolyte system. They have found that that IL based polymer electrolyte PEO + 20 wt.% LiTFSI + X wt.% (X = 10, 15, 20) shows three step decomposition and thermal stability is found in the range 200–220°C as shown in **Figure 6(c)**. Also, on increasing the IL concentration, melting-temperature shifted towards lower temperature side (see **Figure 6(d)**). Therefore, IL based polymer electrolyte is more suitable electrolyte for Li-battery applications at high temperature due to its good thermal stability.

3.3 Effect of IL on the ionic conductivity of polymer electrolyte system

One of the crucial effects of IL on the polymer electrolyte system is ionic conductivity which is usually examined by the complex impedance spectroscopy technique. It has been reported in literature that on addition of IL into the polymer electrolyte system, the conductivity of parent system increases because IL acts as plasticizer which enhances flexibility of polymer electrolyte system and thus ionic conductivity of the system. The ionic conductivity of IL-based polymer electrolyte system is calculated by the equation:

$$\sigma = \frac{1}{R_b} \frac{L}{A} \quad (2)$$

Where L and A are the thickness and area of polymer electrolyte respectively and R_b is the bulk resistance of electrolyte.

Meghnani et al. [41] have reported that on increasing the IL concentration the bulk resistance of polymer electrolyte PEO + 20 wt.% LiFSI + X wt.% PP₁₃FSI (X = 0, 10, 20, 30, 40) decreases and the lowest bulk resistance or highest ionic conductivity is found to be for 40 wt.% IL containing polymer electrolyte as shown in **Figure 7(a,b)**.

This decreasing trend may be due to the plasticizing nature of IL which enhances the flexibility of polymer chain and thus ionic conductivity of polymer electrolyte. They have also studied the temperature dependent conductivity and found that on increasing the temperature, ionic conductivity of the system increases and show Arrhenius type thermally activated behavior:

$$\sigma = \sigma_0 e^{-\frac{E_a}{RT}} \quad (3)$$

Where E_a , K and T are the activation energy, Boltzmann constant and temperature respectively and σ_0 is pre-exponential factor. It is found that activation energy of electrolyte system decreases with increasing the IL concentration as seen from **Figure 7(c)**. In another study Meghnani et al. [8] have reported the conductivity of PEO + 20 wt.% LiFSI + X wt.% BMPyTFSI (X = 10, 15, 20) system and found that on increasing IL content, conductivity of system increases and follows Arrhenius type thermally activated behavior as shown in the **Figure 7(d)**. Also, they have observed that conductivity and activation energy both are inverse in nature (see **Figure 7(e)**). Balo et al. [43] also observed almost similar behavior in PEO + 20 wt.% LiTFSI + X wt.% EMIMFSI (x = 0, 2.5, 5, 7.5, 10, 12.5, and 15) polymer electrolyte system. They found that on increasing the IL concentration upto 10 wt.%, ionic conductivity of system increases and thereafter it is decreases. It is because beyond this IL concertation, formation of ion pairs starts which reduces the ionic conductivity of the system.

3.4 Effect of IL on the Li⁺ diffusion coefficient (D_{Li^+}) and Li-ion ionic conductivity of polymer electrolyte system

For application of IL-based polymer electrolyte system in Li-battery, it is important to know the Li⁺ diffusion coefficient (D_{Li^+}) and Li-ion ionic conductivity. Li⁺ diffusion coefficient is usually estimated by restricted diffusion method [44]. In this method, polymer electrolyte is sandwich between two non-blocking electrodes and constant potential is applied for a fixed period of time to set up constant current. Thereafter, potential is interrupted and drop of potential is recorded with respect to time. By determining the slope of this curve, diffusion coefficient of electrolyte is calculated using the formula [44]:

$$Slope = \frac{-\pi^2 D}{L^2} \quad (4)$$

Where L is the thickness of the electrolyte. Meghnani et al. [41] have estimated the Li⁺ diffusion coefficient (D_{Li^+}) for PEO + 20 wt.% LiFSI + X wt.% (0, 10, 40) PP₁₃FSI system (see **Figure 8(a,b)**). It is found that D_{Li^+} value for PEO + 20 wt.% LiFSI system is $\sim 3.51 \times 10^{-9} \text{ cm}^2\text{s}^{-1}$ at room temperature (RT) while when IL is added in

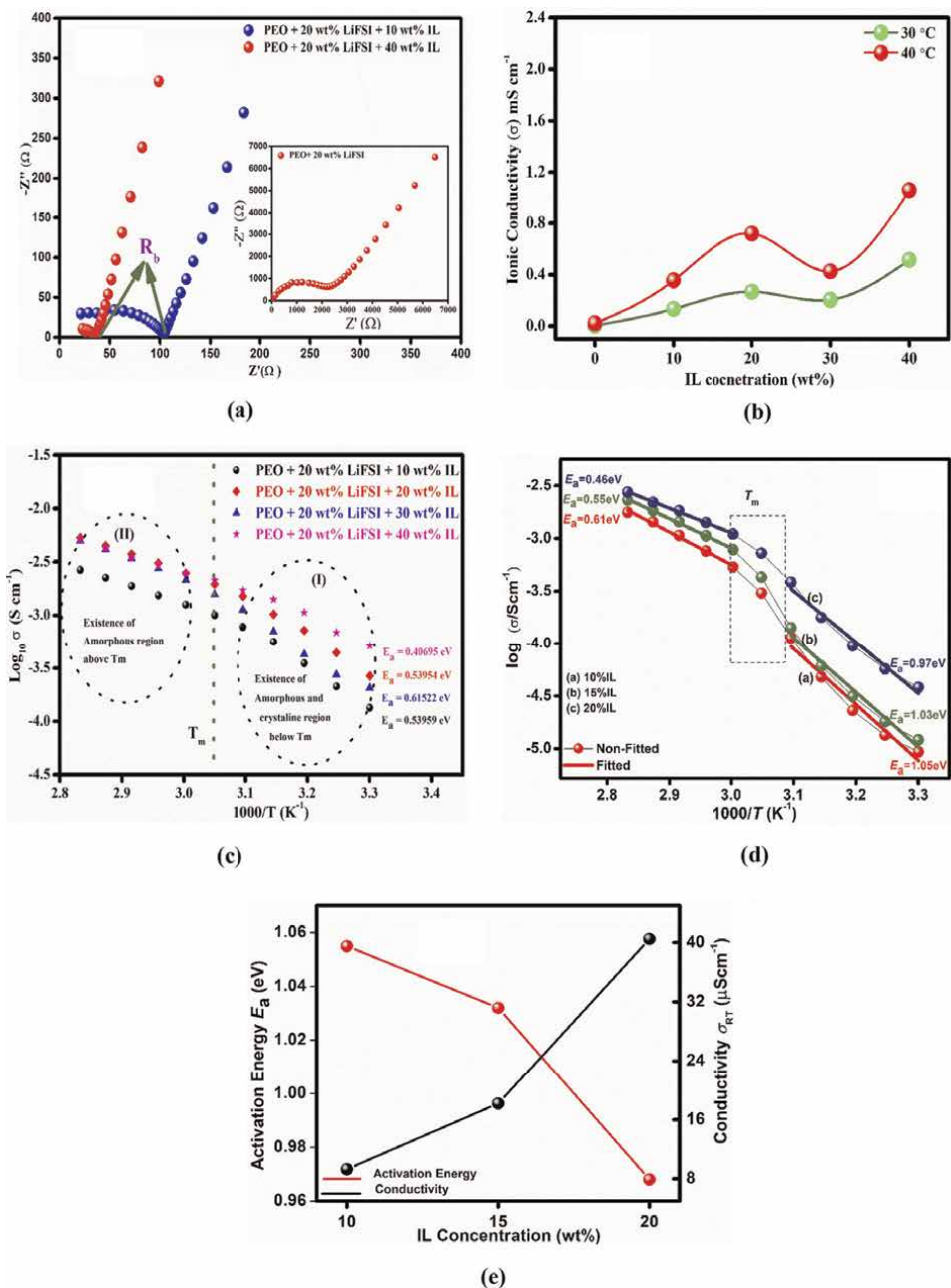


Figure 7. (a) Nyquist plot, (b) variation of conductivity with IL concentration at 30°C and 40°C and (c) Arrhenius plot of the cell SS/PEO + 20 wt.% LiFSI + X wt.% PP₃FSI/SS (X = 0, 10, 20, 30, 40) (d) temperature-dependent conductivity of polymer electrolytes PEO + 20 wt.% LiFSI + X wt.% IL (X = 10, 15, and 20) and (e) variation of conductivity (σ), and activation energy (E_a) with IL concentration.

the PEO + 20 wt.% LiFSI system, D_{Li^+} increases progressively and its maximum value is observed $\sim 1.32 \times 10^{-8} \text{ cm}^2 \text{ s}^{-1}$ for 40 wt.% IL containing polymer electrolyte as shown in the **Figure 8(c)**. This increase in D_{Li^+} value confirms the higher lithium-ion

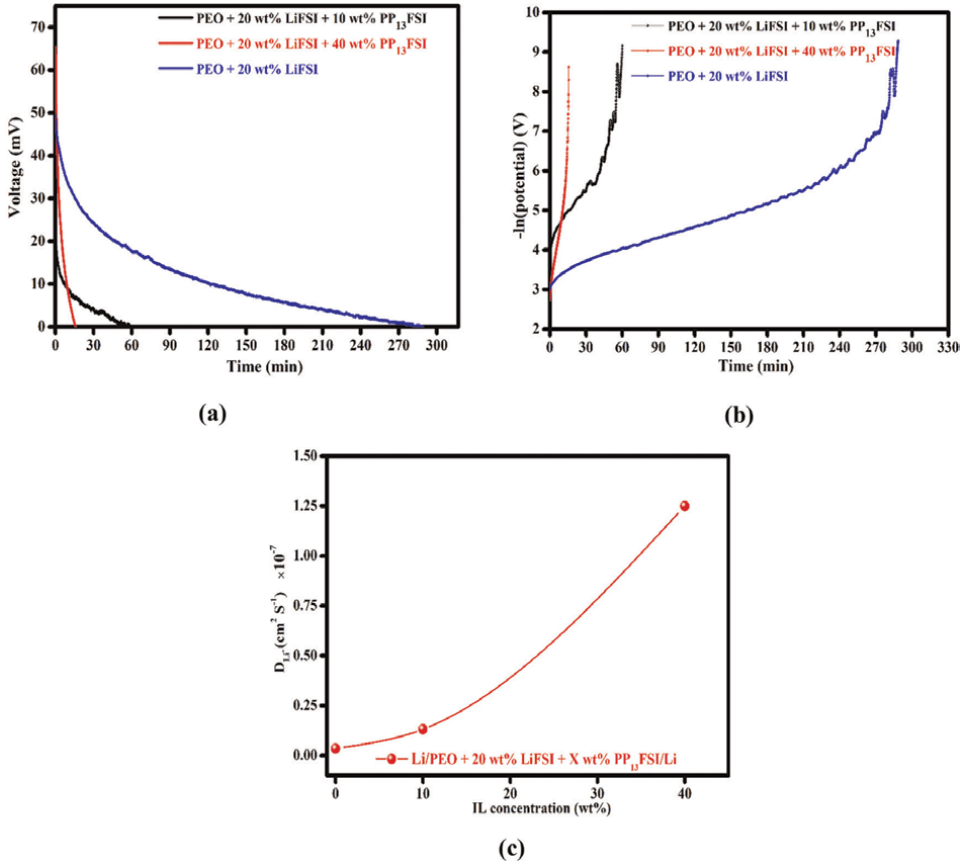


Figure 8. (a-b) Li^+ ion Diffusion coefficient measurement using RDM of the polarized cell Li/PEO + 20 wt.% LiFSI + X wt.% (0, 10, 40) PP₁₃FSI/Li shown by (c) Variation of Li^+ ion diffusion coefficient with respect to IL concentration.

conductivity which makes IL-based electrolyte system more suitable for Li-battery applications.

Besides that, IL also affects the lithium-ion transference number of polymer electrolyte system. Meghni et al. [8] have determined the Li-ion transference number by dc polarization technique. In this technique, IL-based polymer electrolyte is sandwiched between two Li-metal foils (Li/IL-based-PE/Li) and a small constant potential (0.1 V) is applied across this cell configuration for a fixed period of time and corresponding current is recorded with respect to time, as shown in **Figure 9(a)**. Also, the impedance plot is recorded before and after polarization (see **Figure 9(b)**). Authors have calculated the transference number of Li⁺ ion using the Bruce and Vincent' formula [45]:

$$t_{Li^+} = \frac{I_{ss}(\Delta V - I_0 R_0)}{I_0(\Delta V - I_{ss} R_{ss})} \quad (5)$$

Where I_{ss} and R_{ss} are the steady-state current and passive layer resistance after polarization and I_0 & R_0 are the initial current and passive layer resistance before polarization respectively.

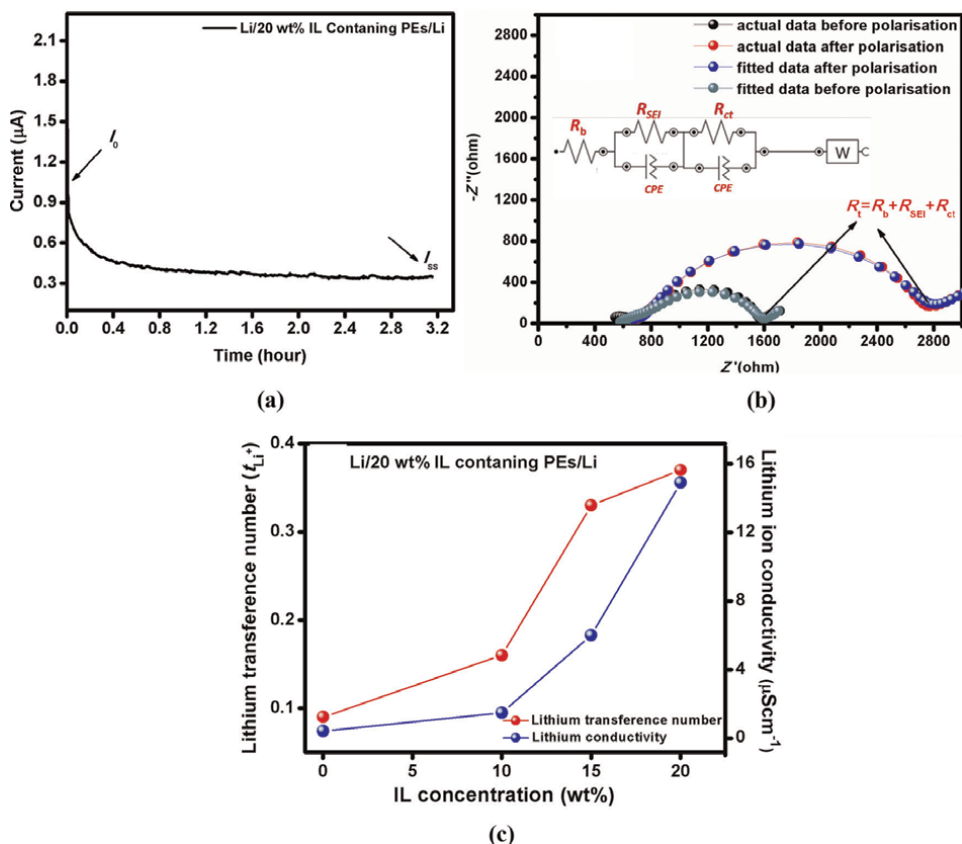


Figure 9. (a) dc polarization curve of cell (Li/20 wt.% IL containing PEs/Li) at the voltage 0.05 V, (b) Nyquist plot of the cell (Li/20 wt.% IL containing PEs/Li) before and after polarization and (c) Variation of Li^+ transference number and Li^+ ion conductivity with IL concentration.

From these studies they found that t_{Li^+} as well Li-ion conductivity both are increased with IL concentration and the maximum t_{Li^+} value is ~ 0.37 for 20 wt.% IL-containing polymer electrolyte as seen from **Figure 9(c)**.

Besides that, Baló et al. [34] also reported the same result for PEO + 20 wt.% LiTFSI + x wt.% EMIMTFSI (x = 0, 2.5, 5, 7.5, 10 and 12.5) IL-based polymer electrolyte system. They found that for PEO + 20 wt.% LiTFSI, t_{Li^+} is around 0.11 while on addition of IL it is reached to 0.16 for PEO + 20 wt.% LiTFSI + 2.5 wt.% EMIMTFSI and increases gradually on increasing the IL concentration and maximum value is found to be ~ 0.39 for PEO + 20 wt.% LiTFSI + 12.5 wt.% EMIMTFSI.

3.5 Effect of IL on the electrochemical stability window of polymer electrolyte

For application of IL-based polymer electrolyte in Li-battery, it is important to know the electrochemical stability window (ESW) of electrolyte. For this motive, Linear sweep voltammetry (LSV) technique is used. In this technique electrolyte is sandwiched between stainless steel electrode which work as reference electrode and Li-electrode which act as working electrode and current is record with respect to voltage. Meghni et al. [41] have observed the effect of IL on the ESW (**Figure 10**)

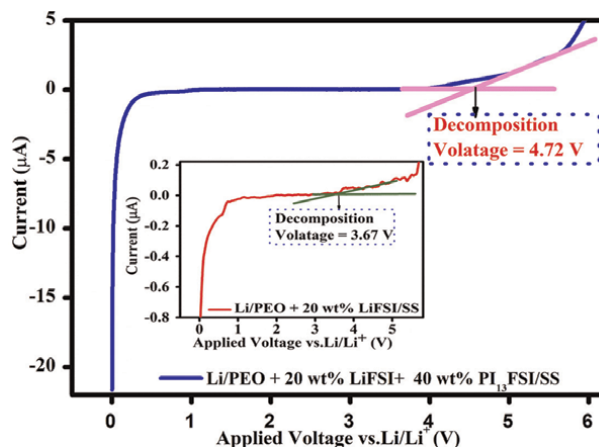


Figure 10. Linear sweep voltammetry measurement of Li/PEO + 20 wt.% LiFSI + X wt.% (0, 40) PP₁₃FSI/SS at scan rate ~ 0.05 mV/s.

and found that for polymer system PEO + 20 wt.% LiFSI without IL, the ESW is ~ 3.67 V vs. Li/Li⁺ [while for 40 wt.% IL containing polymer electrolyte, electrochemically stable window ~ 4.72 V vs. Li/Li⁺. From the above discussion, it can be seen that the presence of IL improves the electrochemical stability window of polymer system significantly which is good for high voltage Li-battery application.

4. Application of IL-based polymer electrolyte in Li-metal battery

In Li-battery, charging and discharging take place by means of electrochemical redox reaction. For Li-ion insertion and extraction during charging-discharging process, electrolyte is required. Electrolyte plays the crucial role in determining the Li-battery performance. Among the different type of electrolytes, IL-based polymer electrolytes have gained more attention due to its some unique properties such as high flexibility, wide ECW, good thermal and mechanical stability as well as high ionic conductivity.

IL-based polymer electrolyte which is most commonly known as gel-polymer electrolyte is widely used in Li-battery carries the hybrid properties of solid electrolyte with an embedded liquid electrolyte that is liquid electrolyte is embedded in the polymer matrix. Due to immobilization of electrolyte, enhanced ionic conductivity as well as wide ESW is achieved when compared to solid and liquid electrolytes. Also, it reduces the probability of short-circuiting due to stable solid-interphase formation (SEI) which reduces in turn the lithium-dendrite growth, there is ease of portability, safety issue of battery enhances due to no electrolyte leakage and absence of volatile reaction. Therefore, IL-based polymer electrolyte is attractive choice for Li-batteries. Among the alternative clean energy resources, Li-metal battery have gained more attention. They are widely used in the market such as portable electronic devices, electric vehicles (EVs), hybrid electric vehicles (HEVs), grid energy storage system and so on [46–48].

Furthermore, from safety point of view specially in lithium-metal battery (LMB), IL-based polymer electrolyte is widely used but still there needs to improve some

IL-based polymer electrolyte	Cathode	Current rate (C-rate)	Number of cycles	Specific discharge capacity (mAh/g)	Coulombic efficiency (%)	Reference
Poly(ionic liquid)s-based polymer electrolyte	$\text{LiNi}_{0.8}\text{Co}_{0.15}\text{Al}_{0.05}\text{O}_2$	0.05 C	20	123	>96	[49]
PEO-LiTFSI-PyT ₄ TFSI	$\text{LiNi}_{0.8}\text{Co}_{0.15}\text{Al}_{0.05}\text{O}_2$	C/15	35	125	~99.75	[50]
PEO + 20 wt.% LiFSI + 40 wt.% PP ₁₃ FSI	BiPO ₄ @NCA	0.2C	150	110	~99.96	[41]
PEO + LiFSI+7.5 wt.% EMIMFSI	LiFePO ₄	C/20	100	143	~100	[37]
PEO + 20 wt.% LiFSI+10 wt.% PYR ₁₃ FSI	GO coated LiFePO ₄	C/10	100	163	~99	[51]
PEO + 20 wt.% LiTFSI +10 wt.% EMIMFSI	LiFePO ₄	C/10	200	145	~100	[43]
PEO + 20 wt.% LiTFSI +10 wt.% EMIMFSI	NCA	C/10	200	175	~100	[43]
PEO + 20 wt.% LiTFSI+30 wt.% BMPyTFSI	LiFePO ₄	C/10	35	106	~100	[52]
P(EO) ₁₀ LiTFSI-PyR ₄ TFSI	LiFePO ₄	C/10	180	170 at 40 °C	~100	[53]
PEO ₂₀ LiTFS [PyT ₁₄ TFSI]	LiFePO ₄	C/10	450	140 at 40°C	~100	[54]
PEO ₂₀ LiTFSI [Pip ₁ .10ITFSI]	Li ₄ Ti ₅ O ₁₂	C/20	40	150	~100	[55]
PEO ₂₀ LiTFSI [Pip ₁ .10ITFSI]	LiFePO ₄	C/20	35	120	~100	[55]
PEO + 20 wt.% LiFSI +20 wt.% BMPyTFSI	NCA	C/5	125	137	~96	[8]
P(EO) ₂₀ LiTFSI + 1.27PP1.3LiTFSI	LiFePO ₄	C/10	20	120	~99	[36]
PEO + 20 wt.% LiTFSI+12.5 wt.% EMIMTFSI	LiMn ₂ O ₄	C/10	100	120	~100	[34]
PEO + 20 wt.% LiTFSI+20 wt.% BMIMTFSI	LiMn ₂ O ₄	C/10	25	90	~100	[30]

Table 2. Electrochemical performance of lithium metal batteries (LMBs) with IL-based polymer electrolytes.

parameters like internal resistance of the cell should be low and also cell must deliver maximum capacity with 100% coulombic efficiency and better capacity retention. For that purpose, IL-based polymer electrolytes having high ionic conductivity must be used in LMBs so that cell resistance as well as SEI layer resistance would be low. The performance of some of LMBs with IL-based polymer electrolytes are listed in **Table 2**.

Meghnani et al. [41] have reported the performance of lithium metal polymer battery (LMPB) using the synthesized IL-based polymer electrolyte, PEO + 20 wt.% LiFSI +40 wt.% PP₁₃FSI in the cell Li/PEO + 20 wt.% LiFSI +40 wt.% PP₁₃FSI/ Pristine NCA and Li/PEO + 20 wt.% LiFSI +40 wt.% PP₁₃FSI/BiPO₄@NCA configuration. In the cell configuration Li/pristine NCA, cell delivers a discharging capacity ~150 mAh. g⁻¹ at C/10 rate while Li/BiPO₄@NCA cell delivers the discharge capacity ~164 mAh. g⁻¹ at C/10 rate as shown in **Figure 11(a,b)**. Also, the coulombic efficiency of the cell Li/BiPO₄@NCA is found to be ~99.96% after 150 cycles and for the cell Li/pristine NCA, it is around ~91.68% as shown in **Figure 11(c,d)**.

Balo et al.[43] have studied the electrochemical performance of Li-battery using the IL based polymer electrolyte, PEO + 20 wt.% LiTFSI+10 wt.% EMIMFSI in the cell Li/ PEO + 20 wt.% LiTFSI+10 wt.% EMIMFSI /GO-LiFePO₄ and Li/PEO + 20 wt.% LiTFSI+10 wt.% EMIMFSI/NCA configuration. They found that the cell Li/GO-

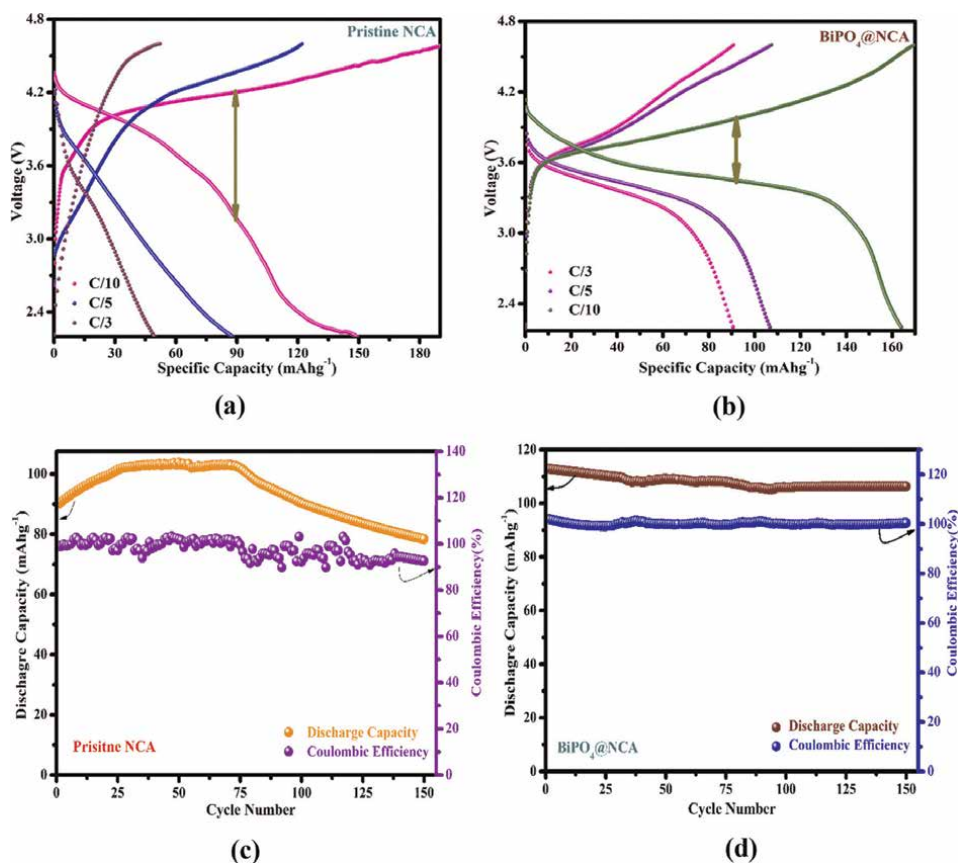


Figure 11. (a,b) charge-discharge curve and (c,d) cyclic stability of cell Li/PEO + 20 wt.% LiFSI + 40 wt.% PP₁₃FSI/Pristine NCA and Li/PEO + 20 wt.% LiFSI + 40 wt.% PP₁₃FSI/BiPO₄@NCA respectively.

LiFePO₄ delivers the maximum discharge capacity 145, 83, 38, 20 mAh/g at C/10, C/5 and 1 C and 2 C rate respectively (see **Figure 12(a)**). While another cell configuration Li/NCA delivers maximum discharge capacity 175, 168, 157, 150 mAh/g at C/10, C/5, 1 C and 2 C rate respectively (**Figure 12(c)**). When these cells are cycled at C/10 upto 200 cycles it is found that for cell Li/GO-LiFePO₄ in the initial few cycles discharge capacity is lower and it reaches to around ~145 mAh/g within the 10th cycle (see **Figure 12(b)**). However, 142 mAh/g capacity remains after 200th cycle. They have also calculated capacity fading per cycle (inset of **Figure 12(b)**). It is seen that it shows linear behavior and there is only 0.01% capacity loss per cycle. From the cyclic performance of the cell Li/NCA it was inferred that the discharge capacity is low (~126 mAh/g) in initial 6–7 cycles thereafter it value increases gradually and attains the maximum capacity ~175 mAh/g (see **Figure 12(d)**). However, after that, the capacity remains constant during the cycling process. The maximum discharge capacity and better cyclic stability with good coulombic efficiency of these two cells may be consistent with the higher lithium-ion conductivity of ionic liquid-based polymer electrolyte and lower interfacial resistance due to better contact with the electrode.

From the above discussion, it can be concluded that IL-based polymer electrolytes are most promising candidate for Li-metal polymer batteries.

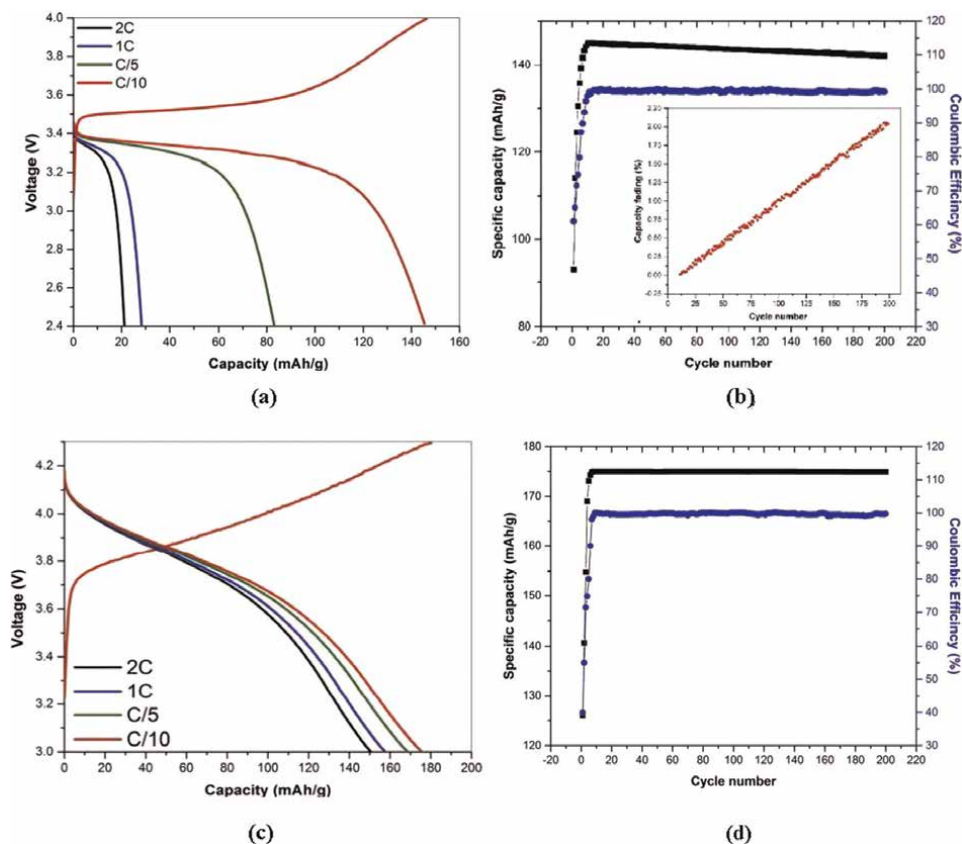


Figure 12.

(a, c) Charge-discharge curve and (b, d) cyclic performance of the cell Li/PEO + 20 wt.% LiTFSI+10 wt.% EMIMFSI/GO-LiFePO₄ and Li/PEO + 20 wt.% LiTFSI+10 wt.% EMIMFSI/NCA.

5. Conclusion


As we can see that electrolyte plays the crucial role in batteries performance. It not only acts as a separator between electrodes but also provides the path for ion transportation. Therefore, electrolyte should possess high ionic conductivity, wide electrochemical window, good thermal and mechanical stability. All these properties are embedded in ionic liquid-based gel polymer electrolyte. IL-based polymer electrolytes not only have high ionic conductivity but also are free from leakage problem, portability issue and short-circuiting problem which is usually faced in case of liquid electrolytes. The unique properties of IL-based polymer electrolytes proves its suitability for battery applications. For this reason, IL-based polymer electrolytes are widely used in Li-battery and it is found that IL-based polymer electrolyte with Li-metal shows better cyclic stability as well good coulombic efficiency. Thus, IL-based polymer electrolytes are most attractive choice for lithium metal polymer battery.

Author details

Dipika Meghnani and Rajendra Kumar Singh*
Ionic Liquid and Solid-State Ionics Lab, Department of Physics, Institute of Science,
Banaras Hindu University, Varanasi, India

*Address all correspondence to: rksingh_17@rediffmail.com;
rajendrasingh.bhu@gmail.com

IntechOpen

© 2022 The Author(s). Licensee IntechOpen. This chapter is distributed under the terms of the Creative Commons Attribution License (<http://creativecommons.org/licenses/by/3.0>), which permits unrestricted use, distribution, and reproduction in any medium, provided the original work is properly cited. 

References

- [1] Nitta N, Wu F, Lee JT, Yushin G. Li-ion battery materials: Present and future. *Materials Today*. 2015;**18**:252-264. DOI: 10.1016/j.mattod.2014.10.040
- [2] Megahed S, Ebner W. Lithium-ion battery for electronic applications. *Journal of Power Sources*. 1995;**54**: 155-162. DOI: 10.1016/0378-7753(94)02059-C
- [3] Tiwari RK, Singh SK, Gupta H, Srivastava N, Meghnani D, Mishra R, et al. Multifaceted ethylenediamine and hydrothermal assisted optimum reduced GO-nanosulfur composite as high capacity cathode for lithium-sulfur batteries. *Electrochemical Science Advances*. 2021; **2**:1-14. DOI: 10.1002/elsa.202100025
- [4] Srivastava N, Singh SK, Gupta H, Meghnani D, Mishra R, Tiwari RK, et al. Electrochemical performance of Li-rich NMC cathode material using ionic liquid based blend polymer electrolyte for rechargeable Li-ion batteries. *Journal of Alloys and Compounds*. 2020;**843**: 155615. DOI: 10.1016/j.jallcom.2020.155615
- [5] Mishra R, Singh SK, Gupta H, Srivastava N, Meghnani D, Tiwari RK, et al. Surface modification of nano Na [Ni_{0.60}Mn_{0.35}Co_{0.05}]O₂ cathode material by dextran functionalized RGO via hydrothermal treatment for high performance sodium batteries. *Applied Surface Science*. 2021;**535**: 147695. DOI: 10.1016/j.apsusc.2020.147695
- [6] Niu H, Wang L, Guan P, Zhang N, Yan C, Ding M, et al. Recent advances in application of ionic liquids in electrolyte of lithium ion batteries. *Journal of Energy Storage*. 2021;**40**:102659. DOI: 10.1016/j.est.2021.102659
- [7] Liu K, Wang Z, Shi L, Jungsuttiwong S, Yuan S. Ionic liquids for high performance lithium metal batteries. *Journal of Energy Chemistry*. 2021;**59**:320-333. DOI: 10.1016/j.jechem.2020.11.017
- [8] Meghnani D, Gupta H, Singh SK, Srivastava N, Mishra R, Tiwari RK, et al. Fabrication and electrochemical characterization of lithium metal battery using IL-based polymer electrolyte and Ni-rich NCA cathode. *Ionics (Kiel)*. 2020;**26**:4835-4851. DOI: 10.1007/s11581-020-03656-9
- [9] Gupta H, Balo L, Singh VK, Chaurasia SK, Singh RK. RSC Advances Effect of phosphonium based ionic liquid on structural, electrochemical and thermal behaviour. *RSC Advances*. 2016; **6**:87878-87887. DOI: 10.1039/C6RA20393K
- [10] Pandey GP, Kumar Y, Hashmi SA. Ionic liquid incorporated polymer electrolytes for supercapacitor application. *Indian Journal of Chemistry - Section A(IJCA)*. 2010;**49**:743-751
- [11] Chaurasia SK, Singh RK. Electrical conductivity studies on composite polymer electrolyte based on ionic liquid. *Phase Transitions*. 2010;**83**: 457-466. DOI: 10.1080/01411594.2010.491434
- [12] Shalu SK, Chaurasia RK, Chandra SS. Thermal stability, complexing behavior, and ionic transport of polymeric gel membranes based on polymer PVdF-HFP and ionic liquid, [BMIM][BF₄]. *The Journal of Physical Chemistry B*. 2013; **117**:897-906. DOI: 10.1021/jp307694q
- [13] Song JY, Wang YY, Wan CC, Open Access Library Song, Wang YY, Wan CC.

Review of gel-type polymer electrolytes for lithium-ion batteries. *Journal of Power Sources*. 1999;**77**:183-197. DOI: 10.1016/S0378-7753(98)00193-1. Available from: <http://www.oalib.com/references/9023829>

[14] Shalu, Singh VK, Singh RK. Development of ion conducting polymer gel electrolyte membranes based on polymer PVdF-HFP, BMIMTFSI ionic liquid and the Li-salt with improved electrical, thermal and structural properties. *Journal of Materials Chemistry C*. 2015;**3**:7305-7318. DOI: 10.1039/c5tc00940e

[15] Sakaebe H, Matsumoto H, Tatsumi K. Application of room temperature ionic liquids to Li batteries. *Electrochimica Acta*. 2007;**53**:1048-1054. DOI: 10.1016/j.electacta.2007.02.054

[16] Nakagawa H, Fujino Y, Kozono S, Katayama Y, Nukuda T, Sakaebe H, et al. Application of nonflammable electrolyte with room temperature ionic liquids (RTILs) for lithium-ion cells. *Journal of Power Sources*. 2007;**174**:1021-1026. DOI: 10.1016/j.jpowsour.2007.06.133

[17] Borgel V, Markevich E, Aurbach D, Semrau G, Schmidt M. On the application of ionic liquids for rechargeable Li batteries: High voltage systems. *Journal of Power Sources*. 2009;**189**:331-336. DOI: 10.1016/j.jpowsour.2008.08.099

[18] Lewandowski A, Świdarska-Mocek A. Ionic liquids as electrolytes for Li-ion batteries-An overview of electrochemical studies. *Journal of Power Sources*. 2009;**194**:601-609. DOI: 10.1016/j.jpowsour.2009.06.089

[19] Singh SK, Shalu L, Balo H, Gupta VK, Singh AK, Tripathi YL, et al. Singh, Improved electrochemical performance of EMIMFSI ionic liquid

based gel polymer electrolyte with temperature for rechargeable lithium battery. *Energy*. 2018;**150**:890-900. DOI: 10.1016/j.energy.2018.03.024

[20] Mishra R, Singh SK, Gupta H, Tiwari RK, Meghnani D, Patel A, et al. Polar β - Phase PVdF-HFP-based freestanding and flexible gel polymer electrolyte for better cycling stability in a Na battery. 2021;**35**:15153-15165. DOI: 10.1021/acs.energyfuels.1c02114

[21] Liu H, Yu H. Ionic liquids for electrochemical energy storage devices applications. *Journal of Materials Science and Technology*. 2019;**35**:674-686. DOI: 10.1016/j.jmst.2018.10.007

[22] Shin JH, Henderson WA, Passerini S. Ionic liquids to the rescue? Overcoming the ionic conductivity limitations of polymer electrolytes. *Electrochemistry Communications*. 2003;**5**:1016-1020. DOI: 10.1016/j.elecom.2003.09.017

[23] Tripathi AK, Singh RK. Application of Ionic Liquids as a Green Material in Electrochemical Devices. *Industrial Applications of Green Solvents*. 2019;**II** (54)106-147. DOI: 10.21741/9781644900314-6

[24] Eftekhari A, Liu Y, Chen P. Different roles of ionic liquids in lithium batteries. *Journal of Power Sources*. 2016;**334**: 221-239. DOI: 10.1016/j.jpowsour.2016.10.025

[25] Tsunashima K, Sugiya M. Physical and electrochemical properties of low-viscosity phosphonium ionic liquids as potential electrolytes. *Electrochemistry Communications*. 2007;**9**:2353-2358. DOI: 10.1016/j.elecom.2007.07.003

[26] Ishikawa M, Sugimoto T, Kikuta M, Ishiko E, Kono M. Pure ionic liquid electrolytes compatible with a graphitized carbon negative electrode in

- rechargeable lithium-ion batteries. *Journal of Power Sources*. 2006;**162**: 658-662. DOI: 10.1016/j.jpowsour.2006.02.077
- [27] Seki S, Ohno Y, Kobayashi Y, Miyashiro H, Usami A, Mita Y, et al. Imidazolium-based room-temperature ionic liquid for lithium secondary batteries. *Journal of the Electrochemical Society*. 2007;**154**:A173. DOI: 10.1149/1.2426871
- [28] Kalhoff J, Eshetu GG, Bresser D, Passerini S. Safer electrolytes for lithium-ion batteries: State of the art and perspectives. *ChemSusChem*. 2015;**8**: 2154-2175. DOI: 10.1002/cssc.201500284
- [29] Agostini M, Rizzi LG, Cesareo G, Russo V, Hassoun J. Characteristics of a graphene nanoplatelet anode in advanced lithium-ion batteries using ionic liquid added by a carbonate electrolyte. *Advanced Materials Interfaces*. 2015;**2**:1-7. DOI: 10.1002/admi.201500085
- [30] Singh VK, Shalu L, Balo H, Gupta SK, Singh RK. Singh, Solid polymer electrolytes based on Li + /ionic liquid for lithium secondary batteries. *Journal of Solid State Electrochemistry*. 2017;**21**:1713-1723. DOI: 10.1007/s10008-017-3529-z
- [31] Simonetti E, Carewska M, Di Carli M, Moreno M, De Francesco M, Appetecchi GB. Towards improvement of the electrochemical properties of ionic liquid-containing polyethylene oxide-based electrolytes. *Electrochimica Acta*. 2017;**235**:323-331. DOI: 10.1016/j.electacta.2017.03.080
- [32] Kumar Y, Hashmi SA, Pandey GP. Lithium ion transport and ion-polymer interaction in PEO based polymer electrolyte plasticized with ionic liquid. *Solid State Ionics*. 2011;**201**:73-80. DOI: 10.1016/j.ssi.2011.08.010
- [33] Gupta H, Shalu L, Balo VK, Singh SK, Chaurasia RK. Effect of phosphonium based ionic liquid on structural, electrochemical and thermal behaviour of polymer poly(ethylene oxide) containing salt lithium bis (trifluoromethylsulfonyl)imide. *RSC Advances*. 2016;**6**:87878-87887. DOI: 10.1039/c6ra20393k
- [34] L. Balo, Shalu, H. Gupta, V. Kumar Singh, R. Kumar Singh, Flexible gel polymer electrolyte based on ionic liquid EMIMTFSI for rechargeable battery application, *Electrochimica Acta*. 2017; **230**:123-131. DOI: 10.1016/j.electacta.2017.01.177
- [35] Cheng H, Zhu C, Huang B, Lu M, Yang Y. Synthesis and electrochemical characterization of PEO-based polymer electrolytes with room temperature ionic liquids. *Electrochimica Acta*. 2007;**52**: 5789-5794. DOI: 10.1016/j.electacta.2007.02.062
- [36] An Y, Cheng X, Zuo P, Liao L, Yin G. Improved properties of polymer electrolyte by ionic liquid PP1.3TFSI for secondary lithium ion battery. *Journal of Solid State Electrochemistry*. 2012;**16**: 383-389. DOI: 10.1007/s10008-011-1340-9
- [37] Balo L, Gupta H, Singh SK, Singh VK, Kataria S, Singh RK. Performance of EMIMFSI ionic liquid based gel polymer electrolyte in rechargeable lithium metal batteries. *Journal of Industrial and Engineering Chemistry*. 2018;**65**:137-145. DOI: 10.1016/j.jiec.2018.04.022
- [38] Singh VK, Shalu SK, Chaurasia RK. Singh, Development of ionic liquid mediated novel polymer electrolyte

membranes for application in Na-ion batteries. *RSC Advances*. 2016;**6**: 40199-40210. DOI: 10.1039/c6ra06047a

[39] Polu AR, Rhee HW. Ionic liquid doped PEO-based solid polymer electrolytes for lithium-ion polymer batteries. *International Journal of Hydrogen Energy*. 2017;**42**:7212-7219. DOI: 10.1016/j.ijhydene.2016.04.160

[40] Meghnani D, Gupta H, Singh SK, Srivastava N, Mishra R. Fabrication and electrochemical characterization of lithium metal battery using IL-based polymer electrolyte and Ni-rich NCA cathode. 2020;**26**:4835-4851.

[41] Meghnani D, Gupta H, Singh SK, Srivastava N, Mishra R, Tiwari RK, et al. Enhanced cyclic stability of LiNi_{0.815}Co_{0.15}Al_{0.035}O₂ cathodes by surface modification with bipo 4 for applications in rechargeable lithium polymer batteries. *ChemElectroChem*. 2021;**8**:2867-2880. DOI: 10.1002/celec.202100629

[42] Chaurasia SK, Singh RK, Chandra S. Dielectric relaxation and conductivity studies on (PEO:LiClO₄) polymer electrolyte with added ionic liquid [BMIM][PF₆]: Evidence of ion-ion interaction. *Journal of Polymer Science Part B: Polymer Physics*. 2011;**49**: 291-300. DOI: 10.1002/polb.22182

[43] Balo L, Gupta H, Singh SK, Singh VK, Tripathi AK, Srivastava N, et al. Development of gel polymer electrolyte based on LiTFSI and EMIMFSI for application in rechargeable lithium metal battery with GO-LFP and NCA cathodes. *Journal of Solid State Electrochemistry*. 2019;**23**:2507-2518. DOI: 10.1007/s10008-019-04321-6

[44] Ma Y, Doyle M, Fuller TF, Doeff MM, De Jonghe LC, Newman J. The measurement of a complete set of transport properties for a concentrated

solid polymer electrolyte solution. *Journal of the Electrochemical Society*. 1995;**142**:1859-1868. DOI: 10.1149/1.2044206

[45] Singh SK, Gupta H, Balo L, Shalu VK, Singh AK, Tripathi YL, et al. Electrochemical characterization of ionic liquid based gel polymer electrolyte for lithium battery application. *Ionics (Kiel)*. 2018;**24**:1895-1906. DOI: 10.1007/s11581-018-2458-x

[46] Cheng XB, Zhang R, Zhao CZ, Zhang Q. Toward safe lithium metal anode in rechargeable batteries: A review. *Chemical Reviews*. 2017;**117**: 10403-10473. DOI: 10.1021/acs.chemrev.7b00115

[47] Li Z, Huang J, Yann Liaw B, Metzler V, Zhang J. A review of lithium deposition in lithium-ion and lithium metal secondary batteries. *Journal of Power Sources*. 2014;**254**:168-182. DOI: 10.1016/j.jpowsour.2013.12.099

[48] Cheng XB, Zhang R, Zhao CZ, Wei F, Zhang JG, Zhang Q. A review of solid electrolyte interphases on lithium metal anode. *Advancement of Science*. 2015;**3**:1-20. DOI: 10.1002/adv.201500213

[49] Girard GMA, Wang X, Yunis R, Howlett PC, Forsyth M. Stable performance of an all-solid-state Li metal cell coupled with a high-voltage NCA cathode and ultra-high lithium content poly(ionic liquid)s-based polymer electrolyte. *Journal of Solid State Electrochemistry*. 2020;**24**: 2479-2485. DOI: 10.1007/s10008-020-04775-z

[50] Wetjen M, Kim GT, Joost M, Appetecchi GB, Winter M, Passerini S. Thermal and electrochemical properties of PEO-LiTFSI-Pyr 14TFSI-

based composite cathodes, incorporating 4 V-class cathode active materials. *Journal of Power Sources*. 2014;**246**: 846-857. DOI: 10.1016/j.jpowsour.2013.08.037

[51] Gupta H, Kataria S, Balo L, Singh VK, Singh SK, Tripathi AK, et al. Electrochemical study of Ionic Liquid based polymer electrolyte with graphene oxide coated LiFePO₄ cathode for Li battery. *Solid State Ionics*. 2018;**320**: 186-192. DOI: 10.1016/j.ssi.2018.03.008

[52] Gupta H, Shalu L, Balo VK, Singh SK, Singh AK, Tripathi YL, et al. Effect of temperature on electrochemical performance of ionic liquid based polymer electrolyte with Li/LiFePO₄ electrodes. *Solid State Ionics*. 2017;**309**: 192-199. DOI: 10.1016/j.ssi.2017.07.019

[53] Appetecchi GB, Kim GT, Montanino M, Alessandrini F, Passerini S. Room temperature lithium polymer batteries based on ionic liquids. *Journal of Power Sources*. 2011;**196**: 6703-6709. DOI: 10.1016/j.jpowsour.2010.11.070

[54] Kim GT, Appetecchi GB, Carewska M, Joost M, Balducci A, Winter M, et al. UV cross-linked, lithium-conducting ternary polymer electrolytes containing ionic liquids. *Journal of Power Sources*. 2010;**195**: 6130-6137. DOI: 10.1016/j.jpowsour.2009.10.079

[55] An Y, Cheng X, Zuo P, Liao L, Yin G. The effects of functional ionic liquid on properties of solid polymer electrolyte. *Materials Chemistry and Physics*. 2011; **128**:250-255. DOI: 10.1016/j.matchemphys.2011.03.007

Chapter 2

High Ionic Conductivities of Ionic Materials as Potential Electrolytes

*Pradip K. Bhowmik, Si L. Chen, Haesook Han,
Khairul Anwar Ishak, Thamil Selvi Velayutham,
Umama Bendaoud and Alfonso Martinez-Felipe*

Abstract

Ionic liquids (ILs) are salts consisting of organic cations and inorganic/organic anions having melting transitions lower than 100°C. They hold promise as engineered materials in a variety of modern fields. They are used as green solvents or catalysts for chemical reactions, biocatalysts, biopolymers processing, active pharmaceutical ingredients in medicine, even as electrolytes for batteries. For batteries applications, ionic liquids must have high ionic conductivity, but most of the ionic liquids (monocationic) have low conductivities. To address this limitation, we describe in this chapter dicationic ionic liquids based on extended viologens. The colossal conductivities, $\sigma_{dc} \sim 10^{-1.5} \text{ S cm}^{-1}$ of new diatonic ionic liquids in the same range of benchmark materials/electrolytes applied in fuel cells and batteries is reported. The relatively new class of ionic liquids consist of extended viologen bistriflimides containing oligoethyleneoxy groups were prepared via Zincke reaction under mild conditions and are excellent candidates as components in devices for energy conversion and storage applications. The synthesis and ionic conductivities of other ionic liquids and dicationic organic salts will be contrasted with dicationic ionic liquids in this chapter.

Keywords: extended viologens, ionic liquids, Zincke salt, dicationic ionic liquid crystals, ionic conductivity, dielectric impedance spectroscopy

1. Introduction

Ionic liquids (ILs) are salts consisting of organic cations and inorganic/organic anions having melting transitions (T_m) lower than 100°C, and even below ambient temperatures, and with cryogenic glass transition temperatures (T_g). ILs can be engineered for a variety of modern applications, including green solvents or catalysts [1, 2], biocatalysts [3], biopolymers [4–7], pharmaceutical ingredients [8], and electrolytes for batteries [9–11]. Despite they were discovered over 30 years ago, interest by researchers and industrialists in ILs continues to grow due to their versatility.

The introduction of multiple charges in low-molar ionic liquids and poly(ionic liquid)s widens the range of physical properties, leading to improvements in density, surface tension and viscosity, facilitated by their higher molecular weights [12, 13]. The large charge densities and electrostatic interactions normally increase the ILs

thermal stabilities [14, 15] and electrical capacities [16, 17], and results in better performance as antimicrobial agents [18] and stationary phases for gas chromatography [19], among others [20, 21].

Multi-charged ILs are particularly attractive as electrolytes used in energy storage and conversion materials and devices, due to their combination of low viscosity (like traditional ILs) and high ionic conductivity (like poly(ionic liquid)s). The physical properties of multi-charged ILs can be fine-tuned by combining different cations and anions, with well-defined chemical structures that avoid polydispersity issues. Current multi-charged ILs include ammonium, phosphonium, imidazolium, pyridinium, pyrrolidinium, piperidinium, triazolium and 4,4'-bipyridinium (viologen) cations, but the perspectives for new and tailored materials are almost unlimited.

In this chapter, we showcase the potential of three series of different ionic liquids as electrolytes in energy applications, by correlating their ionic conductivities to structural effects.

2. Conductivity measurements

The conductivity of the ionic liquids was studied by impedance spectroscopy [22]. Small amounts (few mg) of molten samples were inserted into commercial indium tin oxide (ITO) cells, *via* capillary method (Instec Inc.). The parallel capacitance C_p and the dielectric loss tangent ($\tan(\delta) = \frac{\epsilon''}{\epsilon'}$, where ϵ'' is the dielectric loss factor, and ϵ' the dielectric modulus) were measured in frequency sweeps ranging between $f = 0.1$ Hz and 10^6 Hz, and at different temperatures. Two instruments were used and combined for these impedance measurements: a laboratory-made dielectric spectrometer (10^{-1} – 10^4 Hz) and a commercial impedance analyser (Agilent 4294A) (10^2 – 10^6 Hz). The results were analysed in terms of the complex permittivity, $\epsilon^*(\omega) = \epsilon' - j\epsilon''$, and conductivity, $\sigma^*(\omega) = \sigma' - j\sigma''$, where $\sigma' = \omega\epsilon_0\epsilon''$ and $\sigma'' = \omega\epsilon_0\epsilon'$ with $\omega = 2\pi f$ is the angular frequency ($\text{rad}\cdot\text{s}^{-1}$).

3. Results: materials preparation and conductivity

We have prepared and assessed three series of dicationic salts as novel ionic liquid electrolytes: dicationic stilbazolium salts, dicationic asymmetric viologens, and dicationic ionic liquids. Our general strategy for their synthesis is based on quaternization by S_N^2 aka Menshutkin reactions, followed by metathesis of anions [12–21, 23].

3.1 Dicationic stilbazolium salts and their ionic conductivities

The dicationic stilbazolium salts (I-1 – I-4) were prepared by the reaction of *trans*-4-octyloxy-4-stilbazole with α,ω -methylene ditosylates by S_N^2 , followed by metathesis reaction of the corresponding ditosylates salts with lithium triflimide salt to yield the dicationic stilbazolium bistriflimide salts (II-1– II-4), as shown in **Figure 1**. The detailed synthetic procedures were described elsewhere [24]. Their chemical structures were established by using ^1H , ^{13}C and ^{19}F nuclear magnetic resonance (NMR) spectra and elemental analysis [24].

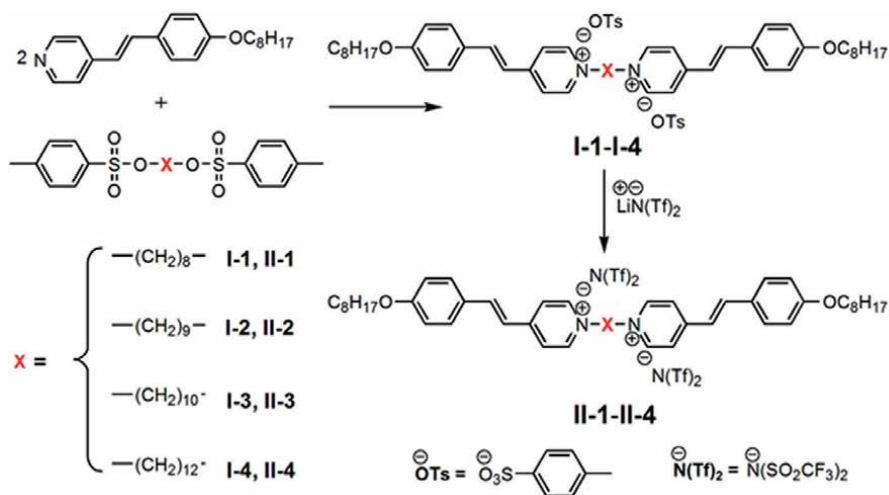


Figure 1.
 Synthesis of dicationic stilbazolium dicationic salts containing bistosylate and bistriflimide counterions.

Despite the presence of mesogenic units, these salts do not display mesomorphic properties, and instead solely exhibit crystalline polymorphism, confirmed by the presence of several peaks in the differential scanning calorimetric thermograms (DSC), **Figure 2**.

We found that the salts containing tosylate ions (**I-*n***) display stronger dielectric response than the triflimide analogues (**II-*n***, see **Figure 3(a)**), and show more complex profiles, associated to the additional aromatic groups. All these dielectric relaxations promote short-range conductivity in the salts, see **Figure 3(b)**, associated to local displacements of the charges. Despite the strong ϵ'' response, the tosylate salts did not develop signs of direct conductivity (σ_{dc}) in the range of temperatures and frequencies under study. We hypothesise that the presence of bulky aromatic groups may hinder long-range transport of ionic charges in these compounds. The triflimide salts, alternatively, show DC values that reach the $10^{-4.5} \text{ S}\cdot\text{cm}^{-1}$ range in the isotropic

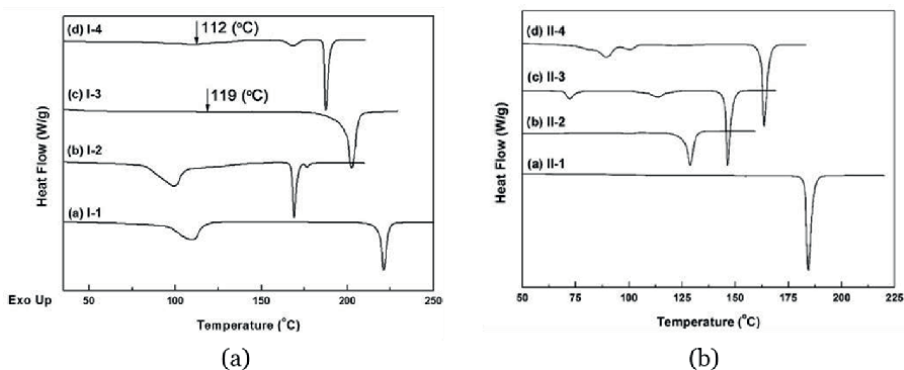


Figure 2.
 Differential scanning calorimetry thermograms (DSC) obtained on heating at $10^\circ\text{C}\cdot\text{min}^{-1}$ for the bistosylate (a) and bistriflimide (b) salts.

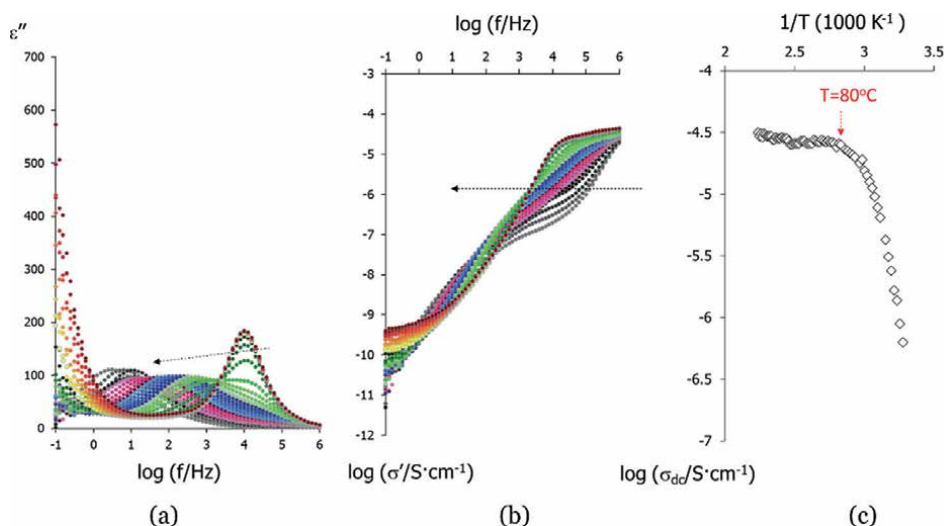


Figure 3. Dielectric results obtained from the impedance frequency sweeps of dicationic stilbazolium salts: (a) dielectric loss factor, ϵ'' and (b) real component of the complex conductivity, σ' of **II-3**; (c) Arrhenius plots for the direct current conductivity (σ_{dc}) obtained for **II-4**.

phase, see **Figure 3c**), but then fall rapidly following a Vogel- Fulcher-Tammann, VFT, profile [24–26].

These correlations between conductivity and structure highlight that the transport of ionic charges in these salts may require an amorphous environment, even if they involve short molecular range. The strong temperature dependence of σ_{dc} also confirms that the conductivity response is strongly coupled to segmental viscous-like motions.

3.2 Dicationic asymmetric viologens, **6BPn(s)**

The synthesis of asymmetric viologens with hexyl terminal groups and different alkyl chain lengths, and their synthetic routes are shown in **Figure 4**. The detailed synthetic procedures were described elsewhere, and their chemical structures were determined by using ^1H , ^{13}C and ^{19}F NMR spectra and elemental analysis [27].

The **6BPn(s)** exhibit Smectic T phases in a broad range of temperatures, including room temperature, confirmed by polarised optical microscopy and X-ray diffraction, see **Figure 5**.

The **6BPn(s)** undergo one main dielectric relaxation, **Figure 6(a)**, associated to the rotation of the molecular core, and high frequency conductivity, **Figure 6(b)**, related to short-range triflate ion-hopping. The materials reach direct current conductivities (σ_{dc}) in the 10^{-5} to 10^{-3} S cm^{-1} range, **Figure 6(c)**, which are very promising for organic media. These dielectric processes depict a clear Vogel-Fulcher-Tammann (VFT) behaviour, indicating that the dielectric and conductivity response of these LCIs is strongly coupled to segmental-type motions [27].

3.3 Dicationic extended viologens and their ionic conductivities

The dicationic extended viologens **1–3** were prepared according to the **Figure 7** (vide infra). The 4-oligoethyleneoxyphenylanilines were prepared according to

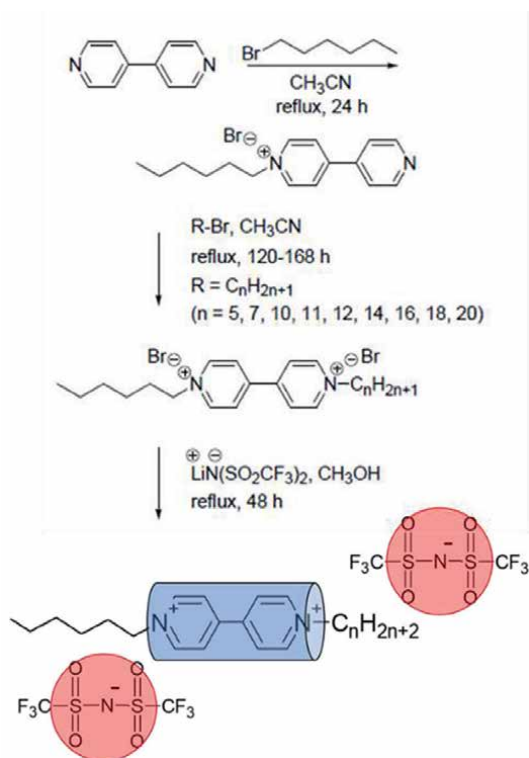


Figure 4. Synthetic routes for the asymmetric viologen bistriflimide salts of a 4,4'-bipyridinium core (BP) alkylated with hexyl group with $n = 5, 7, 10, 11, 12, 14, 16, 18$ and 20 .

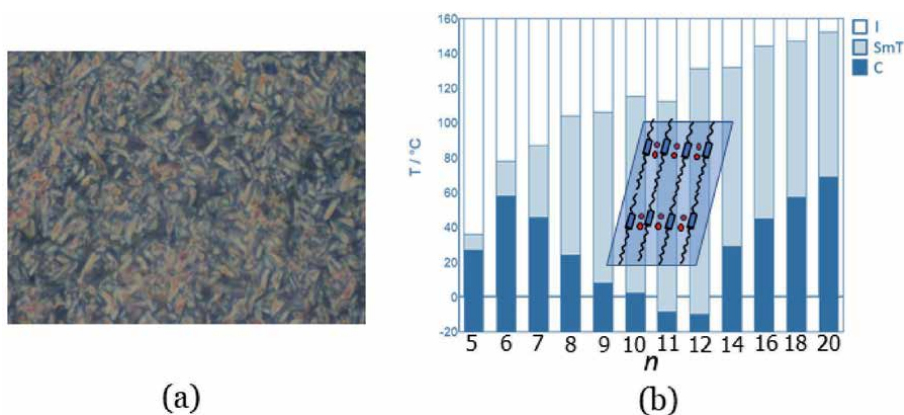


Figure 5. (a) Photomicrograph of **6BP16** obtained under the polarised optical microscope, showing the SmT phase; (b) phase diagram of the **6BPn(s)** as a function of terminal chain, n , showing a sketch of a proposed SmT structure.

modified literature procedures step 1 and step 2 [28, 29]. The synthesis of bis-(4-oligoethyleneoxyphenyl)-4,4'-bipyridinium dichlorides (**P1-P3**) with different ethyleneoxy groups is also summarised in **Figure 7**. The synthetic routes involved: (i) the aromatic nucleophilic substitution between the 1-chloro-2,4-dinitrobenzene

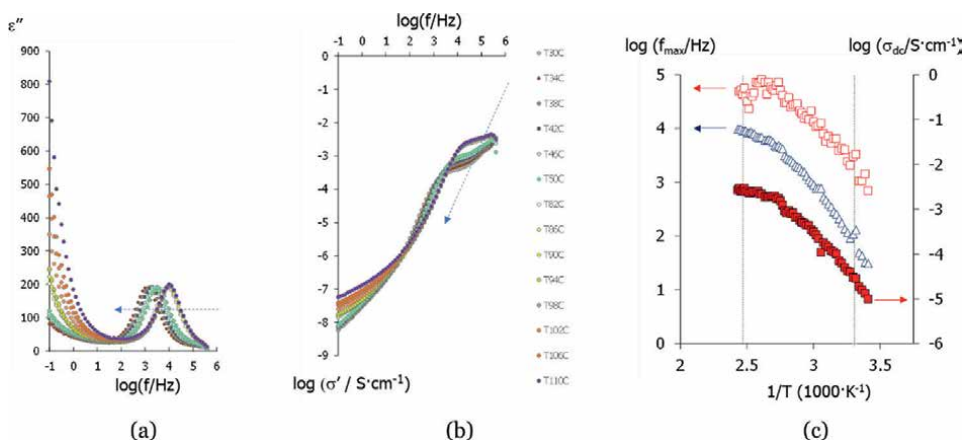


Figure 6.

Dielectric results obtained from the impedance frequency sweeps of **6BP14**: (a) dielectric loss factor, ϵ'' ; (b) real component of the complex conductivity, σ' ; (c) Arrhenius plots for the frequency dependence of ϵ'' and σ' maxima, and direct current conductivities (σ_{dc}).

and 4,4'-bipyridine in acetonitrile on heating to reflux, to yield the so-called Zincke salts [30, 31] (step 3); and (ii) subsequent anionic ring opening and ring closing reactions (ANROC) with the corresponding 4-oligoethyleneoxyphenylanilines, in N,N-dimethylacetamide (DMAc) at room temperature (step 4). Lastly, **P1-P3** were converted to **1-3** by metathesis with lithium triflimides in methanol [32] (step 5). Detailed synthetic procedures and analyses are also given elsewhere [33]. The chemical structures of the intermediates and final products were confirmed by their Fourier-transform infrared (FT-IR) spectra, ^1H , ^{13}C , and ^{19}F spectra in CD_3OD and their purity was determined by elemental analysis [33]. To our knowledge, these are the first examples of ionic liquids prepared *via* Zincke reactions.

Thermogravimetric analysis (TGA), differential scanning calorimetry (DSC), and polarised optical microscopy (POM) were used to determine the thermal properties and phase behaviour of these salts. The three salts' degradation temperatures, T_d , range from ~ 311 to 334°C , with less than 5% weight loss up to 300°C in nitrogen [33]. Although it was anticipated that bistriflimide ions would impart high thermal stabilities, the high T_d values demonstrate that the presence of flexible oxyethylene groups has no destabilising effect on these salts.

The DSC thermograms of salts **1** and **2** exhibit first-order endotherms associated with crystal-to-crystal (**2**) and melting (**1** and **2**) processes, whereas salt **3** only exhibits a low-temperature glass transition ($T_g = -6^\circ\text{C}$) [1–11, 34, 35]. Both **1** and **2** melt upon heating as expected where the increase in the oxyethylene termination length reduces the melting point. Due to inhibition of crystallisation at sufficiently long ethyleneoxy chains, $n = 3$, the absence of first-order transitions in the corresponding thermogram indicates that **3** behaves like an amorphous salt. In subsequent heating and cooling scans, there are no additional thermal events visible for **1** and **2**, suggesting that crystallisation of these samples must be a slow process. The absence of liquid crystal behaviour in these salts, contrasts with the recent report of smectic phases by analogous alkoxy-terminated ($n \geq 6$) viologens (see **Figure 8**) [32] and others [36–38]. Even though comparable lengths of terminal chains would have been expected to promote microphase separation and smectic behaviour in **1-3**, the formation of stronger interactions by the ethyleneoxy

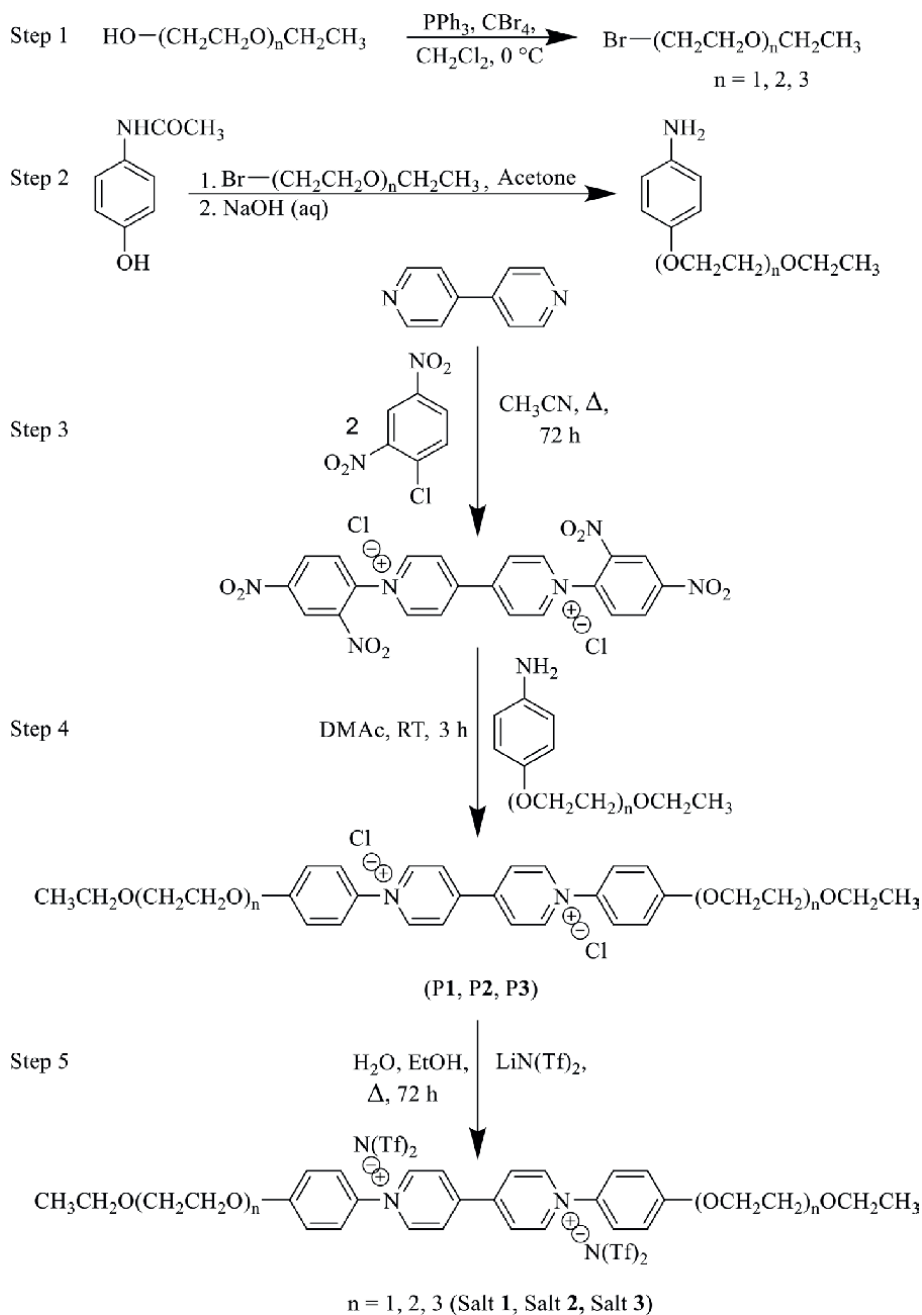


Figure 7. Multiple steps for the synthesis of the ionic liquids and salts 1–3.

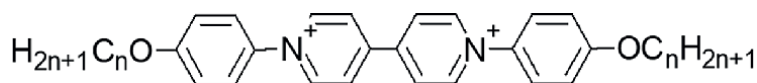


Figure 8. General chemical structures of alkoxy-terminated viologens [32].

groups may limit the local mobility required to yield liquid crystallinity. The effect of terminal chain lengths on nanosegregation between polar chains and aromatic cores in similar viologens is being studied further.

Viologens and their countless derivatives have already been proposed as potential redox active functional materials for use in electrochromic devices, diodes and transistors, memory devices, molecular machines, and dye-sensitised solar cells [39–41]. The incorporation of the oxyethylene(s) terminations is warranted for not one but two distinct reasons. On the one hand, one of our goals is to reduce (at least partially) the rigidity of the four-ring phenyl core (which could increase viscosity). On the other hand, the presence of polar chains can help delocalize the triflimide anions and avoid complexation, both of which would inhibit ion mobility [42]. This is because polar chains have a higher dipole moment.

Figure 9 shows the dielectric and conductivity response of the extended viologens **1–3** as a function frequency measured at room temperature. The complex permittivity and conductivity values of these salts have been found to be extraordinarily high due to the highly polar nature of ionic liquids and salts [33]. The ϵ'' plot demonstrates a linear increase (with slopes of -1) at sufficiently lower frequencies representing the increase in direct current (DC) conductivity [43]. This DC component dominates any potential dielectric relaxation, despite the presence of peaks in the salts **1** in **Figure 9(a)**. The third salt has the highest conductivity values of the three salts. The formation of plateaus in the double logarithmic σ' versus f plots in **Figure 9(b)** [22] confirms the existence of DC conductivity. The exemplary temperature plot of complex permittivity (ϵ^*) and conductivity (σ^*) of salt **2** is shown

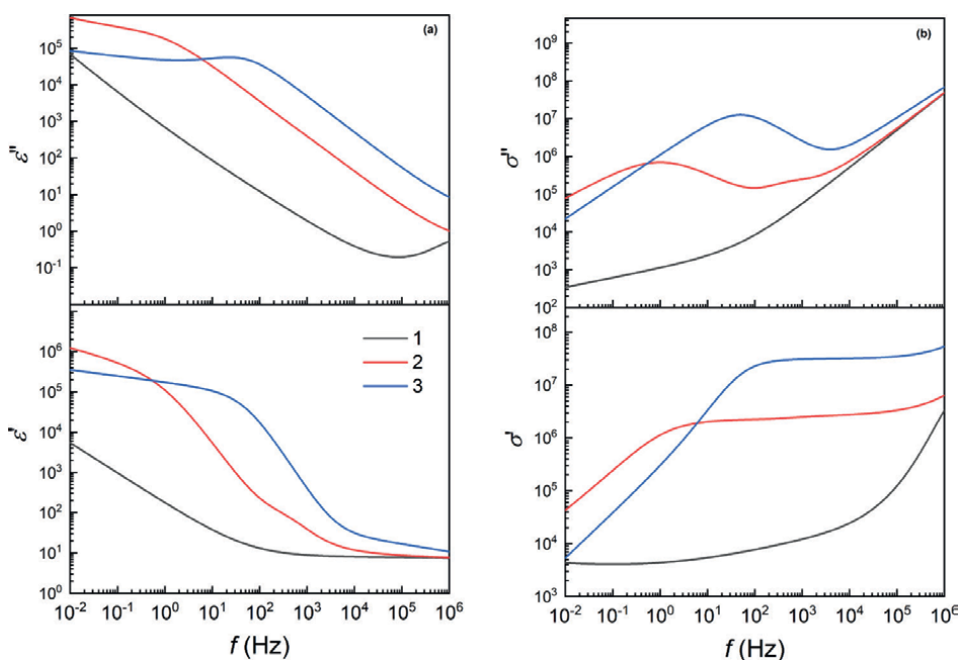


Figure 9. Complex permittivity (a) and conductivity (b) obtained for compounds **1**, **2** and **3** measured at room temperature.

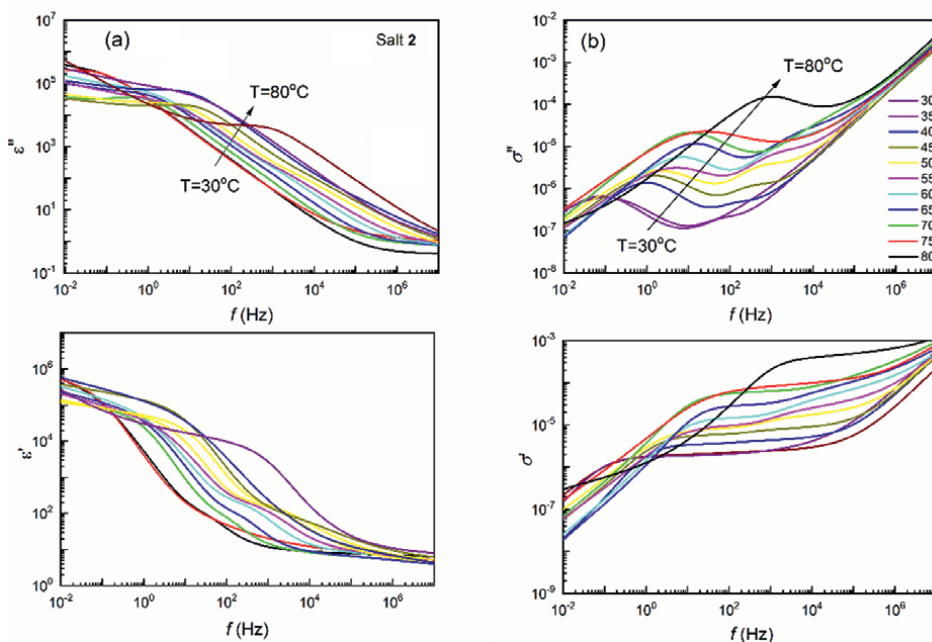


Figure 10. Complex permittivity (a) and conductivity (b) obtained for compounds **2** measured on heating from 30°C (see the arrow).

in **Figure 10**. The DC conductivity values, σ_{dc} , are estimated by extrapolating the constant σ' ranges to $f \rightarrow 0$ at various temperature. The resulting Arrhenius plots (not shown here) were used to evaluate the activation energy E_a of the conductivity process using the equation; $\sigma_{dc} = \sigma_0 \exp(E_a/RT)$, where R is the gas constant, $8.31 \text{ J} \cdot \text{mol}^{-1} \cdot \text{K}^{-1}$, T is the absolute temperature, and σ_0 is a pre-exponential term. Salts **1** and **2** have activation energies of 95.9 kJ/mol and 84.5 kJ/mol , respectively. These values are significantly higher for locally activated processes and are consistent with the occurrence of so-called β -relaxations, which involve the rotation of rod-like molecules (extended viologen moieties) within the crystal lattice around their long axis [33, 44]. When the $-(\text{CH}_2\text{CH}_2\text{O})-$ terminal chains are short, it appears that the motions around the bulky four-phenyl core dominate (and partially hinder) the conductivity process [43, 45–47]. On the other hand, salt **3** shows exceptional σ_{dc} values ($\sim 10^{-1.5} \text{ S/cm}$) comparable to the bench electrolytes used in fuel cells [48] and batteries [49]. Longer ethyleneoxy terminal chains enhance conductivity in salts by a plasticizing effect, thereby promoting ionic motions in the material. Moreover, salt **3** is one of the few examples of an organic salt with such large conductivities under anhydrous conditions and at temperatures close to room temperature [9, 50–54]. The formation of a rubbery phase above its low glass transition $T_g - 6^\circ\text{C}$ (from DSC measurement) with large free volumes that facilitate ionic motion can explain the higher σ_{dc} values observed for **3** within the series [55, 56]. In this molten-like state, conductivity has very weak temperature dependence [57–59]. The ionic liquids **1** and **2**, on the other hand, remain in a glassy state throughout the temperature range under study, and the σ_{dc} values are lower.

4. Conclusions

We have prepared new viologens by using Zincke reactions, which led to the formation of ionic liquids and salts with strong dielectric responses. Our results confirm that a fine balance between local/charge interactions and mobility is needed to optimise phase behaviour and conductivity of the ionic liquids. In general terms, the formation of amorphous, liquid crystalline, or crystal phases, can be tuned by the aspect ratio of the rigid core and the flexible terminations.

Whilst compounds having alkyl terminations still fall some orders of magnitude below those exhibited by reference phosphonium or imidazolium-based ionic liquid electrolytes (10^{-2} S·cm⁻¹) [60, 61], we found that the presence of oxyethylene groups promotes high conductivities in the $10^{-1.5}$ S·cm⁻¹ range, comparable to those required in commercial batteries or fuel cells [48, 49]. The presence of additional polar sites in these terminations may be the key to facilitate long-range transport in these materials. Interestingly, the presence of tosylate ions with a strong dielectric response does not promote long-range conductivity, and triflimide ions appear to be more suitable for ionic transport. Delocalisation of the charges can therefore be a key enabler for high σ_{dc} values.

These results highlight the potential use of these and other ionic liquids in energy devices such as fuel cells, batteries, supercapacitors, or solar cells. By extending the central rigid core, exchanging different cations, or modifying the composition and length of the terminations, this work opens new avenues for the design of ionic liquids with tuned electrostatic interactions and nanostructures.

Acknowledgements

We sincerely acknowledge Dr. Kousaalya Bakthavatchalam for critically reading and making insightful suggestions for the improvement of the article. TSV acknowledges the Ministry of Higher Education under the Fundamental Research Grant Scheme [FRGS/1/2018/STG07/UM/02/6] for the financial support. AMF would like to thank the Carnegie Trust for the Universities of Scotland, for the Research Incentive Grant RIG008586, the Royal Society and Specac Ltd. for the Research Grant RGS\R1\201397, the Royal Society of Edinburgh and the Scottish Government for one Sapphire project, and the Royal Society of Chemistry for the award of a mobility grant (M19-0000). UB thanks the School of Engineering (University of Aberdeen) for the award of one Summer Scholarship.

Conflict of interest

The authors declare no conflict of interest.

Author details

Pradip K. Bhowmik^{1*}, Si L. Chen¹, Haesook Han¹, Khairul Anwar Ishak²,
Thamil Selvi Velayutham³, Umama Bendaoud⁴ and Alfonso Martinez-Felipe⁴

1 Department of Chemistry and Biochemistry, University of Nevada Las Vegas,
Las Vegas, NV, USA


2 Faculty of Science, Institute of Biological Sciences, Universiti Malaya,
Kuala Lumpur, Malaysia

3 Faculty of Science, Department of Physics, Low Dimensional Materials Research
Centre, Universiti Malaya, Kuala Lumpur, Malaysia

4 Chemical Processes and Materials Research Group, School of Engineering, Centre
for Energy Transition, King's College, University of Aberdeen, Old Aberdeen, UK

*Address all correspondence to: pradip.bhowmik@unlv.edu

IntechOpen

© 2022 The Author(s). Licensee IntechOpen. This chapter is distributed under the terms of the Creative Commons Attribution License (<http://creativecommons.org/licenses/by/3.0>), which permits unrestricted use, distribution, and reproduction in any medium, provided the original work is properly cited. 

References

- [1] Welton T. Room-temperature ionic liquids. Solvents for synthesis and catalysis. *Chemical Reviews*. 1999;**99**:2071-2084
- [2] Kar M, Plechkova NV, Seddon KR, Pringle JM, MacFarlane DR. Ionic liquids –further progress on the fundamental issues. *Australian Journal of Chemistry*. 2019;**72**:3-10
- [3] Sheldon RA. Biocatalysis in ionic liquids: State-of-the union. *Green Chemistry*. 2021;**23**:8406-8427
- [4] Swatloski RP, Spear SK, Holbrey JD, Rogers RD. Dissolution of cellulose in ionic liquids. *Journal of the American Chemical Society*. 2002;**124**:4974-4775
- [5] Zhang ZR, Song JL, Han BX. Catalytic transformation of lignocellulose into chemical and fuel products in ionic liquids. *Chemical Reviews*. 2017;**117**:6834-6880
- [6] Ren F, Wang J, Xie F, Zan K, Wang S, Wang S. Applications of ionic liquids in starch chemistry: A review. *Green Chemistry*. 2020;**22**:2162-2183
- [7] Shukla SK, Mikkola J-P. Use of ionic liquids in protein and DNA chemistry. *Frontiers Chemistry*. 2020;**8**:598662
- [8] Egorova KS, Gordeev EG, Ananikov VP. Biological activity of ionic liquids and their applications in pharmaceuticals and medicine. *Chemical Reviews*. 2017;**117**:7132-7189
- [9] Watanabe M, Thomas ML, Zhang SG, Ueno K, Yasuda T, Dokko K. Application of ionic liquids to energy storage and conversion materials and devices. *Chemical Reviews*. 2017;**117**:7190-7239
- [10] Yang QW, Zhang ZQ, Sun XG, Hu YS, Xing HB, Dai S. Ionic liquids and derived materials for lithium and sodium batteries. *Chemical Society Reviews*. 2018;**47**:2020-2064
- [11] Yu LP, Chen GZ. Ionic liquid-based electrolytes for supercapacitor and supercapattery. *Frontiers in Chemistry*. 2019;**7**:272
- [12] Guglielmero L, Mezzetta A, Guazzelli L, Pomelli CS, D'Andrea F, Chiappe C. Systemetic synthesis and properties evaluation of dicationic ionic liquids, and a glance into potential new field. *Frontier in Chemistry*. 2018;**6**:612
- [13] Ikeda T. Facile synthesis of tetra-branched tetraimidazolium and tetrapyrrolidinium ion liquids. *ACS Omega*. 2021;**6**:19623-19628
- [14] Ferdeghini C, Guazzelli L, Pometti CS, Ciccioli A, Brunetti B, Mezzetta A, et al. Synthesis, thermal behavior and kinetic study of N-morpholinium dicationic ionic liquids by thermogravimetry. *Journal of Molecular Liquids*. 2021;**332**:115662
- [15] Clarke CJ, Morgan PJ, Hallett JP, Licence P. Linking the thermal and electronic properties of functional dicationic salts with their molecular structures. *ACS Sustainable Chemistry and Engineering*. 2021;**9**:6224-6234
- [16] Matsumoto M, Shimizu S, Sotoike R, Watanabe M, Iwasa Y, Itoh Y, et al. Exceptionally high electric double layer capacitances of oligomeric ionic liquids. *Journal of the American Chemical Society*. 2017;**139**:16072-16075
- [17] Maruyama Y, Marukane S, Morinaga T, Homma S, Kamijo T, Shomura R, et al. New design of polyvalent ammonium salts for a

- high-capacity electric double layer capacitor. *Journal Power Sources*. 2019;**412**:18-28
- [18] Pernak J, Skrzypezak A, Lota G, Frackowiak E. Synthesis and properties of trigeminal tricationic ionic liquids, Chemistry – A. *European Journal*. 2007;**13**:3106-3112
- [19] Patil RA, Talebi M, Sidisky LM, Berthod A, Armstrong DW. Gas chromatography selectivity of new phosphonium-based dicationic ionic liquid stationary phases. *Journal of Separation Science*. 2018;**41**:4142-4148
- [20] Cui J, Li Y, Chen D, Zhan T-G, Zhang K-D. Ionic liquid-based stimuli-responsive functional materials. *Advanced Functional Materials*. 2020;**30**:2005522
- [21] Yoshida Y, Kitagawa H. Chromic ionic liquids. *ACS Applied Electronic Materials*. 2021;**3**:2468-2482
- [22] Dyre JC. Some remarks on ac conduction in disordered solids. *Journal of Non-Crystalline Solids*. 1991;**135**:219-226
- [23] Jordão N, Cruz H, Branco A, Pina F, Branco LC. Electrochromic devices based on disubstituted oxo-bipyridinium ionic liquids. *ChemPlusChem*. 2015;**80**:202-208
- [24] Bhowmik PK, Koh JJ, King D, Han H, Heinrich B, Donnio B, et al. Dicationic stilbazolium salts: Structural, thermal, optical, and ionic conduction properties. *Journal Molecular Liquids*. 2021;**341**:117311
- [25] Vogel H. The temperature dependence low of viscosity of fluids. *Physikalische Zeitschrift*. 1921;**22**:645-646
- [26] Fulcher GS. Analysis of recent measurements of the viscosity of glasses-reprint. *Journal of the American Ceramic Society*. 1992;**75**:1043-1059
- [27] Bhowmik PK, Noori O, Chen SL, Han H, Fisch MR, Robb CM, et al. Ionic liquid crystals: Synthesis and characterization via NMR, DSC, POM, X-ray diffraction and ionic conductivity of asymmetric viologen bistriflimide salts. *Journal Molecular Liquids*. 2021;**328**:115370
- [28] Sudhakar S, Narasimha Swamy T, Srinivasan KSV. Synthesis, characterization, and thermal properties of 4,4'-bis(4-n-alkoxybenzoyloxy) benzylideneanilines and bis(4-benzylidene-4'-n-alkoxyaniline) terephthalates. *Liquid Crystals*. 2000;**27**:1525-1532
- [29] Kim I-H, Tsai H-J, Nishi K, Kasagami T, Morisseau C, Hammock BD. 1,3-Disubstituted Ureas functionalized with ether groups are potent inhibitors of the soluble epoxide hydrolase with improved pharmacokinetic properties. *Journal of Medicinal Chemistry*. 2007;**50**:5217-5226
- [30] Sharma GD, Saxena D, Roy MS. Studies on electrical and photoelectrical behaviour of ITO/ArV/In Schottky barrier device. *Synthetic Metals*. 1999;**106**:97-105
- [31] Cheng W-C, Kurth MJ. The Zincke reaction. A review. *Organic Preparations and Procedures International*. 2002;**34**:585-608
- [32] Bhowmik PK, Al-Karawi MKM, Killarney ST, Dizon EJ, Chang A, Kim J, et al. Thermotropic liquid-crystalline and light-emitting properties of bis(4-alkoxyphenyl)viologen bis(triflimide) salts. *Molecules*. 2020;**25**:2435

- [33] Bhowmik PK, Chen SL, Han H, Ishak KA, Velayutham TS, Bendaoud U, et al. Dicationic ionic liquids based on bis(4-oligoethyleneoxyphenyl) viologen bistriflimide salts exhibiting high ionic conductivities. *Journal of Molecular Liquids*. 2022;**365**:120126
- [34] Hallett JP, Welton T. Room-temperature ionic liquids: Solvents for synthesis and catalysis. 2. *Chemical Reviews*. 2011;**111**:3508-3576
- [35] Welton T. Ionic liquids: A brief history. *Biophysical Reviews*. 2018;**10**:691-706
- [36] Haramoto Y, Yin M, Matukawa Y, Ujiie S, Nanasawa MA. A new ionic liquid crystal compound with viologen group in the principal structure. *Liquid Crystals*. 1995;**19**:319-320
- [37] Wang R-T, Lee G-H, Lai CK. Anion-induced ionic liquid crystals of diphenylviologens. *Journal Materials Chemistry C*. 2018;**6**:9430-9444
- [38] Veltri L, Cavallo G, Beneduci A, Metrangolo P, Corrente GA, Ursini M, et al. Synthesis and thermotropic properties of new green electrochromic ionic liquid crystals. *New Journal of Chemistry*. 2019;**43**:18285-18293
- [39] Das G, Škorjanc T, Sharma SK, Gándara F, Lusi M, Shankar Rao DS, et al. Viologen-based conjugated covalent organic networks via Zincke reaction. *Journal of the American Chemical Society*. 2017;**139**:9558-9565
- [40] Striepe L, Baumgartner T. Viologens and their application as functional materials. *Chemistry A European Journal*. 2017;**23**:16924-16940
- [41] Ding J, Zheng C, Wang L, Lu C, Zhang B, Chen Y, Li M, Zhai G, Zhuang X. Viologen-inspired functional materials: Synthetic strategies and applications. *Journal of Materials Chemistry* 2019;**A 7**:23337-23360.
- [42] Bishop AG, MacFarlane DR, McNaughton D, Forsyth M. Triflate ion association in plasticized polymer electrolytes. *Solid State Ionics*. 1996;**85**:129-135
- [43] Brown AW, Martinez-Felipe A. Ionic conductivity mediated by hydrogen bonding in liquid-crystalline 4-n-alkoxybenzoic acids. *Journal of Molecular Structure*. 2019;**1197**:487-496
- [44] Zentel R, Strobl GR, Ringsdorf H. Dielectric-relaxation of liquid-crystalline polyacrylates and polymethacrylates. *Macromolecules*. 1985;**18**:960-965
- [45] Bojanowski Z, Knapik J, Diaz M, Ortiz A, Ortiz I, Paluch M. Conductivity mechanism in polymerized imidazolium-based protic ionic liquid [HSO₃-BVIIm][OTf]: Dielectric relaxation studies. *Macromolecules*. 2014;**47**:4056-4065
- [46] Concellón A, Hernández-Ainsa S, Barberá J, Romero P, Serrano JL, Marcos M. Proton conductive ionic liquid crystalline poly(ethyleneimine) polymers functionalized with oxadiazole. *RSC Advances*. 2018;**8**:37700-37706
- [47] Liang SW, O'Reilly MV, Choi UH, Shiao H-S, Bartels J, Chen Q, et al. High ion content siloxane phosphonium ionomers with very low T-g. *Macromolecules*. 2014;**47**:4428-4437
- [48] Mauritz KA, Moore RB. State of understanding of Nafion. *Chemical Reviews*. 2004;**104**:4535-4585
- [49] Luntz AC, McCloskey BD. Nonaqueous Li-air batteries:

a status report. *Chemical Reviews*. 2014;**114**:11721-11750

[50] Bostwick JE, Zanelotti CJ, Yu D, Pietra NF, Williams TA, Madsen LA, et al. Ionic interactions control the modulus and mechanical properties of molecular ionic composite electrolytes. *Journal Materials Chemistry C*. 2022;**10**:947-957

[51] Devaki SJ, Sasi R. Ionic liquids/ionic liquid crystals for safe and sustainable energy storage systems. In: Handy S, editor. *Progress and Developments in Ionic Liquids*. Intech: London, UK; 2017. pp. 313-336

[52] Liu H, Yu H. Ionic liquids for electrochemical energy storage devices applications. *Journal Materials Science and Technology*. 2019;**35**:674-686

[53] Papović S, Gadžurić S, Bešter-Rogač M, Vraneš M. Effect of the alkyl chain length on the electrical conductivity of six (imidazolium-based ionic liquids + γ -butyrolactone) binary mixtures. *Journal of Chemical Thermodynamics*. 2016;**102**:367-377

[54] Xu C, Yang G, Wu D, Yao M, Xing C, Zhang J, et al. Roadmap on ionic liquid electrolytes for energy storage devices. *Chemistry An Asian Journal*. 2021;**16**:549-562

[55] Angell CA, Imrie CT, Ingram MD. From simple electrolyte solutions through polymer electrolytes to superionic rubbers: Some fundamental considerations. *Polymer International*. 1988;**47**:9-15

[56] Angell CA. Relaxation in liquids, polymers and plastic crystals-strong fragile patterns and problems. *Journal of Non-Crystalline Solids*. 1991;**131**:13-31

[57] Vanti L, Alauddin SM, Zaton D, Aripin NFK, Giacinti-Baschetti M,

Imrie CT, et al. Ionically conducting and photoresponsive liquid crystalline terpolymers: Towards multifunctional polymer electrolytes. *European Polymer Journal*. 2018;**109**:124-132

[58] Alauddin SM, Ibrahim AR, Aripin NFK, Velayutham TS, Abou-Zeid OK, Martinez-Felipe A. New side-chain liquid crystalline terpolymers with anhydrous conductivity: Effect of azobenzene substitution on light response and charge transfer. *European Polymer Journal*. 2021;**146**:110246

[59] Alauddin SM, Aripin NFK, Velayutham TS, Martinez-Felipe A. Liquid crystalline polymers containing sulfonic and light-responsive groups: From molecular design to conductivity. *Molecules*. 2020;**25**:2579

[60] Jourdain A, Serghei A, Drockenmuller E. Enhanced ionic conductivity of a 1,2,3-triazolium-based poly(siloxane ionic liquid) homopolymer. *ACS Macro Letters*. 2016;**5**:1283-1286

[61] Maximean DM, Cîrcu V, Paul Ganea CP. Dielectric properties of a bisimidazolium salt with dodecyl sulfate anion doped with carbon nanotubes. *Beilstein Journal of Nanotechnology*. 2018;**9**:164-174

Application of Ionic Liquids in Rechargeable Li-Ion Batteries: A Comprehensive Guide to Design, Synthesis and Computational Aspects

*Kajari Chatterjee, M.K. Sridhar, Akhilesh Kumar Singh
and Kisor Kumar Sahu*

Abstract

The breathtaking pace of the development of smart and wearable gadgets, electric vehicles and many other ultraportable devices has ushered into the era of rapid development of rechargeable batteries with enhanced safety, high-performance, high gravimetric and volumetric energy density. New battery chemistries are being constantly explored to identify better electrolytes that are environmental-friendly, non-flammable, reusable and most importantly ultra-customizable for high-performance applications. Ionic liquid, by virtue of its unique set of tunable properties, is a natural choice from both academic and industrial perspectives. A general guiding principle of ionic liquid synthesis proceeds via an appropriate selection of precursors from the ionic liquid toolbox and reaction with the alkyl halide followed by the metathesis or simple acid-base reaction yielding the final ionic liquid. This study is a complete and extensive treatise on the usage of the ionic liquids in the electrolytes of secondary batteries concerning (i) the design philosophy, (ii) synthesis, (iii) characterization, (iv) new chemistry and electrode material development (v) cell performance, (vi) cell safety, and (vii) comprehensive computational protocols encompassing all the aspects of the electrolyte and electrode-electrolyte interactions.

Keywords: ionic liquids, electrolyte/electrolyte additive, secondary battery, density functional theory, molecular dynamics, Monte Carlo simulations

1. Introduction

Batteries are all around us. They are mainly of two types: primary (non-rechargeable) and secondary (rechargeable). Economically and also from a materials sustainability point of view, rechargeable batteries should replace the primary cells wherever possible. Intense research is going on to make our planet cleaner through

sustainable and ecofriendly technologies. Through constant innovation, battery materials are being perfected in terms of cost effectiveness, cycle lives, energy and power densities, cell voltages and cell safety [1, 2]. Rechargeable batteries are the electrochemical devices which can transform chemical energy into electrical energy and vice versa. This is called the “Rocking Chair” mechanism. The battery mainly consists of three parts: Anode, electrolyte and cathode. When a battery is operated, redox reactions take place: reduction and oxidation take place at cathode and anode respectively during discharge. While charging, the reactions are reversed. In order to maintain the charge balance in a battery driven electrical circuit, the resulting current from anode to cathode need to be compensated by ion transport through electrolyte inside the cell. If the electrolyte is liquid, there is a need for a separator between electrodes to prevent short-circuit.

Among the most popular commercially available rechargeable batteries, lithium ion batteries (LIBs) are having higher gravimetric and volumetric energy densities [3] which make them smaller, lighter and energy dense than others. These parameters are of crucial importance for modern automotive and portable electronic industries.

The other advantages of LIBs are low self-discharge and lack of memory effect. Schematics of internal structure of a LIB is shown in **Figure 1**. LIBs were first commercialized by Sony Corporation in 1991 [4]. The following decade can be marked by intense advanced engineering of LIBs. In 2005, Sony again introduced the first tin based anode battery [5] (Nixelion™) with 30% more battery capacity resulting in an expeditious increase in LIB sales for automotive applications [6].

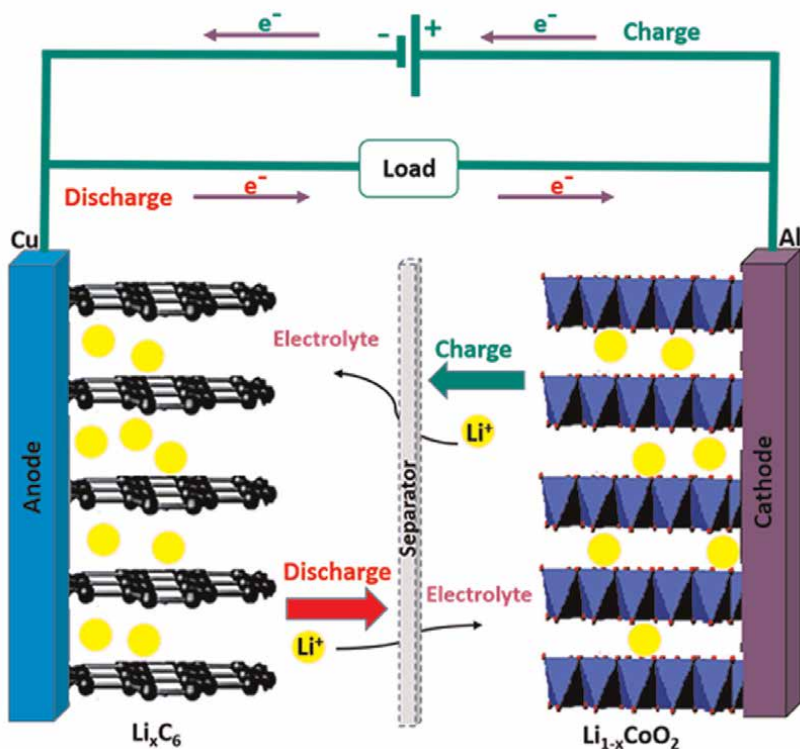


Figure 1. Schematics of internal structure of a lithium ion battery.

Battery electrolyte plays a very crucial role in performances. Electrolyte is a medium of transportation of ions. There are many types of electrolytes available in the market in the form of solid, liquid, gel and polymer. Some important and desirable properties of electrolyte are (i) solid electrolyte interface (SEI) formation which protects the electrodes from degradation and also prevents anion intercalation, (ii) wide electrochemical window which determines the stability range of batteries; and improving: (iii) chemical stability, (iv) ionic conductivity, and (v) salt solubility. Liquid electrolyte is advantageous because of their high ionic conductivity. The most popular commercial LIB electrolytes was developed by Tarascon *et al.* [7], which contains lithium hexafluorophosphate (LiPF_6 , a lithium salt) dissolved in a mixture of organic carbonates (ethylene carbonate and dimethyl carbonate). This electrolyte has high salt dissociation, low viscosity, moderate ionic conductivity and cost-effective. However, it also has serious shortcomings in the form of being flammable, sensitive towards hydrolysis and toxic. There is an urgent need to identify a possible solution for reducing irreversible lithium losses and flammability. One of the most attractive routes to address these problems is through the introduction of additives or optimization of electrolyte composition [8].

The role of additives in electrolyte is to facilitate one or more of the following phenomena: Formation of stable solid electrolyte interface (SEI) on electrodes, protect cathode from over-charge, reduce gas generation, improve thermal stability and ionic conductivity and increase coulombic efficiency. They are typically categorized as SEI supporting, flame retardant and over-charge protective additives. The SEI supporting additives are again classified into three groups: reaction type, reduction type and SEI improver. The reaction type additives react with intermediate solvents and participate in SEI formation. The reduction type additives generally decompose prior to the electrolyte solvent's decomposition while charging and help in formation of SEI. The last type i.e. SEI improvers are re-dissolved in the inorganic SEI layer to prevent continuous growth of SEI further, thus enhancing the performance of LIB. **Figure 2** depicts the design strategy of a high energy rechargeable batteries.

Ionic Liquids (ILs) have been proposed as electrolytes in LIBs for recent years. For example, Kim *et al.* [9] developed the battery prototype of $\text{Li}/\text{LiFePO}_4$ and $\text{Li}_4\text{Ti}_5\text{O}_{12}/\text{LiFePO}_4$ using pyrrolidinium-based ILs and their performance characterization are

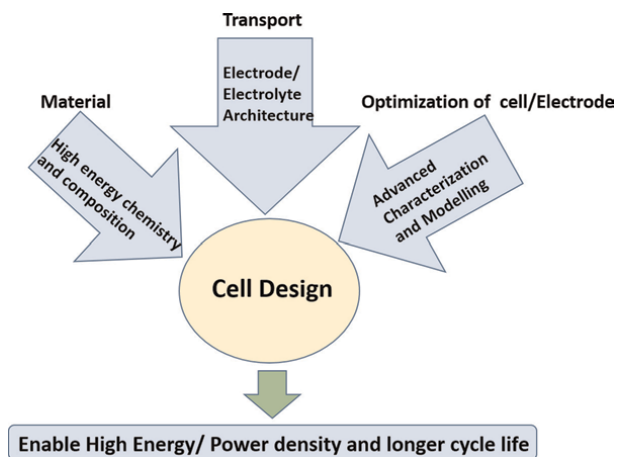


Figure 2.
Design strategy of a high energy rechargeable batteries.

described therein. T. Yim *et al.* [10] discussed the usage of room temperature ILs as an alternative to conventional carbonate-based electrolyte for LIBs. Masayoshi Watanabe *et al.* [11] described the application of ILs in energy storage devices. Sato *et al.* [12] found a novel ammonium IL, *N,N*-diethyl-*N*-methyl-*N*-(2-methoxyethyl)ammonium bis(trifluoromethylsulfonyl)imide) as an electrolyte for electrochemical devices. T.D Vo *et al.* [13]. had studied the safety aspect of 1-ethyl-3-methylimidazolium bis (trifluoromethanesulfonyl) in carbonate solvents (EC-PC). H. Park *et al.* [14] used over-lithiated lithium nickel oxide (Li_2NiO_2) as a sacrificing positive additive for LIBs. Guerfi *et al.* [15] used mixtures of ILs ((trifluoromethylsulfonyl imide) as anion and 1-ethyl-3-methylimidazolium as cation) along with organic electrolyte to enhance cell safety and electrochemical performances. H. Saruwatari *et al.* [16] found that addition of bis(oxalato)borate anion in 1-ethyl-3-methyl-imdazolium tetrafluoroborate formed SEI which improved the performances in battery. N. Plylahan *et al.* [17] showed that for high temperature LIB, pyrrolidinium-based hybrid ILs might be a good choice. In summary, using ILs as an electrolyte/electrolyte additive in lithium ion batteries may resolve many concerns in LIBs.

2. General features, synthesis and characterization of ILs

Green technology refers to the application of scientific principles for the purpose of emission reduction, conservation of water, waste reduction and increasing energy efficiency compared to their conventional counterparts. From the early age of alchemy, there has been huge interest in the study of species in solution. Solvents can be of any type of liquids but sometimes they are hazardous and create environmental pollution. The examples of common solvents are chloroform, dichloromethane, carbon tetrachloride, acetone, chlorofluorocarbon (CFC), ethylene carbonate (EC), dimethyl carbonate (DMC) etc. Traditionally, these solvents have been used as reaction media for the synthesis of fine chemicals, pharmaceuticals, petrochemicals and energy storage applications however, they have some drawbacks: (i) mostly they are used in large amounts, and (ii) usually they are volatile. In the chemical industry, the major problem is the large volume of hazardous wastes as by-products. When these are dumped into the environment it causes air, water and soil pollution. These volatile organic compounds (VOC) which evolve harmful gasses have low thermal stability, pose danger to human life and disbalance the ecosystem. So, introducing greener and cleaner technology in both industry and academia is a high priority agenda [18]. More specifically, green chemistry is the design of processes which can reduce or eliminate the generation of harmful/hazardous substances. Hazardous materials are categorized as physical (e.g. flammable and explosive), toxicological (carcinogenic and mutagenic), and environmental (affecting ozone depletion, climate change, and global warming) [19, 20]. To minimize the chemical wastes from industries, refinements and redesign are necessary for conventional chemical processes [12]. At present scenario, low volatile, recyclable, reusable and thermally stable solvents, in particular, “neoteric solvents” would be ideal for chemical industries. According to the guidelines of Montreal Protocol [21], four alternate technologies are possible. They are (i) solvent free synthesis, (ii) use of supercritical fluids, (iii) use of water as solvent, and (iv) use of room temperature ionic liquid. Solvent free synthesis is not feasible all the time. For supercritical fluids, they need special conditions (e.g. a feasible or at least favorable T_c , P_c etc.). For the last two decades, water has been used as a useful solvent medium but as it is a protic solvent, it has the tendency to hydrolyze. Another major limitation

of water is the low miscibility with organic reagents. So, ILs as reaction media are a better and generic option for many applications.

ILs are molten salts that are liquid below 100°C and consist entirely of ions [22–25]. Mostly ILs are comprised of bulky, asymmetric organic cations and organic or inorganic anions (**Figure 3**).

The most common IL cations are alkylammonium, alkylphosphonium, *N,N*-dialkylimidazolium as well as *N*-alkylpyridinium and alkylthiazolium cations. The anions may be as simple as halides (chloride, bromide or iodide), nitrate, tetrafluoroborate, haloaluminates, hexafluorophosphate etc. Nowadays, alkyl sulfates and alkyl sulfonates and even more often fluorinated and perfluorinated anions such as triflate, $[\text{CF}_3\text{SO}_3]^-$, bis(fluorosulfonyl)imide $[(\text{FSO}_2)_2\text{N}]^-$ and bis(trifluoromethylsulfonyl)imide $[(\text{CF}_3\text{SO}_2)_2\text{N}]^-$ are employed. There are several functionalized cations which are very popular (**Figure 4**).

With permutation and combination of these cations and anions, a large number of ILs can be designed for specific applications [13, 24]. In fact, for 1,3-functionalized

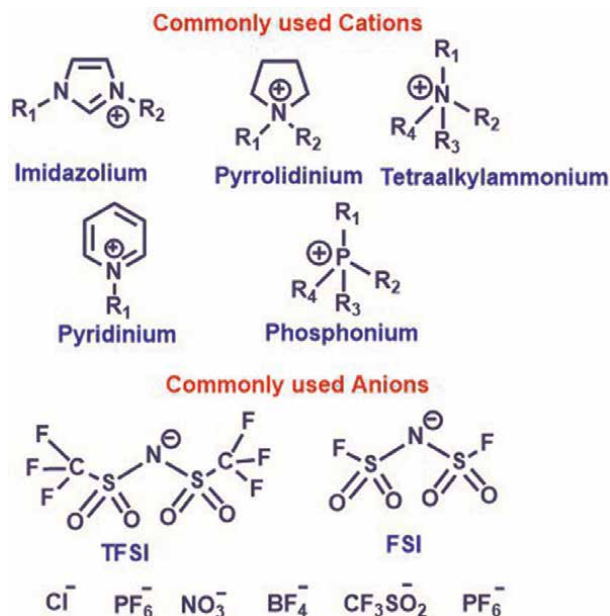


Figure 3.
The ionic liquid tool cabinet: Frequently used cations and anions for ILs.

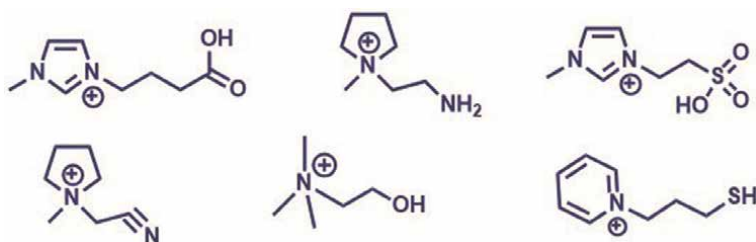


Figure 4.
Functionalized cations of ILs.

imidazolium derivatives, there are 30,000 entries in the CAS database [26]. That is why, RTILs are also known as “designer solvents”.

Although, one can certainly identify an optimal IL for any specific application, there still might be some pros and cons. The choice of cations and anions have a great influence not only on the physical properties but also in thermodynamics and the kinetics of the reactions involved for specific applications. As a rule of thumb, anions control the chemistry and the cations refine the physical properties like viscosity, solubility, flammability, density etc. Thus, for a targeted application, tuning of the properties of ionic liquids is very important. **Figure 5** depicts the number of publications on ILs in rechargeable batteries from 2010 to May 2022.

2.1 Synthesis of room temperature ionic liquids

Depending upon the structures, properties and applications, four different generations of ionic liquids have been reported till date [27, 28]. The first generation ILs are those whose physicochemical properties can be strengthened by simply changing their cations and anions. They have been extensively used as solvent of the reaction media but they are ecotoxic in aquatic environments. When functionalized cations e.g., dialkylimidazolium, alkylpyridinium and phosphonium or anions e.g., tetrafluoroborate and hexafluorophosphate are introduced to play a particular chemical role, it is called second generation ILs. They are stable in aquatic environments and mainly used as lubricants, complex ligands and materials for energy applications. The third generation ILs are synthesized from some low-toxic, biologically active ions e.g., amino acids and choline, which have nearly identical physical properties of classical ILs. These task specific ILs [29] have antifungal and antibacterial properties etc. They are the good choices for drugs/biomolecule delivery, bio sensing and regenerative medicines. Recently, in 2018, the fourth generation ILs [30] have been introduced. Unlike the three previous generations, these ILs go beyond the traditional salt-in-solvent solutions and therefore not readily predictable by simple rule of mixtures. Typically, they are custom-designed aryl-alkyl-substituted ILs. They offer some unique application in bio preservation and offer tremendous future potential owing to their intrinsic biocompatibility.

Since the present study focuses on the ILs for LIB applications, we have confined our discussion only to the synthesis of first and second generation room temperature ILs.



Figure 5. The number of publications on ILs in rechargeable batteries from 2010 to 2022 (all data are taken from “Scifinder” up to 16th of May 2022).

Fewer steps are required for their synthesis. The first synthetic step for both first and second generation ILs [27] are common. First of all, one has to choose the corresponding precursor which after reaction with alkyl halide gives halide intermediate. This intermediate undergoes either metathesis (anion is exchanged with group 1 metal salts) or simple acid-base reaction to give final ionic liquid. The synthetic route of Imidazolium-based ionic liquids were given by Huddleston *et al.* [31] and Stark *et al.* [32]

From **Figure 6**, it can be seen that 1-alkyl-3-methylimidazolium ionic liquid is obtained from corresponding halide precursors either by metathesis or by treatment with acids with stoichiometric ratios. Among halides, chlorides are mostly preferred. Sometimes the alkylation is carried out in an autoclave at elevated temperature and autogenous pressure without addition of any solvent if the chloroalkane (e.g., chloroethane) is gaseous at room temperature. But their higher homologues can be synthesized under reflux at atmospheric pressure. Same method can be followed for the pyridinium, piperidinium or any other ILs. The synthesis of third and fourth generation ILs follow the green path and thus is not very easy to synthesize. Particularly, attaining high purity becomes increasingly challenging for the higher generation ILs and often additional precautions need to be taken [28, 33].

2.2 Characterization of ILs

The synthesized ILs should be free from any impurities such as organic solvents, chloride ions, water etc. because final purity of ILs has a very strong influence on the

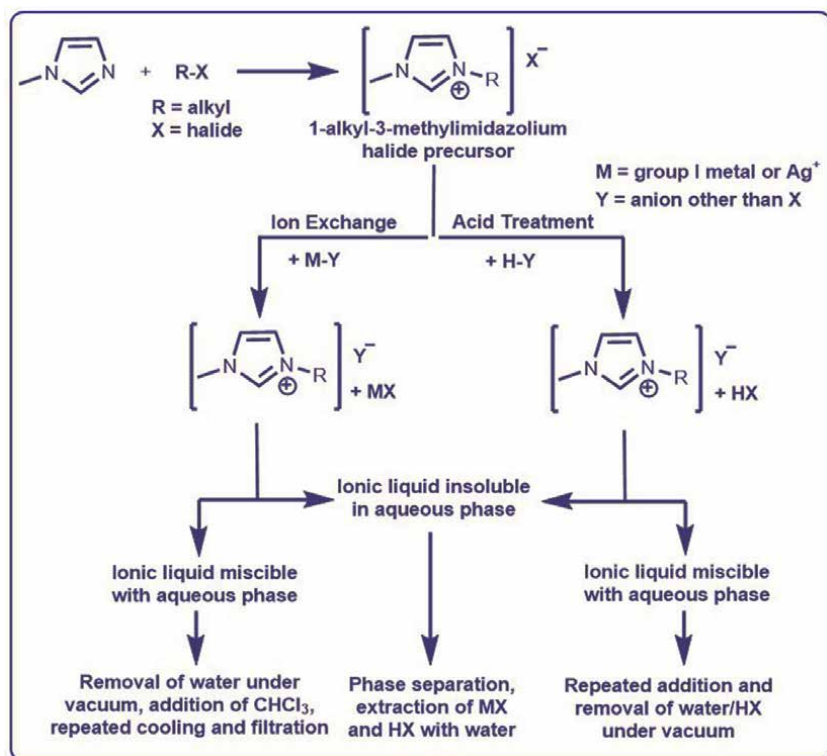


Figure 6. Common synthetic route for the preparation of IL; reproduced from ref. [28].

physicochemical properties. Therefore, during synthesis proper care should be taken. The identity of synthesized ILs are established by Nuclear Magnetic Resonance (NMR) spectroscopy, Fourier Transform Infrared (FT-IR) spectroscopy, Electrospray ionization mass spectrometry (ESI-MS) and Elemental (CHN) analysis. Additionally, Karl Fischer titration is an important technique to quantify the trace amount of water present in the synthesized IL.

2.3 Physicochemical characteristics of ILs

ILs have many interesting properties depending upon the choices, which make them very attractive candidates for diverse applications. Some of them are as follows: (i) very negligible vapor pressure, (ii) high thermal stability, (iii) wide electrochemical window, (iv) tunable properties, (v) nonflammable, and (vi) the most importantly, environment friendly. Thermodynamic properties such as activity coefficients, densities and transport properties like viscosity, conductivity and diffusion coefficients have a great influence in reactivity of ILs towards chemical processes. In a review, Heintz [34] has described the thermodynamics and thermophysics of ILs in non-aqueous solvents.

As ILs are ionic in nature, they are highly conducting materials [35]. This property makes ILs the ideal candidate for applications in electrochemical devices. Just like other properties, conductivity of ILs also can be adjusted by deliberate choice of cations and anions as both moieties can contribute to it. It can also be enhanced by increasing the temperature. Sometimes, the aggregation or ion pairing in neat solution leads to reduction in ion mobility thus reducing the conductivity. As a side note, studies have shown that in the solar cell applications, the conduction is enhanced via Grotthuss hopping alternatively than the typical transfer mechanisms [36, 37].

Viscosity plays a major role in determining the physical properties. Generally, the viscosities of IL are higher than that of common solvents [31]. If alkyl chain length of IL is increased, the viscosity is increased because of more Van der Waals interaction between cations [38]. It can be minimized by functionalization of side chains. The anions also play an important role. The tendency to form hydrogen bonds and symmetry of anions have a great influence on viscosity of ILs. It decreases with increase in temperature due to the reduction in Van der Waals interaction between cations and anions. The impurities such as water, organic solvents and chloride ions have great influence on viscosities [39]. For example, 0.01 molal bmimCl has viscosity of 154 cP whereas 0.5 molal bmimCl has viscosity of 201 cP. Generally, Imidazolium based ILs have lesser viscosities than ammonium based ILs [40]. The viscosities can be tuned by structural modification of ions.

The electrochemical stability window (ESW) of an ionic liquid is the range in electric potential wherein that particular ionic liquid is stable (not decomposed) either by the reduction of constituting cation or by the oxidation of anion [35]. Generally, the window for ILs lie in between 3.0 V and 6.4 V [41–44]. The precise range of electrochemical windows depends on the nature of cations and anions. Fluorine containing anions generally show a wide range. All Imidazolium-based ILs show cathodic stability about -2 V vs saturated calomel electrodes [41–44].

The ILs generally possess high thermal (and radiation, useful for nuclear application) stability because of their negligible vapor pressure. Detail studies have been reviewed by Maton *et al.* [45] and Bier *et al.* [46]. Xue *et al.* [47] described the long-term stability of protic, polymerized and mixtures of ILs in their perspective article. Literature reveals that, their decomposition temperature are generally in the range of

280–490°C. Thermal stability is generally determined by thermogravimetric analysis (TGA). The decomposition temperature is very much dependent on the structure of the consisting cations and anions [48]. Generally, the anions are more responsible than cations for the decomposition of ILs. For same cation, the decomposition temperature is increased with more hydrophobic anions [31] e.g. for $[C_4mim]^+$ the decomposition temperature varies in the following way: Cl^- (254°C) < I^- (265°C) < PF_6^- (349°C) < BF_4^- (403°C) < NTf_2^- (439°C).

ILs are still expensive than conventional solvents. Because of their low vapor pressure, the classical ILs may not be harmful in atmospheric condition but they may cause severe contamination in aquatic environment due to their potential toxicity and nonbiodegradability. To make them economical and environment friendly, there is a need to recycle those ILs for future use. Recyclability of ILs is one of the main reasons for their increasing popularity among the scientists and engineers. There are several processes available for IL recovery. Wu *et al.* [49] have summarized the different IL recovery processes which might be a guide to future researchers. Toxicity is also a major issue for the biomedical application of ILs. Using structure-activity relationship, the toxicity and biocompatibility can be tailored for ILs [50]. Zhao *et al.* [51] and Ranke *et al.* [52] have highlighted some toxicological advances of new generation ILs.

3. Different types of ILs used in rechargeable batteries

Table 1 summarizes the salient features of different IL precursors and their derivatives for specific electrochemical systems to enhance different performance/stability/safety metrics. These can be a good guiding principle for customizing IL for a specific battery application.

IL precursor classes	ILs + additives	Electro-chemical System	Salient features	Reference
Imidazolium-based ILs	HMITFSI, MEMITFSI	Li/LiMn _{1.5} Ni _{0.5} O ₄	Wide (~ 5.5 V) ESW and possible parasitic anodic reactions while charging at the high potentials	[53]
	LiTFSI in AMImTFSI	Li-Sulfur	Lithium polysulfide dissolution is suppressed and exhibit good cycling capacity	[54]
	EMIM ⁺ -encapsuled ionogel	Li/LiFePO ₄	Reversible Li ⁺ intercalation/deintercalation behavior and stable even after 120 cycles at 0.5C	[55]
	IMI _{1,201} TFSI, IMI _{1,10201} TFSI	Li/LiFePO ₄	Increased conductivity with less viscosity, capacity retention is up to 92% at lower current rate	[56]
Pyrolidinium-based ILs	BMPTFSI	Li/LiMn _{1.5} Ni _{0.5} O ₄	Wide (~ 5.5 V) ESW and possible parasitic anodic reactions while charging at the high potentials	[53]
	Py ₂₄ TFSI-LiTFSI + PVdF-HFP + EC + PC	Li/Li	Wide ESW, high degradation temperature and high lithium ion transport	[57]

IL precursor classes	ILs + additives	Electro-chemical System	Salient features	Reference
	PYR _{1(2O1)} TFSI, PYR ₁₄ TFSI	Li/LiFePO ₄	Suppresses crystallinity and increase cation solvation	[55]
	PYR ₁₃ TFSI, PYR ₁₃ FSI	Li/NMC	Ion transport properties is enhanced (about 10 ⁻³ S cm ⁻¹ at -20°C) and wide ESW of 5 V	[58]
	Pyr1,3FSI-LiTFSI	Li-LiCoO ₂	Lithium dendrite growth is effectively suppressed and exhibit good cycling performances at 4.4 V	[59]
	BMPyrTFSI, MPPyrTFSI	Zn stannates / Li	Safer electrolytes and potential candidate to replace graphite as the anode material in more complex devices.	[60]
Pyridinium-based IL	B ₃ MePyTFSI, B ₄ MePyTFSI	Li/LiFePO ₄	High ionic conductivity and exhibit better cycling capacity by enhancing cation solvation	[55]
Tetraalkylammonium-based ILs	N111(1O2) FSI	Li-Air	Possesses low viscosity (~111.4 cP) and initial capacity is 3.75 times higher than reference material	[61]
	DEMETFSA - LiTFSA	Li-LiCoO ₂	Charge/discharge reversibility is increased	[62]
Phosphonium-based IL	mono-(C6) 3PC10- TFSI	Li-LiCoO ₂	High decomposition temperature (355°C), good conductivity (1.7 mS cm ⁻¹) at 100 °C and enhanced specific energy and capacity retention	[63]

Table 1. Representative ILs as electrolytes used in rechargeable battery with corresponding electrochemical systems.

4. Tailoring the properties of rechargeable batteries using IL electrolyte additives

4.1 Ionic conduction

Polymer electrolytes, in spite of its mechanical strength and stability, have a low ionic conductivity at a temperature below its glass transition temperature [64]. ILs have been recently studied as plasticizers in polymer electrolyte. Polymer doping with ILs and polymerization with ILs as solvent are the widely used methods to incorporate ILs in polymer electrolytes [65]. The ions in the ILs react with donor species of the polymer molecule thus reducing the intermolecular interaction. This increases disorder and causes an increase in Li-ion conductivity [66]. Even when polymer is added in small concentration in ionic liquids (gel or polymer-in-salt ionic liquids), the ionic conductivity of the gel polymer is greater than the pure electrolyte, due to the reduction in the overall viscosity of the gel, explained by polymer breathing model [67].

4.2 Solid electrolyte interphase (SEI)

As the ILs [68–70] have high oxidation potential (~ 5.3 V vs. Li^+/Li^0), they may serve as alternative electrolytes for LIBs. The major drawback with ILs is their high viscosity due to which the Li^+ ion conductivity is reduced. Imidazolium-based ILs are the most appropriate candidates for LIBs due to their relatively lower viscosity and a high Li-salt solubility at room temperature. In order to form a stable SEI layer on the graphite anode, some electrolyte additives (EC or VC) must be added because these ILs have poor stability below 1.1 V vs. Li^+/Li^0 [43].

In a stable battery cell, the relative electron energies in the cathode, anode and electrolyte have been schematically depicted in **Figure 7**. Here cathode is the oxidant and anode is the reductant and ΔE_p is the electrochemical stability window (roughly the energy difference between the HOMO and LUMO of the electrolyte). μ_A and μ_C are the chemical potential and ϕ_A and ϕ_C are the work function of anode and cathode respectively. In absence of any passivation layer (SEI), if the chemical potential of anode is more than the LUMO of the electrolyte, then it will reduce the electrolyte by transferring the electron to the LUMO of the electrolyte and if the chemical potential of the cathode is less than the HOMO of the electrolyte, then it will oxidize the electrolyte by transferring the electron to the cathode from the HOMO of the electrolyte. For thermodynamic stability of the battery cell, the following relationship must hold: $e \cdot V_{oc} = \mu_A - \mu_C \leq \Delta E_p$; where e is the electronic charge and V_{oc} is the open circuit voltage of the battery cell. Hence the SEI layer provides the kinetic stability to increase the V_{oc} provided the solvent window of the electrolyte is not too large and the SEI layer formation is ensured by either $\mu_A > \text{LUMO}$ and/or $\mu_C < \text{HOMO}$.

An optimized concentration of ionic liquid as additive to an organic liquid carbonates may tackle the problem of flammability without much compromise in the Li-ion transport and it also helps in SEI formation that in turn provides protection from the degradation of electrode surface [72, 73]. In our previous work, an imidazolium-based

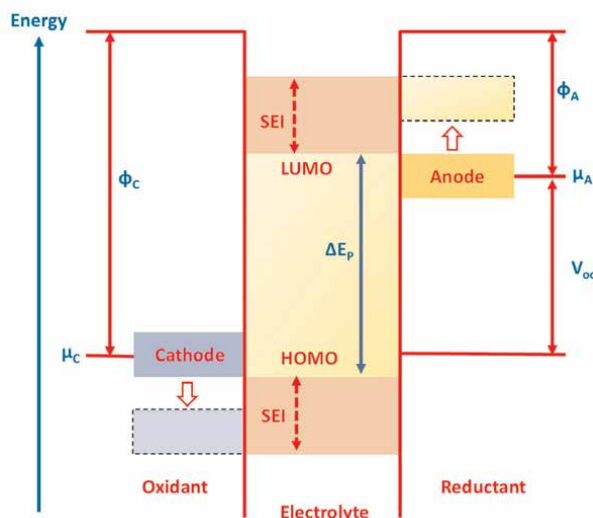


Figure 7. Schematic open-circuit diagram of an electrolyte in a thermodynamically stable battery cell. Copyright; reprinted with permission from ref. [71].

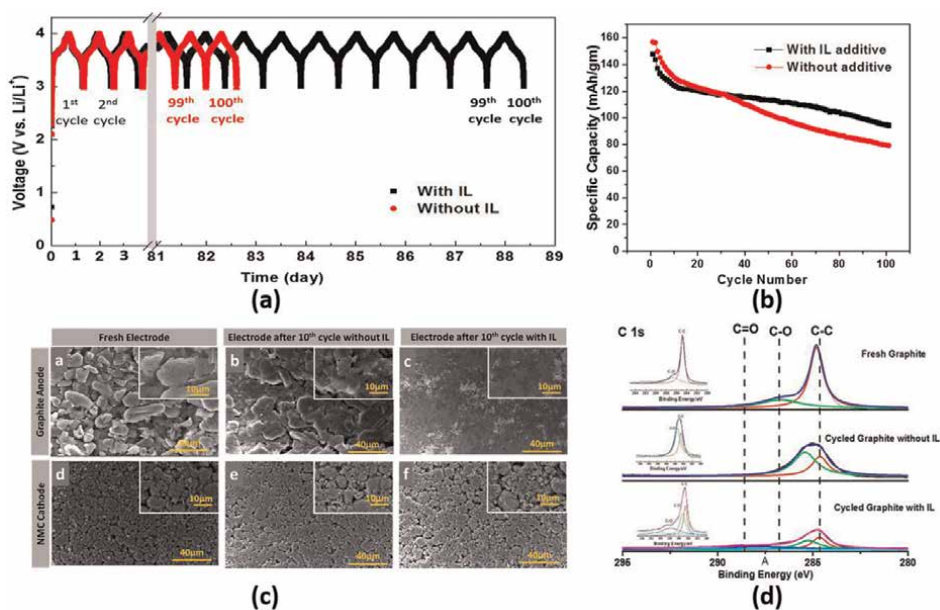


Figure 8. (a) Galvanostatic charging and discharging (100 cycles) of the cells with and without IL with cell voltage between 3.0 V to 4.0 V and a break plot from 3 to 81 days. The cell with IL (black) provides at least 6 days more service than without IL. (b) Cyclic discharge curve of the cell in electrolyte without and with IL, (c) SEM micrographs of both the electrodes before and after cycling, and (d) C 1s XPS spectra of graphite electrodes with IL and without IL; copyright; reprinted with permission from ref. [72]. Copyright 2020 Springer Nature.

non-flammable dicationic ionic liquid was synthesized and was used (20 mM) as an additive to the conventional organic electrolytes for LIBs (**Figure 8**).

It has been found that the addition of IL enhances the discharge capacity of the LIBs by 22% and capacity retention is $\sim 73\%$. The SEM micrographs and XPS study with IL revealed that a stable SEI has been formed during cycling.

Further, this strategy may further increase the oxidation voltage (lower HOMO energy) of the hybrid electrolyte from that of the carbonate. Unfortunately, till date the use of IL as a sole electrolyte for secondary batteries is still a challenge.

5. Theoretical considerations

5.1 Overarching theoretical and computational paradigm

Computational methods have been widely used for the fundamental understanding of many novel materials. Similarly, simulation of the ionic liquids enables researchers to understand its behavior and tailor its properties. When ILs are used as solvents in battery electrolytes the charge present in the solute polarizes the solvent around it, thus a reaction potential acts on the solute which alters its charge distribution with respect to normal charge distribution in the vacuum. Thus, for the simulations of ILs, the solvent effect is of paramount importance in predicting their properties. Two different methods have been developed for studying the effect of solvent on the molecule. One includes consideration of explicit solvent molecules

around the solute and studying it as a single system. The second method involves the usage of average properties of solvent with the assumption that the solvent is a macroscopic continuum medium instead of individual molecules. In the first approach the number of solvent molecules considered explicitly is limited and with a large number of molecules it becomes computationally expensive, especially in first principle calculations. Thus, the second approach is widely used to find the properties of a solute in the presence of a dielectric solvent using first principle calculations. Many continuum solvent models have been proposed such as the Apparent Surface Charge (ASC) method, Born approximation method and so on. One of the widely used methods is the ASC method. In this method the reactive potential due to the continuum solvent is calculated by considering surface charge density on the boundary of the solute. The boundaries enclose the cavities which in turn are formed by the superposition of nucleus centered spheres [74] with Van der Waal radius. The reaction potential is given by Eq. (1)

$$V_{RP}(\vec{r}) = \int_S \frac{\sigma(\vec{s})}{|\vec{r} - \vec{s}|} d^2s \quad (1)$$

where $\sigma(\vec{s})$ is the surface charge density and $V_{RP}(\vec{r})$ is the reaction potential due to the polarized dielectric medium. The ASC method can be further classified mainly into Polarizable Continuum Model (PCM), Integral Equation Function (IEF)-PCM and Solvent Model based on Density (SMD). In a PCM based ASC model, the surface charges are calculated by the Eq. (2)

$$\sigma(\vec{s}) = \frac{\epsilon - 1}{4\pi\epsilon} \frac{\partial(V_M - V_{RP})_{in}}{\partial\vec{n}} \quad (2)$$

where, ϵ is the dielectric constant of the solvent, V_M is the potential due to the charge within the cavity [75] and \vec{n} is the normal vector to the surface. Another method in the ASC is IEF PCM in which the potentials are redefined using green function from which the surface charges are calculated using a unique solution to the Eq. (3)

$$A\sigma = -g \quad (3)$$

where, A and g are the integral operators [76]. The computation used in all the above ASC methods uses boundary element method in which the surface is discretized and each discrete surface element is provided with discrete charges thus modifying the reaction potential given in Eq. (1)–(4)

$$V_{RP}(\vec{r}) = \sum_y \frac{q_y}{|\vec{r} - \vec{s}_y|} \quad (4)$$

where, q_y is the discrete charges present at the center of the surface elements and y is the number of discrete surface elements on the boundary of the solute [77].

In the PCM and IEF-PCM models, the bulk electrostatic interaction between the charge in the cavity and the dielectric continuum medium is considered in calculating the free energy change of solvation. Considerable improvement can be achieved in SMD, which considers additional interaction parameters accounting for the free energy change associated with the solvent cavitation (creating void space in the

continuum media to accommodate the solute), changes in dispersion energy, and local solvent structure changes. The equation governing this interaction is given by Eq. (5)

$$\Delta G_{CDS} = \sum_o \tau_o A_o(R) + \tau_m \sum_o A_o(R) \quad (5)$$

The SMD uses an IEF-PCM model for electrostatic interaction along with the free energy change described in Eq. (5). For ΔG_{CDS} (free energy corresponding to cavitation, dispersion and solvent structure) the boundary of the solute is taken at the Solvent Accessible Surface (SAS) which differs from the actual Van der Waal radii used in finding the reaction potential as shown in **Figure 9**.

5.2 First principle calculations: Density functional theory (DFT)

DFT is based on the foundational assumption that uses electron density as the main variable instead of the many-body wave function of the electrons thereby significantly reducing the computational complexity of the problem. The basis set is a set of one-particle functions generally used to build molecular orbitals in DFT to convert the complex partial differential equations into a simple form of a linear algebraic equation. Determining the properties of ILs as electrolyte in battery applications can be done based on experimental as well as computational method, but obtaining valuable molecular level insights of these properties through first principle methods allow us to make suitable decisions on the cations and anions to be used and tailor their molecular structures. These methods are widely used to study the effect of cation and anion, and their impact on its ESW, Lithium oxidation/reduction rate at the anode/cathode, Lithium ion conductivity, viscosity, solvation shell constituents etc.

The ESW of an ionic liquid can be calculated by finding the values of HOMO and LUMO energies or by using the thermodynamic cycle method. This is of great significance, e.g. for high voltage batteries the main limitation is the narrow ESW of the conventional electrolytes. In a study performed by Kazebiamnavi *et al.*, both the thermodynamic cycle and HUMO/LUMO method was used for finding ESW of methylimidazolium-based cations with different anions, particularly the effect of alkyl chain length of cation and different anions [78]. Thermodynamic cycle method

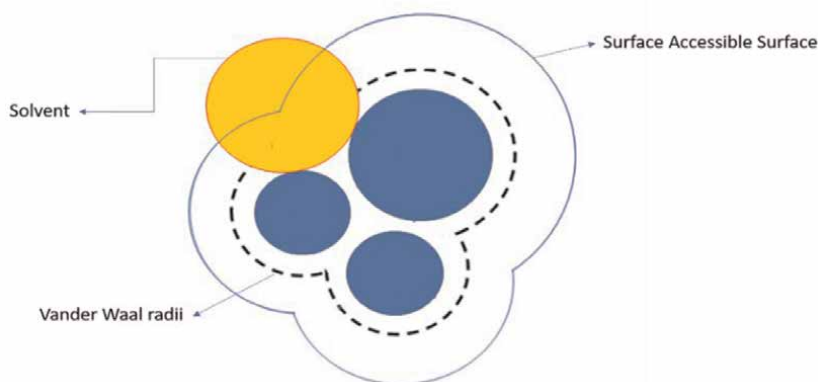


Figure 9. Different cavity boundary surfaces used in SMD method.

splits the charge transfer reaction of the solvated species into three reactions that involve conversion from solvated species to gaseous form, charge transfer reaction of the gaseous form and solvation of the ionized gas [78–80]. The total free energy for oxidation/reduction of a species in a solvent medium is calculated using **Figure 10**.

From the free energy values, the oxidation and reduction potential can be obtained by Eqs. (6) and (7)

$$E_{ox} = -\left(-\Delta G_{sol}^{ox} + \Delta G_{ref}^{ox}\right)/nF \quad (6)$$

$$E_{red} = -\left(-\Delta G_{sol}^{red} + \Delta G_{ref}^{red}\right)/nF \quad (7)$$

where, ΔG_{ref} is the Li/Li + oxidation and reduction Gibbs Free energy and n is the valency for redox couple (for Li/Li+; $n = 1$).

In order to include the effect of the polarizable solvent, a PCM model is used and an iterative self-consistent reaction field (SCRF) is used to calculate the actual charge distribution in the solute cavity. As a first step, the SCRF involves calculation of charge density in a solute molecule with vacuum as its surroundings. The same is then used to calculate the surface charge density that induces the formation of the reaction potential. This reaction potential is then added to the Hamiltonian and the cycle is repeated until the difference in total free energy becomes lesser than the tolerance value [81].

The anions, $[PF_6]^-$ and $[BF_4]^-$ have a lower HOMO and higher LUMO energy when compared to the $[OTf]^-$ and $[TFSI]^-$ ions. This is mainly due to the fact that in $[PF_6]^-$ and $[BF_4]^-$ HOMO and LUMO orbitals are contributed mainly by electronegative Fluorine atoms, while for the latter two it is distributed all over the molecule. The ESW was also calculated using the energy gap between HOMO and LUMO energy levels. It was found that error for thermodynamic cycles peaked up to a value of 15% but for HOMO/LUMO method it peaked around 50% [78].

Another important factor that affects the properties of the IL is the type of solvation shell formed around the Lithium cation. This solvation shell formed around the Lithium determines properties such as viscosity and ionic conductivity. A study done by Angenendt *et al.* [82] uses binding energy of the Lithium salt $[LiAn1]$ and Ionic Liquid anions $[An2]^-$ as means to determine the stable triplets $([Li (An1) (An2)]^-)$

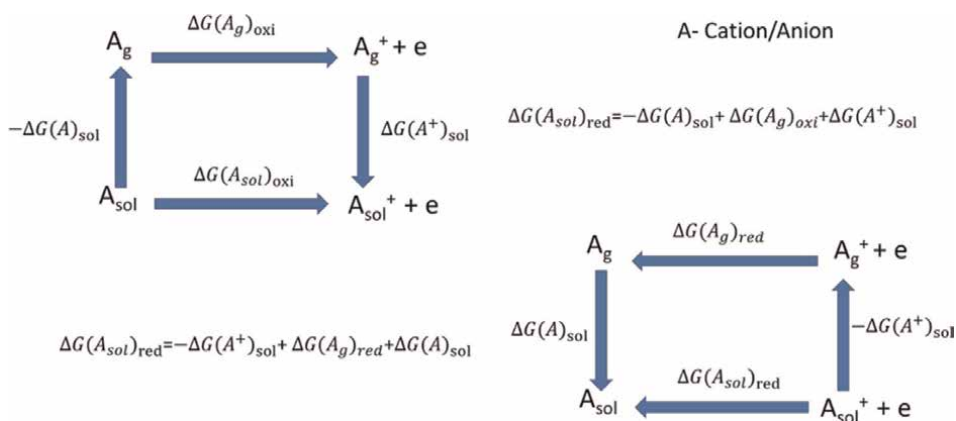
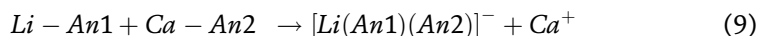
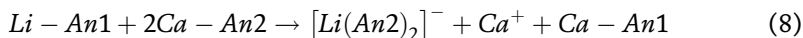


Figure 10. Thermodynamic cycle method for calculating free energy of oxidation and reduction.

formed in the solvation shell (An is used as an acronym for anion). The above method which ignores IL cation interaction is compared with an alternative method which includes interaction of IL cation, which is implemented by Eqs. (8) and (9)



where, An, Ca represents IL anion and cation, respectively. The reaction with lower free energy determines the stable triplet in a ternary system. Even though BF_4^- ions containing triplets were found to be prominent while considering binding energies with the Lithium salt, the cation interaction makes the BF_4^- ion containing triplets less favorable. Kiratidis *et al.* [83] have studied the effect of confined ionic liquids between two surfaces using DFT and found that the surface forces depend on the bulk density of the ionic liquids as well as on the adsorption potential. They have also observed a qualitative similarity in the trend of surface forces for neutral and similarly charged surfaces. Venkataraman *et al.* [84] have studied the interaction between Estrone and Imidazolium-Hydrophobic Ionic liquids using B3LYP/6-31G(d) level of theory. The affinity of Estrone towards the IL with PF_6^- anion is the highest among all other ILs and the interaction is found to have a non-covalent nature. Chen *et al.* [85] have developed an ab initio method to predict the melting point of ionic liquids. SMD-generic-IL solvation model along with the Born-Fajans-Haber cycle is used and found to be in good agreement in comparison to the experimental results with a mean absolute error of 30.5 K and a mean relative error of 8.5%.

5.3 Molecular dynamics studies

Unlike the first-principle methods, MD simulations consider atoms of IL as charged hard spheres. The partial charges are obtained from the Restrained Electrostatic Potential (RESP) algorithm which involves fitting DFT derived Electrostatic Potential (ESP) values calculated at different distances from the molecule's Van der Waal surface. The fitting is an optimization protocol generally based on the least square method which minimizes the sum of mean square error between the actual and fitted potential and a weighted harmonic or hyperbolic function which captures the difference between target and the fitted charge on each atom in a molecule [86]. These partial charges obtained from first principle calculations can only cover the coulombic force acting between charged atoms and ignores the change in the charge distribution within the atoms. Thus, potentials that incorporate the phenomenon of polarization have been developed for MD simulations of ILs. These potentials can be classified broadly into non-polarizable and polarizable potentials. In non-polarizable potential, the partial charge on each atom of the molecule is kept constant throughout the MD simulation. To incorporate the effect of polarization the partial charge obtained from the first principle calculations are scaled by a factor less than unity as a mean field approximation. This model predicted slower dynamics for IL in comparison with experimental results [87]. As the scaling factor is determined for a specific ionic liquid, it lacks transferability between different ILs and it fails to produce good results in case of IL mixtures [88, 89]. To overcome the above limitations, polarizable force fields have been developed for MD simulations of ILs. The polarizable force fields commonly used are Fluctuating Charge method, Drude oscillator method and Induced point dipole method.

5.3.1 Induced point dipole method (IPD)

In the IPD method, a point dipole is considered at the center of each atom in a molecule. For the i^{th} atom in a molecule the induced dipole moment is given by Eq. (10)

$$\mu_i = \alpha_i E_T \quad (10)$$

where, E_T is the total electric field. The total electric field acting on the atom in an induced dipole method is given by Eq. (11)

$$E_T = E_i - \sum_{j=1, i \neq j}^N T_{ij} \mu_j \quad (11)$$

where, E_i corresponds to the electric field acting on atom i due to permanent partial charges and the second term corresponds to the dipole interaction with T_{ij} corresponds to the dipole-dipole tensor and μ_j corresponds to the dipole moment of atom j . The main assumption in this model is that the dipole moment is considered isotropic and the model fails when the distance between two atoms approach $4(\alpha_i \alpha_j)^{1/6}$ in case of a two-atom system. Thus, a Thole damping factor is combined with the standard induced point dipole model to overcome the problem and this combined model is widely used in MD simulations for explicitly using polarizable force fields [90]. Bedrov *et al.* have used APPLE&P [91] force field to study the effect of the induced point dipole method on the thermodynamic properties of several ILs. When the induced point dipole interaction is turned off, the density and the average molecular dipole values are underestimated while the enthalpy of vaporization increases by 20–30%. This was explained by the larger difference in energy for the gas phase between polarized and non-polarized force fields in comparison to the liquid phase. The dynamic properties such as the diffusion coefficient was calculated by the mean square displacement and fitting it with a linear relation. The diffusion coefficient calculated using a non-polarizable field was found to have a lower value when compared to the polarizable fields [92]. The effect of polarizability on the simulation is also observed by considering the site-site partial radial density function. Due to the screening effect provided by the polarizable field no oscillations or small peaks were seen at larger distances in the partial radial density function when compared to the non-polarizable field. In another study by Zhao *et al.* [93], a MD simulation with AMBER potential force field (induced point dipole method) was used to find the effect of pressure on the ionic liquid [C₄mim][PF₆] and a phase change was observed when pressure increased from 5000 bar to 6000 bar. A sudden increase in density was observed, which was in agreement with the Raman spectroscopy results. Further analysis on the possible conformal change of both cation and anion have been performed to correlate with the phase change. The anion had the least effect but the dihedrals of the alkyl chain in the cation changed in such a way that it bends towards the cationic ring causing an increase in density. The radial distribution function showed that the atom near to the ring had no change in dihedral angles but the carbon atom in the farthest of the alkyl chain was displaced a lot towards the ring, thus making ILs with large cationic alkyl chain easily compressible.

5.3.2 Drude oscillator model (DOM)

In DOM, the polarizability of a given atom with partial charge q is modeled by considering two particles, a mobile drude particle at a distance $\vec{d}_{j,\gamma}$ carrying a charge

q_d connected by a harmonic spring of spring constant k and a fixed charge of $-q_d$ placed at the center of the atom. The Total electric field $E_{i,\beta T}$ acting on the atom β of molecule v is given by Eq. (12)

$$E_{v,\beta T} = E_{v,\beta} + q_d \sum_w \sum_\gamma \frac{|\vec{r}_{v,\beta} - \vec{r}_{w,\gamma}|}{|\vec{r}_{v,\beta} - \vec{r}_{w,\gamma}|^3} - \frac{|\vec{r}_{v,\beta} - (\vec{r}_{w,\gamma} + \vec{d}_{w,\gamma})|}{|\vec{r}_{v,\beta} - (\vec{r}_{w,\gamma} + \vec{d}_{w,\gamma})|^3} \quad (12)$$

where, $E_{v,\beta}$ is the electric field acting on the atom β due to the partial charges of the atoms γ in different molecules w and the second term corresponds to the electric field acting on the atom β due to the drude pairs. The force acting on the drude particle can be represented by Eq. (13) [94].

$$q_d E_{v,\beta T} = k \vec{d}_{v,\beta} \quad (13)$$

When this electric field acts on the drude particle, it oscillates about a point at a distance $\vec{d}_{v,\beta}$ from the center of the atom from which the average induced dipole moment can be obtained. The average isotropic dipole moment on atom β is given by Eq. (14)

$$\mu_{v,\beta} = \frac{q_d^2 E_{v,\beta T}}{k} \quad (14)$$

Taylor's expansion with an assumption of negligible distance between the atom and drude particle, reduces Eqs. (12) to (11). As the deflection of the spring can be resolved into its three cartesian coordinates, it incorporates anisotropy in the polarization of the atom which offers an advantage over the previous method [95]. Schroder *et al.* [96] have studied the effect of DOM polarization and compared it with non-polarizable and charge-scaled model on 1-ethyl-3-methylimidazolium trifluoromethanesulfonate. The study revealed that charge-scale method could be used to determine collective dynamics of ILs such as diffusion coefficient of ions in IL. But the local dynamics such as the atomic and molecular dipole values and anion positioning around the cation in first solvation shell were well represented by the DOM. Schmollngruber *et al.* [95] compared the effect of IPD and DOM polarization methods on IL with EMIM⁺ cation and CF₃SO₃⁻ anion. In cases of smaller values of polarizability, both the model predicts similar trends for properties such as ion-pair polarizabilities, mean squared displacement values and the coordination of anions around the cation. At high polarizable levels the models tend to deviate and the IPD model have higher impact on the properties of the simulated ionic liquid.

5.3.3 Fluctuating charge model (FCM)

In all the above cases the dipoles are induced using drude particles or atoms that have induced dipole moment while the actual charge on the atom remains fixed throughout the simulation. In the FCM the charge on each atom in the molecule is changed every timestep in such a way that the potential energy is minimized. The Lagrangian multiplier method is used to find the minimal combination of partial charges on the atom based on the constraint that the sum of charges on the atoms in a molecule is constant. This indirectly specifies that in this model the electronegativity

of every atom in the molecule is considered as constant, thus also referred as charge equilibration or chemical potential equilibration model [97]. Cavalcante *et al.* [98] have studied the effect of FCM polarization in the structural rearrangement of anions (PF_6^- and Cl^-) around the cations (1-ethyl-3-methylimidazolium, 1-butyl-3-methylimidazolium). The cations were simulated as non-polarizable molecules while the polarizability model was applied to the anions. The parameters such as electro-negativity and hardness used in FCM was calibrated using Mulliken charges obtained by quantum chemical calculations at the MP2 level, with the basis function 6-311G*. The fixed charge model placed the anions around the C2 carbon atom in imidazolium ring. After introducing polarizability in the anions, the high probability region for the position of the anions shifts off-plane (away from the plane of the ring) and is further placed above and below the ring center. This position of PF_6^- ions are in accordance with the experimental results. Apart from structural aspects it could also reproduce the natural trend of diffusion coefficients with increase in their melting point.

5.4 Monte Carlo (MC) simulations

The main difference between the MD and MC simulation is that the former method tries to trace the exact trajectory of the atoms while the latter deals with only the equilibrium states and the simulation proceeds by sampling microstates following different functions depending upon different ensembles being used. MC simulation involves performing the metropolis algorithm. A lattice is chosen for defining the sites, on which the events of the process to be simulated, are performed. The events are chosen in such a way that the probability of acceptance of any event P_{acc} is given by Eq. (15)

$$P_{acc} = \min \{1, x\} \quad (15)$$

where, x is the ratio of probabilities of the new and the old state. The function used to calculate x depends mainly on the type of ensemble being used.

Phase equilibrium of the electrolytes is one of the factors that decides the operating range of the electrolyte in terms of operating temperature [99]. For phase equilibrium calculations using MC, NPT, Grand Canonical (GC) and Gibbs ensemble MC simulations are found to be suitable ensembles rather than canonical ensembles. In the grand canonical model, a generalized form of canonical ensemble is developed by keeping the system in an ideal gas reservoir in such a way that the system volume is kept constant while the number of particles within the system is allowed to change by accepting or donating particles to the ideal-gas reservoir. The events in this ensemble involve all the events in the canonical ensemble (particle displacements within the system) along with insertion and rejection of particles from the system.

In a study by Rane *et al.* [100] the standard GCMC method is extended for ionic liquids by considering separate ideal gas reservoirs for cations and anions and to maintain neutrality the insertion of ion-pair took place simultaneously. In order to eliminate low acceptance probability, instead of choosing the insertion sites randomly, it is based on distance biasing insertion/deletion methods. In this method, the first ion insertion site is randomly chosen while the site for the counter ion is chosen with a probability which decreases exponentially with increasing interionic distance. Restrictive Primitive Model (RPM), a simple model, which assumes ions as small spheres was used to simulate the liquid-vapor phase change of the ILs and the above GCMC method was found to be efficient for this study.

The temperature at which the phase transformation in RPM occurs does not provide enough driving force for the single ions to move from one lattice site to the other, making the equilibration of the system a time-consuming process. Orkoulas *et al.* [101] added new MC multi-particle movements for canonical ensemble steps, where a low density induces a ion-pair movement in contrast to the cluster movement at high density regime along with the distance biased insertion and destruction of the ion pairs for GCMC Simulations. The dipole and cluster movement led to equilibration of the system within 5×10^5 MC steps with smaller total energy compared to the normal simulation with single ion movements which could not converge.

In the NPT model, the system to be simulated is kept isolated but in thermal and mechanical contact with an ideal gas reservoir. A study was done by Shah [102] on 1-n-butyl-3-methylimidazolium hexafluorophosphate using NPT ensemble. Apart from the combined displacement of ion pair movement described in the Canonical ensemble a volume change Monte Carlo move was also carried out for every two cycles. The molar volume calculated was within 5% of the experimental values. The method also shows good agreement for values such as isothermal compressibility and cubic expansion coefficient with experimental results.

One of the widely used MC methods for phase equilibrium calculation is the Gibbs Ensemble Monte Carlo (GEMC) simulation. Here a constant volume is divided into two regions with each region allowing particle transfer interaction, volume change and particle movement within each other thus having events belonging to both NPT and GCMC simulations. However, the method used for ionic liquids involves transfer of single ions with a background charge to maintain neutrality [103]. Orkoulas *et al.* [101] extended the distance biased ion-pair insertion method to GEMC and found that the results produced were in agreement with the conventional GEMC for RPM with increased efficiency.

6. Future perspectives

Rechargeable LIBs are the suitable systems to store energy for powering electric or hybrid vehicles. They have very high energy density, capacity and efficiency among all commercially available electrochemical storage systems. The technologies of LIBs have reached a very advanced stage [104]. The safety concerns towards the flammable nature of conventional electrolytes may be tackled to a great extent by using ILs as additive to them. There is a great future scope and a dream to use ILs as a sole electrolyte (ILs-based gels or polymer electrolytes) containing lithium salts in combination with the advanced electrode materials to provide high thermal stability. In order to fulfill this dream, one needs to exploit the underlying thermodynamic and kinetic stabilities of these ILs with respect to electrode materials. Some task specific ILs may be designed which will facilitate the formation of SEI layer to protect the electrodes during the charge discharge cycle of the battery cell. Customizing the cations and anions of the ILs used in LIBs, one may fine tune the SEI formation during charge -discharge cycle. Also, there is a need for the development of an alternative to the aluminum as current collectors because it has tendency to corrode at high operating voltage of LIBs. Although the typical ILs used in LIBs are hydrophobic, the dissolved lithium salt makes them very water sensitive. To tackle this problem, new salts may be designed as an alternative to the presently used lithium salts. ILs presents plausible future solutions to the problems encountered during the high-power demand at the start-up and acceleration in electric or hybrid vehicle technology.

7. Conclusion

ILs are very attractive candidates for electrolyte and electrolyte-additive owing to their highly customizable configurations leading to unique electrochemical properties that are of great importance for high performance LIBs. ILs have many desirable properties such as (i) very negligible vapor pressure, (ii) high thermal stability, (iii) wide electrochemical window, (iv) tunability, (v) non flammability, and (vi) environment friendly. Some of the representative ILs used as electrolytes in rechargeable batteries with corresponding electrochemical systems have been tabulated. Schematic open-circuit-diagram of an electrolyte and SEI formation in a thermodynamically stable cell has been discussed from the viewpoint of electronic energy levels. Simulations of the ILs to understand and exploit the solvation effect is of paramount importance in imparting performance enhancement in LIBs and their properties. The first principle methods have been widely used to study the effect of cation and anion used, on its ESW, Lithium oxidation/reduction rate at the anode/cathode, Lithium ion conductivity, viscosity, solvation shell constituents. An iterative SCRF can be used to calculate the actual charge distribution in the solute cavity. Typical error in ESW estimation by thermodynamic cycles method is $\sim 15\%$ while that for HOMO/LUMO is $\sim 50\%$. Non-polarizable model predicts slower dynamics for IL in comparison to the experimental results. A scaling factor, accounting for partial charge, is determined for a specific IL therefore, it lacks transferability between different ILs and it fails to produce good results in case of IL mixtures. The Drude oscillator model incorporates anisotropy in the polarization of the atom, which is advantageous over the IPD method. Phase equilibrium calculations using NPT, Grand Canonical and Gibbs ensemble MC simulations are found to be suitable rather than canonical ensembles. The ion-pair and cluster movement leads to equilibration of the system within reasonable (5×10^5) MC steps with smaller total energy compared to the normal simulation. GCMC and GEMC simulation can also be modified with the ion-pair and cluster movement and are more efficient for phase transformation simulation.

Acknowledgements

K.C. and M.K.S acknowledge IIT Bhubaneswar for the fellowship. KKS acknowledges funding from UAY projects.

Conflict of interest

The authors declare no conflict of interest.

Author details

Kajari Chatterjee¹, M.K. Sridhar¹, Akhilesh Kumar Singh^{2*} and Kisor Kumar Sahu^{1,3*}


1 School of Minerals, Metallurgical and Materials Engineering, Indian Institute of Technology Bhubaneswar, Bhubaneswar, India

2 School of Basic Sciences, Indian Institute of Technology Bhubaneswar, Bhubaneswar, India

3 Center of Excellence for Novel Energy Materials (CENEMA), Indian Institute of Technology Bhubaneswar, Bhubaneswar, India

*Address all correspondence to: aksingh@iitbbs.ac.in and kisorsahu@iitbbs.ac.in

IntechOpen

© 2022 The Author(s). Licensee IntechOpen. This chapter is distributed under the terms of the Creative Commons Attribution License (<http://creativecommons.org/licenses/by/3.0>), which permits unrestricted use, distribution, and reproduction in any medium, provided the original work is properly cited. 

References

- [1] Haregewoin AM, Wotango AS, Hwang B-J. Electrolyte additives for lithium ion battery electrodes: Progress and perspectives. *Energy and Environmental Science*. 2016;**9**(6): 1955-1988. DOI: 10.1039/C6EE00123H
- [2] Kaseem M, Fatimah S, Nashrah N, Ko YG. Recent progress in surface modification of metals coated by plasma electrolytic oxidation: Principle, structure, and performance. *Progress in Materials Science*. 2021;**117**:100735. DOI: 10.1016/j.pmatsci.2020.100735
- [3] Tarascon J-M, Armand M. Issues and challenges facing rechargeable lithium batteries. In: *Materials for Sustainable Energy*. UK: Co-Published with Macmillan Publishers Ltd; 2010. pp. 171-179. DOI: 10.1142/9789814317665_0024
- [4] Blomgren GE. The development and future of lithium ion batteries. *Journal of the Electrochemical Society*. 2017; **164**(1):A5019-A5025. DOI: 10.1149/2.0251701jes
- [5] "sony nexelion." [Online]. Available from: <https://www.sony.com/en/SonyInfo/News/Press/200502/05-006E/>
- [6] Ding Y, Cano ZP, Yu A, Lu J, Chen Z. Automotive Li-ion batteries: Current status and future perspectives. *Electrochemical Energy Reviews*. 2019; **2**(1):1-28. DOI: 10.1007/s41918-018-0022-z
- [7] Tarascon J, Guyomard D. New electrolyte compositions stable over the 0 to 5 V voltage range and compatible with the $\text{Li}_{1+x}\text{Mn}_2\text{O}_4$ /carbon Li-ion cells. *Solid State Ionics*. 1994;**69**(3-4):293-305. DOI: 10.1016/0167-2738(94)90418-9
- [8] Zhang SS. A review on electrolyte additives for lithium-ion batteries. *Journal of Power Sources*. 2006;**162**(2): 1379-1394. DOI: 10.1016/j.jpowsour.2006.07.074
- [9] Kim G-T et al. Development of ionic liquid-based lithium battery prototypes. *Journal of Power Sources*. 2012;**199**: 239-246. DOI: 10.1016/j.jpowsour.2011.10.036
- [10] Yim T, Kwon M-S, Mun J, Lee KT. Room temperature ionic liquid-based electrolytes as an alternative to carbonate-based electrolytes. *Israel Journal of Chemistry*. 2015;**55**(5): 586-598. DOI: 10.1002/ijch.201400181
- [11] Watanabe M, Thomas ML, Zhang S, Ueno K, Yasuda T, Dokko K. Application of ionic liquids to energy storage and conversion materials and devices. *Chemical Reviews*. 2017;**117**(10): 7190-7239. DOI: 10.1021/acs.chemrev.6b00504
- [12] Sato T, Maruo T, Marukane S, Takagi K. Ionic liquids containing carbonate solvent as electrolytes for lithium ion cells. *Journal of Power Sources*. 2004;**138**(1-2): 253-261. DOI: 10.1016/j.jpowsour.2004.06.027
- [13] Vo TD, Nguyen HV, Nguyen QD, Phung Q, Tran VM, Le PLM. Carbonate solvents and ionic liquid mixtures as an electrolyte to improve cell safety in sodium-ion batteries. *Journal of Chemistry*. 2019;**2019**:1-10. DOI: 10.1155/2019/7980204
- [14] Kim J, Kang H, Hwang K, Yoon S. Thermal decomposition study on Li_2O_2 for Li_2NiO_2 synthesis as a sacrificing positive additive of lithium-ion batteries. *Molecules*. 2019;**24**(24):4624. DOI: 10.3390/molecules24244624

- [15] Guerfi A et al. Improved electrolytes for Li-ion batteries: Mixtures of ionic liquid and organic electrolyte with enhanced safety and electrochemical performance. *Journal of Power Sources*. 2010;**195**(3):845-852. DOI: 10.1016/j.jpowsour.2009.08.056
- [16] Saruwatari H, Kuboki T, Kishi T, Mikoshiba S, Takami N. Imidazolium ionic liquids containing LiBOB electrolyte for lithium battery. *Journal of Power Sources*. 2010;**195**(5):1495-1499. DOI: 10.1016/j.jpowsour.2009.08.081
- [17] Plylahan N, Kerner M, Lim D-H, Matic A, Johansson P. Ionic liquid and hybrid ionic liquid/organic electrolytes for high temperature lithium-ion battery application. *Electrochimica Acta*. 2016; **216**:24-34. DOI: 10.1016/j.electacta.2016.08.025
- [18] Anastas PT. Green chemistry and the role of analytical methodology development. *Critical Reviews in Analytical Chemistry*. 1999;**29**(3): 167-175. DOI: 10.1080/10408349891199356
- [19] Anastas PT, Kirchoff MM. Origins, current status, and future challenges of green chemistry. *Accounts of Chemical Research*. 2002;**35**(9):686-694. DOI: 10.1021/ar010065m
- [20] Horváth IT, Anastas PT. Innovations and green chemistry. *Chemical Reviews*. 2007;**107**(6):2169-2173. DOI: 10.1021/cr078380v
- [21] U. N. Environment. About Montreal protocol. Ozonaction. 2018. Available from: <http://www.unep.org/ozonaction/who-we-are/about-montreal-protocol> [Accessed: June 7, 2022]
- [22] Welton T. Room-temperature ionic liquids. *Solvents for synthesis and catalysis*. *Chemical Reviews*. 1999; **99**(8):2071-2084. DOI: 10.1021/cr980032t
- [23] Plechkova NV, Seddon KR. Applications of ionic liquids in the chemical industry. *Chemical Society Reviews*. 2008;**37**(1):123-150. DOI: 10.1039/B006677J
- [24] Wilkes JS. A short history of ionic liquids—From molten salts to neoteric solvents. *Green Chemistry*. 2002;**4**(2): 73-80. DOI: 10.1039/b110838g
- [25] Freemantle M. *An Introduction to Ionic Liquids*. Cambridge, UK: RSC Pub; 2010
- [26] Zingg SP, Dworkin AS, et al. Reactivity of anthracene in liquid SbCl₃–AlCl₃–N–(1-butyl) Pyridinium chloride mixtures. *Journal of the Electrochemical Society*. 1984;**131**(7): 1602-1608. DOI: 10.1149/1.2115917
- [27] Kianfar E, Mafi S. Ionic liquids: Properties, application, and synthesis. *Fine Chemical Engineering*. 2020;**2**: 22-31. DOI: 10.37256/fce.212021693
- [28] Nikfarjam N et al. Antimicrobial ionic liquid-based materials for biomedical applications. *Advanced Functional Materials*. 2021;**31**(42): 2104148. DOI: 10.1002/adfm.202104148
- [29] Giernoth R. Task-specific ionic liquids. *Angewandte Chemie, International Edition*. 2010;**49**(16): 2834-2839. DOI: 10.1002/anie.200905981
- [30] MacFarlane DR et al. New dimensions in salt–solvent mixtures: A 4th evolution of ionic liquids. *Faraday Discussions*. 2018;**206**:9-28. DOI: 10.1039/C7FD00189D
- [31] Huddleston JG, Visser AE, Reichert WM, Willauer HD, Broker GA,

Rogers RD. Characterization and comparison of hydrophilic and hydrophobic room temperature ionic liquids incorporating the imidazolium cation. *Green Chemistry*. 2001;**3**(4): 156-164. DOI: 10.1039/b103275p

[32] John Wiley & Sons, Inc, editor. Kirk-Othmer Encyclopedia of Chemical Technology. 1st ed. Hoboken, NJ, United States: John Wiley & Sons, Inc.; 2000. DOI: 10.1002/0471238961

[33] Chavan SS, Sharma YO, Degani MS. Cost-effective ionic liquid for environmentally friendly synthesis of 3,4-dihydropyrimidin-2(1H)-ones. *Green Chemistry Letters and Reviews*. 2009;**2**(3):175-179. DOI: 10.1080/17518250903252260

[34] Heintz A. Recent developments in thermodynamics and thermophysics of non-aqueous mixtures containing ionic liquids. A review. *The Journal of Chemical Thermodynamics*. 2005;**37**(6): 525-535. DOI: 10.1016/j.jct.2005.04.003

[35] Endres F, Zein El Abedin S. Air and water stable ionic liquids in physical chemistry. *Physical Chemistry Chemical Physics*. 2006;**8**(18):2101. DOI: 10.1039/b600519p

[36] Matsumoto H, Matsuda T, Tsuda T, Hagiwara R, Ito Y, Miyazaki Y. The application of room temperature molten salt with low viscosity to the electrolyte for dye-sensitized solar cell. *Chemistry Letters*. 2001;**30**(1):26-27. DOI: 10.1246/cl.2001.26

[37] Papageorgiou N et al. The performance and stability of ambient temperature molten salts for solar cell applications. *Journal of the Electrochemical Society*. 1996;**143**(10): 3099-3108. DOI: 10.1149/1.1837171

[38] Hagiwara R, Ito Y. Room temperature ionic liquids of

alkylimidazolium cations and fluoroanions. *Journal of Fluorine Chemistry*. 2000;**105**(2):221-227. DOI: 10.1016/S0022-1139(99)00267-5

[39] Seddon KR, Stark A, Torres M-J. Influence of chloride, water, and organic solvents on the physical properties of ionic liquids. *Pure and Applied Chemistry*. 2000;**72**(12):2275-2287. DOI: 10.1351/pac200072122275

[40] Mikkola J-P, Virtanen P, Sjöholm R. Aliquat 336®—A versatile and affordable cation source for an entirely new family of hydrophobic ionic liquids. *Green Chemistry*. 2006;**8**(3):250. DOI: 10.1039/b512819f

[41] Noda A, Watanabe M. Highly conductive polymer electrolytes prepared by in situ polymerization of vinyl monomers in room temperature molten salts. *Electrochimica Acta*. 2000;**45**(8-9):1265-1270. DOI: 10.1016/S0013-4686(99)00330-8

[42] Bonhôte P, Dias A-P, Papageorgiou N, Kalyanasundaram K, Grätzel M. Hydrophobic, highly conductive ambient-temperature molten salts. *Inorganic Chemistry*. 1996;**35**(5): 1168-1178. DOI: 10.1021/ic951325x

[43] Fuller J, Carlin RT, Osteryoung RA. The room temperature ionic liquid 1-Ethyl-3-methylimidazolium Tetrafluoroborate: Electrochemical couples and physical properties. *Journal of the Electrochemical Society*. 1997;**144**(11):3881-3886. DOI: 10.1149/1.1838106

[44] McEwen AB, Ngo HL, LeCompte K, Goldman JL. Electrochemical properties of imidazolium salt electrolytes for electrochemical capacitor applications. *Journal of the Electrochemical Society*. 1999;**146**(5):1687-1695. DOI: 10.1149/1.1391827

- [45] Maton C, De Vos N, Stevens CV. Ionic liquid thermal stabilities: Decomposition mechanisms and analysis tools. *Chemical Society Reviews*. 2013; **42**(13):5963. DOI: 10.1039/c3cs60071h
- [46] Bier M, Dietrich S. Vapour pressure of ionic liquids. *Molecular Physics*. 2010; **108**(2):211-214. DOI: 10.1080/00268971003604609
- [47] Xue Z, Qin L, Jiang J, Mu T, Gao G. Thermal, electrochemical and radiolytic stabilities of ionic liquids. *Physical Chemistry Chemical Physics*. 2018; **20**(13):8382-8402. DOI: 10.1039/C7CP07483B
- [48] Ngo HL, LeCompte K, Hargens L, McEwen AB. Thermal properties of imidazolium ionic liquids. *Thermochimica Acta*. 2000; **357-358**: 97-102. DOI: 10.1016/S0040-6031(00)00373-7
- [49] Wu B, Liu W, Zhang Y, Wang H. Do we understand the recyclability of ionic liquids? *Chemistry—A European Journal*. 2009; **15**(8):1804-1810. DOI: 10.1002/chem.200801509
- [50] Jastorff B et al. How hazardous are ionic liquids? Structure–activity relationships and biological testing as important elements for sustainability evaluation. This work was presented at the green solvents for catalysis meeting held in Bruchsal, Germany, 13–16th October 2002. *Green Chemistry*. 2003; **5**(2):136-142. DOI: 10.1039/b211971d
- [51] Zhao D, Liao Y, Zhang Z. Toxicity of ionic liquids. *CLEAN—Soil Air Water*. 2007; **35**(1):42-48. DOI: 10.1002/clen.200600015
- [52] Ranke J, Stolte S, Störmann R, Arning J, Jastorff B. Design of Sustainable Chemical Products. The example of ionic liquids. *Chemical Reviews*. 2007; **107**(6):2183-2206. DOI: 10.1021/cr050942s
- [53] Borgel V, Markevich E, Aurbach D, Semrau G, Schmidt M. On the application of ionic liquids for rechargeable Li batteries: High voltage systems. *Journal of Power Sources*. 2009; **189**(1):331-336. DOI: 10.1016/j.jpowsour.2008.08.099
- [54] Peng Y, Badam R, Jayakumar TP, Wannapakdee W, Changtong C, Matsumi N. Drastic effect of salt concentration in ionic liquid on performance of lithium sulfur battery. *Journal of the Electrochemical Society*. 2022; **169**(5):050515. DOI: 10.1149/1945-7111/ac6bc6
- [55] Lin X et al. Cation effect on ionic liquid-involved polymer electrolytes for solid-state lithium metal batteries. *New Journal of Chemistry*. 2022; **46**: 10379-10385. DOI: 10.1039/D1NJ06210G
- [56] Ferrari S et al. Alkoxy substituted imidazolium-based ionic liquids as electrolytes for lithium batteries. *Journal of Power Sources*. 2013; **235**:142-147. DOI: 10.1016/j.jpowsour.2013.01.149
- [57] Sirisopanaporn C, Fernicola A, Scrosati B. New, ionic liquid-based membranes for lithium battery application. *Journal of Power Sources*. 2009; **186**(2):490-495. DOI: 10.1016/j.jpowsour.2008.10.036
- [58] Moreno M et al. Ionic liquid electrolytes for safer lithium batteries: I. investigation around optimal formulation. *Journal of the Electrochemical Society*. 2017; **164**(1): A6026-A6031. DOI: 10.1149/2.0051701jes
- [59] Zhang H et al. Ionic liquid electrolyte with highly concentrated LiTFSI for lithium metal batteries. *Electrochimica*

Acta. 2018;**285**:78-85. DOI: 10.1016/j.electacta.2018.07.231

[60] Quezada D, Honores J, Ruiz-León D. Zinc Stannate as anode and Pyrrolidinium-based room temperature ionic liquid as electrolyte for Lithium-ion cells. *International Journal of Electrochemical Science*. 2021;**21**:210212. DOI: 10.20964/2021.02.34

[61] Yoon H, Shin S, Park S, Shin MW. Low-viscosity quaternary ammonium-based ionic liquid electrolytes for lithium air batteries. *Journal of Molecular Liquids*. 2022;**359**:119352. DOI: 10.1016/j.molliq.2022.119352

[62] Seki S et al. Quaternary ammonium room-temperature ionic liquid/lithium salt binary electrolytes: Electrochemical study. *Journal of the Electrochemical Society*. 2008;**155**(6):A421. DOI: 10.1149/1.2899014

[63] Lin X, Kaviani R, Lu Y, Hu Q, Shao-Horn Y, Grinstaff MW. Thermally-responsive, nonflammable phosphonium ionic liquid electrolytes for lithium metal batteries: Operating at 100 degrees celsius. *Chemical Science*. 2015;**6**(11):6601-6606. DOI: 10.1039/C5SC01518A

[64] Hema M, Selvasakerpandian S, Hirankumar G, Sakunthala A, Arunkumar D, Nithya H. Structural and thermal studies of PVA:NH4I. *Journal of Physics and Chemistry of Solids*. 2009; **70**(7):1098-1103. DOI: 10.1016/j.jpics.2009.06.005

[65] Rathnayake RMLL, Perera KS, Vidanapathirana KP, Polymer Electronics Research Laboratory, Department of Electronics, Wayamba University of Sri Lanka, Kuliyaipitiya, Sri Lanka. Past, present and future of ionic liquid based polymer electrolytes. *AIMS Energy*. 2020;**8**(2):231-251. DOI: 10.3934/energy.2020.2.231

[66] Yusuf SNF, Yahya R, Arof AK. Ionic liquid enhancement of polymer electrolyte conductivity and their effects on the performance of electrochemical devices. In: Handy S, editor. *Progress and Developments in Ionic Liquids*. London: InTech; 2017. DOI: 10.5772/65752

[67] Chandra S. Proton-conducting gel electrolyte. *Solid State Ionics*. 2002;**154-155**:609-619. DOI: 10.1016/S0167-2738(02)00505-2

[68] Koch VR, Dominey LA, Nanjundiah C, Ondrechen MJ. The intrinsic anodic stability of several anions comprising solvent-free ionic liquids. *Journal of the Electrochemical Society*. 1996;**143**(3):798-803. DOI: 10.1149/1.1836540

[69] Markevich E, Baranchugov V, Aurbach D. On the possibility of using ionic liquids as electrolyte solutions for rechargeable 5V Li ion batteries. *Electrochemistry Communications*. 2006;**8**(8):1331-1334. DOI: 10.1016/j.elecom.2006.06.002

[70] Wang Y, Zaghbi K, Guerfi A, Bazito FFC, Torresi RM, Dahn JR. Accelerating rate calorimetry studies of the reactions between ionic liquids and charged lithium ion battery electrode materials. *Electrochimica Acta*. 2007; **52**(22):6346-6352. DOI: 10.1016/j.electacta.2007.04.067

[71] Goodenough JB, Kim Y. Challenges for rechargeable Li batteries. *Chemistry of Materials*. 2010;**22**(3):587-603. DOI: 10.1021/cm901452z

[72] Chatterjee K, Pathak AD, Lakma A, Sharma CS, Sahu KK, Singh AK. Synthesis, characterization and application of a non-flammable dicationic ionic liquid in lithium-ion battery as electrolyte additive. *Scientific*

Reports. 2020;**10**(1):9606. DOI: 10.1038/s41598-020-66341-x

[73] Chatterjee K, Pathak AD, Sahu KK, Singh AK. New Thiourea-based ionic liquid as an electrolyte additive to improve cell safety and enhance electrochemical performance in lithium-ion batteries. *ACS Omega*. 2020;**5**(27):16681-16689. DOI: 10.1021/acsomega.0c01565

[74] Marenich AV, Cramer CJ, Truhlar DG. Universal solvation model based on solute electron density and on a continuum model of the solvent defined by the bulk dielectric constant and atomic surface tensions. *The Journal of Physical Chemistry. B*. 2009;**113**(18): 6378-6396. DOI: 10.1021/jp810292n

[75] Tomasi J, Mennucci B, Cammi R. Quantum mechanical continuum solvation models. *Chemical Reviews*. 2005;**105**(8):2999-3094. DOI: 10.1021/cr9904009

[76] Tomasi J, Mennucci B, Cancès E. The IEF version of the PCM solvation method: An overview of a new method addressed to study molecular solutes at the QM ab initio level. *Journal of Molecular Structure: THEOCHEM*. 1999; **464**(1-3):211-226. DOI: 10.1016/S0166-1280(98)00553-3

[77] Miertuš S, Scrocco E, Tomasi J. Electrostatic interaction of a solute with a continuum. A direct utilization of AB initio molecular potentials for the prevision of solvent effects. *Chemical Physics*. 1981;**55**(1):117-129. DOI: 10.1016/0301-0104(81)85090-2

[78] Kazemiabnavi S, Zhang Z, Thornton K, Banerjee S. Electrochemical stability window of imidazolium-based ionic liquids as electrolytes for lithium batteries. *The Journal of Physical Chemistry. B*. 2016;**120**(25):5691-5702. DOI: 10.1021/acs.jpcc.6b03433

[79] Shao N, Sun X-G, Dai S, Jiang D. Electrochemical windows of sulfone-based electrolytes for high-voltage Li-ion batteries. *The Journal of Physical Chemistry. B*. 2011;**115**(42):12120-12125. DOI: 10.1021/jp204401t

[80] Zhang X, Pugh JK, Ross PN. Computation of thermodynamic oxidation potentials of organic solvents using density functional theory. *Journal of the Electrochemical Society*. 2001; **148**(5):E183-E188. DOI: 10.1149/1.1362546

[81] Chen JL, Noodleman L, Case DA, Bashford D. Incorporating solvation effects into density functional electronic structure calculations. *The Journal of Physical Chemistry*. 1994;**98**(43): 11059-11068. DOI: 10.1021/j100094a013

[82] Angenendt K, Johansson P. Ionic liquid based lithium battery electrolytes: Charge carriers and interactions derived by density functional theory calculations. *The Journal of Physical Chemistry. B*. 2011;**115**(24):7808-7813. DOI: 10.1021/jp2036108

[83] Kiratidis AL, Miklavcic SJ. Density functional theory of confined ionic liquids: A survey of the effects of ion type, molecular charge distribution, and surface adsorption. *The Journal of Chemical Physics*. 2019;**150**(18):184502. DOI: 10.1063/1.5093552

[84] Saravanan S, Venkataramanan A, Anantharaj R. DFT study on interaction of Estrone and imidazolium-based hydrophobic ionic liquids. In: Bulnes F, Stavrou VN, Morozov O, Bourdine AV, editors. *Advances in Quantum Communication and Information*. London: IntechOpen; 2020. DOI: 10.5772/intechopen.86821

[85] Chen L, Bryantsev VS. A density functional theory based approach for

predicting melting points of ionic liquids. *Physical Chemistry Chemical Physics*. 2017;**19**(5):4114-4124.
DOI: 10.1039/C6CP08403F

[86] Bayly CI, Cieplak P, Cornell W, Kollman PA. A well-behaved electrostatic potential based method using charge restraints for deriving atomic charges: The RESP model. *The Journal of Physical Chemistry*. 1993; **97**(40):10269-10280. DOI: 10.1021/j100142a004

[87] Chen M, Pendrill R, Widmalm G, Brady JW, Wohlert J. Molecular dynamics simulations of the ionic liquid 1-*n*-Butyl-3-Methylimidazolium chloride and its binary mixtures with ethanol. *Journal of Chemical Theory and Computation*. 2014;**10**(10):4465-4479.
DOI: 10.1021/ct500271z

[88] Cui K, Yethiraj A, Schmidt JR. Influence of charge scaling on the solvation properties of ionic liquid solutions. *The Journal of Physical Chemistry. B*. 2019;**123**(43):9222-9229.
DOI: 10.1021/acs.jpcc.9b08033

[89] Son CY, McDaniel JG, Schmidt JR, Cui Q, Yethiraj A. First-principles united atom force field for the ionic liquid BMIM⁺ BF₄⁻: An alternative to charge scaling. *The Journal of Physical Chemistry. B*. 2016;**120**(14):3560-3568.
DOI: 10.1021/acs.jpcc.5b12371

[90] Thole BT. Molecular polarizabilities calculated with a modified dipole interaction. *Chemical Physics*. 1981; **59**(3):341-350. DOI: 10.1016/0301-0104(81)85176-2

[91] Bedrov D, Borodin O, Li Z, Smith GD. Influence of polarization on structural, thermodynamic, and dynamic properties of ionic liquids obtained from molecular dynamics simulations. *The Journal of Physical*

Chemistry. B. 2010;**114**(15):4984-4997.
DOI: 10.1021/jp911670f

[92] Yan T, Wang Y, Knox C. On the structure of ionic liquids: Comparisons between electronically polarizable and nonpolarizable models I. *The Journal of Physical Chemistry. B*. 2010;**114**(20): 6905-6921. DOI: 10.1021/jp9089112

[93] Zhao Y et al. The behavior of ionic liquids under high pressure: A molecular dynamics simulation. *The Journal of Physical Chemistry. B*. 2012;**116**(35): 10876-10884. DOI: 10.1021/jp3070568

[94] Lemkul JA, Huang J, Roux B, MacKerell AD. An empirical polarizable force field based on the classical Drude oscillator model: Development history and recent applications. *Chemical Reviews*. 2016;**116**(9):4983-5013.
DOI: 10.1021/acs.chemrev.5b00505

[95] Schmollngruber M, Lesch V, Schröder C, Heuer A, Steinhäuser O. Comparing induced point-dipoles and Drude oscillators. *Physical Chemistry Chemical Physics*. 2015;**17**(22): 14297-14306. DOI: 10.1039/C4CP04512B

[96] Schröder C. Comparing reduced partial charge models with polarizable simulations of ionic liquids. *Physical Chemistry Chemical Physics*. 2012; **14**(9):3089. DOI: 10.1039/c2cp23329k

[97] Chen J. Theory and applications of fluctuating-charge models. 2010.
DOI: 10.48550/arXiv.1004.0186

[98] Cavalcante A d O, Ribeiro MCC, Skaf MS. Polarizability effects on the structure and dynamics of ionic liquids. *The Journal of Chemical Physics*. 2014; **140**(14):144108. DOI: 10.1063/1.4869143

[99] Self J, Bergstrom HK, Fong KD, McCloskey BD, Persson KA. A

theoretical model for computing freezing point depression of lithium-ion battery electrolytes. *Journal of the Electrochemical Society*. 2021;**168**(12): 120532. DOI: 10.1149/1945-7111/ac3e47

[100] Rane KS, Errington JR. Using Monte Carlo simulation to compute liquid–vapor saturation properties of ionic liquids. *The Journal of Physical Chemistry. B*. 2013;**117**(26):8018-8030. DOI: 10.1021/jp404207x

[101] Orkoulas G, Panagiotopoulos AZ. Free energy and phase equilibria for the restricted primitive model of ionic fluids from Monte Carlo simulations. *The Journal of Chemical Physics*. 1994; **101**(2):1452-1459. DOI: 10.1063/1.467770

[102] Shah JK, Brennecke JF, Maginn EJ. Thermodynamic properties of the ionic liquid 1-n-butyl-3-methylimidazolium hexafluorophosphate from Monte Carlo simulations. *Green Chemistry*. 2002; **4**(2):112-118. DOI: 10.1039/b110725a

[103] Panagiotopoulos AZ. Molecular simulation of phase equilibria: Simple, ionic and polymeric fluids. *Fluid Phase Equilibria*. 1992;**76**:97-112. DOI: 10.1016/0378-3812(92)85080-R

[104] Armand M, Endres F, MacFarlane DR, Ohno H, Scrosati B. Ionic-liquid materials for the electrochemical challenges of the future. In: *Materials for Sustainable Energy*. UK: Co-Published with Macmillan Publishers Ltd; 2010. pp. 129-137. DOI: 10.1142/9789814317665_0020

Section 2

Specific Ionic Liquids for
Industrial Applications

Perspective Chapter: Applications of Novel Ionic Liquids as Catalyst

Ganesan Kilivelu

Abstract

Ionic liquids have much interesting attention in the area of biomedical and it's an alternative to traditional organic solvents owing to their unique chemical, physical properties and environmentally eco-friendly catalytic responses. Ionic liquids have distinct properties like tunability that allows their physical and chemical behaviors to be changed as desired by changing the organic cations with inorganic anions or inorganic cations with organic anions or both cation and anion from organic moieties. Most of the organic reactions are carried out with assistance of catalyst, usually commercially available catalyst are very expensive, more hydroscopic in nature, thermally unstable and very difficult to recycle them but ionic liquids are acted as potential Lewis acidic behaviors, thermally stable, easily recycle inexpensive compared to commercial catalyst and easy to prepare electrically neutral organic cation which are loosely bind with inorganic anions, and organic (pyridinium/imidazolium/piperidinium) cation could be easily accelerate (or) activate the functional group for most of the organic reactions. Hence, ionic liquids plays a vital role in modern organic synthetic field and may be inevitable in future research.

Keywords: substituted dimeric imidazolium cation, trimeric imidazolium salt, catalyst regenerations, pyrimidine derivative, one pot preparation

1. Introduction

Ionic liquids have attracted increasing interest from chemist in the last few decades because of their distinguishable properties including chemical stability, non-flammability, non-volatility and high thermal stability. Commercially available catalysts are very expensive, more hydroscopic in nature, thermally unstable and very difficult to recycle, whereas ionic liquids are thermally stable, easily recyclable, inexpensive compared to commercial catalyst, easy to prepare and have potential Lewis acidic behavior and so, nowadays it plays a vital role in catalysis. Ionic liquids are electrically neutral molecule consist of organic cations which are loosely bind with inorganic anions, hence organic pyridinium/imidazolium/piperidinium cation can easily accelerate (or) activate the functional group in most of the organic reactions. Most of the organic reactions are carried out with the assistance of catalyst [1, 2]. for example, in one pot preparation of 3,4-dihydro-3-substituted oxazine derivatives at room temperature, 1-ethylimidazolium sulphonate is used as a catalyst [3]. Acid based

bifunctional pyridinium salt used as a catalyst in Knoevenagel condensation reaction with and without solvent [4]. *N*-Methyl pyridinium bromide acted as highly efficient reagent for aliphatic nucleophilic substitution reaction of sulphate aryl substituted aliphatic ether [5]. 1,4-Diazobicyclo[2.2.2]octane based quarternary ammonium bromide which is recyclable, cheaper and environmentally friendly are used in the preparation of bisnaphtholmethane [6]. Chiral biaryl aluminate anion with imidazolium salt showed excellent catalytic response for asymmetric Baeyer-villiger oxidation with higher percentage of conversion [7]. Preparation of hydroxyl methyl substituted furfural in higher yield with shorter reaction time is achieved in the presence of chiral dimeric ionic liquids [8]. Bronsted acidic ionic liquid is used as a catalyst in the preparation of pyridylimidazopyridine [9].

Lewis acid accepts the pair of electrons to attain the octet electronic configuration. Acid is the electron deficient positive charged species that accepts the electrons to form a covalent bond. Base is the electron rich negative charged species that donates to electron deficient ions to form a covalent bond. Organic molecule containing electro positive nitrogen are acted as second-generation Lewis acid. Lewis acid such as $ZnCl_2$, BF_3 , $SnCl_3$, $AlCl_3$ and CH_3AlCl_2 catalyze the reaction between electron rich diene and electron deficient dienophile and also catalyze the inverse electron demand Diels Alder reaction. In most of the organic reactions like Aldol condensation reaction, Friedel craft alkylation and acylation, carbon-carbon (or) carbon-nitrogen/carbon-sulfur/carbon-oxygen bond formation can be catalyzed by Lewis acid. Most of the organic reactions are carried out with polar/non-polar organic solvents rather than water, because the reactants are insoluble/sparingly soluble or unstable/decompose in water. Now a days, despite few disadvantages, water plays a crucial role as a solvent for organic reactions due to its more polar nature, environment friendly, non-toxic, moderate boiling solvent, easily available and more abundant solvent in the earth. In recent years, Ionic liquids became a very interesting area of research in catalysis, drug delivery system and electro chemical aspects. ionic liquids are excellent alternate for the toxic organic solvents because of its low volatile nature, thermally stable and non-toxic nature. In this book chapter, we will discuss about the catalytic importance and plausible organic reaction mechanism of novel mono, di and trimeric imidazolium and pyridinium salts (ionic liquid) as a catalyst in Aldol condensation, Biginelli reaction, Erlenmeyer reaction, Mannich reaction and Pechmann reaction.

2. Novel 6,6'-(butane-1,4-diylbis(oxy))bis(methylene)bis(2,4-dimethyl-3-nitro-1-(4-nitrobenzyl)pyridinium) bromide used as a catalyst in Aldol condensation reaction

In Aldol condensation reaction, β -hydroxy derivatives are formed from α -hydrogen containing aldehyde (or) ketone in the presence of strong alkali. In this reaction, strong alkali abstracts the proton from α -hydrogen containing carbonyl compound and carbanion will attack another carbonyl group to form β -keto derivatives. There are two types of Aldol condensation reaction (simple and mixed Aldol condensation reactions). If both the reacting substrate are similar, then it is called simple Aldol reaction and if two different α -hydrogen containing carbon compounds are involved, then it is called mixed Aldol condensation reaction (**Figure 1**). α -Hydrogen containing aliphatic aldehydes are more reactive than the α -hydrogen containing ketones. In mixed Aldol condensation reaction, one α -hydrogen containing aliphatic aldehyde can react with or without α -hydrogen containing carbonyl compounds. The presence of

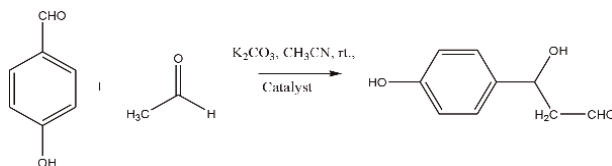


Figure 1.
Mixed Aldol Condensation reaction.

Lewis acid enhances the carbanion attack with (or) without α -hydrogen carbonyl compound in Aldol condensation reaction.

In the above reaction, a very expensive chiral catalysts are used to prepare α -hydroxy derivatives. Simple Aldol condensation reaction is more advantageous than the mixed Aldol condensation [10, 11].

Lewis acid facilitates the carbonyl compound to attack enolate nucleophile. Hongxin Liu and co-workers used very expensive catalyst which consumes longer reaction time and lesser β -hydroxy derivatives [12]. The literature shows that catalyst such as $TiCl_4$, $AlCl_3$, BF_3 , $AlCl_3$ or $ZnCl_2$ are used in Aldol condensation reaction. These catalysts activate only one carbonyl compound to facilitate the enolate attack (**Figure 2**) whereas, dimeric pyridinium salt in a very low concentration i.e. one equivalence of pyridinium salt activates two equivalence of carbonyl compounds (**Figure 3**). After completion of inter (or) intra-molecular Aldol condensation reaction, the catalyst is easily recovered, recycled and used upto four cycles [13].

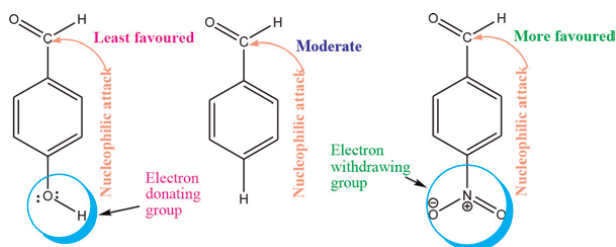


Figure 2.
Feasibility of nucleophilic attack.

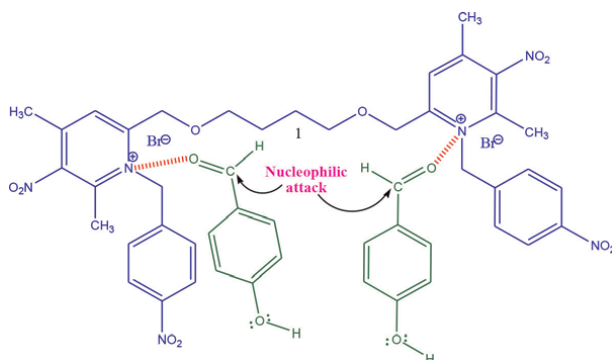


Figure 3.
Aldol condensation catalyzed by dimeric ionic liquid 1.

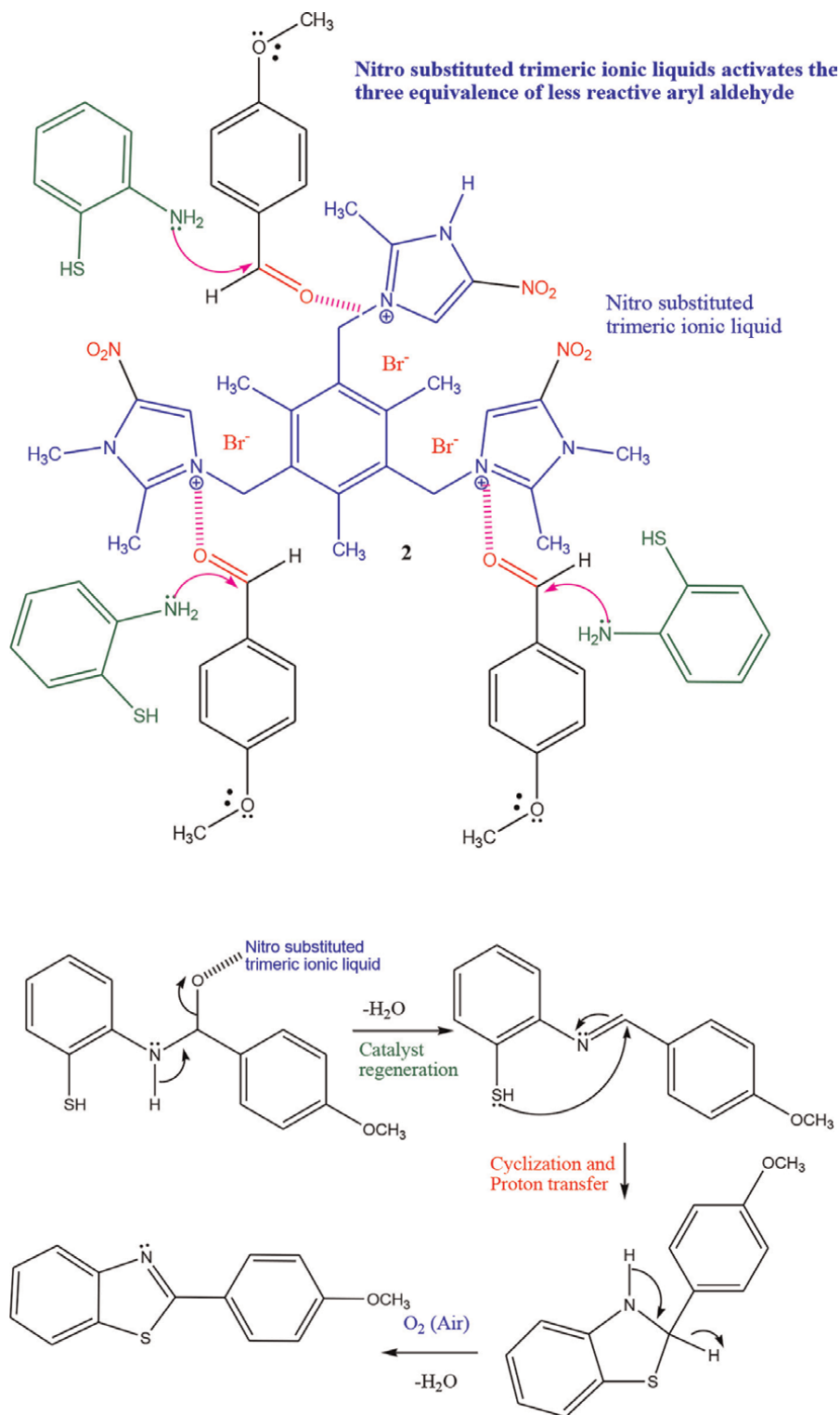


Figure 4. Plausible mechanism for benzoxazole formation with trimeric imidazolium salt 2.

2.1 Novel 3,3'-(2,4,6-trimethyl-5-((2-methyl-5-nitro-1H-imidazol-1-ium-3-yl)methyl)-1,3-phenylene)bis(methylene)bis(1,2-dimethyl-5-nitro-1H-imidazol-3-ium) bromide as a catalyst in the preparation of benzoxazole

Synthesis of dimeric and trimeric substituted imidazolium cation with different anion is carried out using easily available starting materials under conventional as well as solvent free solid supported method [14]. Benzoxazole and its derivatives are prepared using very low concentration of catalyst (dimeric/trimeric substituted imidazolium salts). Trimeric imidazolium salt showed excellent catalytic response than the dimeric substituted imidazolium salts. 0.33 equivalent of trimeric substituted imidazolium salt is sufficient to accelerate the benzoxazole formation where as other catalyst requires equal molar ratio. Benzoxazole and its derivatives are prepared by reaction between substituted aryl aldehyde and *o*-amino phenol (or) *o*-amino thiol in the presence/absence of solvents. With the required equivalence of starting materials, in the absence of catalyst for 10 hours gives only 48% of yield whereas addition of catalyst {trimeric imidazolium salt (2.2458×10^{-4} mmol)} in CH₃CN solvent under refluxing condition for 30 min. gives 89% of benzoxazole derivatives. From the above reaction, trimeric substituted imidazolium salts activate three equivalence of substituted aryl aldehyde and then *o*-phenol is more facile for cyclization (**Figure 4**). Same benzoxazole and its derivatives are prepared using trimeric substituted imidazolium salts in the absence of solvent and reaction is completed in shorter reaction time with the higher yield and with the easy purification process. It is environment friendly due to the absence of solvent. Benzoxazole is prepared with optimum concentration of trimeric substituted imidazolium salts in the presence of polar and moderately polar solvents such as CHCl₃, THF, Acetone, C₂H₅OH and DMSO. Among these solvents, DMSO showed higher percentage of benzoxazole formation in shorter reaction time [15].

2.2 Biginelli reaction catalyzed by novel 2,2'-(butane-1,4-diylbis(oxy))bis(1-(4-nitrobenzyl)pyridinium) bromide

Preparation of pyrimidone derivatives from one pot multi component reaction using ethyl acetoacetate, diamide and simple/substituted aryl aldehyde with the assistance of Lewis acid. The literature shows that, the Biginelli reaction required longer reaction time, expensive catalyst and gives very low percentage of yield [16–19].

Preparation of pyrimidine derivatives from conventional method [6] takes 24 hours to complete the reaction, whereas flexible dimeric pyridinium cation as catalyst showed excellent catalytic activity even at very low concentration by

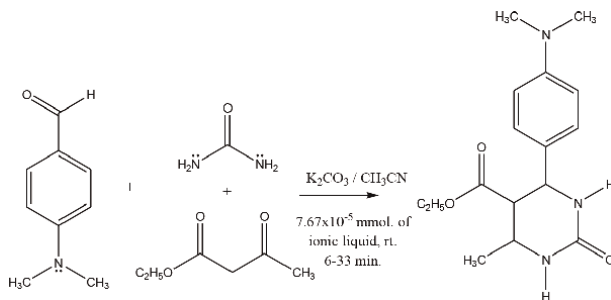


Figure 5.
Pyrimidone formation under Biginelli reaction.

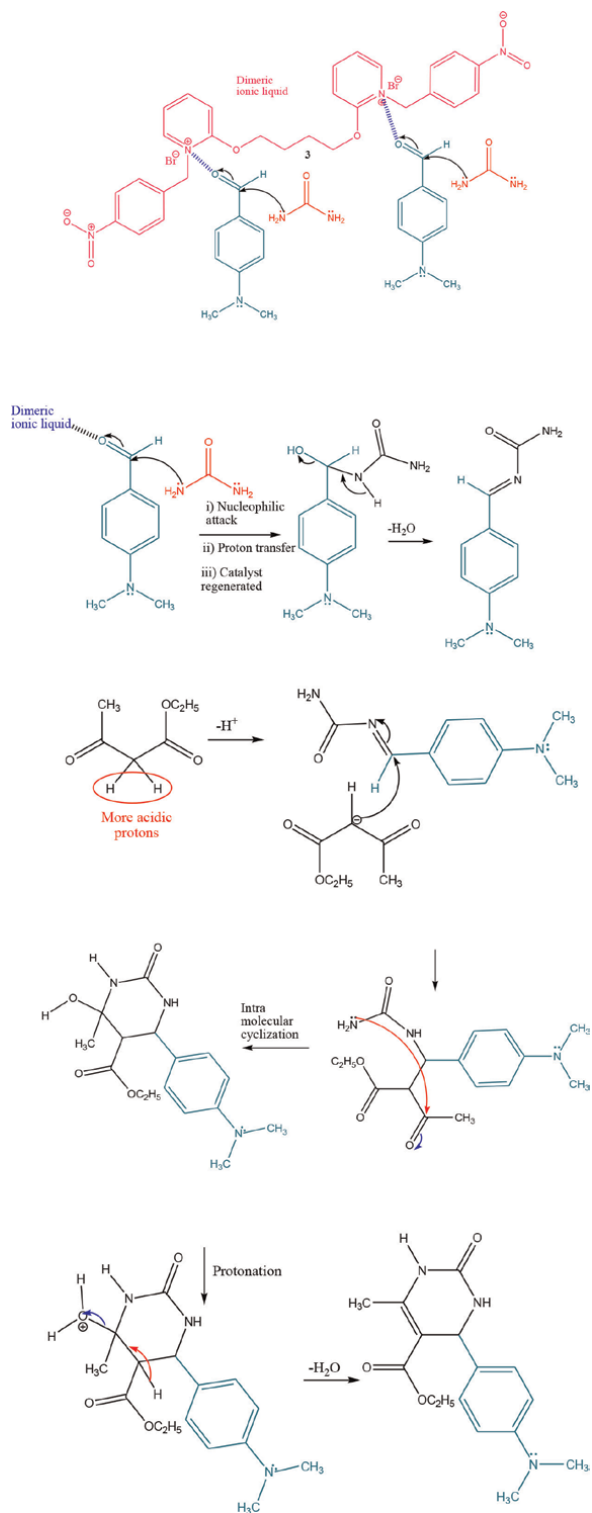


Figure 6. Plausible mechanism for formation Pyrimidone catalyzed by flexible dimeric pyridinium ionic liquid 3.

activating the substituted benzaldehyde even in half the equivalence of dimeric pyridinium salts (**Figure 5**). In this reaction (**Figure 6**), various counter anions such as Br^- , BF_4^- , PF_6^- and CF_3SO_3^- are used. Among these, bromide counter anion containing flexible dimeric pyridinium cation showed effective catalysis. Here, the size of the counter anion plays a crucial role in catalytic response. Bromide counter anion containing dimeric pyridinium cations are freely available, which in turn easily activate the simple/substituted aryl aldehyde when compared with other counter anions [20].

2.3 Novel 1,1',1''-(2,4,6-trimethylbenzene-1,3,5-triyl)tris(methylene)tris(4-(4-nitrophenyl)pyridinium) bromide as a catalyst Erlenmeyer reaction

Preparation of benzylidene oxazolone by Erlenmeyer reaction is carried out between aryl aldehyde and hippuric acid in the presence of anhydrous K_2CO_3 and acetic acid without any catalyst at room temperature for 5 hours. There is no interesting findings are observed. Some of the recent report states that, benzylidene oxazolone derivatives are also prepared using special reaction setup with higher concentration of ionic liquids (20%) at high temperature using expensive catalyst [21–23]. Hence, 4-Nitro benzyl substituted monomeric, dimeric and trimeric pyridinium bromides are tried as a catalyst for Erlenmeyer reaction. 4-Nitro benzyl substituted pyridinium salts showed excellent catalytic response and suitable for Erlenmeyer reaction when compared with other literature catalyst due to inexpensive starting material and stability. 5.7×10^{-5} mmol. concentration of 4-nitro benzyl substituted pyridinium salt is sufficient to complete Erlenmeyer reaction in short time at room temperature with higher yield. 4-Nitro benzyl substituted trimeric pyridinium cation showed excellent catalytic activity than the 4-nitro benzyl substituted dimeric pyridinium salt. Dimeric pyridinium salt showed good catalytic response than the monomeric substituted pyridinium salt. One equivalence of 4 nitro benzyl substituted pyridinium cation will activate three equivalence of carbonyl compounds (**Figure 7**), hence 0.33 equivalence of 4-nitro substituted trimeric pyridinium cation is sufficient for Erlenmeyer reaction [24].

2.4 Novel 1-benzyl-2-methoxypyridinium bromide and 1-benzyl-2,6-dimethoxypyridinium bromide as a catalyst in Mannich reaction

Aliphatic triaryl amine is one of the most important functional groups in the active pharmaceutical ingredients because of its interaction *via* H-bond donor/acceptor with the target binding site. Hence, β -amino carbonyl compound containing triaryl amine plays a crucial role in medicinal chemistry. One pot preparation of oxirane derivatives from easily available aryl amine, phenol and paraformaldehyde (**Figure 8**).

2-Methoxy benzyl substituted pyridinium salts showed excellent catalytic properties than the 2, 6-dimethoxy benzyl substituted pyridinium salts. In the catalyst, methoxy group acted as an electron donating group. If electron withdrawing group is more in the Lewis acid, then the activation of carbonyl group may be less or inactive. So, 2, 6-dimethoxy benzyl substituted pyridinium salts catalytic activity is lesser than the 2-methoxy benzyl substituted pyridinium salts. Different inorganic counter anions such as Br^- , BF_4^- , PF_6^- and CF_3SO_3^- containing 2-methoxy benzyl substituted pyridinium salts plays a crucial role in the activation of carbonyl group because of its bulkier (or) less electro negative nature. The pyridinium carbon is freely

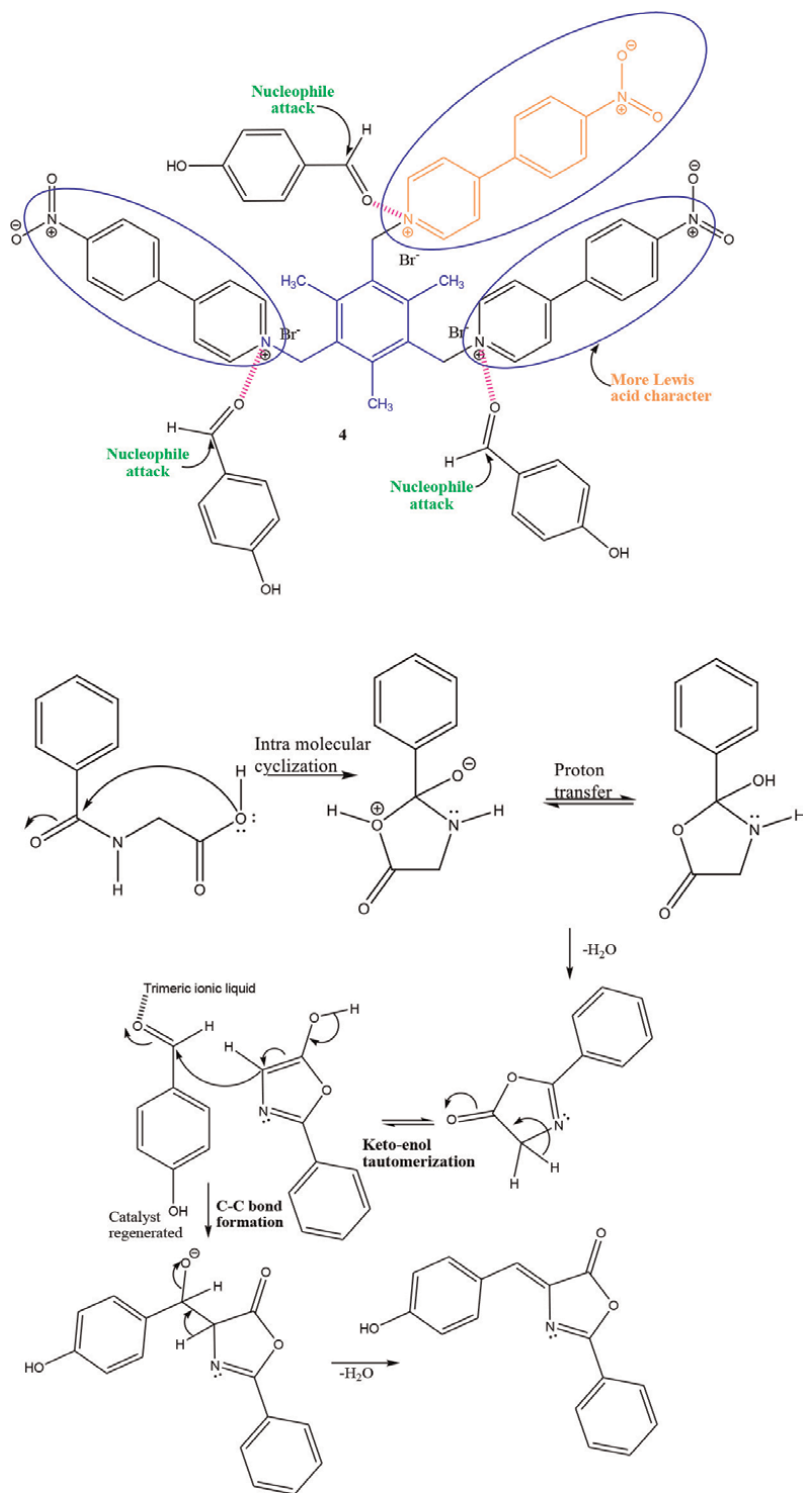


Figure 7.
Plausible mechanism for Erlenmeyer reaction.

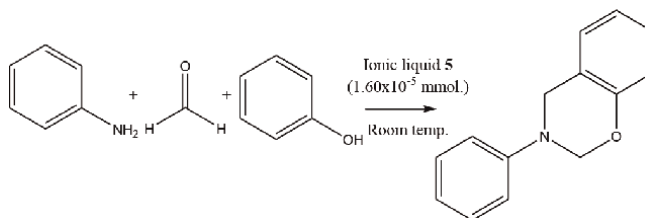


Figure 8.
Mannich reaction catalyzed by monomeric pyridinium ionic liquid 4.

available and its easily bind and activate the carbonyl compounds. The Mannich reaction is tried with 2-methoxy benzyl substituted pyridinium cation with Br^- , BF_4^- , PF_6^- and CF_3SO_3^- . Among the catalyst, bromide counter anion containing catalyst showed excellent catalytic response than the BF_4^- , PF_6^- and CF_3SO_3^- . The catalytic efficiency depends on electron deficient and freely available pyridinium cation [25]. One pot multi component Mannich reaction is carried out with the assistance of flexible longer alkyl chain containing substituted dimeric imidazolium cation with various counter anions (Br^- , BF_4^- , PF_6^- and CF_3SO_3^-). Flexible dimeric substituted imidazolium cation acted as a potential catalyst when compared with 2-methoxy benzyl substituted pyridinium cation. One equivalence of flexible dimeric substituted imidazolium cation activates two equivalences of carbonyl compound. The catalytic efficiency of flexible dimeric substituted imidazolium cation with bromide anion showed excellent catalytic response than the others. 1.66×10^{-4} mmol. (optimum concentration) of catalyst is sufficient to form Mannich product with shorter reaction time. Reuse of flexible dimeric substituted imidazolium salts showed same efficiency even after fourth cycle [26]. Substituted oxazine derivatives are acted as an important candidate in the area of medicinal industries [27, 28]. One pot multi component preparation of oxazine derivative of naphtho heterocyclic substituted compounds using various Lewis acids and Ionic liquids showed poor yield and longer reaction time [29–31]. 1,2-Dimethyl benzyl substituted imidazolium salt is used as a third generation Lewis catalyst for the preparation of naphtho heterocyclic substituted oxazine derivatives instead of expensive/inexpensive catalyst which gives poor yield with longer reaction time. 1,2-Dimethyl benzyl substituted imidazolium cation showed shorter reaction time and higher yield due to its effective activation of carbonyl compound (**Figure 9**). The efficiency of the recycled catalyst is also the same even after the fourth cycle [32].

2.5 Novel 5-methyl-2-nitro-3-(4-nitrobenzyl)-1H-imidazol-3-ium bromide as a catalyst in Pechmann reaction

2-Methyl-5-nitro substituted imidazolium salts are prepared by conventional and solid supported muffle furnace method. Quaternization of 2-methyl-5-nitro imidazole with benzyl bromide/4-nitro benzyl bromide under refluxing condition requires 13 hours for completion, whereas solvent free Muffle furnace method requires only 1/4th of reaction period. Electron Donating/electron withdrawing substituent containing phenol (**Figure 10**) is treated with ethyl acetoacetate in the presence of optimum concentration of 2.0128×10^{-4} mmol. afforded substituted chromenone derivatives. 4-chloro phenol is treated with ethyl acetate along with 2.0128×10^{-4} mmol. of

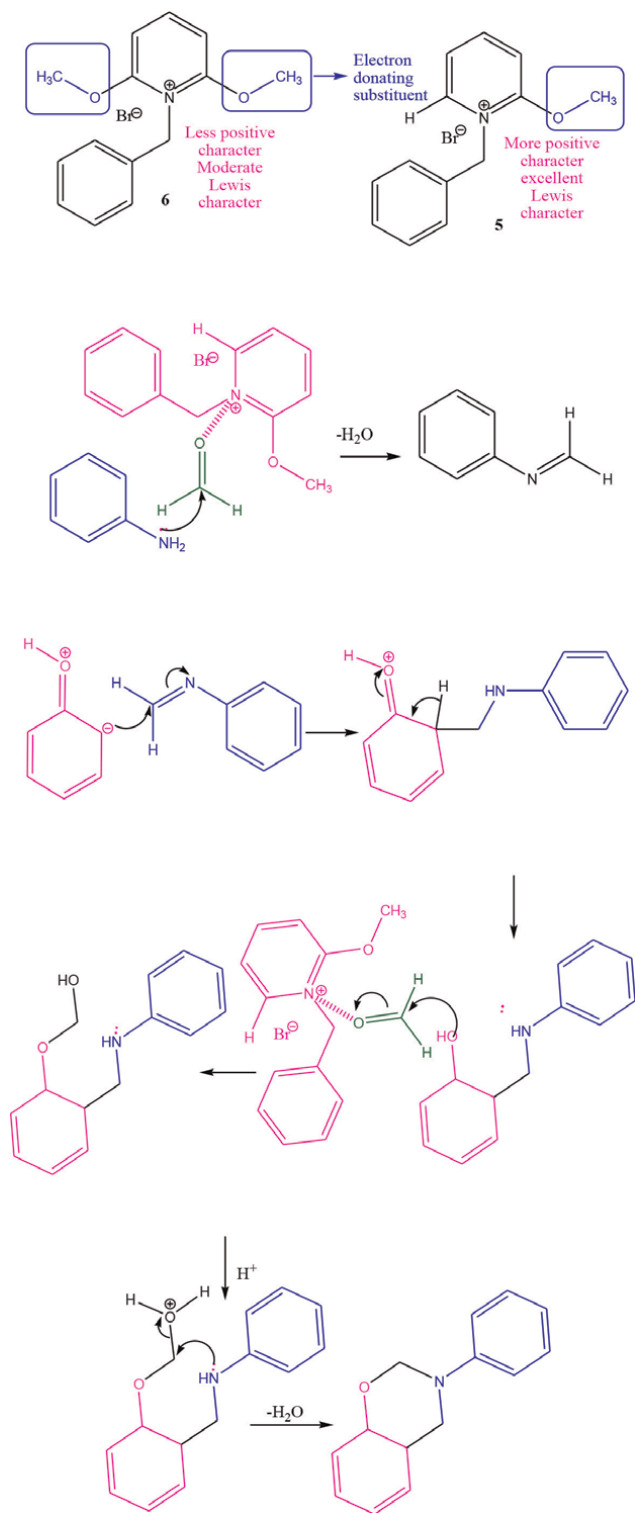


Figure 9. Plausible mechanism for Mannich reaction catalyzed by mono meric pyridinium ionic liquid **5** & **6**.

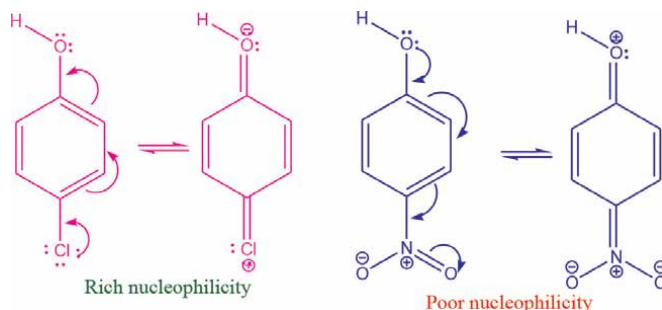


Figure 10.
Reactive probability of substituted phenols.

2-methyl-5-nitro substituted imidazolium type of ionic liquids as a catalyst and gives 6-chloro-4-methylchromenone derivative in 80% of yield in 30 minutes. Whereas, same optimized concentration of 2-methyl-5-nitro substituted imidazolium type of ionic liquid is used in the reaction between 4-nitro phenol and ethyl acetoacetate and afforded 75% of Pechmann product (**Figure 11**) in longer reaction time [33].

Pechmann reaction is tried with various concentrations such as 8.385×10^{-5} mmol, 1.3418×10^{-4} mmol, 2.012×10^{-4} mmol, and 2.683×10^{-4} mmol. Among these concentrations, 2.012×10^{-4} mmol of catalyst showed higher percentage of conversion with shorter reaction time. There is no appreciable progress in both reaction time and percentage of yield, when increasing the concentration of the catalyst to 2.683×10^{-4} mmol, so the optimum concentration of the catalyst is 2.012×10^{-4} mmol for Pechmann reaction. Preparation of 6-chloro-4-methyl chromonone derivative from required equivalence of starting materials in various solvents such as THF, acetone, ethanol, methanol and DMSO. Among these solvents, DMSO showed higher yield with shorter reaction time compared with other solvents.

2.6 Preparation of Xanthene and its derivatives using novel 3,3',3''-(2,4,6-trimethylbenzene-1,3,5-triyl)tris(methylene)tris(1,2-dimethyl-1H-imidazol-3-ium) as a catalyst

Xanthene and its derivatives play a crucial role in pharmaceutical applications as analgesic, antiviral, antibacterial and anti-inflammatory drugs [34–36]. One pot preparation of benzoxanthene and its derivatives in the presence of various expensive and nano-particle supported catalyst [37–41]; and it has some limitations such as very high toxic halogenated solvents, high reaction temperature, tedious purification procedure and very low percentage of conversion. 2:1 ratio of β -naphthol and simple/substituted benzaldehyde with or without catalyst in the presence or absence of solvent afforded aryl substituted benzoxanthene and its derivatives [34–36]. The reaction is tried with electron donating/electron withdrawing substituted containing aryl aldehyde with two equivalence of β -naphthol. In these reactions, the electron withdrawing substituent containing aryl aldehyde reacts faster than the electron donating substituent containing aryl aldehyde because of the carbanion in β -naphthol which easily attack more electro positive carbonyl carbon of aryl aldehyde. The β -naphthol carbanion is much more facile to attack, if the catalyst is trimeric substituted imidazolium salts. In benzoxanthene and its derivatives preparation, various polar and non-polar solvents are tried under conventional method. Dimethyl sulphoxide (DMSO) solvent showed excellent response,

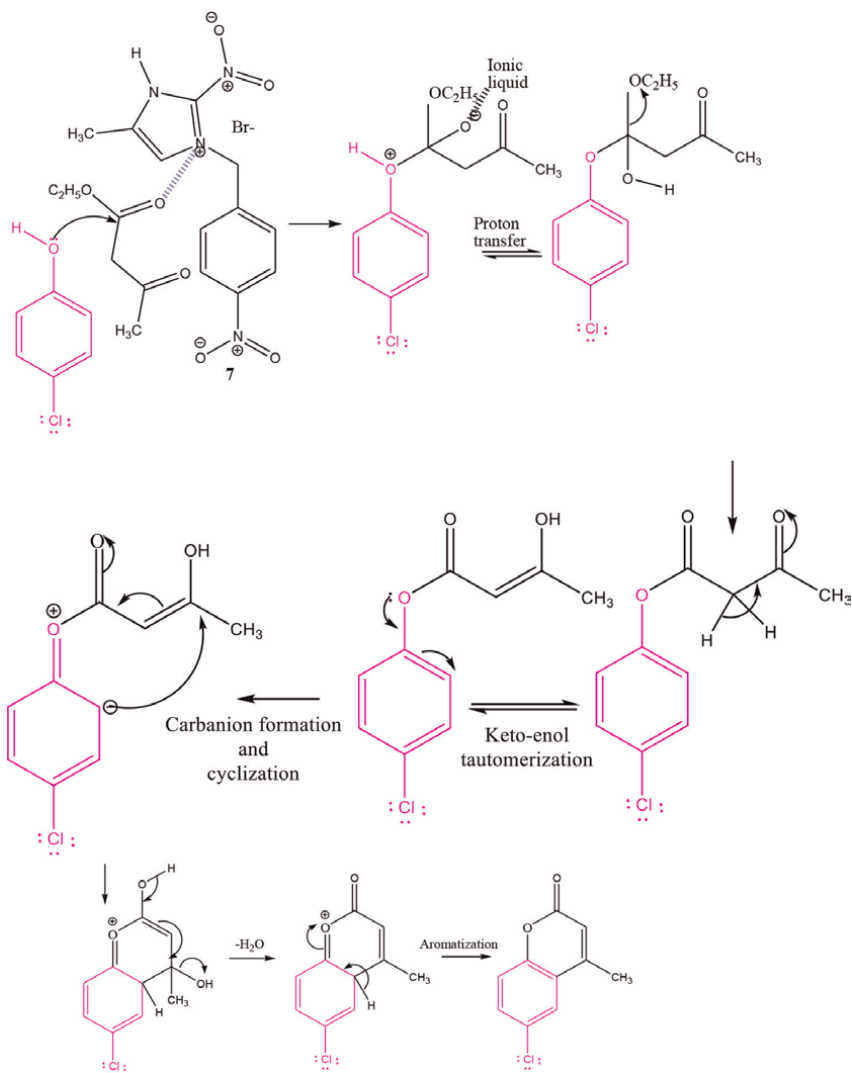


Figure 11.
Plausible mechanism for Pechmann reaction.

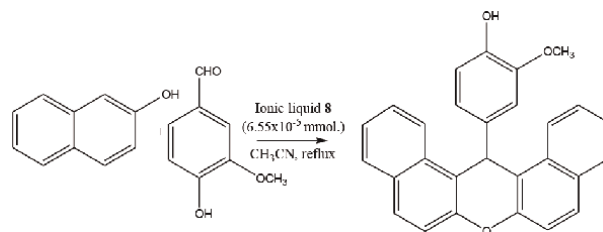


Figure 12.
Xanthene derivative formation catalyzed by trimeric imidazolium salt 8.

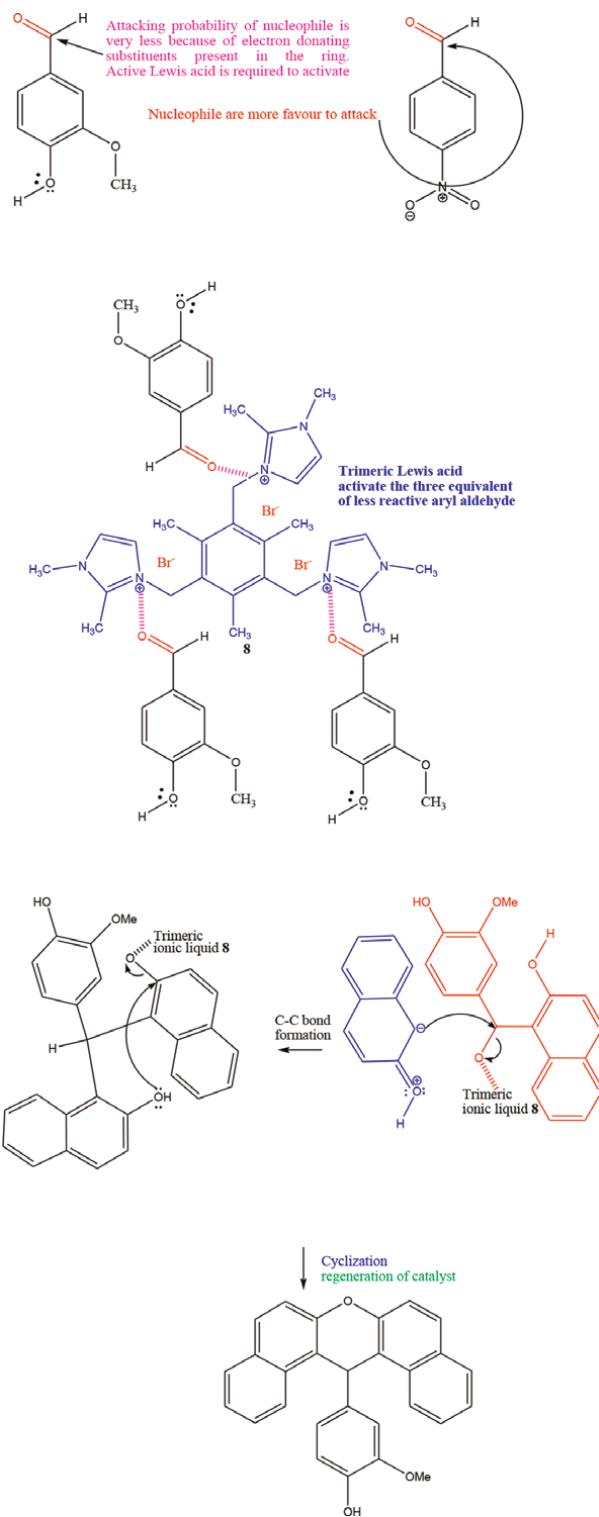


Figure 13.
 Plausible mechanism for formation of xanthene catalyzed by trimeric ionic liquid 8.

such as higher yield in shorter reaction time when compared with other solvents such as THF, ethyl alcohol, chloroform and acetone [32]. In β -naphthol, hydroxy group is an electron donating group, hence, it is acted as *o* and *p*-directing group for aromatic electrophilic substitution reaction. In this regard, *para* position is already substituted, only two possible positions are available to make C-C bond formation with aryl aldehyde. The C-C bond formation is mostly at the first position of β -naphthol (Figures 12 and 13).

3. Conclusions

Mono, di and trimeric imidazolium and pyridinium salts are more useful in catalysis to prepare biologically important intermediate and target molecules from novel synthetic methodology. We have synthesized novel mono, di and trimeric imidazolium and pyridinium salts (ionic liquids) and used these ionic liquids as a catalyst in the following reactions. Oxazolone derivatives which has antibacterial, anti-inflammatory, anti-fungal and immunomodulatory properties are prepared by Erlenmeyer reaction with the assistance of trimeric nitro substituted pyridinium salts as catalyst with higher yields. Inexpensive flexible dimeric nitro substituted dimeric pyridinium salts are used in the preparation of biologically active β -hydroxy substituted alkanal in excellent yield. In one pot multi component reaction, oxirane and its derivatives are prepared by Mannich reaction in the presence of very low concentration of recyclable 2-methoxy benzyl substituted pyridinium salts under normal reaction condition. In general, Biginelli reaction requires longer reaction time and gives moderate yield even in the presence of expensive catalyst. Whereas, inexpensive, recyclable flexible longer alkyl chain linked dimeric pyridinium bromide gives excellent response. Flexible longer alkyl chain linked methyl substituted imidazolium bromide acted as an excellent Lewis catalyst for Mannich reaction in the formation of xanthene and its derivatives. $1/3$ rd of 2.245×10^{-4} mmol. concentration of trimeric mesityl core connected imidazolium bromide is sufficient to prepare benzoxazole and its derivatives. In Pechmann reaction, minimum concentration of monomeric, dimeric and trimeric substituted imidazolium/pyridinium salts showed excellent catalytic response.

Acknowledgements

Author thanks Mrs. Revathi Ganesan, Dr. P. Ganapathi, Dr. C. Manikandan, Dr. R. Tamilarasan, Dr. R. Sundaram, Dr. N. Arunagirinathan, Dr. N. Vijayakanth, Dr. A. Aravind, Mr. R. Naveenkumar, Mrs. R. Rajalakshmi, Mr. Senthilnathan Govindaraj, Mr. Sadaiyan Govindaraj for their great support, hard work and co-operation.

Conflict of interest


“The authors declare no conflict of interest.”

Author details

Ganesan Kilivelu
PG and Research Department of Chemistry, Presidency College, Chennai, India

*Address all correspondence to: kiliveluganesan@yahoo.co.in

IntechOpen

© 2022 The Author(s). Licensee IntechOpen. This chapter is distributed under the terms of the Creative Commons Attribution License (<http://creativecommons.org/licenses/by/3.0>), which permits unrestricted use, distribution, and reproduction in any medium, provided the original work is properly cited. 

References

- [1] Peter W, Wilhelm K. Ionic liquids—New “Solutions” for transition metal. *Angewandte Chemie International Edition*. 2000;**39**:3772-3789. DOI: 10.1002/1521-3773(20001103)39:21
- [2] Jasminka P, Marko Z, Kenneth KL, Stojan S. Halogenation of organic compounds in ionic liquids. *Tetrahedron*. 2009;**65**:5625-5662. DOI: 10.1016/j.tet.2009.04.092
- [3] Kategaonkar AH, Sonar SS, Shelke KF, Shingate BB, Shingare MS. Ionic liquid catalyzed multicomponent synthesis of 3,4-dihydro-3-substituted-2H-naphtho[2,1-e][1,3]oxazine derivatives. *Organic Communications*. 2010;**3**:1-7
- [4] Mingjue Z, Pingping Z, Yan L, Guojian C, Jun E, Jun H. Schiff base structured acid–base cooperative dual sites in an ionic solid catalyst lead to efficient heterogeneous Knoevenagel condensations. *Chemistry—A European Journal*. 2012;**18**:12773-12782. DOI: 10.1002/chem.201201338
- [5] Yajun L, Yongnan X, Sun HJ, Junghyun C. A facile and green protocol for nucleophilic substitution reactions of sulfonate esters by recyclable ionic liquids [bmim][X]. *Synlett*. 2012;**23**:2692-2698. DOI: 10.1055/s-0032-1317473
- [6] Jun T, Cheng Y, Da-zhen X. Ionic liquid [DABCO-H][HSO₄] as a highly efficient and recyclable catalyst for Friedel–Crafts alkylation in the synthesis of Bis(naphthol)methane and Bis(indolyl)methane derivatives. *Synthesis*. 2016;**48**:3559-3566. DOI: 10.1055/s-0035-1561655
- [7] Agnieszka D, Magdalena BF, Anna C. Stable chiral complexes of ionic liquids with aluminium and biaryl ligands as efficient catalysts for the synthesis of chiral lactones. *Synlett*. 2014;**25**:559-563. DOI: 10.1055/s-0033-1340518
- [8] Subbiah S, Luís FV, José MSSE, Luís PNR, Carlos AMA. Organocatalyzed one-step synthesis of functionalized N-Alkyl-pyridinium salts from biomass derived 5-hydroxymethylfurfural. *Organic Letters*. 2015;**17**:5244-5247. DOI: 10.1021/acs.orglett.5b02573
- [9] Siddiqui SA, Potewar TM, Lahoti RJ, Srinivasan KV. Ionic liquid promoted facile one-pot synthesis of 1-pyridylimidazo[1,5-*a*]pyridines from dipyritylketone and aryl aldehydes. *Synthesis*. 2006;**17**:2849-2854. DOI: 10.1055/s-2006-942522
- [10] Gröger H, Vogel EM, Shibasaki M. New catalytic concepts for the asymmetric aldol reaction. *Chemistry - A European Journal*. 1998;**4**:1137-1141. DOI: 10.1002/(SICI)1521-3765(19980710)4:7<1137:AID-CHEM1137>3.0.CO;2-Z
- [11] Yamada YMA, Yoshikawa N, Sasai H, Shibasaki M. Direct catalytic asymmetric aldol reactions of aldehydes with unmodified ketones. *Angewandte Chemie, International Edition in English*. 1996;**36**:1871-1873. DOI: 10.1002/anie.199718711
- [12] Parveen M, Ahmad V, Malla A, Azaz S, Silva M, Pereira Silva PS. Solvent-free, [Et₃NH][HSO₄] catalyzed facile synthesis of hydrazone derivatives. *New Journal of Chemistry*. 2015;**39**:469-481. DOI: 10.1039/C4NJ01666A
- [13] Salami-Ranjbaran E, Khosropour AR, Mohammadpoor Baltork I, Moghadam V, Tangestaninejad S, Mirkhani V. A Novel pseudo-four-

component domino reaction for the synthesis of naphtho[2,1-b]furan-2(1H)-ones using a nanocatalyst. ACS Combinatorial Science. 2015;17(8): 452-458. DOI: 10.1021/acscombsci.5b00018

[14] Manikandan C, Ganesan K. Silica-supported solvent approaches more facile than the conventional for erlenmeyer synthesis with our pyridinium salts. Journal of Heterocyclic Chemistry. 2018;55:929. DOI: 10.1002/jhet.3120

[15] Manikandan C, Ganesan K. Synthesis, characterization and catalytic behavior of methoxy, dimethoxy substituted pyridinium type ionic liquids. Synthetic Communications. 2014;44:3362. DOI: 10.1080/00397911.2014.941503

[16] Ganapathi P, Ganesan K. Synthesis and characterization of methyl substituted imidazolium dimeric ionic liquids and their catalytic activities. American Journal of Applied Chemistry. 2014;1:40

[17] Burke WJ, Murdock KC, Ec G. Condensation of hydroxy aromatic compounds with formaldehyde and primary aromatic amines. Journal of the American Chemical Society. 1954; 76:1677-1679. DOI: 10.1021/ja01635a065

[18] Voruenrates SM, Wit WF, Tongeren JV. Lange, Efavirenz: A review. Expert Opinion on Pharmacotherapy. 2007;8:851-871. DOI: 10.1517/14656566.8.6.851

[19] Nagrik MD. One-pot preparation of β -amino carbonyl compounds by mannich reaction using MgO/ZrO₂ as effective and reusable catalyst. International Journal of Chemistry. 2010;2:98. DOI: 10.5539/ijc.v2n2p98

[20] Agag T. Preparation and properties of some thermosets derived from allyl-functional naphthoxazines. Journal of Applied Polymer Science. 2006;100: 3769-3777. DOI: 10.1002/app.23502

[21] Mathew BP, Nath M. One-pot three-component synthesis of dihydrobenzo- and naphtho[e]-1,3-oxazines in water. Journal of Heterocyclic Chemistry. 2009; 46:1003-1006. DOI: 10.1002/jhet.147

[22] Ganapathi P, Ganesan K. Synthesis and characterization of 1,2-dimethyl imidazolium type of ionic liquids and its catalytic activities. Synthetic Communications. 2015;45:2135

[23] Ganapathi P, Ganesan K. Synthesis and characterization of antibacterial ionic liquids moieties under multiple routes and their catalytic responses. Journal of Drug Research and Development. 2017;4:1

[24] Kamna G, Smritilekha B, Man S, Dhananjay M. Synthesis of dual functional pyrimidinium ionic liquids as reaction media and antimicrobial agents. RSC Advances. 2016, 2016;6(6):106806, 106806-106820. DOI: 10.1039/C6RA21865B

[25] Shahid-ul I, Butola BS, Faqeer M. Silver nanomaterials as future colorants and potential antimicrobial agents for natural and synthetic textile materials. RSC Advances. 2016;6:44232-44247. DOI: 10.1039/C6RA05799C

[26] Hafez HN, Hegab MI, Farag ISA, Gazzar ABA. A facile regioselective synthesis of novel *spiro*-thioxanthene and *spiro*-xanthene-9',2-[1,3,4] thiadiazole derivatives as potential analgesic and anti-inflammatory agents. Bioorganic & Medicinal Chemistry Letters. 2008;18:4538. DOI: 10.1016/j.bmcl.2008.07.042

- [27] Qiang Z, Hong S, Jun L, Yunyang W. A magnetic nanoparticle supported dual acidic ionic liquid: A “quasi-homogeneous” catalyst for the one-pot synthesis of benzoxanthenes. *Green Chemistry*. 2012;**14**:201-208. DOI: 10.1039/C1GC16031A
- [28] Kotaskova M, Oglou O, Helm M. Synthesis of new asymmetric xanthene dyes *via* catalyst-free S_NAr with sulfur nucleophiles. *Organic & Biomolecular Chemistry*. 2014;**12**:3816. DOI: 10.1039/C4OB00533C
- [29] Maleki B, Davoodi A, Azghandi MV, Baghayeri M, Akbarzadeh E, Veisi H, et al. Facile synthesis and investigation of 1,8-dioxooctahydroxanthene derivatives as corrosion inhibitors for mild steel in hydrochloric acid solution. *New Journal of Chemistry*. 2016;**40**: 1278-1286. DOI: 10.1039/C5NJ02707A
- [30] Kumar A, Sharma S, Maurya RA, Sarkar J. Diversity oriented synthesis of benzoxanthene and benzochromene libraries via one-pot, three-component reactions and their anti-proliferative activity. *Journal of Combinatorial Chemistry*. 2010;**12**:20. DOI: 10.1021/cc900143h
- [31] Nandi GC, Samai S, Kumar R, Singh MS. Cyclization of alkynoic acids with gold catalysts: A surprising dichotomy between Au^I and Au^{III}. *Tetrahedron*. 2009;**65**(36):1871-1879. DOI: 10.1016/j.tet.2008.10.112
- [32] Liu H, Li G, Wang Y, Zhang S, Tang Z. Synthesis and photochemistry of a new photolabile protecting group for propargylic alcohols. *Synlett*. 2017;**28**: 560-564. DOI: 10.1055/s-0036-1588915
- [33] Manikandan C, Govindaraj S, Ganesan K. Greener synthetic approach for the preparation of substituted flexible dimeric pyridinium salts and its importance. *Journal of Heterocyclic Chemistry*. 2021;**58**:1749. DOI: 10.1002/jhet.4305
- [34] Ganapathi P, Ganesan K. Anti-bacterial, catalytic and docking behaviours of novel di/trimeric imidazolium salts. *Journal of Molecular Liquids*. 2017;**233**:452
- [35] Zhang L, Zhang Z, Liu Q, Liu T, Zhang G. Iron-catalyzed vinylogous aldol condensation of biginelli products and its application toward pyrido[4,3-d]pyrimidinones. *The Journal of Organic Chemistry*. 2014;**79**:2281. DOI: 10.1021/jo402773r
- [36] Shen Z, Xu X, Ji S. Brønsted base-catalyzed one-pot three-component biginelli-type reaction: An efficient synthesis of 4,5,6-Triaryl-3,4-dihydropyrimidin-2(1H)-one and mechanistic study. *The Journal of Organic Chemistry*. 2010;**75**:1162-1167. DOI: 10.1021/jo902394y
- [37] Chandra Nandi G, Samai S, Singh M. Biginelli and Hantzsch-type reactions leading to highly functionalized dihydropyrimidinone, thiocoumarin, and pyridopyrimidinone frameworks via ring annulation with β-oxodithioesters. *The Journal of Organic Chemistry*. 2010;**75**:7785. DOI: 10.1021/jo101572c
- [38] Fuchs D, Nasr-Esfahani M, Diab L, Mejkal T, Breit B. Tandem Hydroformylation–Biginelli Reaction. *Synlett*. 2013;**24**:1657-1662. DOI: 10.1055/s-0033-1339298
- [39] Manikandan C, Ganesan K. Solid-supported synthesis of flexible dimeric pyridinium salts and their catalytic activities. *Synlett*. 2016;**27**:1527
- [40] Flavio C, Nicole K, Thimma R, Thamos Williamson R, Thomas C.

Substituents effect on the
erlenmeyer–plöchl reaction:
Understanding an observed process
reaction time. *Organic Process Research
and Development*. 2010;**14**:579-584.
DOI: 10.1021/op100032s

[41] Ganapathi P, Ganesan K. Solid phase
synthesis of Xanthene derivatives
assisted by imidazolium salts. *Journal of
Advanced Catalysis Science and
Technology*. 2018;**5**:19

Iron-Based Ionic Liquids for Magnetic Resonance Imaging Application

Praveen Singh Gehlot and Arvind Kumar

Abstract

In the biomedical treatment, identification of diseases and their diagnosis are running with help of many biomedical techniques including imaging such as magnetic resonance imaging (MRI). MRI technique requires an identification of targeted cell or lesion area which can be achieved by contrast agent. For clinical use, T_1 positive MRI contrast agents and T_2 negative MRI contrast agents are being used. However, these contrast agents have several drawbacks such as toxic effect of metal centre, poor resolution, weak contrast, low intensity image and short signal for long-term in vivo measurement. Therefore, development of new contrast agents is imperative. Ionic liquids with their unique properties have been tried as novel contrasting materials. Particularly, iron-containing amino-acid-based ionic liquids or amino-acid-based paramagnetic ionic liquids (PMILs) have been reported and demonstrated as MRI contrast agents. These PMILs have shown superior features over reported contrast agents such as dual-mode contrast, biofriendly nature, involvement of non-toxic magnetic centre (Fe), stable aqueous solution, better image intensity at low concentration level and easy to synthesis. PMILs have been characterized well and studied with animal DNA using various techniques. The result revealed that animal DNA is remain safe and stable structurally up to 5 mmol.l^{-1} . These cost-effective PMILs opened the greater opportunity in the field of contrast-based biomedical applications.

Keywords: ionic liquids, paramagnetic, contrast agents, magnetic resonance imaging, MRI, relaxativity, DNA

1. Introduction

It is well known that, among various biomedical imaging modalities, magnetic resonance imaging (MRI) is one of the most powerful, ionizing-radiation-free and non-invasive imaging technique, and principally it resembles NMR (Nuclear Magnetic Resonance) technique. Image is formed by spatially encoding NMR signals received from the proton relaxation of the molecules under applied magnetic field [1, 2]. During imaging, the identification of targeted cell or lesion can be visualized by using some of tracking or sensing agent. In the X-ray techniques, BaSO_4 will be used to enhance the contrasting level and make difference in brightness of background to

target or lesions area. Similarly, in the magnetic resonance imaging (MRI) technique, MRI contrasting agents are widely used to boost up the image sensitivity and achieve anatomical differentiation or detection accuracy by enhancing the contrast of the image. According to the nature of generating contrast, MRI contrast agents used clinically are T_1 MRI contrast agents and T_2 MRI contrast agents. T_1 contrast (positive contrast) enhances brightness in T_1 -weighted images; however, T_2 contrast (negative contrast) enhances darkness in T_2 -weighted images [2]. Clinically used contrast agent is mostly composed of gadolinium metal ion. These contrast agents are metal–ligand structure. Gadolinium-based contrast agents (GBCAs) show T_1 positive contrast during imaging process [3]. Most commonly, a contrast agent exhibits either T_1 or T_2 contrasting nature in domination, but recently dual-contrasting nature in single agent with significant T_1 and T_2 relaxivity values has been reported. Most of these dual-contrasting agents are either multi-layered core-shell nanoparticle or nanoparticle-Gd-chelate complexes which need a highly precise multistep and sophisticated synthesis procedure [4, 5]. But at present, none of the dual (T_1 and T_2) contrasting agents are commercially available for MRI diagnosis. For GBCAs, it is reported that a severe nephrogenic systemic fibrosis (NSF) complication is recently recognized. Deposited Gd metal ion can induce critical clinical problems such as chronic kidney disease (CKD) and acute kidney injury, etc. to the patient [6]. Thus, in short, there are adverse effects of such contrast agents which are dominant and need to remove or overcome these obstacles either in performance or health issues. For sake of knowledge, the contrast agents can be grouped broadly into three categories depending upon their function and nature of contrast. T_1 contrast agent: gadolinium (Gd)-chelate-based contrast agents (GBCAs) such as Magnevist®, Dotarem® and Omniscan™ are commonly used in daily present clinical practice for T_1 contrast in most of clinical aspects [5]. The Magnevist is ionic contrast agent and has N-methylglucamine counter positive ion. It is used for the visualization of abnormal vascularity. However, these GBCAs have higher osmolality values [7]. Theoretically, the origin of T_1 response is related to the longitudinal relaxivity (r_1) of aqueous solutions metal–ligand-bearing contrast agent. The main parameters such as the number of water molecules in the first coordination sphere of the metal ion (q), their residence time in the first coordination sphere (t_M) and the molecular tumbling time (t_R) are optimized to determine the value of r_1 . These parameters are related to water exchanging process between the first coordination sphere of paramagnetic metal ions–ligand moiety and the surrounding water [8]. Most of GBCAs for which q value falls in the range of 1–3 have sufficient thermodynamic and kinetic stability [9, 10]. T_2 contrast agents: superparamagnetic iron oxide nanoparticles (SPIOs)-based contrast agents such as Resovist®, Feridex® and Gastromark™ are commercially available and clinically approved T_2 contrasting agents. They have higher relaxivity value and considered as negative contrast agent due to enhancement of darkness in T_2 images [11, 12]. To prevent agglomeration, either each of these particles is covered with a core-shell or magnetic crystallite embedded in a coating. For example, ferumoxide is made from dextran, whereas ferumoxsil is made of siloxanes. Size of the core determines the relaxivity property of particle. Here also, parameters such as t_R are governed transverse relaxivity (r_2), which is further related to T_2 contrast. The relaxation induced by superparamagnetic particles can be explained by the classic outer-sphere relaxation theory [13]. According to this theory, the relaxation rates of water protons diffusing nearby the unpaired electrons present in paramagnetic ions are responsible for the particle's magnetization [14]. Enhancement in T_2 relaxation increases with the particle size [15, 16]. Therefore, SPIOs were firstly developed as T_2

contrast agents due to their larger size [17]. According to the overall size of the particles, superparamagnetic iron oxides are classified [7]. Ultra-small superparamagnetic iron oxide (USPIO) nanoparticles [18] have a diameter less than 50 nm, whereas small superparamagnetic iron oxide (SSPIO) nanoparticles have size between 1 nm and 50 nm. Micron-sized particles of iron oxide (MPIO) nanoparticles are large particles with a diameter of several microns. Since T_1 - and T_2 -weighted contrast agents exhibit great response and possess unique qualities, but there are some reports which have described their limitations. Therefore, synergic integration of these two functions (T_1 and T_2) for MRI is expected to get more comprehensive and cooperative diagnostic information over the single T_1 or T_2 contrast agent [19–21]. The development of dual-mode contrast agent of MRI in a single instrumental system could proficiently eliminate certain difficulties. It could also improve the diagnostic accuracy for most of diseases. It is reported that some functionalized or mixed nanomaterials exhibit intrinsic dual-contrast effects in magnetic resonance imaging. The FeCo nanoparticles (NPs) reported by H. Dai show high T_1/T_2 contrast effects, but there is a lack of understanding of the dual-mode contrast mechanism [22]. Many researchers have reported the Gd^{3+} -containing magnetite (Fe_3O_4) NPs, MnO-containing nanoparticles and SPIONs as dual-MRI contrast agents [4, 5, 23–29]. A recent patent shows pH-sensitive nano-formulates (PMNs) contrast agent comprising extremely small iron oxide nanoparticles (ESIONs) [30]. Songjun Zeng and Jianhua Hao have been used a hybrid lanthanide nanoparticle as a dual-mode contrast agent for imaging-directed tumor diagnosis [31]. The iron oxide nanoparticles coated with Gd-DTPA and fibrin-binding peptides have also been reported by Xu et al. for the detection and localization of thrombosis [32]. Similarly, the cyclic RGD functionalized liposomes (cRGD@MLP-Gd) encapsulated with gadolinium diethylenetriamine penta-acetic acid (Gd-DTPA) and superparamagnetic iron oxide (SPIO) are prepared by Fang Yang and Chun-Jian Li and used for thrombus-targeted imaging activity [33].

Each and every researcher is familiar with Ionic Liquids (ILs) and its functionality. Due to its tuneable nature, ionic liquids have gained special attention. Ionic liquids are compounds comprising entirely of ions where at least one ion should be asymmetric organic ion and melts below the 100°C [34]. It is already reported that the physicochemical properties of ILs depend on the nature of cation, anion and alkyl substitutions [35], and properties can be altered by varying the nature of ions, thus making them task-specific [36]. Task-specific ionic liquids with characteristic physicochemical properties produced many advantages and have been used in various applications widely [37–40]. Researchers have introduced the inherent magnetic properties by using transition metal at molecular level. First time paramagnetic magnetic ionic liquid (PMIL) has been reported by Hayashi Satoshi et al. and their magnetic property explained. These ionic liquids are composed of iron metal halide ($FeCl_4^-$ ion) [41]. Due to inherent paramagnetic character, these ionic liquids were termed as paramagnetic ionic liquids (PMILs). PMILs are made up of a distinct group with versatile properties such as magnetic character and widely used in a various applied fields. For example, the PMILs have been used in desulfurizations [42], organic synthesis [43], microextraction [44, 45], electrocatalysis [46], probe for vesicles [47], self-assembling media for surfactants [48], acidic catalysis [49, 50], density measurements [51], paramagnetic polymer synthesis [52, 53], microemulsion formulation [54], synthesis of chitosan supported magnetic ionic liquid based catalysis [55], CO_2 separation [56], application in analytical science [57] and other various applications [58]. Kumar et al. have reported paramagnetic surface-active ionic liquids (PMSAILs), another class of PMILs. Paramagnetic surface-active ionic liquids (PMSAILs) are long chain bearing those ionic liquids which have amphiphilic nature and

Type	Name of amino acid	Abbreviation	Chemical Structure
Without esterification	Proline	Pro[FeCl ₄]	
	Glutamic Acid	Glu[FeCl ₄]	
With methyl esterification	Proline	ProC ₁ [FeCl ₄]	
	Glutamic Acid	GluC ₁ [FeCl ₄]	
	Valine	ValC ₁ [FeCl ₄]	
	Alanine	AlC ₁ [FeCl ₄]	

Reproduced from Ref. [63] with permission from Royal Society of Chemistry respectively.

Table 1.

Name of amino acid and chemical structures of used in the study as contrast agents.

have ability to form nano-aggregates such as micelle and vesicles in their solution. The PMSAILs are demonstrated as contrast agent in aqueous solution for MRI application and also studied with animal DNA to check its structural stability [59]. Many ionic liquids have been prepared using amino acid, and their biocompatible and biofriendly nature [60, 61] have been checked. Since L-amino acid is biological monomer that is the building block of proteins. L-amino-acid-based chiral PMILs have been synthesized and studied by Isiah M. Warner et al. [62]. Here, the iron-containing amino-acid-based PMILs are studied and first time explored the application as contrast agents which more promisingly interact with essential biological molecules and surprisingly enhance the contrast intensity with retention time. These PMILs-based contrast agents were made of biofriendly amino acid and iron halide. Authors have studied broadly and investigated its interaction with DNA through various techniques including CD, fluorescence, ITC, zeta and gel electrophoresis. MRI property of these PMILs is also investigated and claimed their superior contrast activity. Since these are made of amino acid and iron moiety, therefore, they are non-hazardous, toxic-metal-free and biofriendly contrast agent (**Table 1**) [63]. This work is patented in Indian patent office [64].

2. Paramagnetic ionic liquids as contrast agents

As it has been already mentioned in introduction, ionic liquids (ILs) have gained special attention due their flexibility and versatility. Thus, ionic liquids have been used in various applications, and ionic liquid is still being used. In the continuation of the applications, Carla I. Daniel et al. have mentioned the possibility of low-toxic magnetic ionic liquid as contrast agent at end of conclusion. They have conducted a proton nuclear magnetic relaxation dispersion ¹H NMRD study of the molecular dynamics in mixtures of phosphonium-based magnetic ionic liquid [P₆₆₆₁₄][FeCl₄] with [P₆₆₆₁₄][Cl] ionic liquid and mixtures of [P₆₆₆₁₄][FeCl₄] with dimethyl sulfoxide (DMSO). The enhancement in r_1 relaxation rate of MIL in mixture of ILs + [P₆₆₆₁₄][FeCl₄] with DMSO solvent [65]. The relaxation enhancement is directly linked with contrast property as we know. The proton spin-lattice relaxation dispersion rate (r_1), was measured for both these systems, and the rate indicates a much larger paramagnetic relaxation enhancement for [P₆₆₆₁₄][FeCl₄] with [P₆₆₆₁₄][Cl], in comparison with that

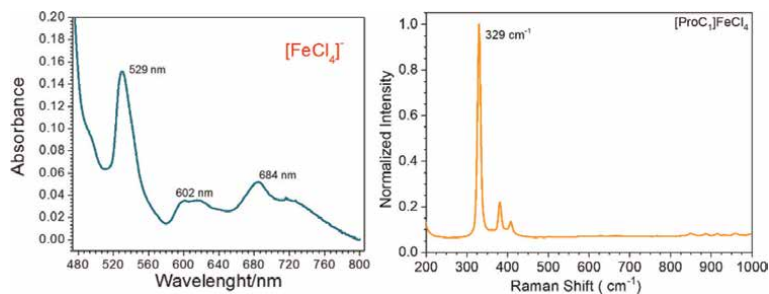


Figure 1. Representative UV and Raman spectrum of PMIL ($\text{ProC}_1[\text{FeCl}_4]$). Reproduced from Ref. [63] with permission from Royal Society of Chemistry respectively.

observed for the mixtures of $[\text{P}_{66614}][\text{FeCl}_4]$ with DMSO. This difference has reflected that in this mixture, the proton spin–lattice relaxation does not depend on the concentration of paramagnetic ions $[\text{FeCl}_4]^-$ linearly. The paramagnetic ions $[\text{FeCl}_4]^-$ seem to disturb the local molecular organization, molecular order, dynamics and packing in the $[\text{P}_{66614}][\text{Cl}]$ ionic medium as compared with non-ionic organic solvent DMSO. Thus, here, aqueous solution of iron-containing PMILs is examined for imaging, and their relaxivity rate at various concentrations is studied.

Kumar et al. have synthesized amino-acid-based PMILs [63]. These amino acids are used in two forms—esterified and without esterified. Esterified amino acids are prepared as reported earlier in the literature [61, 66]. Chloro halide salt of amino acid is simply mixed with ferric chloride in equimolar ratio in the ethanol solvent. Dark brown PMILs are obtained at end of process after solvent evaporation. So, these PMILs are easy to synthesize and can be cost-effective. These PMILs are characterized well, and structural verification of $[\text{FeCl}_4]^-$ ion is done by UV and Raman shift using Shimadzu UV-2700 UV–VIS spectrophotometer, Japan, and LabRAM HR Evolution Horiba Jobin Yvon Raman spectrometer, Japan, at 298.15 K (**Figure 1**). The Raman shift value for $[\text{FeCl}_4]^-$ ion should be near 334 cm^{-1} [67, 68]. The paramagnetic nature of PMILs is confirmed by the EPR spectrum using mt-MiniScope MS5000 ESRStudio by Freiberg instrument at 298.15 K. The EPR spectrum of PMILs in solution phase indicates a single isotropic EPR line which appeared due to mixed $^6\text{S}_1$ state. EPR spectrum of magnetic centre, here Fe^{3+} ion, strongly depends on its tetrahedral environment [69]. The amount of Fe in each PMILs is measured and calculated using Perkin Elmer ICP optima 2000 DV ICP-OES (Inductively Coupled Plasma–Optical Emission Spectroscopy) analyzer. In the terms of Fe, aqueous solutions from 0.1 to 5 mmol.l^{-1} are prepared for further experiments including interaction with DNA and magnetic resonance imaging.

3. Physiochemical properties of PMILs

Degradation and glass transition temperature of PMILs was investigated using NETZSCH TG 209 F1 Libra TGA and NETZCH DSC 204 F1 Phoenix DSC, respectively. A presentative differential scanning calorimetry (DSC) and thermogravimetric analysis (TGA) thermograms are given in **Figure 2**. Combinedly, these are thermal analyses, and it is the technique in which physical properties of a substance or a mixture of substances are measured against either of temperature or time, wherein the substances are subjected to a controlled temperature programme system. If the

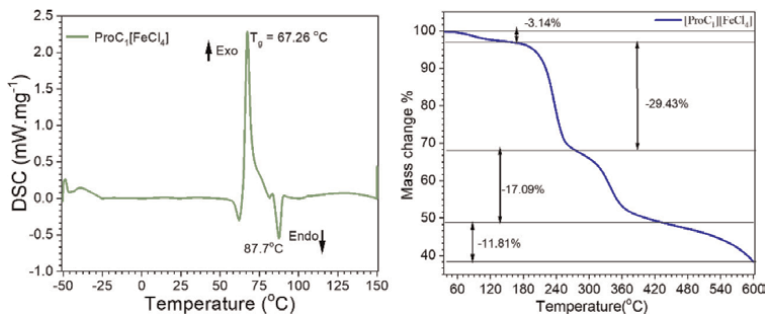


Figure 2. Representative DSC and TGA thermogram ($\text{ProC}_1[\text{FeCl}_4]$). Reproduced from Ref. [63] with permission from Royal Society of Chemistry respectively.

physical property is weight, then it is termed as a TGA. In thermogravimetric analysis (TGA), weight changes or % of the mass loss of PMILs is measured as a function of temperature. Thermogravimetric curves (graph between % mass loss versus temperature) allow an evaluation of thermal stabilities. Degradation temperature (T_g) was marked where maximum mass changes occur [70–73]. In the figure, initial loss in mass is due to moisture or water elimination at near 120–200°C. After that maximum loss in mass was observed at 200–300°C. For the TGA thermogram, onset temperature (T_{onset}) is the intersection of the baseline of weight (after the loss of the water) and the tangent of the weight versus temperature curve or simply, a temperature at which the sample loses weight with fastest rate. The start temperature (T_{start}) is beginning of decomposition [72]. For ionic liquid, glass transition temperature is measured due to its amorphous nature. Glass transition temperatures (T_g) for PMILs are found below 100°C. There is assumption that lowering the melting point of ionic liquids is achieved due to distortion in the lattice of crystal, and these disturbances generate low lattice enthalpy and weak ionic attraction between asymmetric ions. However, like branching or enlargement of substituent is majorly responsible of disruption in crystal packing [74]. In DSC, the sample and reference are kept at the same temperature, and the energy $d(\Delta q)/dt$ required to preserve zero temperature differential ($\Delta T = 0$) between the sample and the reference is measured on the function of temperature during a thermal event in the sample. As a result, the endothermic peak indicates absorption of heat, and the exothermic peak will rise when heat is released. Depending on the nature of peaks, glass transition temperature (T_g), melting point (T_m), crystallization transition (T_c) and heat capacity can be calculated [71, 75–77]. Since, T_g values are less than 100°C and fulfilled the criteria of an IL [78], therefore our product will be called as paramagnetic ionic liquids (PMILs).

4. Interaction of PMILs with animal DNA

To explore the biofriendly nature and structural stability of animal DNA, the physical interaction of this PMILs has been investigated. For this whole investigation, 90–92 ng ul^{-1} concentration of DNA was prepared in buffer solution using NanoDrop® Spectrophotometer ND-1000. After that, PMILs are studied with animal (salmon fish) double-stranded β -DNA (ds- β -DNA) and studied the conformational and structural stability of DNA in aqueous medium. For this, PMILs were examined

with DNA using various techniques including circular dichroism (CD), fluorescence, isothermal thermal calorimetry (ITC), zeta potential and Agarose gel-electrophoresis, and the concentration regime where DNA remains safe in native form is identified. It is found that long-chain-bearing PMILs undergo complex formation (DNA-PMILs) in the form of precipitate at higher concentration [59].

4.1 Circular dichroism (CD) and fluorescence

To investigate the structural and conformational stability, CD (Jasco J-815 CD spectrometer under the N_2 environment at temperature 298.15 K) and fluorescence spectra of DNA are recorded in the presence of aqueous solution of PMILs, and the spectra are shown in **Figure 3**. It is well known that the presence of a positive band at about 276 nm and a negative band near 245 nm with crossover point at nearby 258 nm collectively indicates the existence of native pure DNA in buffer solution. These values indicate that used pure DNA is the fully hydrated double-helix β form and dextrorotatory in nature [79]. The secondary structure of DNA remained same as native DNA within the concentration range ($0.1\text{--}5\text{ mmol.l}^{-1}$ Fe); after that, at higher concentrations (above 3 mmol.l^{-1} Fe), PMIL underwent interaction process with negative sites of DNA, and consequently, bands are distorted. Thus, at low concentration of PMILs, CD bands of DNA unchanged and are likely to superimpose on native bands representing the structural and conformational stability of DNA in these concentration ranges. For tertiary structure confirmation, interaction of PMILs with DNA was observed by Ethidium Bromide (EB) exclusion assay using a Fluorolog horiba Jobin Yvon fluorescence spectrophotometer. Fluorescence intensity of intercalating dye EB abruptly enhanced when

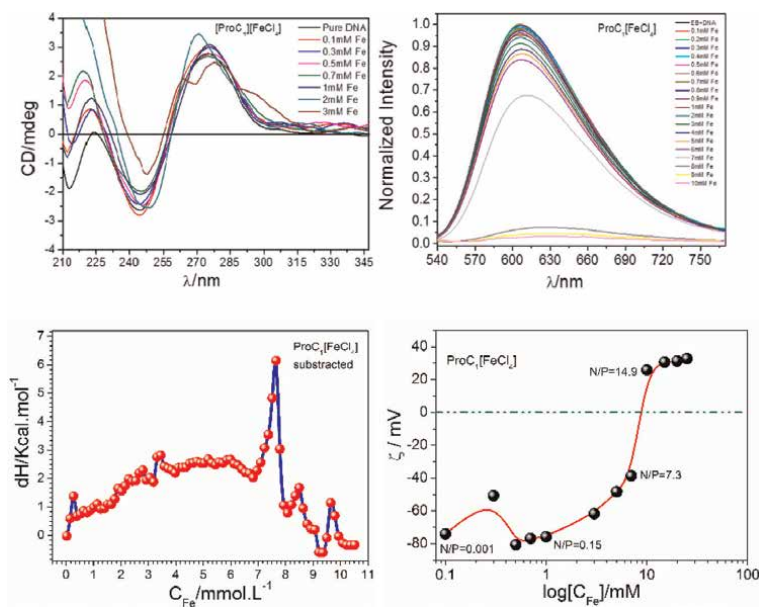


Figure 3. Representative CD spectra, fluorescence spectra of ED-DNA complex, ITC binding enthalpogram and zeta potential at various concentrations ($ProC_1[FeCl_4]$). Reproduced from Ref. [63] with permission from Royal Society of Chemistry respectively.

dye intercalate at minor grooves of DNA with order of 20–25 times with respect to alone EB in buffer medium. Here, water is responsible which acts as a strong quencher [80–83]. From **Figure 3**, it can be observed that intensity peak height is similar to EB-Native DNA complex at low concentration ($0.1\text{--}3\text{ mmol.l}^{-1}$) that means PMILs did not bind to the EB-DNA complex efficiently. But at higher concentration, intensity peak height reduces due to involvement of cationic counterpart to the EB-DNA complex. Positive counter ion of PMILs started to interact with the minor negative groove of DNA via strong electrostatic interaction after complete removal of the spine of hydration, and consequently, EB dislocates effectively from its hydrophobic environment [84, 85]. It is assumed that more hydrated small cation-containing PMILs are incompetent to dislocate the EB efficiently due to weak electrostatic interactions, but these interactions become dominant when concentration is increased. In the case of long-chain-containing PMILs, DNA showed compaction phenomenon at higher concentration [59]. DNA compaction is confirmed by distortion in intensity and shifting in band position due to formation of cationic surfactant complex (lipoplex) [86]. So, from figure it can be judged that CD spectra and fluorescence spectra confirmed conformational and structural stability of DAN, which remains similar to native DNA at low concentration of PMILs.

4.2 Isothermal titration calorimeter and zeta potential

To investigate the interaction of PMILs with DNA thermodynamically, binding isothermal enthalpogram is measured from Isothermal Titration Calorimetry (ITC) experiments using MicroCal ITC200 microcalorimeter instrument with controlled Hamiltonian syringe. Measured enthalpy in the ITC experiment is a combination of overall heat produced from various phenomena involving the binding of PMILs on DNA through the electrostatic and hydrophobic interactions, hydration of PMILs and the change in the conformation of hydrated DNA [87]. From **Figure 3**, it is observed that variation in enthalpy (ΔH) of DNA-PMILs interaction process is less at low concentration and shows negligible DNA-PMILs binding. But, at higher concentration, a characteristic large enthalpic peak appeared which revealed significant DNA-PMILs interactions or can say complex formation [59, 88], which means PMILs have a significant impact on DNA after certain critical concentration. In the continuation, the effect of PMILs on DNA negative surface is observed by measuring zeta potential (ζ) using a Zetasizer Nano ZS light scattering apparatus (Malvern Instruments, U.K.) with a He-Ne laser (633 nm, 100 mW) at 298.15 K. The trend of changes in zeta potential with respect to concentration of PMILs is negative to positive. Initially it is negative due to surface charge of DNA alone or less binding of PMILs at low concentration. After that, it is passed through neutral point to positive value at higher concentration. It can be understood like, initially a few molecules of PMILs interact with DNA surface and at this time, some hidden negative charges of core area of the DNA chains become exposed outside; consequently, zeta value initially decreases [89]. After that, more positive counter ions of PMILs started to bind with exposed negative surface of DNA when overall exposed negative surface of DNA was neutralized, and then, subsequently, zeta value shifted to its positive values and then finally reached its maximum positive value. The neutralized negative surface of DNA makes PMIL-DNA complex formation, and such a complex occurs when all negative phosphate groups bind with available positive cations [90–93]. This observation also coincides with ITC enthalpogram.

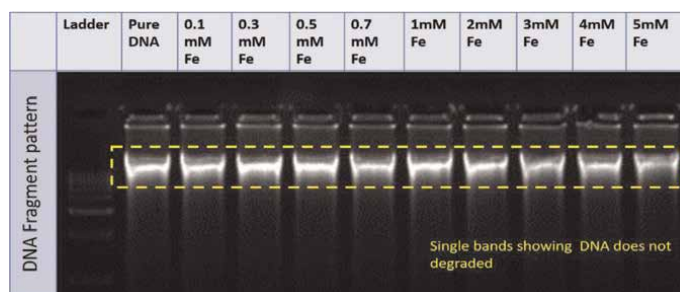


Figure 4. Representative agarose gel-electrophoresis electrophoresis pattern of DNA in the presence of PMILs at various concentrations ($\text{ProC}_4[\text{FeCl}_4]$). Reproduced from Ref. [63] with permission from Royal Society of Chemistry respectively.

4.3 Agarose gel electrophoresis

Whether DNA breaks down or not in the presence of PMILs, with this objective, the agarose gel electrophoresis experiment was performed using Electrophoresis Power supply BGPS 300/400. In **Figure 4**, initial bright bands are similar to pure DNA at low concentration (up to 5 mM Fe) which indicates the presence of unbound DNA molecules. It was ensured that DNA degradation does not happen in lower concentration regimes after that the band becomes remarkably vague at higher concentration; further these illuminated vague bands disappear when concentration increases. Disappearance of band tells that all DNA molecules have been bound with PMILs, and there are no free DNA molecules available. Moreover, the absence of multiple bands like a ladder confirmed that DNA did not degrade or break in the presence of PMILs molecules [94].

Therefore, collectively it can be summed that these PMILs are safer in terms of biofriendly nature, structural stability and degradation of DNA at certain range of concentration. These PMILs are safe and free from any adverse effect on animal DNA. This concentration range is selected for magnetic resonance imaging experiment.

5. Relaxation study of PMILs and its outcomes

Magnetic resonance imaging and relaxation study has been carried to demonstrate the utility and effectiveness of PMILs as an MRI contrast agent (CA). MR imaging experiment and relaxivity measurement were carried out using 11.7 Tesla MRI instrument (Brücker Advance 500 MHz proton NMR) using a micro-imaging probe and Paravision imaging software at CSIR CSMCRI, India. T_1 - and T_2 -weighted MRI images of aqueous phantoms of each PMIL at different concentration (0.3, 0.5, 0.7 and 1.0-mM Fe) are measured using the spin-echo pulse sequences (RAREVTR and MSME) with acquisition parameters FOV = 0.4 cm, TR = 350 ms, TE = 8 ms, 128×128 matrix and FOV = 0.4 cm, TR = 2000 ms, TE = 36, 128×128 matrix respectively for PMSAILs. T_1 and T_2 relaxation times of aqueous phantoms are measured using Bruker RAREVTR (FOV = 0.4 or 0.5 cm, TE = 8 ms, TR = 250 to 2850 ms and 128×128 matrix) and MSME (FOV = 0.4 or 0.5 cm, TE = 12 to 72 ms, TR = 2000 ms and 128×128 matrix) MRI pulse sequences respectively. T_1 and T_2 relaxivity values were calculated through Eq. (1) by linear curve fitting of relaxation rate ($1/T_1$ and $1/T_2$) versus Fe concentration using Paravision software.

The study has explored its utility and estimated the effectiveness of the PMILs as MRI contrast agents and can be used for diagnosis. Generally, the intensity of MRI image depends on the population of ^1H nuclei of water molecules present in the biological tissue or cell or solvent, relaxation time and their relaxation rate also. Relaxation rate belongs to spin–spin relaxation and spin–lattice relaxation. Relaxation rate greatly influenced by environment of water molecules that are going to exchange process between magnetic centre or surrounding. Thus, relaxation rate (r) can vary with the variation of the local magnetic field and magnetic field inhomogeneity around the ^1H nuclei of the sample. Incorporation of a magnetic entity such as gadolinium chelates and superparamagnetic nanoparticles of Gd, Fe, Mn, into the samples will bring changes in relaxation rate via generating a variation in the local magnetic field and magnetic field inhomogeneity around the ^1H nuclei of the concerned sample.

The relaxation rate of PMILs obeys a linear relationship with Fe concentration and can be represented mathematically by the following expression [95].

$$\frac{1}{T_{i,C}} = \frac{1}{T_{i,0}} + r_i C \quad (1)$$

$T_{i,C}$ and $T_{i,0}$ ($i = 1$ or 2) are relaxation time of sample at C concentration and absence of contrast reagent respectively, and r_i is the relaxivity of the contrast agent. T_1 - and T_2 -weighted images are recorded via using spin echo (SE) MRI pulse sequence, and the signal intensity for SE pulse sequence can be expressed as [2].

$$I = I_0 \left(1 - e^{-TR/T_1}\right) \left(e^{-TE/T_2}\right) \quad (2)$$

Intensity of T_1 - and T_2 -weighted image is totally T_1 - and T_2 -dependent; T_1 and T_2 weighting can be achieved by eliminating one term in the presence of other. For T_1 -weighted image, T_2 term should be eliminated and the same for T_2 -weighted image, T_1 term should be eliminated with the selection of the appropriate combination of TE (time of echo) and TR (time of repetition) values. Further, it can be seen from Eqs (1) and (2) that the intensity increases in T_1 -weighted image but decreases in T_2 -weighted images with the increase of Fe concentration and vice versa too. Local magnetic field inhomogeneity generated by Fe constituent also affects the transverse relaxation time (T_2), and due to this involvement of local field inhomogeneity, T_2 converts into T_2^* . T_2^* relaxation time is a combination of true T_2 relaxation time with relaxation rate generated due to local magnetic field inhomogeneity, and its value is always larger than T_2 relaxation time and can be mathematically expressed as [96].

$$\frac{1}{T_{2,C}^*} = \frac{1}{T_{2,C}} + \gamma \Delta B \quad (3)$$

where γ is the gyromagnetic ratio, ΔB is magnetic field inhomogeneity across the voxel and $1/T_2$ is the relaxation rate contribution of magnetic field inhomogeneity. T_2^* -weighted MRI images are obtained with gradient echo pulse sequence by choosing appropriate values of TE, TR and flip angle (α) of the excitation pulse to minimize the T_1 effect in the images. Signal intensity under this pulse sequence can be illustrated as

$$I = I_0 \frac{(1 - e^{-TR/T_1}) \sin \alpha}{(1 - e^{-TR/T_1}) \cos \alpha} e^{-TE/T_2^*} \quad (4)$$

In order to investigate the contrast property of PMILs, five different concentrations (0.0, 0.3, 0.5, 0.7 and 1.0 mM Fe) were prepared, and T_1 , T_2 and T_2^* -weighted MRI images of aqueous phantoms were obtained. Their relaxation times were determined by using Eq. (2) for T_1 , T_2 , and Eq. (4) for T_2^* . T_1 and T_2 -weighted MRI images of PMILs are shown in **Figure 2**. An intensity reduction in T_2 and T_2^* -weighted images and simultaneously an intensity enhancement in T_1 -weighted image were observed along with Fe concentration. This intensity variation found in MRI images with respect to Fe concentration reveals contrast property of aqueous PMILs qualitatively and further suggests that these PMILs have negative as well as positive contrast behavior or can say PMLs can be used as T_1 and T_2 contrast agents.

Figure 5 represent a linear relationship of relaxation rate (r) with Fe concentration of PMILs which is found similar as reported in the literature available for various contrast agents [97]. This contrast property of PMILs is determined quantitatively for PMILs; r_1 , r_2 and r_2^* relaxivity measured by a linear curve fitting of their corresponding curves (Eq. (1)). The measured r_1 and r_2 values are given in **Table 2**.

It is also found that these PMILs are able to generate dual contrast with intermediate r_2/r_1 value like metal nanoparticles. Low value of r_2/r_1 represents the positive contrast, whereas high value indicates negative, but intermediate value of this represents dual nature of contrast agent.

Tegafaw et al. reported that the r_2/r_1 value for Gd-Dy oxide made hybrid nanoparticles is near 6 and claimed its dual nature [5]. $Fe_2O_3 + Fe_3O_4$ nanoparticles (Resovist) also have r_2/r_1 value near 5.9 [3]. Similarly, r_2/r_1 value for these PMILs is also observed near 5.2 and which is greater than Gd-BOPTA ($r_2/r_1 \approx 1.1$). Therefore, it can be summarized that the synthesized nanoparticle-free and biofriendly PMILs are potential T_2 and T_1 dual-mode contrast agents. These PMILs can take position in the list of newly discovered or clinically used contrast agents.

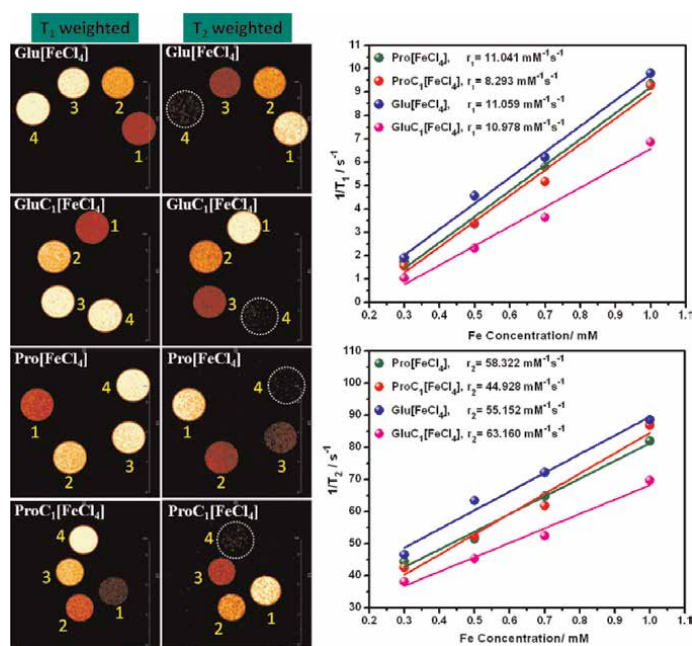


Figure 5. T_1 - and T_2 -weighted MR images and relaxivity pattern of amino-acid-based PMILs at various Fe concentrations. Reproduced from Ref. [63] with permission from Royal Society of Chemistry respectively.

PMILs	Osmolality ^a Osmol.Kg ⁻¹	r_1 (mM ⁻¹ .s ⁻¹)	r_2 (mM ⁻¹ .s ⁻¹)	r_2/r_1
Pro[FeCl ₄]	2.7	11.04	58.32	5.28
ProC ₁ [FeCl ₄]	3.1	8.29	44.93	5.42
Glu[FeCl ₄]	2.8	11.06	55.15	4.99
GluC ₁ [FeCl ₄]	3.3	10.98	63.16	5.75
AlaC ₁ [FeCl ₄]	3.2	6.64	37.27	5.61
ValC ₁ [FeCl ₄]	3.2	6.81	38.43	5.64
Gd-BOPTA	1.9	4.31	4.95	1.20

Data reproduced from Ref. [63] with permission from Royal Society of Chemistry respectively.

Table 2. Osmolality, relaxivity values (r_1 and r_2) and ratio of r_2 and r_1 (r_2/r_1) for PMILs and Gd-BOPTA.

6. Conclusion and future prospect

PMILs has been explored as a dual-responsive (T_1 and T_2) contrast agents for magnetic resonance imaging, and such dual-behavior contrast agents are reported by rare researchers [4, 5]. PMILs have green nature (use of biofriendly amino acid moiety) and magnetic property (use of biocompatible non-toxic Fe (III) ion). Use of Fe eliminated the adverse effect of toxic metal ion like Gd(III) on cell functionality [98] or any Gd metal concerned diseases [99]. However, it is also reported that metallic nanoparticles used for single as well as dual contrast agents have also showed the harmful effect on cell and its physiology [100–102]. For the sake of knowledge, Maureen R. Gwinn and Val Vallyathan have reviewed and reported the toxic effect of nanoparticles (NPs)-based contrast agents which similarly act as air-borne UFPs (Ultra-Fine Particles) and cause diseases with long latency [102]. Similarly, Meng Tang et al. have also reviewed the various adverse effects of NPs on cell organelles and reported that NPs create mitochondrial dysfunction, endoplasmic reticulum stress and lysosomal rupture [103]. Even clinically used Gd-based contrast agents (GBCAs) are also under the question mark with their health-related issues and lengthy synthesis. The report from FDA drug safety newsletter also has criticized the GBCAs and explained the drastic effect of Gd on kidney-related issues such as fibrosing disease, NSF (Nephrogenic Systemic Fibrosis) with acute or chronic severe renal (kidney) insufficiency and renal dysfunction. Some other reports are also available where researchers have reported the accumulation of gadolinium in the renal tissue of patients suffering from NSF [98]. In this study, PMILs have been studied, and their possible use in imaging techniques such as MRI contrast agent with some better advantage has been revealed. Most frequently used Gd metal has been replaced with Fe as a magnetic source in PMILs for imaging due to kidney-related issues. The efficacy of these PMILs is also compared with clinically approved ongoing Gd-based contrast agent. If we compare, PMILs neither contain any metallic nanoparticles nor metal with bulky ligand complex. These PMILs are found to be free from the issue of metal leaching, and any adverse or side effect which is common for nanomaterials when they are used as contrast agents. These PMILs are easy to synthesize and cost-effective, and at certain concentration, they are safe in reference to animal DNA. However, for real effect on cell or health, there is research still ongoing. So, targeted and specific uses of these PMILs need further deep investigations with living cells or organisms.

The comparative study of PMILs with commercially available and FDA-approved Gd-based contrast agents is also completed to examine the comparative performance. Gadobentae Diglumine (Gd-BOPTA) is used as a model contrast agent for this studied. All the experiments were carried out under the similar conditions, and it was found that PMILs-based contrast agents have remarkable properties with significant imaging responses and relaxivity values. The relaxivity values (r_1 and r_2) for Gd-BOPTA are much less compared with PMILs and wherein the ratio of r_2/r_1 is found around 1.2 for Gd-BOPTA which makes it positive contrast agent (T_1 mode) only. The relaxivity values (r_1 and r_2), ratio of r_2/r_1 and osmolality value of PMILs with Gd-BOPTA are given in **Table 2**. The measured osmolality values are found in range of 3 Osmol.Kg⁻¹ for PMILs which is comparable to Gd-BOTA contrast agent. Low osmolality helps to reduce the pain and other contrary effect during injection [104]. From the results discussed above, it can be concluded that PMILs have several advantages over existing contrast agents (NPs and GBCAs). The PMILs have following advantages:

1. The synthesis of PMILs is easy, less tedious, green and cost-effective.
2. There is no need of a long and lengthy pre-synthesis of ligands moiety, costly precursors, reactants, toxic reagents and volatile organic solvents for synthesis like other MRI contrast agents.
3. The problems related to thermodynamic instability and metal leaching problem can be avoided in PMILs.
4. The use of Fe metal in PMILs eliminates the severe health problems which occur due to toxic metals such as Gd.

It can be said that any biological moiety including proteins, vitamin, nitrogen contain sugar moiety, nitrogen-containing heterocycles or drug molecules or any molecule which can be turned into positive ions may be used to synthesize the PMILs via given synthetic procedure in the literature [63]. This study opens other new potential applications of PMILs in the fields of medical, pharma and analytical science. Moreover, such study also triggered further investigations into cytotoxicity, effect on biological process, cancer cell growth, tracking of drug molecules in body and its other uses in physical constant verification and measurement. In the field of imaging, PMILs may become most potential and promising contrast agent with suitable modification. However, research is still ongoing to explore new molecules with better advantages of such iron (III)-containing ionic-liquid-based contrast agents.

Acknowledgements

Praveen Singh Gehlot gratefully acknowledges the Commissioner of Higher Education Department, Government of Gujarat, India, and his former fellowship (JRF & SRF) granted by University Grant Commission, India. Authors also acknowledge financial support through Department of Science and Technology (DST), India. Authors are thankful to CSIR-CSMCRI, India, for providing the place for research work and additional assistance.

Conflict of interest

The authors declare no conflict of interest.

Author details

Praveen Singh Gehlot¹ and Arvind Kumar^{2,3*}


1 Department of Chemistry, Government Science College, Pardi, Gujarat, India

2 CSIR-Central Salt and Marine Chemicals Research Institute (CSIR-CSMCRI), Bhavnagar, Gujarat, India

3 Academy of Scientific and Innovative Research, Ghaziabad, India

*Address all correspondence to: arvind@csmcri.res.in

IntechOpen

© 2022 The Author(s). Licensee IntechOpen. This chapter is distributed under the terms of the Creative Commons Attribution License (<http://creativecommons.org/licenses/by/3.0>), which permits unrestricted use, distribution, and reproduction in any medium, provided the original work is properly cited. 

References

- [1] Bottomley PA, Foster TH, Argersinger RE, Pfeifer LM. A review of normal tissue hydrogen NMR relaxation times and relaxation mechanisms from 1–100 MHz: Dependence on tissue type, NMR frequency, temperature, species, excision, and age. *Medical Physics*. 1984; **11**(4):425-448
- [2] Lasser EC. Basic mechanisms of contrast media reactions: Theoretical and experimental considerations 1. *Radiology*. 1968; **91**(1):63-65
- [3] Hifumi H, Yamaoka S, Tanimoto A, Citterio D, Suzuki K. Gadolinium-based hybrid nanoparticles as a positive MR contrast agent. *Journal of the American Chemical Society*. 2006; **128**(47): 15090-15091
- [4] Shin T-H, Choi J-s, Yun S, Kim I-S, Song H-T, Kim Y, et al. T 1 and T 2 dual-mode MRI contrast agent for enhancing accuracy by engineered nanomaterials. *ACS Nano*. 2014; **8**(4):3393-3401
- [5] Tegafaw T, Xu W, Ahmad MW, Baeck JS, Chang Y, Bae JE, et al. Dual-mode T1 and T2 magnetic resonance imaging contrast agent based on ultrasmall mixed gadolinium-dysprosium oxide nanoparticles: Synthesis, characterization, and in vivo application. *Nanotechnology*. 2015; **26**(36):365102
- [6] Neuwelt EA, Hamilton BE, Varallyay CG, Rooney WR, Edelman RD, Jacobs PM, et al. Ultrasmall superparamagnetic iron oxides (USPIOs): A future alternative magnetic resonance (MR) contrast agent for patients at risk for nephrogenic systemic fibrosis (NSF)? *Kidney International*. 2009; **75**(5): 465-474. DOI: 10.1038/ki.2008.496
- [7] Gerald CF, Laurent S. Classification and basic properties of contrast agents for magnetic resonance imaging. *Contrast Media & Molecular Imaging*. 2009; **4**(1):1-23
- [8] Norek M, Peters JA. MRI contrast agents based on dysprosium or holmium. *Progress in Nuclear Magnetic Resonance Spectroscopy*. 2011; **59**(1):64-82. DOI: 10.1016/j.pnmrs.2010.08.002
- [9] Tóth É, Helm L, Merbach A. Relaxivity of gadolinium(III) complexes: Theory and mechanism. In: *The Chemistry of Contrast Agents in Medical Magnetic Resonance Imaging*. Wiley; 2013. pp. 25-81. DOI: 10.1002/9781118503652.ch2
- [10] Caravan P, Zhang Z. Targeted MRI contrast agents. In: *The Chemistry of Contrast Agents in Medical Magnetic Resonance Imaging*. Wiley; 2013. pp. 311-342. DOI: 10.1002/9781118503652.ch7
- [11] Muller RN, Vander Elst L, Roch A, Peters JA, Csajbok E, Gillis P, et al. Relaxation By Metal-Containing Nanosystems. In: *Advances in Inorganic Chemistry*. Vol. 57. Academic Press; 2005. pp. 239-292. DOI: 10.1016/S0898-8838(05)57005-3
- [12] Laurent S, Forge D, Port M, Roch A, Robic C, Vander Elst L, et al. Magnetic Iron oxide nanoparticles: Synthesis, stabilization, vectorization, physicochemical characterizations, and biological applications. *Chemical Reviews*. 2008; **108**(6):2064-2110. DOI: 10.1021/cr068445e
- [13] Gueron M. Nuclear relaxation in macromolecules by paramagnetic ions: A novel mechanism. *Journal of Magnetic Resonance (1969)*. 1975; **19**(1):58-66. DOI: 10.1016/0022-2364(75)90029-3
- [14] Gillis P, Koenig SH, Transverse relaxation of solvent protons induced by

magnetized spheres: Application to ferritin, erythrocytes, and magnetite. *Magnetic Resonance in Medicine*. 1987; **5**(4):323-345. DOI: 10.1002/mrm.1910050404

[15] Koenig SH, Kellar KE. Theory of $1/T_1$ and $1/T_2$ NMRD profiles of solutions of magnetic nanoparticles. *Magnetic Resonance in Medicine*. 1995;**34**(2): 227-233. DOI: 10.1002/mrm.1910340214

[16] Roch A, Muller RN, Gillis P. Theory of proton relaxation induced by superparamagnetic particles. *The Journal of Chemical Physics*. 1999;**110**(11): 5403-5411. DOI: 10.1063/1.478435

[17] Vogl TJ, Hammerstingl R, Schwarz W, Mack MG, Müller PK, Pegios W, et al. Superparamagnetic iron oxide-enhanced versus gadolinium-enhanced MR imaging for differential diagnosis of focal liver lesions. *Radiology*. 1996;**198**(3):881-887. DOI: 10.1148/radiology.198.3.8628887

[18] Ahlström KH, Johansson LO, Rodenburg JB, Ragnarsson AS, Åkeson P, Börseth A. Pulmonary MR angiography with ultrasmall superparamagnetic iron oxide particles as a blood pool agent and a navigator echo for respiratory gating: Pilot study. *Radiology*. 1999;**211**(3):865-869. DOI: 10.1148/radiology.211.3.r99jn10865

[19] Chen J, Zhang W-J, Guo Z, Wang H-B, Wang D-D, Zhou J-J, et al. pH-responsive iron manganese silicate nanoparticles as T1-T2* dual-modal imaging probes for tumor diagnosis. *ACS Applied Materials & Interfaces*. 2015; **7**(9):5373-5383. DOI: 10.1021/acscami.5b00727

[20] Yang L, Zhou Z, Liu H, Wu C, Zhang H, Huang G, et al. Europium-engineered iron oxide nanocubes with high T1 and T2 contrast abilities for MRI

in living subjects. *Nanoscale*. 2015;**7**(15): 6843-6850. DOI: 10.1039/C5NR00774G

[21] Zhou Z, Wu C, Liu H, Zhu X, Zhao Z, Wang L, et al. Surface and interfacial engineering of Iron oxide nanoplates for highly efficient magnetic resonance angiography. *ACS Nano*. 2015; **9**(3):3012-3022. DOI: 10.1021/nn507193f

[22] Seo WS, Lee JH, Sun X, Suzuki Y, Mann D, Liu Z, et al. FeCo/graphitic-shell nanocrystals as advanced magnetic-resonance-imaging and near-infrared agents. *Nature Materials*. 2006;**5**(12): 971-976. DOI: 10.1038/nmat1775

[23] Cheng K, Yang M, Zhang R, Qin C, Su X, Cheng Z. Hybrid nanotrimers for dual T1 and T2-weighted magnetic resonance imaging. *ACS Nano*. 2014; **8**(10):9884-9896. DOI: 10.1021/nn500188y

[24] Bae KH, Kim YB, Lee Y, Hwang J, Park H, Park TG. Bioinspired synthesis and characterization of gadolinium-labeled magnetite nanoparticles for dual contrast T1- and T2-weighted magnetic resonance imaging. *Bioconjugate Chemistry*. 2010;**21**(3):505-512. DOI: 10.1021/bc900424u

[25] Wang X, Zhou Z, Wang Z, Xue Y, Zeng Y, Gao J, et al. Gadolinium embedded iron oxide nanoclusters as T1-T2 dual-modal MRI-visible vectors for safe and efficient siRNA delivery. *Nanoscale*. 2013;**5**(17):8098-8104. DOI: 10.1039/C3NR02797J

[26] Yang H, Zhuang Y, Sun Y, Dai A, Shi X, Wu D, et al. Targeted dual-contrast T1- and T2-weighted magnetic resonance imaging of tumors using multifunctional gadolinium-labeled superparamagnetic iron oxide nanoparticles. *Biomaterials*. 2011;**32**(20): 4584-4593. DOI: 10.1016/j.biomaterials.2011.03.018

- [27] Shin T-H, Choi J-s, Yun S, Kim I-S, Song H-T, Kim Y, et al. T1 and T2 dual-mode MRI contrast agent for enhancing accuracy by engineered nanomaterials. *ACS Nano*. 2014;**8**(4):3393-3401. DOI: 10.1021/nn405977t
- [28] McDonagh BH, Singh G, Hak S, Bandyopadhyay S, Augestad IL, Peddis D, et al. L-DOPA-coated manganese oxide nanoparticles as dual mri contrast agents and drug-delivery vehicles. *Small*. 2016;**12**(3):301-306. DOI: 10.1002/smll.201502545
- [29] Zhu H, Zhang L, Liu Y, Zhou Y, Wang K, Xie X, et al. Aptamer-PEG-modified Fe₃O₄@Mn as a novel T1- and T2-dual-model MRI contrast agent targeting hypoxia-induced cancer stem cells. *Scientific Reports*. 2016;**6**(1): 39245. DOI: 10.1038/srep39245
- [30] Hyeon T, Na K, Ling D, Park W, Kim BH, Yim H, et al. inventors; SNR R & DB FOUNDATION (KR); INSTITUTE FOR BASIC SCIENCE (KR); THE CATHOLIC UNIVERSITY OF KOREA INDUSTRY—ACADEMIC (KR), assignee. MRI contrasting agent for contrasting cancer cell. Korea Patent US9765187B2. 2017
- [31] Yi Z, Li X, Lu W, Liu H, Zeng S, Hao J. Hybrid lanthanide nanoparticles as a new class of binary contrast agents for in vivo T1/T2 dual-weighted MRI and synergistic tumor diagnosis. *Journal of Materials Chemistry B*. 2016;**4**(15): 2715-2722. DOI: 10.1039/C5TB02375K
- [32] Ta HT, Arndt N, Wu Y, Lim HJ, Landeen S, Zhang R, et al. Activatable magnetic resonance nanosensor as a potential imaging agent for detecting and discriminating thrombosis. *Nanoscale*. 2018;**10**(31):15103-15115. DOI: 10.1039/C8NR05095C
- [33] Ye S, Liu Y, Lu Y, Ji Y, Mei L, Yang M, et al. Cyclic RGD functionalized liposomes targeted to activated platelets for thrombosis dual-mode magnetic resonance imaging. *Journal of Materials Chemistry B*. 2020;**8**(3):447-453. DOI: 10.1039/C9TB01834D
- [34] Hallett JP, Welton T. Room-temperature ionic liquids: Solvents for synthesis and catalysis. 2. *Chemical Reviews*. 2011;**111**(5):3508-3576. DOI: 10.1021/cr1003248
- [35] Tokuda H, Hayamizu K, Ishii K, Susan MABH, Watanabe M. Physicochemical properties and structures of room temperature ionic liquids. 2. Variation of alkyl chain length in imidazolium cation. *The Journal of Physical Chemistry B*. 2005;**109**(13): 6103-6110. DOI: 10.1021/jp044626d
- [36] Davis JH. James task-specific ionic liquids. *The Journal of Physical Chemistry Letters*. 2004;**33**(9): 1072-1077. DOI: 10.1246/cl.2004.1072
- [37] MacFarlane DR, Tachikawa N, Forsyth M, Pringle JM, Howlett PC, Elliott GD, et al. Energy applications of ionic liquids. *Energy & Environmental Science*. 2014;**7**(1):232-250. DOI: 10.1039/C3EE42099J
- [38] Keskin S, Kayrak-Talay D, Akman U, Hortaçsu Ö. A review of ionic liquids towards supercritical fluid applications. *The Journal of Supercritical Fluids*. 2007;**43**(1):150-180. DOI: 10.1016/j.supflu.2007.05.013
- [39] Olivier-Bourbigou H, Magna L, Morvan D. Ionic liquids and catalysis: Recent progress from knowledge to applications. *Applied Catalysis A: General*. 2010;**373**(1):1-56. DOI: 10.1016/j.apcata.2009.10.008
- [40] Rogers RD. Green Industrial Applications of Ionic Liquids. Vol. XXIV,

553 p. Dordrecht: Springer; 2002.
DOI: 10.1007/978-94-010-0127-4

[41] Satoshi H, Hiro-o H. Discovery of a magnetic ionic liquid [bmim]FeCl₄. *Chemistry Letters*. 2004;**33**(12): 1590-1591. DOI: 10.1246/cl.2004.1590

[42] Yao T, Yao S, Pan C, Dai X, Song H. Deep extraction desulfurization with novel guanidinium-based strong magnetic room-temperature ionic liquid. *Energy & Fuels*. 2016;**30**:4740-4749

[43] Shi F, Peng J, Deng Y. Highly efficient ionic liquid-mediated palladium complex catalyst system for the oxidative carbonylation of amines. *Journal of Catalysis*. 2003;**219**(2):372-375. DOI: 10.1016/S0021-9517(03)00198-2

[44] Chatzimitakos T, Binellas C, Maidatsi K, Stalikas C. Magnetic ionic liquid in stirring-assisted drop-breakup microextraction: Proof-of-concept extraction of phenolic endocrine disrupters and acidic pharmaceuticals. *Analytica Chimica Acta*. 2016;**910**:53-59. DOI: 10.1016/j.aca.2016.01.015

[45] Trujillo-Rodríguez MJ, Nacham O, Clark KD, Pino V, Anderson JL, Ayala JH, et al. Magnetic ionic liquids as non-conventional extraction solvents for the determination of polycyclic aromatic hydrocarbons. *Analytica Chimica Acta*. 2016;**934**:106-113

[46] Wang KF, Zhang L, Zhuang RR, Jian FF. An iron (III)-containing ionic liquid: Characterization, magnetic property and electrocatalysis. *Transition Metal Chemistry*. 2011;**36**(8):785-791

[47] Kim S, Bellouard C, Eastoe J, Canilho N, Rogers SE, Ihiwakrim D, et al. Spin state as a probe of vesicle self-assembly. *Journal of the American Chemical Society*. 2016;**138**(8):2552-2555

[48] Klee A, Prevost S, Gradzielski M. Self-assembly of imidazolium-based surfactants in magnetic room-temperature ionic liquids: Binary mixtures. *ChemPhysChem*. 2014;**15**(18): 4032-4041. DOI: 10.1002/cphc.201402548

[49] Konwar M, Elnagdy HMF, Gehlot PS, Khupse ND, Kumar A, Sarma D. Transition metal containing ionic liquid-assisted one-pot synthesis of pyrazoles at room temperature. *Journal of Chemical Sciences*. 2019;**131**(8):80. DOI: 10.1007/s12039-019-1659-9

[50] Khalafi-Nezhad A, Mohammadi S. Magnetic, acidic, ionic liquid-catalyzed one-pot synthesis of spirooxindoles. *ACS Combinatorial Science*. 2013;**15**(9): 512-518

[51] Bwambok DK, Thuo MM, Atkinson MB, Mirica KA, Shapiro ND, Whitesides GM. Paramagnetic ionic liquids for measurements of density using magnetic levitation. *Analytical Chemistry*. 2013;**85**(17):8442-8447

[52] Thévenot J, Oliveira H, Sandre O, Lecommandoux S. Magnetic responsive polymer composite materials. *Chemical Society Reviews*. 2013;**42**(17):7099-7116

[53] Döbbelin M, Jovanovski V, Llarena I, Marfil LJC, Cabañero G, Rodriguez J, et al. Synthesis of paramagnetic polymers using ionic liquid chemistry. *Polymer Chemistry*. 2011;**2**(6):1275-1278

[54] Klee A, Prevost S, Kunz W, Schweins R, Kiefer K, Gradzielski M. Magnetic microemulsions based on magnetic ionic liquids. *Physical Chemistry Chemical Physics*. 2012;**14**(44):15355-15360

[55] Khalafi-Nezhad A, Mohammadi S. Chitosan supported ionic liquid: A recyclable wet and dry catalyst for the

direct conversion of aldehydes into nitriles and amides under mild conditions. *RSC Advances*. 2014;**4**(27): 13782-13787

[56] Santos E, Albo J, Rosatella A, Afonso CA, Irabien Á. Synthesis and characterization of magnetic ionic liquids (MILs) for CO₂ separation. *Journal of Chemical Technology and Biotechnology*. 2014;**89**(6):866-871

[57] Clark KD, Nacham O, Purslow JA, Pierson SA, Anderson JL. Magnetic ionic liquids in analytical chemistry: A review. *Analytica Chimica Acta*. 2016; **934**:9-21

[58] Joseph A, Żyła G, Thomas VI, Nair PR, Padmanabhan A, Mathew S. Paramagnetic ionic liquids for advanced applications: A review. *Journal of Molecular Liquids*. 2016;**218**:319-331

[59] Gehlot PS, Gupta H, Kumar A. Paramagnetic surface active ionic liquids: Interaction with DNA and MRI application. *Colloid and Interface Science Communications*. 2018;**26**:14-23. DOI: 10.1016/j.colcom.2018.07.004

[60] Santos de Almeida T, Júlio A, Saraiva N, Fernandes AS, Araújo MEM, Baby AR, et al. Choline- versus imidazole-based ionic liquids as functional ingredients in topical delivery systems: Cytotoxicity, solubility, and skin permeation studies. *Drug Development and Industrial Pharmacy*. 2017;**43**:1-8. DOI: 10.1080/03639045.2017.1349788

[61] Trivedi TJ, Rao KS, Singh T, Mandal SK, Sutradhar N, Panda AB, et al. Task-specific, biodegradable amino acid ionic liquid surfactants. *ChemSusChem*. 2011;**4**(5):604-608

[62] Li M, De Rooy SL, Bwambok DK, El-Zahab B, DiTusa JF, Warner IM.

Magnetic chiral ionic liquids derived from amino acids. *Chemical Communications*. 2009;(45):6922-6924

[63] Gehlot PS, Gupta H, Rathore MS, Khatri K, Kumar A. Intrinsic MRI contrast from amino acid-based paramagnetic ionic liquids. *Materials Advances*. 2020;**1**(6):1980-1987. DOI: 10.1039/D0MA00339E

[64] Kumar A, Gupta H, Gehlot PS, Rathore MS, inventors Novel amino acid based compounds useful as paramagnetic ionic liquids for T1 and T2 dual mode MRI contrast. INDIA Patent Indian Patent No. IN201711043528. 2019

[65] Daniel CI, Vaca Chávez FN, Portugal CA, Crespo JG, Sebastiao PJ. 1H NMR relaxation study of a magnetic ionic liquid as a potential contrast agent. *The Journal of Physical Chemistry. B*. 2015;**119**(35):11740-11747. DOI: 10.1021/acs.jpcc.5b04772

[66] Li J, Sha Y. A convenient synthesis of amino acid methyl esters. *Molecules*. 2008;**13**(5):1111-1119. DOI: 10.3390/molecules13051111

[67] Del Sesto RE, McCleskey TM, Burrell AK, Baker GA, Thompson JD, Scott BL, et al. Structure and magnetic behavior of transition metal based ionic liquids. *Chemical Communications*. 2008;(4):447-449

[68] Yoshida Y, Saito G. Influence of structural variations in 1-alkyl-3-methylimidazolium cation and tetrahalogenoferrate(III) anion on the physical properties of the paramagnetic ionic liquids. *Journal of Materials Chemistry*. 2006;**16**(13):1254-1262. DOI: 10.1039/B515391C

[69] Dariusz W, Artur S, Julia K, Jerzy M, Emilia S, Zygmund W. Crystal structure and magnetic characteristics of a new

3-methylisoquinolinium tetrachloridoferrate(III). *Zeitschrift für anorganische und allgemeine Chemie*. 2009;**635**(8):1249-1253. DOI: 10.1002/zaac.200801257

[70] Bhadani A, Singh S. Synthesis and properties of thioether spacer containing gemini imidazolium surfactants. *Langmuir*. 2011;**27**(23):14033-14044

[71] Douglas A, Skoog FJH, Crouch SR. TGA DTA DSC thermal method. In: Douglas A, FJH S, Crouch SR, editors. *Principle of Instrumental Analysis*. Thomson Higher Education; 2007. pp. 894-904

[72] Fredlake CP, Crosthwaite JM, Hert DG, Aki SN, Brennecke JF. Thermophysical properties of imidazolium-based ionic liquids. *Journal of Chemical & Engineering Data*. 2004; **49**(4):954-964

[73] Kamboj R, Singh S, Bhadani A, Kataria H, Kaur G. Gemini imidazolium surfactants: Synthesis and their biophysicochemical study. *Langmuir*. 2012;**28**(33):11969-11978

[74] Kapustinskii A. Lattice energy of ionic crystals. *Quarterly Reviews, Chemical Society*. 1956;**10**(3):283-294

[75] Mohan R, Lorenz H, Myerson AS. Solubility measurement using differential scanning calorimetry. *Industrial & Engineering Chemistry Research*. 2002;**41**(19):4854-4862

[76] Bruylants G, Wouters J, Michaux C. Differential scanning calorimetry in life science: Thermodynamics, stability, molecular recognition and application in drug design. *Current Medicinal Chemistry*. 2005;**12**(17):2011-2020

[77] Tian T, Hu X, Guan P, Tang Y. Investigation of surface and solubility

properties of *N*-vinylimidazolium tetrahalogenidoferrate (III) magnetic ionic liquids using density functional theory. *Journal of Chemical & Engineering Data*. 2016;**61**(2):721-730

[78] Rogers RD, Seddon KR. Ionic liquids–Solvents of the future? *Science*. 2003;**302**(5646):792-793. DOI: 10.1126/science.1090313

[79] Chang Y-M, Chen CK-M, Hou M-H. Conformational changes in DNA upon ligand binding monitored by circular dichroism. *International Journal of Molecular Sciences*. 2012;**13**(3):3394-3413

[80] Le Pecq J-B, Paoletti C. A new fluorometric method for RNA and DNA determination. *Analytical Biochemistry*. 1966;**17**(1):100-107

[81] Jadhav V, Maiti S, Dasgupta A, Das PK, Dias RS, Miguel MG, et al. Effect of the head-group geometry of amino acid-based cationic surfactants on interaction with plasmid DNA. *Biomacromolecules*. 2008;**9**(7):1852-1859

[82] Barreleiro P, Lindman B. The kinetics of DNA-cationic vesicle complex formation. *The Journal of Physical Chemistry. B*. 2003;**107**(25):6208-6213

[83] Dasgupta A, Das PK, Dias RS, Miguel MG, Lindman B, Jadhav VM, et al. Effect of headgroup on DNA-cationic surfactant interactions. *The Journal of Physical Chemistry. B*. 2007; **111**(29):8502-8508

[84] Satpathi S, Sengupta A, Hridya V, Gavvala K, Koninti RK, Roy B, et al. A green solvent induced DNA package. *Scientific Reports*. 2015;5:9137-9146

[85] Chandran A, Ghoshdastidar D, Senapati S. Groove binding mechanism of ionic liquids: A key factor in long-term stability of DNA in hydrated ionic

liquids? *Journal of the American Chemical Society*. 2012;**134**(50): 20330-20339

[86] Felgner P, Barenholz Y, Behr J, Cheng S, Cullis P, Huang L, et al. Nomenclature for synthetic gene delivery systems. *Human Gene Therapy*. 1997;**8**(5):511-512

[87] Ding Y, Zhang L, Xie J, Guo R. Binding characteristics and molecular mechanism of interaction between ionic liquid and DNA. *The Journal of Physical Chemistry. B*. 2010;**114**(5):2033-2043

[88] Vashishat R, Chabba S, Mahajan RK. Surface active ionic liquid induced conformational transition in aqueous medium of hemoglobin. *RSC Advances*. 2017;**7**(22):13041-13052. DOI: 10.1039/C7RA00075H

[89] Zhao X, Shang Y, Liu H, Hu Y. Complexation of DNA with cationic gemini surfactant in aqueous solution. *Journal of Colloid and Interface Science*. 2007;**314**(2):478-483

[90] Xu L, Feng L, Hao J, Dong S. Compaction and decompaction of DNA dominated by the competition between counterions and DNA associating with cationic aggregates. *Colloids and Surfaces B: Biointerfaces*. 2015;**134**:105-112

[91] Grueso E, Cerrillos C, Hidalgo J, Lopez-Cornejo P. Compaction and decompaction of DNA induced by the cationic surfactant CTAB. *Langmuir*. 2012;**28**(30):10968-10979

[92] Rawat K, Pathak J, Bohidar H. Effect of persistence length on binding of DNA to polyions and overcharging of their intermolecular complexes in aqueous and in 1-methyl-3-octyl imidazolium chloride ionic liquid solutions. *Physical Chemistry Chemical Physics*. 2013; **15**(29):12262-12273

[93] Hou S, Ziebacz N, Wieczorek SA, Kalwarczyk E, Sashuk V, Kalwarczyk T, et al. Formation and structure of PEI/DNA complexes: Quantitative analysis. *Soft Matter*. 2011;**7**(15):6967-6972

[94] He Y, Shang Y, Liu Z, Shao S, Liu H, Hu Y. Interactions between ionic liquid surfactant [C12mim]Br and DNA in dilute brine. *Colloids and Surfaces B: Biointerfaces*. 2013;**101**:398-404. DOI: 10.1016/j.colsurfb.2012.07.027

[95] Rhee I, Kim C. The concentration dependence of relaxation times of hydrogen proton in the aqueous solution of iron ferrite magnetic nanoparticles. *Journal of Magnetism and Magnetic Materials*. 2003;**261**(3):410-414

[96] Chavhan GB, Babyn PS, Thomas B, Shroff MM, Haacke EM. Principles, techniques, and applications of T2*-based MR imaging and its special applications 1. *Radiographics*. 2009; **29**(5):1433-1449

[97] Gupta H, Paul P, Kumar N, Baxi S, Das DP. One pot synthesis of water-dispersible dehydroascorbic acid coated Fe₃O₄ nanoparticles under atmospheric air: Blood cell compatibility and enhanced magnetic resonance imaging. *Journal of Colloid and Interface Science*. 2014;**430**:221-228

[98] High WA, Ayers RA, Chandler J, Zito G, Cowper SE. Gadolinium is detectable within the tissue of patients with nephrogenic systemic fibrosis. *Journal of the American Academy of Dermatology*. 2007;**56**(1):21-26

[99] White DL. Paramagnetic iron (III) MRI contrast agents. *Magnetic Resonance in Medicine*. 1991;**22**(2): 309-312. DOI: 10.1002/mrm.19102 20230

[100] Agarwal M, Murugan M, Sharma A, Rai R, Kamboj A, Sharma H, et al.

Nanoparticles and its toxic effects: A review. *International Journal of Current Microbiology and Applied Sciences*. 2013;2(7682):39

[101] Hoshyar N, Gray S, Han H, Bao G. The effect of nanoparticle size on in vivo pharmacokinetics and cellular interaction. *Nanomedicine*. 2016;11(6): 673-692

[102] Gwinn MR, Vallyathan V. Nanoparticles: Health effects: Pros and cons. *Environmental Health Perspectives*. 2006;114:1818-1825

[103] Liu N, Tang M. Toxic effects and involved molecular pathways of nanoparticles on cells and subcellular organelles. *Journal of Applied Toxicology*. 2020;40(1):16-36. DOI: 10.1002/jat.3817

[104] Peters JA, Djanashvili K. An introduction to MRI contrast agents. In: *Reference Module in Materials Science and Materials Engineering*. Elsevier; 2016. DOI: 10.1016/B978-0-12-803581-8.01826-9

Compatibility of Filter Materials Used with Ionic Liquids' Uses in Hydraulic Drive Control Systems and a Filterability Test

Darko Lovrec and Vito Tič

Abstract

Developments in the field of ionic liquids have led to industrial applications within various industrial processes, as they can be tailored to a specific purpose of use. Due to certain excellent physico-chemical properties, the first industrial applications also appear in the field of hydraulic drives. In these cases, efficient filtration of the hydraulic fluid is extremely important, as the safe, reliable, as well as long-lasting and economical operation of a heavily loaded hydraulic system depends on the efficiency of the filter and the cleanliness of the fluid. In the case of ionic hydraulic fluids, the question of compatibility with the materials of hydraulic components, including filters, arises. The chapter addresses the issue of compatibility of ionic hydraulic fluids with all filter materials, including the filter material that does the actual filtering. At the forefront of the discussion is the issue of incompatibility with cellulose-based filter material, which is considered the most effective when filtering conventional hydraulic fluids. The discussion is also related to off-line filter devices and the standardised filterability test, which prescribes cellulose filter membranes, and the resulting problems of practical and credible implementation of the standardised filterability test.

Keywords: ionic liquids, hydraulic drives, filter materials, compatibility, filterability test

1. Introduction

Filtering technical fluids used in various processes on a variety of machines and devices is very important, if not a key task that we must address, both before and during the operation of the machine or device. Only an appropriate clean fluid ensures the integrity of a particular process and the long service life of both the fluid itself and the individual components and the entire device. This is especially true for hydraulic fluids, which are one of the most loaded technical fluids – liquid lubricants and working media at the same time. In addition to the transmission of forces and the movement of actuators as basic tasks, hydraulic fluid performs several other important tasks. These include cooling all hydraulic components and flushing wear particles

from the gaps between the moving parts of components and transporting them to the filter, where they are trapped and removed from the system. In this way, we ensure and maintain a limited, permissible amount and size of the particles. This ensures low component wear and, consequently, minimal leakage losses, as well as unforeseen machine and device downtime due to sudden component failure [1, 2].

Wear particles and other contaminants that occur in the hydraulic system can be of various origins. Solid particles in the form of metal parts, abrasive dust, welding residues, sand, etc. already occur during the manufacture and installation of the device. Even fresh oil is not clean. The number of contaminants in new, freshly supplied hydraulic fluid is often significantly higher than allowed during operation. During operation, dust, fine sand particles and water or moisture from the surroundings can enter the hydraulic fluid through the filling opening on the tank. Particles of wear on metal parts, as well as seals, also occur in the hydraulic system. Chemical changes in the fluid due to temperature, pressure and shear stresses lead to ageing products such as sediments and acids.

To achieve the cleanest possible hydraulic fluid, and the required cleanliness level of the fluid defined by the requirements of each installed component, filters are installed in different places on the hydraulic device. The locations of the various filters in the hydraulic system are shown in **Figure 1**.

Optionally installed suction filters protect the hydraulic pump from possible dirt in the tank, and pressure filters protect the high-quality, high-performance control valves. Filtration of the fluid returned to the tank is the most used variant. These return line filters are installed either on the return line or on the reservoir cover. Due to the low pressure on the return line, these filters are quite affordable, easy to maintain and include cleaning of the entire amount of fluid returned to the tank. Depending on whether we filter only a part, or the entire flow supplied by the pump, we distinguish between part-flow and main-flow filters. In addition, a separate filter circuit is also possible in combination with a fluid cooler.

Depending on the purpose of the filter, the place of its installation and the associated height of the present pressure, the filters are designed differently and made of different

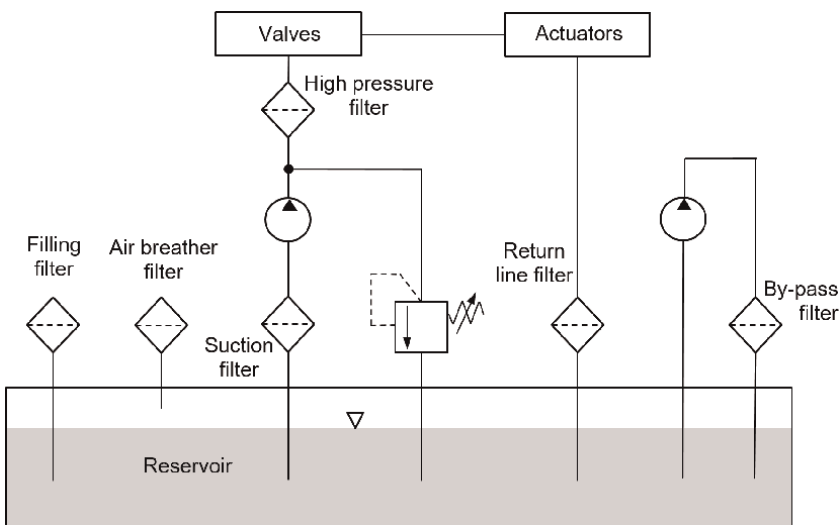


Figure 1.
Location of various types of filters in the hydraulic system.

materials. In the present case, we will focus in more detail on the filters of the total pump flow – i.e. filtering the entire fluid flow. At the forefront will be low-pressure return filters, which we consider a mandatory, indispensable part of every hydraulic device.

In the case of using conventional types of hydraulic fluids, designers and users of hydraulic devices do not prioritise the compatibility of the materials installed in the filter or in the filter component, but they only choose it for a specific type of fluid, usually hydraulic mineral-based oil. Thus, the filter is chosen mainly according to the required degree of cleanliness of the hydraulic fluid and the flow rate.

In the case of new or special hydraulic fluids, before using them, it is necessary to pay a lot of attention to the compatibility of the fluid with all the built-in materials in the filter. This is the task of both the filter manufacturers and later also the users, who must follow the given guidelines and recommendations of the manufacturer to select the appropriate filter with the appropriate materials installed. This dilemma certainly arises in the case of ionic liquids, which are now also used as hydraulic fluids – ionic hydraulic fluids. The first step in this direction is certainly a good knowledge of the filter structure with the various materials incorporated, as well as knowledge of the physico-chemical properties of the used fluid.

2. Filter structure and materials

When it comes to the basic properties of the hydraulic filter, such as type and size of filter, its compressive strength, pressure drop across the filter, filter cartridge collapse pressure, filter efficiency in removing and retaining solid contaminants, the compatibility of all filter materials with the hydraulic fluid used is very important. The latter requirement applies not only to the actual filter material but also all materials built into the filter cartridge and filter housing. A schematic illustration of the flow and filtration process, as well the cross-section of a hydraulic filter and typical structure of a filter cartridge, is shown in **Figure 2**.

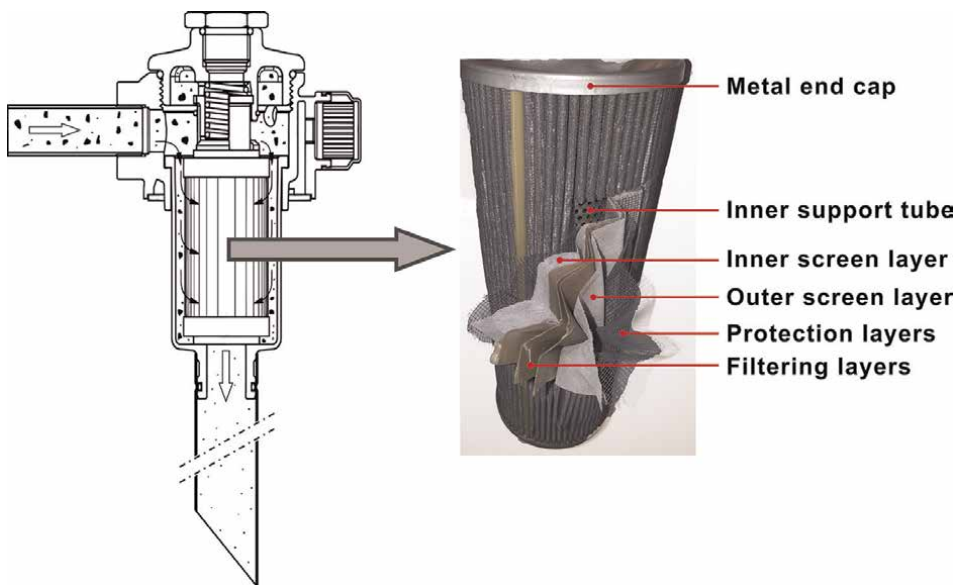


Figure 2.
Flow through filter (left) and typical structure of a filter cartridge (right).

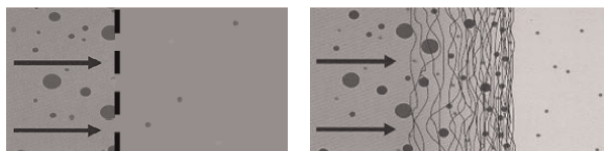


Figure 3.
Principle of the operation of the surface (left) and depth filter (right).

In addition, it is necessary to mention the design of the filter element, which determines the principle of filtering. In the case of hydraulic filters, we distinguish two principles of filter operation and the resulting types of filters: surface filters (mesh and sieve) and depth filters (with a fibrous filter insert) [3–5].

Surface filters are mainly meshing, with pores that are smaller than the particles we want to eliminate – usually pore sizes from 25 μm to 100 μm . The surface filter material is usually a mesh of metal or plastic. To increase the surface area and, thus, increase the filtering effect, the filter mesh folds into a star-like, pleated shape.

Depth filters differ from surface filters in that the deposition and accumulation of particles takes place inside it. Depth filters consist of fibrous materials, metal fibres or plastics in the form of wool (fleece or yarn). This group also includes deep pressure filters made of sintered or glued metal balls. All depth filters have a high capacity to accumulate particles, cause a small pressure drop, are relatively affordable and able to retain longer parts inside, e.g. fibres. The principle of the operation of both types of filters is shown in **Figure 3**.

A whole range of different materials are used, depending on the type of filter and its structure, as well as the type of medium we want to filter.

A complete filter, consisting of a housing and a filter cartridge, is made of different types of materials and not just a material that performs the actual filtering function. When we mention the compatibility of a filter or filter cartridge, we usually think only of the material we use for the actual filtering and pay too little attention to other built-in materials. This includes the inner and outer support material of the filter cartridge, both cartridge covers, the seals on the cartridge and the housing where the filter cartridge is inserted [6–8].

2.1 Materials for filter housing and filter media support

The hydraulic filter housing body is the outer part of the filter. The material for a hydraulic filter housing is a critical part that needs to be considered when selecting a hydraulic filter housing. Proper filter operation depends on the ability of the housing material to withstand fluid operational pressure. Also, the material needs to withstand external factors, such as the environment in which it is operating, as well the type of filtered media inside the housing.

Filter manufacturers most commonly offer three different types of material used for the filter housing. Most hydraulic filter housing bodies are made of copper, carbon steel or stainless steel. All housing materials used must have adequate strength and be compatible with the filtered fluid present inside the filter housing.

At both ends of the filter element are circular caps – end discs. The end discs in a hydraulic filter element are available in different forms and shapes and are of plastic or metal material. These caps play an essential role in squeezing the other parts of the fluid power element into position. In the long run, it offers support to these parts, which ensures that they can withstand the fluid pressure (**Figure 2**).

The protecting cage is an outer section of the filter cartridge and is usually perforated. The cage protects integral parts of the hydraulic filter element from damage and has two main functions. First, it allows for continuous flow of the fluid, which enables filtration to take place; it also offers mechanical support to the entire filter element against external damage. The protective cages are available in different shapes, sizes and materials.

On the innermost part of the filter element is a perforated support body which is usually either of a metallic or plastic material. The function of this body is to offer support and strength to the filter element.

The supporting tube holds or supports the filter media, either from inside or outside. In many cases, the supporting tube is made of stainless steel. Basically, it should support the weight of the filter media and should withstand high pressure and fluctuating temperature. A supporting tube is perforated and allows flow of the hydraulic fluid from the filtration material and basically represents the skeleton of the hydraulic filter element. It is usually made of stainless or corrosion-resistant material.

Seals on the filter cartridge prevent fluid from flowing past the cartridge. A seal can be fixed, but, in certain cases, it is replaceable and can be selected according to the type of liquid to be filtered. NBR (Nitrile/Perbunan/Buna-N) and FKM (Viton) are most used as sealing materials. When selecting sealing material you should, besides the filtration requirements of the application, consider the resistance of the material to breaking or bursting (the burst strength of the sealing material), the flexibility of the fabric you choose, the tensile strength of the material to withstand the mounting temperature and pressure, the outgassing behaviour of the material and the radiation resistance of the material. The chemical compatibility of the material with the type of hydraulic fluid and resistance of the material to corrosion from corrosive agents should also be considered. For these purposes, in the case of new hydraulic fluids or new formulations of existing ones, it makes sense (i.e. urgently) to carry out tests to verify these properties.

2.2 Filter media material

When the fluid passes through the filter media, the actual filtration is performed by retaining contaminants and allowing the cleaner fluid to pass. For example, a filter media of different large pores can filter particles in the range of 3–50 microns. The filter media is mainly a pleated material which can either be plastic, fibreglass, (e.g. Polyester, Nylon, Dacron ...) paper, fleece, cellulose, phenolic-impregnated cellulose or stainless steel mesh [9, 10].

Stainless steel wire mesh filter media is also a popular material in hydraulic filter. This is a type of metal screen with stainless or standard steel. It is woven to make a mesh with different pore sizes. It is also resistant to corrosion. Stainless steel filter media is also used in extreme conditions such as high temperature and pressure.

Fibreglass/micro glass is one of the best media for hydraulic filter elements because it has uniform pores. Manufacturers often choose a co-pleat material, because it is more durable than paper. You are likely to find hydraulic filters having co-pleats with other types of materials, such as polymer mesh, stainless steel wire clothes or annealed epoxy-coated steel wire.

Activated carbon as a filter media material is identified and used due to its ability to remove certain contaminants in very effective way. One gram of the activated carbon has a wide surface area of about 500–3000 square metres. The massive and wide surface area will allow active carbon to have better efficacy in absorbing

contaminants. As the hydraulic fluids flow through the activated carbon, the contaminants such as chemicals stick to the carbon. It removes certain types of 'stubborn' contaminants actively, e.g. dissolved solids that include salts, minerals and metals, most of the microbial contaminants in the hydraulic fluid and inorganic contaminants, including lead. However, activated carbon can only last for a short period of time; therefore, you need to check it every week. Due to this aspect, it is less common in hydraulic systems, as it requires much more attention and control than the other mentioned filter materials.

Paper as a filter media is suitable for disposable hydraulic filter elements. Paper is cheap material though good at absorbing water in hydraulic fluid. Manufacturers use polytetrafluoroethylene (PTFE) or polyester fibre in making the hydraulic filter paper. Also, the pore size and thickness vary, depending on the application.

2.3 Cellulose filter media

Cellulose filters (usually in the form of a filter paper) are generally considered to be versatile and diverse microfiltration agents that work by trapping particles in a random matrix of cellulosic fibres. According to the manufacturers, cellulose filters are generally excellent in terms of separation effect, and they are considered economical filters because they can be removed in an environmentally friendly way; they are harmless from a medical point of view and, thus, to the user, and they are reliable and very effective [11].

Experts dealing with filtration efficiency often recommend the use of cellulose depth filters to achieve efficiency. Cellulose depth filtration is a relatively old but reliable technology. The 'depth' fibre matrix of cellulose-based material is used to trap suspended particles, separating them from their filtered fluid. Working by adsorption and absorption, it has the unique filtration ability to trap particles and moisture.

Deep filtration is most used in applications where exceptional lubricant cleanliness is required. For this purpose, and to achieve the best results, certain filter manufacturers recommend the use of deep cellulose type filters, which, with proper operation and design of the filter, can achieve a filtration rate of up to 3-micron particles. In the case of hydraulic drive technology, this level of cleanliness is suitable for high-tech hydraulic servo drive systems.

Cellulose filter paper is also used as a filter paper to determine the approximate degree of cleanliness level of a hydraulic fluid using on-site testing kits for real-time contamination results or bottle sampling options for ISO counts, wear metals and fluid property determination. The simple process is based on manual sampling of the fluid and filtering through a membrane filter disc. The filter membrane is made of mixed cellulose esters (MCE).

3. Ionic liquids and compatibility of filter materials

The materials used in the filter are very compatible with common types of hydraulic fluids, especially in the case of the most used hydraulic mineral-based oil. In the case of fire-resistant glycol-based hydraulic fluids – HFC fluid (water glycol hydraulic fluid), care must be taken in the selection of seal materials and other materials. Namely, there are some application limitations due to compatibility when using water glycol fluids. Regarding metals, the HFC fluid is corrosive to zinc, cadmium and non-anodised aluminium, and the reaction with these metals causes rapid

deterioration of the fluid. The synthetic rubber seal and gasket compatibility is good; however, polyurethane, leather or cork materials should be avoided. Typical paints will soften in the presence of water glycols; therefore, painted surfaces should be painted with epoxy resin paints.

In the case of a completely new type of hydraulic fluid such as ionic hydraulic fluids, the compatibility of the individual material in the filter must be checked individually with each type of fluid.

Recently, (about the last 10 years), ionic liquids have been moving increasingly from the development pilot phases to real industrial, commercial use. Industrial applications cover many diverse technical fields and even megatrends such as mobility, health and the green economy.

Ionic liquid applications are implemented based on publicly available data and approved personal communications of the author with the industry in almost every technical field, e.g. solvents, energy, catalysts, electrolytes, Nanotechnology, chemicals, electronics, paper and pulp, textiles, pharmaceuticals, biotech, nutrition, health, personal care, metal processing, oil and gas, the automobile industry and all the way to the area of hydraulic drives and systems [12, 13].

Ionic liquids applied in the fields of Lubricants, Heat Transfer and Storage Fluids, Heating, Ventilation, Air Conditioning (HVAC), sealing fluids, cutting and drilling fluids, pressure transmission fluids (hydraulics) and generally as operating liquids in process machines are summarised as ionic engineering fluids. Thus, it is evident that ionic liquids, due to their excellent lubricating and other properties, are also used as lubricants and as hydraulic fluids – ionic hydraulic fluids [14–18].

In most of the mentioned cases, especially in the case of using ionic liquid as a lubricant or as a working fluid within hydraulic drive control systems, fluid filtration is required for the purpose of maintaining the prescribed cleanliness level of the fluid. In this case, the use of effective filters is crucial. This raises the question of the compatibility of filter materials with ionic hydraulic fluids, especially, because several different types of materials are used in the filter (see Section 2).

Methods and standards related to the determination and testing of the material properties of lubricants and the compatibility of materials relate mostly to petroleum-based lubricants. This includes hydraulic fluids, the most commonly used mineral-based hydraulic oils, as well as hydraulic fluids of other types, e.g. fire-resistant hydraulic fluids of the HF type or biodegradable, faster degradable hydraulic fluids of the HE type.

The compatibility of metallic and non-metallic filter materials with ionic hydraulic fluids has been tested in various ways. In cases where there are standards with precisely described procedures and testing conditions, these have been consistently followed. In cases where there is no standard available for testing a particular material or component and only recommendations are given, these have been taken into account. In the case when there are no recommendations or guidelines, a practical, non-standard test was performed. In this case, the conditions present on the real device were taken into account, e.g. applied paint as in the case of a real component, a tested part completely or partially immersed in liquid and similar. However, in cases where the components' part is exposed to the surrounding environment, we have come close to these conditions (there are minor deviations between the industrial environment and the laboratory environment, but these do not significantly affect the main conclusions and findings).

3.1 Determining the compatibility of metallic filter materials

When selecting a filter as a complete component and suitable materials from which it is made (if this information is known and if the choice is possible), we must know the properties of the hydraulic fluid to be filtered well. Given that we encounter different types of metallic and non-metallic materials in the filters (Section 2.1), checking the compatibility of the material with the type of fluid used is a primary and extensive task. This is especially important when it comes to a completely new type of hydraulic fluid, such as ionic hydraulic fluid in our case.

Good lubricating properties and good corrosion protection are the basic aspects of any hydraulic fluid. Unlike other hydraulic components (pumps, valves, hydraulic cylinders and hydro motors), lubricating properties are not at the forefront in the case of filters, but the corrosivity of the fluid to different filter metal materials.

Since ionic liquids are salts, the risk of corrosion can be expected to be one of the most difficult aspects to achieve compared with conventional hydraulic fluids, especially mineral-based oils. That was confirmed within extensive pre-studies and laboratory tests, particularly, in a corrosion test in a humid chamber, where most of the tested ionic liquids proved to be considerably worse than the mineral hydraulic oil (more details are given in the literature, e.g. [19]).

In addition to the humid chamber test (According Standard DIN 51386-1), the corrosion protection capacity was determined by the standard method of determination of corrosiveness to copper (according to ASTM D 130-04) and practical method of determination of corrosion in the open air (practical method, in accordance with the real operating atmosphere conditions).

In the latter case, it was a practical method of immersing and exposing characteristic materials for hydraulic components to various ionic hydraulic liquids. One part of the tested component was completely immersed in the liquid, part was just wetted with IL and exposed to the surrounding ambient air (temperature between 20°C and 22°C, humidity between 35% and 40%) - **Figure 4**.

In this case, parts of the different valve housings (made of cast iron GG30, DIN 169, steel 10,718, steel Hyt 60R), a valve control spool (made from steel 10,715, case hardened 0.4 mm and hardened to 58-62 HRC, steel 16MnCr5), springs (made of steel spring wire according to DIN 17223-1), a washer (made of steel DC01), a bolt (steel 10,715 without subsequent thermal treatment), piston housing (made of steel 42CrMo4 without subsequent thermal treatment) were used as test pieces. Similar materials were used in the case of other hydraulic components. Similar materials are also present in other components of the hydraulic system, such as for pumps, hydraulic cylinders, fittings and piping, as well as filters [19].

The possibility of using filter parts made of copper was also mentioned, and in some cases, aluminium parts could also be encountered. Testing the corrosive or oxidative stability of any parts of the aluminium filter can be performed in the same



Figure 4. Hydraulic valve samples during test of compatibility with ionic liquids.

way as the described immersion test, except that, in this case, either aluminium tape or an aluminium part is used. Alternatively, testing is as available for copper test specimens in the form of test strips, this procedure being specified in the ASTM D 130 Standard.

According to this Standard, the results are given as the corrosiveness to Cu with the designation of the corrosion degree determined by comparison with the tested etalon. Based on the results of our own preliminary testing of different ionic liquids, there were no visible colour changes of the Cu strip, meaning that the (tested) ionic liquids were compatible with materials containing copper. We have come to the same conclusion with other tested ILs – corrosiveness to copper is much lower than that of steel and does not represent any problems. For more details, see [19].

According to the results of the compatibility test, corrosion problems are not to be expected in the practical use of most of the ionic liquids used within the hydraulic system, unless water or increased humidity is present in the ionic liquid. The risk of corrosion could occur if the metal wetted with ionic liquid is exposed to surrounding air with an increased level of humidity (e.g. relative humidity above cca. 60%). As the filter housing is completely filled with fluid and is not in contact with the ambient air, no corrosion problems are expected when using ionic liquid. In addition, most filter housings are made of stainless steel, so there is no risk of corrosion in this case.

3.2 Determining the compatibility of the non-metallic materials in the filter

Regarding the non-metallic materials present in the filter, various plastic materials (for example, both filter cartridge covers, perforated outer protection cover ...) and filter cartridge seals were mentioned. In certain cases, painted parts can also possibly be found. In the case of any protective paint coat inside the filter and its compatibility with the ionic hydraulic fluid used, the problem is like the case of testing the compatibility of the internal protective paint coating of steel hydraulic reservoirs. Only in these cases can the hydraulic fluid be in direct contact with the paint.

Concerning protective coatings, in particular the compatibility of the protective paint regarding the type of hydraulic fluid, there is not a specific standard which would be related to this issue in detail. There are just recommendations or Recommended Practices (RP), linked mostly to related areas, providing guidance on achieving effective corrosion control in storage tanks. They contain information pertinent to the selection of lining materials, surface preparation, lining application, cure and inspection of tank bottom linings for existing and new storage tanks, e.g. the API RP 652 Standard – Linings of Aboveground Petroleum Storage Tank Bottoms. Thus, manufacturers of lubricants are using simple, practical experiments, e.g. testing by continuous contact through the immersion of painted metal samples in the liquid under test, at constant room temperature: 20–25°C.

In our case of testing, the paint coat compatibility was performed with two different types of ionic liquids. The test metal plates were painted with two paints typically used for tank interiors and exteriors. The interior was painted with an epoxy type priming coat, while the exterior was additionally coated with an epoxy-type thick-layer finishing coat. The painted test plates were first completely soaked with the selected ionic liquid and then half immersed in the liquid.

As a result, after a few days of testing (five to six), it turned out that, in the case of one ionic liquid, there were no changes in the paint coat, and in the case of the other, there was wrinkling and swelling and deviation of the paint coat from the metal plate [19]. Given this, each type of ionic hydraulic fluid should be tested separately with the

type of paint used before use. This represents additional work that should be done by either the filter manufacturer or the ionic hydraulic fluids manufacturer, but only in the case if the inside of the filter housing is painted. There are no such paint coat compatibility problems with standard filter housing designs or in the case of a stainless-steel filter housing.

The next non-metallic material present in the filter is seals placed between the filter cartridge and the housing. As mentioned in Section 2.1, NBR or Viton seals are the most used for filter cartridge seals. These materials were also used in the compatibility test with various ionic liquids suitable for use as hydraulic fluids.

The test was performed in accordance with the ASTM D 1414 Standard, with the emphasis on the first three of the six tests (volume swell, shrinkage, hardness change, tensile strength change, elongation change, work function change). According to the test procedure, the thermal loading of the seal in the tested fluid, according to the Standard, takes place for different durations of time (in our case 70, 250, and 500 hours) at a temperature of 90°C [20].

After the elapsed time of thermal loading, the parameters of hardness of the tested seal material and change of geometry were checked, and deviations of values in comparison with deviations valid for mineral hydraulic oils were checked (e.g. permissible changes in % for the case of 500 hours of testing: volume swell –20%, shrinkage: –4%, hardness change: +/- 10% in relation to baseline values before testing).

Visible changes in the colour, shape, geometry and hardness of the seal, for the case of two different seal materials and two different ionic liquids (B2002b® suitable for use in hydraulic systems and EMIM EtSO4 ‘conventional’ ionic liquid, both manufactured by proionic), are shown in **Table 1**.

NBR and Viton materials are quite resistant to thermal stress with various ionic liquids, or they are very compatible with them. This is especially true for the NBR,









Test duration	NBR and B2002b®	FPM and EMIM EtSO4
0 h	 Change in a) Volume: b) Shrinkage: c) Hardness:	 Change in a) Volume: b) Shrinkage: c) Hardness:
After 70 h, 90°C Usually for oil: Vol. swell: +15 Shrinkage: –3 Hardness: +/- 7	 a): +13 b): –6 c): +1	 a): +9 b): –8 c): –10
After 250 h, 90°C Usually for oil: Vol. swell: +15 Shrinkage: –4 Hardness: +/- 8	 a): +20 b): –11 c): +1	 a): +55 b): –6 c): –10
After 500 h, 90°C Usually for oil: Vol. swell: +20 Shrinkage: –4 Hardness: +/- 10	 a): +20 b): –6 c): +3	 a): +55 b): –6 c): –15

Table 1. Changes in geometry and hardness in the case of two seal materials and two ionic liquids compared with the values typical of mineral hydraulic oils.

which shows comparable results compared with conventional hydraulic mineral oils. However, this does not apply to all types of ionic liquids (due to their different chemical structures) and other types of sealing materials. Therefore, in the case of using ionic hydraulic fluid, it is necessary to check its compatibility individually with the seal material used in the filter.

3.3 Determining the compatibility of filter media material

Section 2.2 mentioned the different types of materials used commonly for filtration, and point 2.3 highlighted the cellulose-based filter material that filter manufacturers consider to be very effective. Such cellulose filters in the form of filter membranes are also used in on-site and in laboratory tests to determine the cleanliness class of hydraulic fluid (based on the gravimetric method, with weighing and/or visual evaluation of particle size and quantity). In the following, due to the specificity of cellulosic materials, we will focus on their compatibility with different ionic liquids.

The authors dealing with ionic liquids have already reported on the degradability of cellulose with ionic liquids, and based on this knowledge, ionic liquids were also used for the purpose of cellulose decomposition. For example, Swatloski et al. [21] found that the ILs can dissolve cellulose in a microwave oven as well as in a conventional oven. They reported about initial results that demonstrate that cellulose can be dissolved without activation or pre-treatment in, and regenerated from, 1-butyl-3-methylimidazolium chloride and other hydrophilic ionic liquids. This may enable the application of ionic liquids as alternatives to environmentally undesirable solvents currently used for dissolution of this important bioresource. Ren et al. [22] reported that imidazolium-based chloride ILs can be used to dissolve and regenerate cellulose into a variety of physical forms. They found that 1-allyl-3-methylimidazolium chloride ([AMIM]Cl) showed better capability for dissolving cellulose than [BMIM]Cl. Zhang et al. [23] also found that [AMIM] Cl can be used as solvent for the dissolution and regeneration of cellulose without any pre-treatment or activation. The research results indicated that cellulose with a degree of polymerisation as high as 650 can be dissolved in [AMIM] Cl within 30 min. In these applications, recycling of IL is highly necessary from the points of view of economics, IL disposal and toxicity.

It should be emphasised again that this property of ionic liquids is more or less known to experts in the field of chemistry, to those who deal with ionic liquids. Experts in the field of construction of hydraulic devices, who encounter this type of liquid during their first applications, certainly not.

To test the compatibility of the cellulose-based filter material, a 47 mm diameter membrane white filter paper was used, gridded (to facilitate possible deformation of the filter paper) with a pore size of 0.8 μm and made of mixed cellulose ester (MCE), manufactured by Millipore.

Five different types of ionic liquids were used to test the compatibility of ionic liquids with the cellulose filter material: IL1 (Trioctylmethylammonium dibutyl phosphate), IL2 (EMIM EtSO₄), IL3 (B2001®), IL4 (B2002a®) and IL5 (B2002b®). All mentioned ionic liquids are from the manufacturer proionic. For this purpose, the filter paper was covered with 3 ml of ionic liquid, and the effect of the liquid on the filter material was observed after 1 hour and after 2 days (at normal ambient air conditions). The results of the simple test of the compatibility of tested ionic liquids with a cellulose filter, based on visual observation, are shown in **Figure 5**.

In the present case of testing, the compatibility of the ionic liquid with the cellulose-based filter material, in all cases the deformation of the filter paper occurred

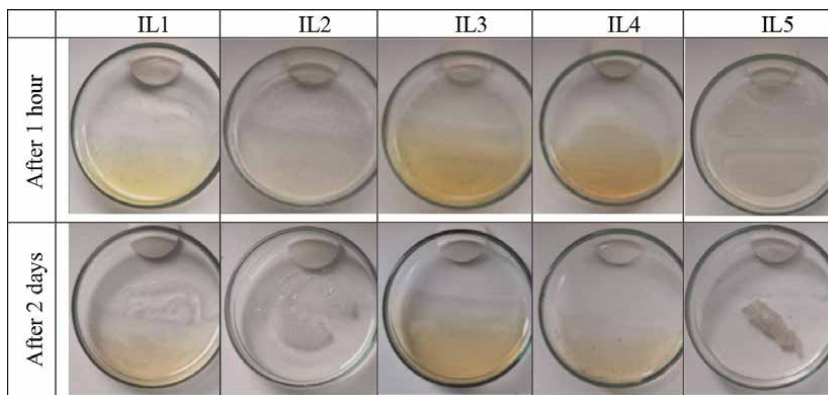


Figure 5.
Effect of ionic liquid on cellulose-based filter material.

first, followed a little later by the disintegration of the paper or another type of deformation. As a result of greater or lesser degradation of the cellulose membrane, a part of the cellulose is definitely present in the ionic liquid and was not visible to the naked eye. We did not measure the amount of cellulose in the ionic hydraulic fluid, because in this case the compatibility of the cellulose filter was in the foreground. The resulting deformation and decomposition are a big enough warning that ionic liquids are not compatible with cellulose filters, which is why it is necessary to use another type of filter material.

4. Tests related to filters and filterability test

There are a wide range of fluid filters used in industry, especially in the filtration of fuel, water and lubricants, including hydraulic filters. Hydraulic filters are required to be compliant with the international contamination code of cleanliness for the fluid contamination levels (ISO 4406) and corresponding filtration standards (e.g. ASTM D3948–14). The required filtration efficiency and dirt holding capacity for the removal of solid particles, water droplets and water moisture from lubricants depend on the filtration system used, the required cleanliness levels of the fluid and the fluid properties (e.g. type, viscosity, surface tension, etc.), which influence the fibre wetting process in fluid filtration. There are many Standards defining performance requirements and test methods for fuel and lubricant filtration [24].

For example, methods for characterising the porous structure and integrity of a filter are defined in ISO 2942 and EN 24003; different methods of testing filtration efficiency and retention capacity are defined in the ISO 4548-12, ISO 16889, ISO 19438 and ISO 23369 Standards; the other test standards also include diesel fuel–water separator performance (ISO 16332 and SAE J1488/J1839), performance of fuel filters for diesel engines (for road vehicles) (ISO 4020), an online automatic particle counter calibration test rig (ISO 11943) and single-pass/gravimetric fuel filter test rigs (SAE J1985 and SAE J905).

In addition to the mentioned standardised tests, the filterability test is important for determining the efficiency of the filter material. The filterability of hydraulic oils is a measure of the ability of a clean fluid to pass through a standard filter without clogging or plugging. Solid additives in hydraulic oils affect filterability largely. This is

especially important, because modern hydraulic systems with narrow gap tolerances, high operating pressures and ever finer filters place increasing demands on the filterability of hydraulic oils. To determine this precisely, the filterability test has been developed in accordance with ISO 13357 and included in the DIN 51524 Standard for HLP hydraulic oils [25].

Using filterability tests in which oil flows through a filter, often under intensified conditions, the interaction between the filter membrane and oil is examined in more detail. Most 'static' filterability tests are carried out as internal tests, due to the lack of a Standard, using different membrane pore sizes and liquid volumes under a vacuum or pressure conditions. However, the results can vary enormously according to the procedure used and often depend on the individual experiences of the laboratory. Since the early 1980s, scientists have been searching for a test capable of becoming a Standard. This has now been passed as the ISO 13357 filterability test parts 1 and 2 [26, 27].

The ISO 13357 Standard test is intended for fresh hydraulic oils with a viscosity grade up to ISO VG 100. The test is divided into the 'wet' filterability test, in which the oil is replaced by water (ISO 13357, part 1) and the test with 'dry' oil (ISO 13357, part 2). The quantity of 300 ml of hydraulic oil is flowed – filtered through a dried 0.8 µm membrane filter under the pressure specified in the Standard. The filtration volume and time are recorded during this process. The filterability is calculated by determining the volume-time relationships at the start, for a test duration of between 10 and 50 seconds (level I) and between 200 and 300 seconds (level II). The test ends when the required data have been recorded or the filtration time exceeds 2 hours. The filterability is indicated by the letter 'F'. If the value is $F > 50$, the test is concluded as 'passed' according to the Standard. The closer 'F' is to 100, the better the filterability. If $F < 50$, the test is deemed to have 'failed'. If the filtration time exceeds 2 hours, the test liquid must be marked as 'unable to filter'.

As already mentioned, Standard ISO 13357-1 and ISO 13357-2 prescribe the use of a cellulose membrane filter with the specified pore size of 0.8 µm, which is not problematic in case of the testing of mineral-based oils and HFD fluids. However, it is not known what may happen in the case of testing the filterability of another type of hydraulic fluid. As shown in Section 3.3, ionic liquids (at least tested), including ionic hydraulic fluids, are not compatible with cellulosic filter materials, as they deform rapidly and, in some cases, degrade completely.

According to the results when testing the filterability in conformity with the ISO 13357 Standard and compatibility with the cellulose filter paper discussed at this point, it can be concluded that the ionic liquids are incompatible with the cellulose filter paper. Therefore, the use of cellulose filter elements in hydraulic systems is not recommended. The filterability in the case of using the filter elements from other materials, for example, glass fibres, should not be problematic; however, they still need to be tested.

The same applies to all other systems that use a certain type of ionic liquid as a liquid which also needs to be filtered. Because there are many types of ionic liquids used for different purposes and in different processes, care must be taken when using cellulose-based materials. It is best to avoid them carefully or, at least, to check the compatibility of the ionic liquid with the cellulose filter before use.

However, regarding standard filterability testing strictly according to the ISO 13357 Standard, it is not feasible, as the use of a cellulose membrane filter is problematic. Other types of filter materials are usually used in today's hydraulic devices. The filterability through filter elements made from other material, for example, glass

fibres, should not be a problem regarding filter material and fluid compatibility. However, the compatibility test must still be established and, of course, to supplement the standard filterability test procedure for these types of fluids.

5. Conclusion

The trend of development of modern hydraulic systems is moving towards more efficient systems with higher energy density and the use of new, high-tech hydraulic fluids. Modern hydraulic components are, thus, made with ever narrower tolerances, smaller gaps between internal moving parts, better materials are used and better surface quality. As a result, higher operating pressures can be used, making hydraulic components smaller, lighter and less space consuming. Due to the smaller tanks, a smaller amount of hydraulic fluid is also used, which is, therefore, much more loaded. As well as in the field of hydraulic fluids, development is taking place in the direction of more energy-efficient fluids, with better lubricating properties, a wider temperature operating range, non-flammability and greater environmental friendliness.

Thus, new types of hydraulic fluids are appearing, which have certain physical and chemical properties that are much better than classic hydraulic fluids. Among them certainly belong ionic liquids suitable for use in hydraulic systems – ionic hydraulic fluids.

Regardless of the type of hydraulic fluid, effective filtering is crucial to achieve adequate operational reliability and a long service life of the components and the entire system. Thus, the average pore size of filters has been reduced from 10 to 20 μm to today's 3 to 12 μm , and new and better filter materials are being used. In the case of new hydraulic fluids, however, the question arises of their compatibility with the materials used commonly in hydraulic components, including filters.

The paper discusses in more detail the issue of compatibility of new ionic hydraulic fluids with the materials used in filters. The emphasis is on return filter materials, which are considered an indispensable component of any hydraulic system. All filter materials are considered, including the filter housing, seals, filter cartridge as a whole, as well as the filter material itself.

Extensive research has shown that no problems can be expected with the metal materials we use for filter housings. Corrosion of steel parts can occur in certain cases only if moisture is present. However, since the filter housing is usually filled with liquid, this problem is not to be expected. However, a problem may arise if the inside of the filter housing is painted with protective paint. In certain cases, softening, wrinkling and peeling of the paint can occur, which can be problematic. It is necessary to individually check the compatibility of a certain type of ionic hydraulic fluid with a certain type of paint before use. If the filter housing and other metal materials of the filter are not painted or are made of other materials (for example, based on copper or stainless steel), these problems do not exist.

We have also not detected any compatibility issues of ionic hydraulic fluids with the plastic materials present on the filter. The same applies to the seals, if they are made of NBR or Viton, the seal material most often found in the filter.

However, it is necessary to be careful with the material of the filter cartridges. In the event that plastic, fibreglass or micro glass (e.g. Polyester, Nylon, Dacron...) is used as the filter material, we did not detect any problems during durability testing on a real device under real operating conditions. However, a compatibility problem arises when using cellulose-based filters. These are considered the most efficient in the field

of hydraulics, but unfortunately ionic hydraulic fluids degrade them (deform and partially decompose).

Cellulose filter membranes are also used in the case of the use of portable off-line devices to determine the cleanliness class of hydraulic fluid. Cellulose-based filter material has proven to be incompatible with ionic liquids.

However, cellulose membranes are also prescribed for determination a very important parameter of filter efficiency, i.e. its filterability. The test is standardised but is mainly intended for testing the filterability of conventional fluids, including hydraulic fluids. Since ionic liquids degrade cellulose-based materials, it will be necessary to update the standardised filterability test for cases where ionic hydraulic fluids are used.

Findings regarding the compatibility of filter materials must be considered, not only when determining the filterability but also when choosing the materials of all filter components. This is true in general and especially in all cases where we do not use classic hydraulic and other technical fluids.

Acknowledgements


This research was supported by the company proionic GmbH from Grambach, Austria, which provided all the samples of ionic liquids and was a very cooperative partner in the IL-selection process, for sharing their wisdom with us. We are also grateful to the company OLMA d.o.o. from Ljubljana, Slovenia, which allowed us to use their equipment and facilities, as well as the personnel to carry out very extensive experimental work. We are thankful to all colleagues in both companies who provided their expertise and skills that assisted this research greatly.

Author details

Darko Lovrec* and Vito Tič
Faculty of Mechanical Engineering, University of Maribor, Maribor, Slovenia

*Address all correspondence to: darko.lovrec@um.si

IntechOpen

© 2022 The Author(s). Licensee IntechOpen. This chapter is distributed under the terms of the Creative Commons Attribution License (<http://creativecommons.org/licenses/by/3.0>), which permits unrestricted use, distribution, and reproduction in any medium, provided the original work is properly cited. 

References

- [1] Sutherland K. *Filters and Filtration Handbook*. 5th ed. Oxford, UK: Elsevier Ltd; 2008. p. 523. DOI: 10.1016/B978-1-85617-464-0.X0001-6. ISBN 978-1-85617-464-0
- [2] Blok P. *The Management of Oil Contamination in Hydraulic Equipment*. Netherlands: Koppen & Lethem, Aandrijftechniek B.V.; 1995. p. 328. ISBN 90-9008458-4
- [3] Chase G, Sparks T. *Filters and Filtration Handbook*. 6th ed. Oxford, UK: Elsevier Ltd; 2015. p. 431. DOI: 10.1016/C2012-0-03230-9. ISBN 978-0-08-099396-6
- [4] Hydac International. *Filter Handbook*. Brochure No.: E7011-3-11-16. Sulzbach/Saar, Germany: Hydac International; 2016. p. 22
- [5] Hydac International. *Filter Elements for Use in Hydac Filters*. TDS No.: E7.200.11/03.12. Sulzbach/Saar, Germany: Hydac International; 2012. pp. 38-46
- [6] Filson Filters. *Hydraulic Filter Element: The Ultimate Guide* [Internet]. 2021. Available from: <https://www.filsonfilters.com/hydraulic-filter-element>. [Accessed: January 14, 2022]
- [7] PAL. *Athalon™ Filters - The Ultimate In Hydraulic & Lube Oil Filter Performance* [Internet]. 2022. Available from: <https://www.pall.com/en/industrial-manufacturing/landing/athalon.html> [Accessed: April 14, 2022]
- [8] Argo Hytos. *Filtration – Products*. [Internet]. 2022. Available from: <https://www.argo-hytos.com/products/filtration.html> [Accessed: April 14, 2022]
- [9] Cosford J. *What do you know about hydraulic filter media?* [Internet]. 2015. Available from: <https://www.mobilehydraulictips.com/what-do-you-know-about-hydraulic-filter-media/#:~:text=They%20can%20be%20used%20to,though%20the%20filter%20is%20clogged>. [Accessed: April 14, 2022]
- [10] Power & Motion. *Hydraulic Filtration*. [Internet]. 2012. Available from: <https://www.powermotiontech.com/hydraulics/hydraulic-filters/article/21882787/hydraulic-filtration>. [Accessed: April 14, 2022]
- [11] Rettenmaier & Soehne GmbH + Co KG. *Why Cellulose Filter Aids?* [Internet]. 2022. Available from: http://www.jrs.eu/jrs_en/fiber-solutions/bu-filtration/why-organic-filter-aids/. [Accessed: April 14, 2022]
- [12] Kalb SR. *Ionic liquids – A new generation of high-tech engineering liquids*. In: *International Conference Fluid Power 2015*. Maribor: University of Maribor. Proceedings; 2015. pp. 49-77
- [13] Kalb SR. *Toward industrialization of ionic liquids*. In: *Commercial Applications of Ionic Liquids; Green Chemistry and Sustainable Technology*. Cham, Switzerland: Springer; 2020. pp. 261-282. DOI: 10.1007/978-3-030-35245-5_11
- [14] Kondo Y, Koyama T, Sasaki S. *Ionic Liquids – New Aspects for the Future*. London, UK: InTech Open; 2013. pp. 127-141
- [15] Schneider MC, Zehnacker O, Schneider R, Seiler M. *Working Fluid for Absorption Heat Pumps*. Patent EP2636715. Munich, Germany: European Patent Office; 11 Sep 2013
- [16] Regueira T, Lugo L, Fernandez J. *Ionic liquids as hydraulic fluids*

Comparison of several properties with those of conventional oil. *Lubrication Science*. 2014;**26**(7–8):488-499

[17] Schluecker E, Wasserscheid P. Ionic liquids in mechanical engineering. *Chemie Ingenieur Technik*. 2011;**83**(9): 1476-1484

[18] Lovrec D. Ionic liquids – The path to the first industrial application. In: *International Conference Fluid Power 2021*. Maribor: Conference proceedings, University of Maribor, University Press; 2021. pp. 211-224. DOI: 10.18690/978-961-286-513-9.17

[19] Kambič M, Kalb R, Tič V, Lovrec D. Compatibility of ionic liquids with hydraulic system components. *Advances in production engineering & management*. 2018;**13**(4):492-503. DOI: 10.14743/apem2018.4.306

[20] Kalb R, Lovrec D. Seal material compatibility test procedure. In: *Conference Proceedings. International Conference Fluid Power 2019*. 1st ed. Maribor: University of Maribor Press; 2019. pp. 133-146

[21] Swatloski RD, Spear SK, Holbrey JD, Rogers RD. Dissolution of cellulose with ionic liquids. *Journal of the American Chemical Society*. 2002;**124**: 4974-4975

[22] Ren Q, Wu J, Zhang J, He JS, Guo ML. Synthesis of 1-allyl-3-methylimidazolium-based room-temperature ionic liquid and preliminary study of its dissolving cellulose. *Acta Polymer. Sin.* 2003;**3**:448-451

[23] Zhang H, Wu J, Zhang J, He J. 1-Allyl-3-methylimidazolium chloride room temperature ionic liquid: A new and powerful nonderivatizing solvent for cellulose. *Macromolecules*. 2005;**38**: 8272-8277

[24] Mao N. Methods for characterisation of nonwoven structure, property, and performance. *Advances in Technical Nonwovens*. Woodhead Publishing Series in Textiles. 2016;**181**:155-211. DOI: 10.1016/B978-0-08-100575-0.00006-1

[25] Day M. Filterability Testing of Paper Machine Oils. *Machinery Lubrication*. 2001. [Internet]. Available from: <https://www.machinerylubrication.com/Read/264/filterability-testing-oil>. [Accessed: April 15, 2022]

[26] ISO 13357-1:2017. Petroleum products - Determination of the filterability of lubricating oils – Part 1; Procedure for oils in the presence of water

[27] ISO 13357-2:2017. Petroleum products – Determination of the filterability of lubricating oils – Part 2: Procedure for dry oils

Development of Low-Friction Ion Gels for Industrial Applications

*Toshio Kamijo, Hiroyuki Arafune, Takashi Morinaga
and Takaya Sato*

Abstract

Friction reduction is imperative for improving the service life and energy efficiency of mechanical systems. Ion gels using ionic liquids (ILs) as swelling agents are expected to be stable gel lubricants owing to the high thermal stability and negligible volatility of ILs; they can maintain their swollen state even under harsh conditions. Therefore, we investigated two types of ion gels: an IL-substituted double-network gel (DN ion S-gel), in which the water in the DN hydrogel is replaced by the IL 3-ethyl-1-methyl-imidazolium ethylsulfate; and a DN ion gel containing N,N-diethyl-N-(2-methoxyethyl)-N-methyl-ammonium bis(trifluoromethylsulfonyl) imide (DEME-TFSI), where one of the polymer backbones is a network of poly(N,N-diethyl-N-(2-methacryloylethyl)-N-methylammonium bis(trifluoromethylsulfonyl) imide), an IL-type polymer based on our previous synthetic study of IL polymer technology. The DN ion S-gel and DN ion gel achieved compression strengths of 25 and 30 MPa, respectively, and were thermally stable until 196°C and 335°C (10% weight-loss temperature), respectively. The coefficient of friction remained stable and low (0.02) after repeated measurements under harsh conditions (high temperature or vacuum conditions), affirming the durability of the DN ion gel.

Keywords: double-network gel, ionic liquid, low friction, highly robust, high vacuum

1. Introduction

Low-friction materials are demanded for energy and resource conservation. As 75% of machine failures are attributed to friction wear [1], friction reduction would improve the service life and energy efficiency of mechanical systems [2]. Low-friction materials can be modeled on the human joint, which has a low coefficient of friction ($\text{CoF} = 10^{-3}$) at pressures above 10^2 atm and remains lubricated for decades [3]. The gel-like structure of human joints, comprising proteoglycans and collagen fibers with a high water content (75–80 wt%), has inspired extensive research on gel lubricants [2–4]. In the early 2000s, researchers in Japan developed hydrogels with high mechanical strength [4–7], promoting the application of gel as biomaterials. Double-network (DN) hydrogels with high mechanical strength, low friction, and biocompatibility are representative gel-lubricant materials [8] and suitable candidates for artificial human joints or cartilages [9]. However, the evaporation of the solvent (water) and

consequent loss of the swollen state have limited the industrial exploitation of gels with these benefits.

Previously, we developed ion gels comprising monodisperse silica nanoparticles and ionic liquids (ILs). In these gels, the silica surface is densely grafted by a well-defined polymer, forming a colloidal self-assembled crystal with a face-centered cubic structure [10]. The ionic conductivity and diffusion coefficients of our gels exceeded those of the bulk polymer. We thus considered the possibility of introducing the highly mobile ions in ion gels to a low-frictional gel surface. To test this idea, we combined ILs with gel lubricants. Owing to their high thermal and oxidative stability, ultralow volatility, and low friction [11–13], IL swelling agents are expected to retain the swelling state of low-friction gels. Whereas DN hydrogels have been targeted as tough hydrogels for biomaterial applications [14], DN ion gels have been mainly studied as gas separation membranes obtained by replacing the water in DN hydrogels with amino-acid-based ILs [15]. As shown in our recent study, IL-based lubrication systems and compatible polymer brushes grafted on Si substrates are efficient and robust lubricants [16]. These lubricants are composed of an IL called N,N-diethyl-N-(2-methoxyethyl)-N-methyl-ammonium bis(trifluoromethylsulfonyl)imide (DEME-TFSI) and high-density IL-type polymer brushes comprising N,N-diethyl-N-(2-methacryloylethyl)-N-methylammonium bis(trifluoromethyl-sulfonyl)imide (DEMM-TFSI), which is a derivative of DEME-TFSI with a polymerizable group. The CoF of the IL-type polymer brushes remained as low as 0.003 over 4,000 cycles.

The present study proposes two types of DN ion gels: an IL-substituted gel in which the water in the DN hydrogel is replaced by an IL [17], and a gel in which one of the polymer backbones of the DN ion gel is a network of poly(DEMM-TFSI) (hereafter, these two gels will be named DN ion S-gel and DN ion gel, respectively). The IL-type polymer in the latter gel is based on our previous synthetic study [18].

The ILs we used, 3-ethyl-1-methylimidazolium ethyl sulfate (EMI-EtSulf) and DEME-TFSI, are commercially readily available and were selected for their compatibility with the gel networks. EMI-EtSulf was also chosen because it can easily substitute water in the hydrogels and has low toxicity. DEME-TFSI has been used for a long time in our material development due to its low viscosity and high electrochemical and thermal stability [13, 16–20]. We are also considering its eventual industrial applications. This IL has been approved by the Japan Chemical Substances Control Law, thereby indicating its potential for industrial mass production and significant cost reductions. Considering the compatibility with this IL, we designed monomers and developed polymerization technology. Therefore, we are developing functional materials by combining DEME-TFSI and poly(DEMM-TFSI) with a maximum consideration of compatibility.

The present study discusses and compares the different tribological properties of DN hydrogels, DN ion S-gels, and DN ion gels. Specifically, it evaluates the gel immobilization techniques of the gels on substrates, the mechanical and thermal stabilities of the ion gels, their lubrication properties in a vacuum, and other required functions for industrial applications.

2. Two types of DN ion gels for industrial applications

2.1 IL-substituted DN gel (DN ion S-gel)

Figure 1 is a schematic of an IL-substituted DN gel. First, a DN hydrogel was fabricated via sequential photopolymerization [6]. A solution of 2-acrylamido

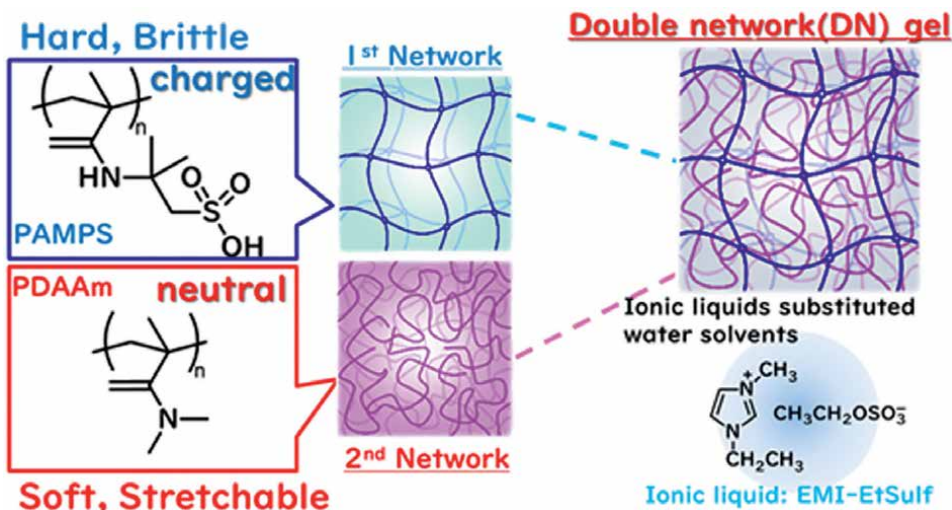


Figure 1.
 Schematic of the IL-substituted DN gel (DN ion S-gel).

methylpropane sulfonic acid (AMPS) as the first monomer, α -Ketoglutaric acid as the initiator, N,N-methylene bisacrylamide (MBAA) as the cross-linker, and water as the solvent was mixed and transferred to a Schlenk tube. Using an injection syringe, the solution was inserted into a reaction cell formed by sandwiching 1-mm-thick Si rubber between two glass plates. After 18 h of rotation under ultraviolet (UV) irradiation, the first gel was obtained. This gel was polymerized under Ar atmosphere, then immersed in a second gel solution comprising dimethylacrylamide as a second monomer, α -Ketoglutaric acid as the initiator, MBAA as the cross-linker, and water as the solvent. Once swelling equilibrium was reached, the second gel solution (i.e., the swelled first gel) was set in the reaction cell and rotated for 18 h under UV light irradiation. The obtained gel was washed with acetonitrile and EMI-EtSulf (volume ratio 1:1), then vacuum-dried at 70°C for 12 h to obtain the substituted DN ion gel. The gel prepared using this method is called DN ion S-gel. The synthesis is detailed elsewhere [17].

2.2 DN ion gel comprising IL and IL polymer, DN ion gel

Figure 2 schematizes the DN ion gel comprising an IL and its polymer (DN ion gel). The first and second networks were composed of DEMM-TFSI and poly (methylmethacrylate) (PMMA), respectively. DEMM-TFSI as the IL monomer, IRGACURE 369 as the initiator, triethyleneglycol dimethacrylate (TEGDMA) as the cross-linker, and DEME-TFSI as the solvent were mixed in a Schlenk tube and deoxygenated by Ar bubbling for 5 min. Using an injection syringe, the solution was injected into a reaction cell formed by sandwiching 2-mm-thick Si rubber between a pair of glass plates. The first gel was rotated for 18 h under UV light irradiation to promote polymerization in an Ar atmosphere. The polymerized gel was washed with acetonitrile to remove impurities and then swollen with DEME-TFSI (poly(DEMM-TFSI) gel as a reference material. PMMA gel was prepared similarly by replacing DEMM-TFSI with methyl methacrylate (MMA) at the same weight ratio. The first gel was polymerized and immersed in a second gel solution comprising MMA monomer, benzophenone

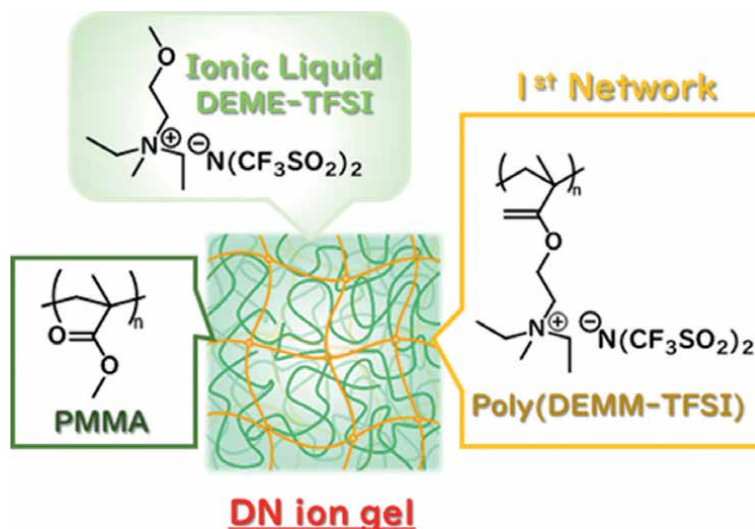


Figure 2. Schematic of the DN ion gel composed of an IL and an IL polymer (DN ion gel).

as the initiator, TEGDMA as the cross-linker, and propylene carbonate as the solvent. After immersion for 2 days to reach swelling equilibrium, the swollen first gel was placed in a reaction cell and rotated for 18 h under UV irradiation. The resulting second gel was washed with an acetonitrile and DEME-TFSI (volume ratio 1:1) to remove the impurities and then vacuum-dried at 70°C for 12 h. The resulting DN ion gel was rich in DEME-TFSI (75 wt%). The synthesis is detailed elsewhere [18].

2.3 Gel immobilization technology on substrates

Figure 3 is a schematic of the gel immobilization technique. The DN ion gels were covalently immobilized on glass substrates via a silane coupling reaction [21]. Briefly, a mixture of ethanol and 3-(trimethoxysilylpropyl) methacrylate was slowly dropped into mixed ethanol and 25-wt% ammonia solution while stirring. The solution was used to immerse a washed glass substrate for 16 h at room temperature to impart the vinyl moieties that covalently anchor the gel to the glass surface. The resulting substrate coated one side of the reaction cell. During the second gel synthesis, the DN ion gel was covalently bonded to the surface silanol groups of a glass substrate. The same technique can prepare DN hydrogels. It is also applicable to other substrates if their surfaces possess hydroxyl groups that can be modified by a silane coupling reagent with vinyl groups, which can help anchor the gel.

3. Characterization of DN and DN ion gels

3.1 Mechanical properties from stress-strain curves

The mechanical strengths of the DN ion gels were evaluated at 25°C and 40% relative humidity using a universal testing machine (Instron 3342, Instron Japan, Kawasaki, Japan). From the stress-strain curves, the compression fracture stresses of the DN

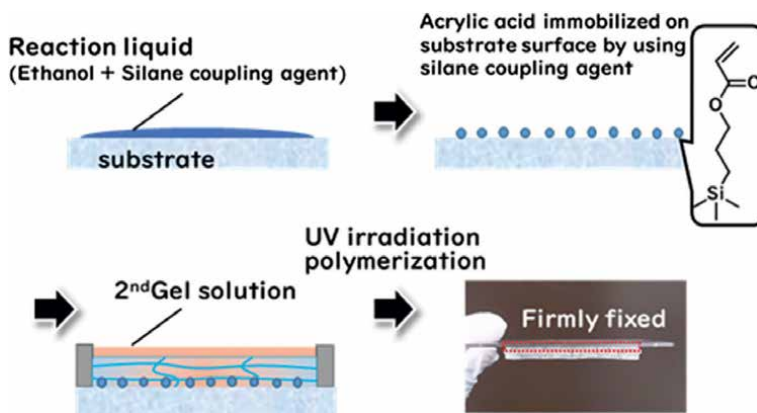


Figure 3. Schematic of gel immobilization technology.

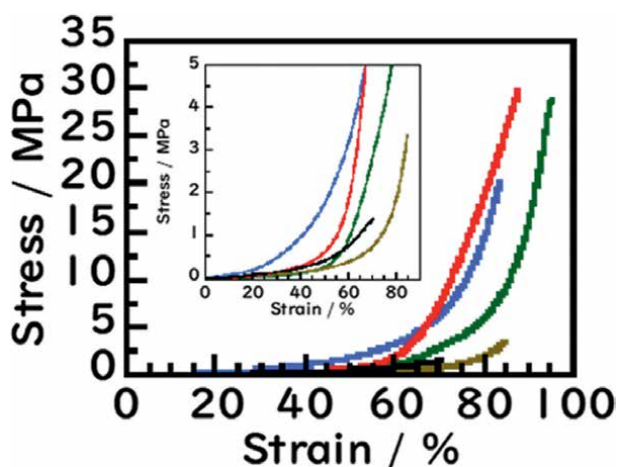


Figure 4. Stress-strain curves of DN hydrogel (blue), DN ion S-gel (green), single DEMM-TFSI gel (brown), and DN ion gel (red). Inset is an expansion of the change region of the curves.

hydrogel and DN ion S-gel were found to be 20 and 25 MPa, respectively (**Figure 4**), which were comparable to those of DN ion gel substituted with tetrabutylphosphonium proline [14]. The stress-strain curve of DN ion gel presented a smaller initial slope than that of DN hydrogel; the loss of hydration force softened the DN ion gel. PAMPS is an electrolyte polymer that swells in pure water via hydration of negatively charged AMPS. In addition, its surface charge is easily shielded in ionic salt at high concentration. The DN ion gel shrank after displacement, suggesting that it softened through loss of hydration power caused by the high ionic strength of EMI-EtSulf.

Moreover, the compressive fracture stress of the DN ion gel was 30 MPa at 87% strain (**Figure 4**), which is 10 MPa higher than that of the DN hydrogel (20 MPa) and DN ion S-gel (25 MPa). The compressive fracture stresses of single-network gels were much lower (1 MPa for poly(DEMM-TFSI) and 3 MPa for PMMA), suggesting that the high mechanical strength of the combined materials derives from the formed DN structure. Because conventional DN gels substituted with amino-acid-based

ILs exhibit similarly high mechanical strengths (>25 MPa) [14], we concluded that combining ILs with compatible polymers can boost the mechanical strength without hydration assistance from electrolyte polymers.

3.2 Thermal properties of the gels

The thermal properties of DN ion S-gel, DN ion gel, and DN hydrogel were evaluated using thermogravimetric analysis (TGA), and the results were compared with those of pure ILs and the conventional lubricants poly- α -olefin (PAO) and glycerol. **Figure 5** compares the TGA curves of DN hydrogel (blue), DN ion S-gel (light blue), EMI-EtSulf (green), DN ion gel (red), DEME-TFSI (light green), PAO (gray), and glycerol (black). The initial weight loss (up to 100°C) in the TGA curves of DN ion S-gel and EMI-EtSulf was attributed to release of absorbed moisture. The secondary weight loss at ~150°C indicated pyrolysis of the sulfonate and sulfate portion of PAMPS and EMI-EtSulf [22]. The 10% weight-loss temperatures (T_{10}) of DN ion S-gel and EMI-EtSulf were determined as 196°C and 247°C, respectively. The T_{10} of DN hydrogel was much lower (39°C), thereby indicating that replacing water with ILs decidedly improves the thermal stability of DN gels ($\Delta T_{10, \text{DN ion S-gel}} = 157^\circ\text{C}$). The DN ion gel thermally decomposed at nearly 300°C with a weight loss 10% at 335°C. The obtained T_{10} value of DN ion gel was much higher than that of the DN hydrogel ($\Delta T_{10, \text{DN ion gel}} = 295^\circ\text{C}$) and 139°C higher than that of the S-gel. The 10% weight loss of DN ion gels occurred at a much higher temperature than that of glycerol (165°C) and PAO (241°C); therefore, DN ion gel can be used as stable and efficient lubricant under high-temperature conditions for industrial applications.

4. Tribological properties of the DN ion gel

4.1 Sliding-speed dependence of CoF on gel properties

For the friction test using a ball-on-plate-type reciprocating tribometer (Shinto Scientific Co., Ltd, Tokyo, Japan), the gel sample was fixed on a sliding table and a glass ball sample ($\phi 10$ mm) was placed in a ball holder connected to a load cell. To

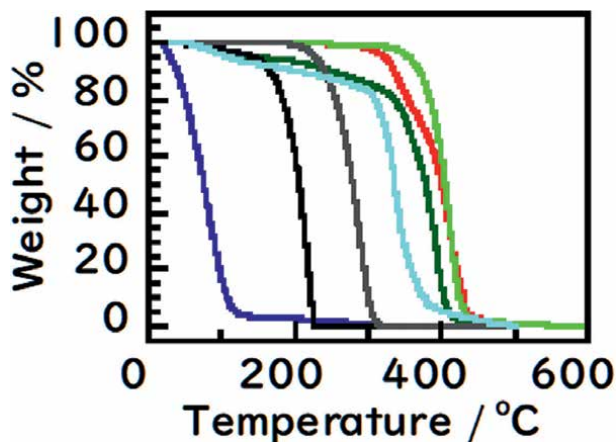


Figure 5. TGA curves of DN hydrogel (blue), DN ion S-gel (right blue), EMI-EtSulf (green line), DN ion gel (red), DEME-TFSI (light green), PAO (gray), and glycerol (black).

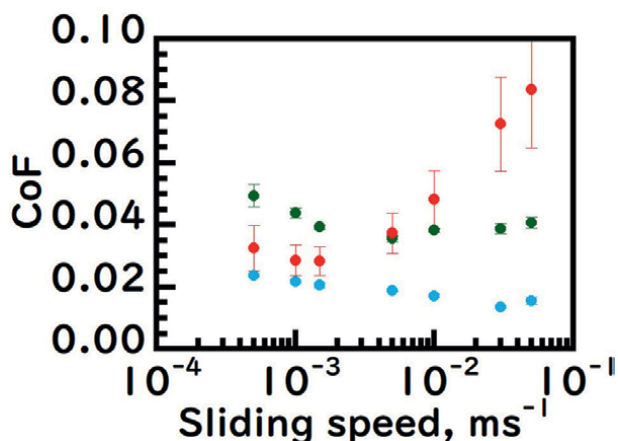


Figure 6. Sliding-speed dependence of CoF at glass ball/DN hydrogel (light blue circles), glass ball/DN ion S-gel (green circles), and glass ball/DN ion gel (red circles).

evaluate the lubrication properties, the ball/substrate frictional force was measured at different loads and sliding speeds. **Figure 6** plots the CoFs as functions of sliding speed for the ball/DN hydrogel (light blue circles), glass ball/DN ion S-gel (green circles), and glass ball/DN ion gel (red circles) under an applied load of 0.98 N. The CoF of the glass ball/DN hydrogel remained within 0.01–0.02 over the range of measured sliding speeds. The minimum CoF at $3.0 \times 10^{-2} \text{ ms}^{-1}$ indicated a shift from the elastic lubrication regime to mixed lubrication. By contrast, the CoFs of the glass ball/DN ion S-gel ranged from 0.04 to 0.05 over the sliding-speed range and were minimized at a speed six times slower ($5.0 \times 10^{-3} \text{ ms}^{-1}$) than that of the DN hydrogel. These results can be attributed to the following factors: (1) high viscosity of the swelling agent incorporated in the DN gels, and (2) increased polymer adhesion after substituting water with IL. As the viscosities of water and EMI-EtSulf at 25°C are 0.89 and 71 MPa·s, respectively, a fluid film of IL is much thicker than a water film. Therefore, the viscosity change could not explain the disparate lubrication properties of DN ion S-gel and DN hydrogel. Regarding factor (2), PAMPS and the glass surface easily dissociate to produce negative charges in pure water, and the fluid film thickness is preserved by electrostatic repulsion between the glass surface and PAMPS [23, 24]. Electrostatic repulsion is essential for lowering the friction at an electrolyte interface. Using a surface force apparatus, Raviv et al. [23] studied the friction between polymer brush layers adsorbed on a molecularly smooth mica surface in water. The friction induced by the shear force between the polyelectrolyte brush layers (CoF = 0.0006–0.001) was lower than that induced between neutral brush layers. In the former case, friction was decreased by electrostatic repulsion between the negatively charged tribopaired polymer brushes. Dunlop et al. [24] measured the normal and shear forces between polyelectrolyte brush layers grafted on a mica surface. After examining the contribution of ionic strength to friction, they found that salt at high concentrations shielded the electric double layer, thereby increasing the shear forces. Being fully composed of cations and anions, EMI-EtSulf has a high salt concentration (≈ 5 molar); therefore, it shielded almost all of the hydroxyl groups on the glass surface and the sulfonate groups on PAMPS. The higher friction of the DN ion gel than of the DN hydrogel was thus attributed to polymer adhesion on the glass surface, enabled by electrostatic shielding of the glass and PAMPS surfaces.

The red circles in **Figure 6** plot the relationship between CoF and sliding speed of the glass ball/DN ion gel under a 0.98-N load. The CoF decreased as the sliding velocity increased to $1.5 \times 10^{-3} \text{ ms}^{-1}$ and increased slowly thereafter, indicating a transition from a mixed (elastic fluid) to a fluid lubrication regime. The higher CoF of the DN ion gel than of the hydrogels and DN ion S-gel at sliding velocities above $5.0 \times 10^{-3} \text{ ms}^{-1}$ may be explained by the smaller elastic deformation (and consequent entry to the fluid lubrication regime) of the synthesized DN ion gel. The CoF of the DN ion gel exceeded those of the DN hydrogel and ion S-gel in the same velocity region. Meanwhile, the effect of surface-to-surface contact becomes significant at velocities below $1.5 \times 10^{-3} \text{ ms}^{-1}$ (in the mixed lubrication regime). The smaller CoF of the DN ion gel than that of the DN ion S-gel in the slow-velocity region means a smaller interaction between the glass surface and DN ion gel than between the glass surface and DN ion S-gel; however, the former interaction exceeded the interaction between the glass surface and DN hydrogel. The CoF of the DN hydrogel was lower at room temperature when water was not volatilized (that is, under the experimental conditions of the present study).

4.2 Repeated durability and thermal stability of gels

Figure 7 shows the temporal changes in the measured CoFs of glass balls/DN ion S-gel and glass balls/DN ion gel at different temperatures under a 0.98 N load and a sliding speed of $5.0 \times 10^{-3} \text{ ms}^{-1}$. At 25°C, 80°C, and 100°C, the CoF values of the glass ball/DN ion S-gel were 0.067, 0.054, and 0.037, respectively, and those of the glass balls/DN ion gel were 0.025, 0.017, and 0.013, respectively. Both sets of CoFs monotonically decreased with increasing temperature. Higher temperatures promote gel softening and decrease the average contact pressure. They also increase the fluid film thickness and hence the viscous resistance. Therefore, decreased polymer adhesion is considered as the main cause of the friction reduction. At 50°C, the CoF of the DN hydrogels jumped by more than 10-fold during repeated measurements, probably due to thermal aggregation of the dried polymer [18] as the water solvent evaporated. In contrast, the CoF of the DN ion gel remained stable after 500 friction cycles even at 100°C because it did not volatilize, indicating that the DN ion S-gel and DN ion gels were more thermally stable than the DN hydrogel. Therefore, they can potentially be applied as lubricating gels in high-temperature applications that are unsuitable for hydrogels.

4.3 Lubricating properties of gels in a vacuum and future development of gel materials

Figure 8 shows the stability of the DN ion gel under a high vacuum during repeated friction measurements of glass balls/DN ion gel. The sliding velocity, load, and pressure were $5.0 \times 10^{-3} \text{ ms}^{-1}$, 0.20 N, and $2.2 \times 10^{-4} \text{ Pa}$, respectively. For this test, a custom-made ball-on-plate-type tribometer was installed in a vacuum chamber [25]. The tribopairs of DN ion gel with glass balls and SUJ2 balls showed a stable response (CoF = 0.023) after 500 friction cycles, indicating that the low-friction surface of the DN ion gel remained stable under high-vacuum conditions. Along with the temperature stability results in **Figure 7**, this result affirms that DN ion gels can reduce the friction and improve the energy efficiency of mechanical systems operating under high-temperature and high-vacuum conditions, such as bearings and mechanical seals.

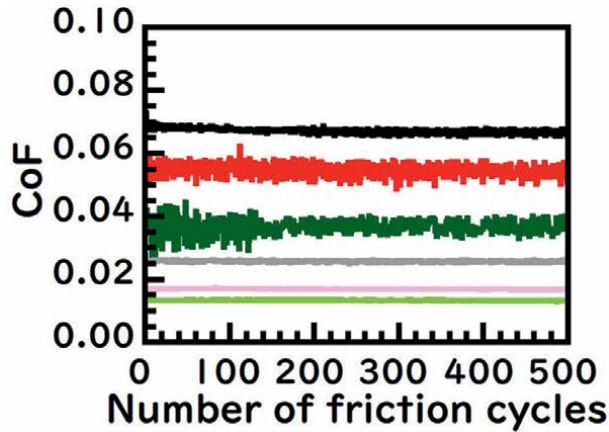


Figure 7. CoF versus number of friction cycles for glass ball/DN ion S-gel (black: 25°C, red: 80°C, green: 100°C) and glass ball/DN ion gel (gray: 25°C, pink: 80°C, yellow-green: 100°C). All measurements were taken at $5.0 \times 10^{-3} \text{ ms}^{-1}$ under a load of 0.98 N.

Thus, we combined DN gels and ILs and evolved them into an industrially viable material. For widespread usage of this material, we must halt the metal corrosion of ILs and replace the expensive ILs with cheaper alternatives such as deep eutectic solvents (DES) [26]. In DES compounds, hydrogen-bond donors are mixed with hydrogen-bond acceptors (either or both solid) at a certain ratio, forming a liquid at room temperature. DESs exhibit similar properties to ILs but are inexpensive and their combination possibilities are numerous. We plan to develop new materials based on DESs.

In addition, the DN gel with IL in this study requires a two-step preparation, which is difficult to synthesize in large quantities. This issue must also be resolved in industrial preparations. Currently, we are developing a one-step preparation method for DN gels [27].

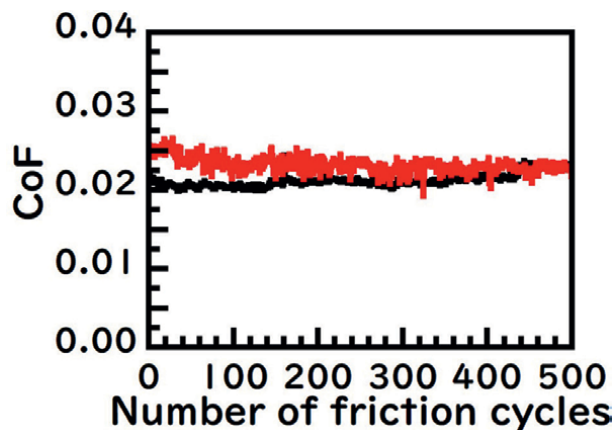


Figure 8. CoF versus number of friction cycles for glass ball/DN ion gel (black) and SUJ2 ball/DN ion gel (red), measured at $5.0 \times 10^{-3} \text{ ms}^{-1}$ under a 0.20 N load and $2.2 \times 10^{-4} \text{ Pa}$.

5. Conclusion

In this study, we investigated gels comprising two types of ILs for industrial applications: DN ion S-gel in which the water in the hydro-DN gel is replaced by an IL EMI-EtSulf, and DN ion gel containing IL DEME-TFSI where one of the polymer backbones of the DN ion gel becomes a network of poly(DEMM-TFSI), an IL-type polymer developed through our previous IL polymer technology.

The obtained DN ion S-gel and DN ion gel achieved high compression strengths (25 and 30 MPa, respectively) and were thermally stable up to 196°C and 335°C (the 10% weight-loss temperature), respectively. The decomposition behavior of the DN ion S-gel and DN ion gel reflects their thermal stabilities after incorporating EMI-EtSulf and DEME-TFSI, respectively. This phenomenon is commonly observed in ion gels. The CoF of the DN ion gel was low (0.02) and stable after repeated measurements at high temperature and under vacuum conditions, confirming the durability of this gel even under harsh conditions.

This study elucidated the fabrication of lubricant gels with high mechanical strength and robustness. The gels are expected to reduce the energy and resource consumption of materials in the temperature range at which conventional hydrogels cannot be used (DN ion S-gel: $\Delta T_{10, \text{DN ion S-gel}} = 157^\circ\text{C}$, DN ion gel; $\Delta T_{10, \text{DN ion gel}} = 295^\circ\text{C}$).

Acknowledgements


This study was supported in part by the e “Green Tribology Innovation Network” Advanced Environmental Materials Area, Green Network of Excellence (GRENE) Program, the ACCEL program and Grants-in-Aid for Scientific Research (No.20H02060, No. 25810091, and No. 26820034) sponsored by the Ministry of Education, Culture, Sports, Science and Technology (MEXT) in Japan. The authors would like to thank Enago (www.enago.jp) for the English language review.

Author details

Toshio Kamijo*, Hiroyuki Arafune, Takashi Morinaga and Takaya Sato
Department of Creative Engineering, National Institute of Technology, Tsuruoka
College, Tsuruoka, Japan

*Address all correspondence to: kamijo@tsuruoka-nct.ac.jp

IntechOpen

© 2022 The Author(s). Licensee IntechOpen. This chapter is distributed under the terms of the Creative Commons Attribution License (<http://creativecommons.org/licenses/by/3.0>), which permits unrestricted use, distribution, and reproduction in any medium, provided the original work is properly cited. 

References

- [1] Adachi K, Yamaguchi T, Ishimine Y, Kato K. Tribologically-based design of precise positioning stage. *Tribological Series*. 2003;**41**:461-468. DOI: 10.1016/S0167-8922(03)80160-8
- [2] Holmberg K, Andersson P, Erdemir A. Global energy consumption due to friction in passenger cars. *Tribology International*. 2012;**47**:221-234. DOI: 10.1016/j.triboint.2011.11.022
- [3] Klein J. Hydration lubrication. *Friction*. 2013;**1**:1-23. DOI: 10.1007/s40544-013-0001-7
- [4] Okumura Y, Ito K. The polyrotaxane gel: A topological gel by figure-of-eight cross-links. *Advanced Materials*. 2001;**13**:485-487
- [5] Haraguchi K, Takehisa T. Nanocomposite hydrogels: A unique organic-inorganic network structure with extraordinary mechanical, optical, and swelling/de-swelling properties. *Advanced Materials*. 2002;**14**:1120-1124. DOI: 10.1002/1521-4095(20020816)14:16
- [6] Gong J, Katsuyama Y, Kurokawa T, Osada Y. Double-network hydrogels with extremely high mechanical strength. *Advanced Materials*. 2003;**15**:1155-1158. DOI: 10.1002/adma.200304907
- [7] Sakai T, Matsunaga T, Yamamoto Y, Ito C, Yoshida R, Suzuki S, et al. Design and fabrication of a high-strength hydrogel with ideally homogeneous network structure from tetrahedron-like macromonomers. *Macromolecules*. 2008;**41**:5379-5384. DOI: 10.1021/ma800476x
- [8] Kaneko D, Tada T, Kurokawa T, Gong JP. Mechanically strong hydrogels with ultra-low frictional coefficients. *Advanced Materials*. 2005;**17**:535-538. DOI: 10.1002/adma.200400739
- [9] Tanabe Y, Yasuda K, Azuma C, Taniguro H, Onodera S, Suzuki A, et al. Biological responses of novel high-toughness double network hydrogels in muscle and the subcutaneous tissues. *Journal of Materials Science. Materials in Medicine*. 2008;**19**:1379-1387. DOI: 10.1007/s10856-007-3255-7
- [10] Sato T, Morinaga T, Marukane S, Narutomi T, Igarashi T, Kawano Y, et al. Novel solid-state polymer electrolyte of colloidal crystal decorated with ionic-liquid polymer brush. *Advanced Materials*. 2011;**23**:4868-4872. DOI: 10.1002/adma.201101983
- [11] Zhou F, Liang Y, Liu W. Ionic liquid lubricants: Designed chemistry for engineering applications. *Chemical Society Reviews*. 2009;**38**:2590-2599. DOI: 10.1039/B817899M
- [12] Somers A, Howlett P, MacFarlane D, Forsyth M. A review of ionic liquid lubricants. *Lubricants*. 2013;**1**:3-21. DOI: 10.3390/lubricants1010003
- [13] Kamijo T, Arafune H, Morinaga T, Honma S, Sato T, Hino M, et al. Lubrication properties of ammonium-based ionic liquids confined between silica surfaces using resonance shear measurements. *Langmuir*. 2015;**31**:13265-13270. DOI: 10.1021/acs.langmuir.5b03354
- [14] Moghadam F, Kamio E, Yoshizumi A, Matsuyama H. An amino acid ionic liquid-based tough ion gel membrane for CO₂ capture. *Chemical Communications*. 2015;**51**:13658-13661. DOI: 10.1039/C5CC04841A

- [15] Haque MA, Kurokawa T, Gong J. Super tough double network hydrogels and their application as biomaterials. *Polymer*. 2012;**53**:1805-1822. DOI: 10.1016/j.polymer.2012.03.013
- [16] Arafune H, Kamijo T, Morinaga T, Honma S, Sato T, Tsujii Y. A robust lubrication system using an ionic liquid polymer brush. *Advanced Materials Interfaces*. 2015;**2**:1500187. DOI: 10.1002/admi.201500187
- [17] Arafune H, Muto F, Kamijo T, Honma S, Morinaga T, Sato T. Tribological properties of double-network gels substituted by ionic liquids. *Lubricants*. 2018;**6**:89. DOI: 10.3390/lubricants6040089
- [18] Arafune H, Honma S, Morinaga T, Kamijo T, Miura M, Furukawa H, et al. Highly robust and low frictional double-network ion gel. *Advanced Materials Interfaces*. 2017;**4**:1700074. DOI: 10.1002/admi.201700074
- [19] Sato T, Masuda G, Takagi K. Electrochemical properties of novel ionic liquids for electric double layer capacitor applications. *Electrochimica Acta*. 2004;**49**:3603-3611. DOI: 10.1016/j.electacta.2004.03.030
- [20] Maruyama Y, Marukane S, Morinaga T, Honma S, Kamijo T, Shomura R, et al. New design of polyvalent ammonium salts for a high-capacity electric double layer capacitor. *Journal of Power Sources*. 2019;**412**:18-28. DOI: 10.1016/j.jpowsour.2018.10.093
- [21] Morinaga T, Sato T, Kamijo T, Arafune H, Furukawa H. Double network gel-solid hybrid, JP Patent 5892570. 2015
- [22] Qiao J, Hamaya T, Okada T. New Highly Proton-conducting membrane poly(vinylpyrrolidone) (PVP)modified poly(vinyl alcohol)/2-acrylamido-2-methyl-1-propanesulfonic acid (PVA-PAMPS) for Low-temperature Direct Methanol Fuel Cells (DMFCs). *Polymer*. 2005;**46**:10809-10816. DOI: 10.1016/j.polymer.2005.09.007
- [23] Raviv U, Giasson S, Kampf N, Gohy JF, Jérôme R, Klein J. Normal and frictional forces between surfaces bearing polyelectrolyte brushes. *Langmuir*. 2008;**24**:8678-8687. DOI: 10.1021/la7039724
- [24] Dunlop IE, Briscoe WH, Titmuss S, Jacobs RMJ, Osborne VL, Edmondson S, et al. Direct measurement of normal and shear forces between surface-grown polyelectrolyte layers. *The Journal of Physical Chemistry. B*. 2009;**113**:3947-3956. DOI: 10.1021/jp807190z
- [25] Kasahara A, Goto M, Tosa M, Yoshihara K. Measurement of friction force electrochemical buffing and chemical polishing to decrease sliding friction in high vacuum with control of surface nano roughness. *Journal of Electroanalytical Chemistry*. 2003;**559**:45-48. DOI: 10.1016/S0022-0728(03)00090-1
- [26] Zhang Q, Vigier KD. Deep eutectic solvents: Syntheses, properties and applications. *Chemical Society Review*. 2012;**41**:7108-7146. DOI: 10.1039/c2cs35178a
- [27] Arafune H, Watarai Y, Kamijo T, Honma S, Sato T. Mechanical and lubrication properties of double network ion gels obtained by a one-step process. *Materials*. 2022;**15**:2113. DOI: 10.3390/ma15062113

Edited by Fabrice Mutelet

Due to their very low volatility, high thermal stability, and ability to dissolve a wide variety of compounds, ionic liquids appear to meet the rigorous criteria for industrial applications. Among other uses, ionic liquids appear to be efficient for gas capture, biomass pretreatment, separation problems, and electrochemistry. They are also used in electrolytes, as lubricants, catalysts, or as antistatic agents. This book discusses the various uses of ionic liquids. Chapters discuss such topics as the use of ionic liquids in batteries, new mono, di, and trimeric imidazolium and pyridinium ionic liquids as catalysts in organic chemistry, the physico-chemical properties of ionic liquid-substituted double-network gels for industrial applications, the use of paramagnetic ionic liquids in magnetic resonance imaging, the compatibility of filter materials used with ionic liquids, and the development of low-friction ion gels for industrial applications.

Published in London, UK

© 2023 IntechOpen
© neirfy / iStock

IntechOpen

